Søvind Marl - Behaviour of a plastic fissured Eocene clay

Grønbech, Gitte Lyng

DOI (link to publication from Publisher):
10.5278/vbn.phd.engsci.00023

Publication date:
2015

Document Version
Publisher's PDF, also known as Version of record

SØVIND MARL - BEHAVIOUR OF A PLASTIC FISSURED EOCENE CLAY

BY
GITTE LYNG GRØNBECH

DISSERTATION SUBMITTED 2015

AALBORG UNIVERSITY
DENMARK

Søvind Marl - Behaviour of a plastic fissured Eocene clay

Ph.D. Dissertation

Gitte Lyng Grønbech

Dissertation submitted January 30, 2015

Thesis submitted:	January 30, 2015
PhD supervisor:	Prof. Lars Bo Ibsen Aalborg University
Assistant PhD supervisor:	Assoc. Prof. Benjaminn Nordahl Nielsen Aalborg University
PhD committee:	Prof. Emeritus Niels Nielsen Foged Technical University of Denmark
	Prof. David Zeng Case Western Reserve University
	Assoc. Prof. Lars Vabbersgaard Andersen Aalborg University
PhD Series:	Faculty of Engineering and Science, Aalborg University

ISSN: 2246-1248
ISBN: 978-87-7112-227-5

Published by:
Aalborg University Press
Skjernvej 4A, 2nd floor
DK – 9220 Aalborg Ø
Phone: +45 99407140
aauf@forlag.aau.dk
forlag.aau.dk

Printed in Denmark by Rosendahls, 2015

Thesis Details

Mandatory page in PhD theses:
For any PhD thesis where one or more submitted or published papers are used in the thesis the PhD student should pay close attention to proper citation of the work. If the paper(s) are co-authored the student cannot normally use the papers as if the student was the sole author. To protect the student while still proving some freedom in using material developed during the PhD study a mandatory page including the following must be included:

1. Title:
Søvind Marl - Behaviour of a plastic fissured Eocene clay

2. PhD student:
Gitte Lyng Grønbech

3. Supervisors:
Professor Lars Bo Ibsen
Associate professor Benjaminn Nordahl Nielsen

4. List of published papers:

- Grønbech, G.L., Nielsen, B.N. and Ibsen, L.B.: "Comparison of Liquid Limit of highly plastic clay by means of Casagrande and Fall Cone Apparatus". Symposium Proceedings: 64^{th} Canadian Geotechnical Conference and the 14^{th} Pan-American Conference on Soil Mechanics and Engineering. 5^{th} Pan-American Conference on Teaching and Learning of Geotechnical Engineering. October 2^{nd} to 6^{th} 2011. Toronto, Canada. Paper no. 1100
- Grønbech, G.L., Ibsen, L.B. and Nielsen, B.N.: "Interpretation of Consolidation Test on Søvind Marl". Proceedings of the 16^{th} Nordic Geotechnical Meeting. Vol. 1 May 9^{th} to 12^{th} 2012. Copenhagen, Denmark. Pp. 85-93.
- Grønbech, G.L., Nielsen, B.N., Ibsen, L.B. and Stockmarr, P.: "Geotechnical Classification of Søvind Marl". Proceedings of the 16^{th} Nordic Geotechnical

Meeting. Vol. 1 May 9th to 12th 2012. Copenhagen, Denmark. Pp. 95-102. (Not included in thesis)

- Grønbech, G.L., Nielsen, B.N., Ibsen, L.B. and Stockmarr, P.: "Geotechnical properties of Søvind Marl - a plastic Eocene clay". Canadian Geotechnical Journal. Vol. 52. 2015
- Grønbech, G.L., Ibsen, L.B. and Nielsen, B.N.: "Preconsolidation of Søvind Marl - a highly fissured Eocene clay". Accepted with modifications for publication in Geotechnical Testing Journal. 2014
- Grønbech, G.L., Ibsen, L.B. and Nielsen, B.N.: "Earth Pressure at Rest of Søvind Marl - a highly overconsolidated Eocene clay". Submitted to Engineering Geology. 2015

5.

This thesis has been submitted for assessment in partial fulfillment of the PhD degree. The thesis is based on the submitted or published scientific papers which are listed above. Parts of the papers are used directly or indirectly in the extended summary of the thesis. As part of the assessment, co-author statements have been made available to the assessment committee and are also available at the Faculty. The thesis is not in its present form acceptable for open publication but only in limited and closed circulation as copyright may not be ensured.

Curriculum Vitae

Gitte Lyng Grønbech

E-mail: ggronbech@gmail.com
glg@civil.aau.com
Date of birth: April 28^{th}, 1983
Place of birth: Frederikshavn, Denmark
Degree: Master of Science in Civil Engineering
Alumni: Aalborg University, Denmark

Higher education

June 2010 — Master of Science in Civil Engineering
Aalborg University, Aalborg, Denmark
Thesis: *Geotechnical Testing of Søvind Marl*
- Subjects within: soil mechanics, structural dynamic, wave hydraulic, offshore constructions, material modeling and load and safety.
- Working in self-managed study groups.
- Individual self-managed project including advanced laboratory work during thesis.

June 2007 — Bachelor of Science in Civil Engineering
Aalborg University, Aalborg, Denmark
- Subjects including: General constructions, including materials, stability and loads as well as foundation, urban planning, traffic engineering, urban environment, indoor environment and construction management.
- Gained general knowledge within the field of civil engineering.
- Experience in the use of theories in student projects.

Professional Experience

December 2010 to January 2015	Ph.D. student at the Department of Civil Engineering, Aalborg University - Research within geotechnical engineering with focus on the properties and behaviour of plastic Eocene clays. - The use, development and maintenance of advanced laboratory equipment. - Distribution of knowledge through lectures at conferences and geotechnical workshops. - Teaching within geotechnical subjects. - Publishing scientific papers in conference proceedings at scientific journals.
September to December 2012	Research Assistant at the Department of Civil Engineering, Aalborg University - Assisting research done at Aalborg University - Development of testing procedure manuals. - Assisting bachelor and master students working in the geotechnical laboratory.

Teaching Experience

Master level	- Advanced Geotechnical Engineering - Geotechnics and Foundation - Supervision of 1st semester Cand. Scient. Tech. student groups
Bachelor level	Research Assistant at the Department of Civil Engineering, Aalborg University - Geology and Geotechnics - Highway Construction and Pavements - Foundation and Earth Pressure

Scientific Publications

Journal papers

- Grønbech, G.L., Nielsen, B.N., Ibsen, L.B. and Stockmarr, P.: *Geotechnical properties of Søvind Marl - a plastic Eocene clay*. Canadian Geotechnical Journal. Vol. 52. 2015
- Grønbech, G.L., Ibsen, L.B. and Nielsen, B.N.: *Preconsolidation of Søvind Marl - a highly fissured Eocene clay*. Accepted with changes in Geotechnical Testing Journal. 2015
- Grønbech, G.L., Ibsen, L.B. and Nielsen, B.N.: *Earth Pressure at Rest of Søvind Marl - a highly overconsolidated Eocene clay*. Submitted to Engineering Geology. 2015

Conference papers

- Grønbech, G.L., Nielsen, B.N. and Ibsen, L.B.: *Comparison of Liquid Limit of highly plastic clay by means of Casagrande and Fall Cone Apparatus*. Symposium Proceedings: 64th Canadian Geotechnical Conference and the 14th Pan-American Conference on Soil Mechanics and Engineering. 5th Pan-American Conference on Teaching and Learning of Geotechnical Engineering. October 2nd to 6th 2011. Toronto, Canada. Paper no. 1100
- Grønbech, G.L., Ibsen, L.B. and Nielsen, B.N.: *Interpretation of Consolidation Test on Søvind Marl*. Proceedings of the 16th Nordic Geotechnical Meeting. Vol. 1 May 9th to 12th 2012. Copenhagen, Denmark. Pp. 85-93.

Grønbech, G.L., Nielsen, B.N., Ibsen, L.B. and Stockmarr, P.: *Geotechnical Classification of Søvind Marl*. Proceedings of the 16th Nordic Geotechnical Meeting. Vol. 1 May 9th to 12th 2012. Copenhagen, Denmark. Pp. 95-102.

Technical reports

- Grønbech, G.L., *Comparison of Plasticity Index of Søvind Marl found by use of Casagrande Cup, Fall Cone apparatus and Loss on Ignition*, DCE Technical Report No. 087, Department of Civil Engineering, Aalborg University
- Grønbech, G.L., *Chloride concentration and pHs influence on the Atterberg limits of Søvind Marl*, DCE Technical Report No. 088, Department of Civil Engineering, Aalborg University
- Grønbech, G.L., *Determination of the deformation properties of Søvind Marl*, DCE Technical Report No. 089, Department of Civil Engineering, Aalborg University

Preface

The present thesis "Søvind Marl - Behaviour of a plastic fissured Eocene clay" is the result of a PhD study within the period December 2010 to January 2015 at the Department of Civil Engineering, Aalborg University, Aalborg, Denmark. The thesis is presented as a collection of peer-reviewed articles published within this period in a number of journals and conferences. The study is financed by the Faculty of Engineering and Science at Aalborg University. The funding is sincerely acknowledged.

I would like to thank my supervisor Professor Lars Bo Ibsen for providing me with the opportunity to realise this PhD study and for the guidance during my studies. I also wish to thank my co-supervisor Associate Professor Benjaminn Nordahl Nielsen for his advice and enlightening discussions and for always taking the time to guide and counsel me. Both supervisor's time and guidance is sincerely acknowledged.

During the PhD study, a large quantity of experimental tests were carried out at the Moust Jacobsen Geotechnical Laboratory at the Department of Civil Engineering, Aalborg University. I wish to thank the technical staff for their help and guidance during the laboratory work. Their help is gratefully acknowledged. I especially wish to thank Engineer Constructor Anette Næslund Pedersen for her ability to keep my spirits high in times of adversity.

I would like to thank my colleagues at the Department of Civil Engineering, Aalborg University for their enlightening discussions and support during my PhD study.

Finally, I would like to thank my family and friends for their support and everlasting encouragement during my study. In the loving memory of my father.

Aalborg, January 2015 Gitte Lyng Grønbech

Summary in English

Denmark has a large presence of fat Tertiary plastic clays, which are located just below the subsoil in a narrow band throughout the country, as well as under younger deposits several other places. These fat clays have a large content of plastic clay minerals, resulting in a significant ability to absorb large quantities of water and thereby making it highly prone to swelling and shrinking. Another distinguishing feature of these clays is their fissured structure, which has a large influence on the behaviour of the clays. The plastic clays have been known for many years, yet the scientific knowledge of their behaviour is limited. Extensive development activity is currently ongoing on locations where the subsoil consists of these plastic clays, increasing the need for a better understanding of these plastic clays.

This thesis deals with the characteristics and behaviour of the plastic Eocene clay Søvind Marl. This is in order to gain a better understanding of the plastic clay group and their geotechnical properties. Søvind Marl has an extremely high plasticity and is highly calcareous, with calcite content reaching up to 75% of the soil specimen. The structure of Søvind Marl is highly fissured, as unstructured fissures run throughout the layers. The clay samples used all originate from two locations at Aarhus Harbour where Søvind Marl is present from just below the surface to great depths.

A literature study on the influence of structure is made to gain an understanding of the influence of the structure on the clay. Both the influence of a general post-sedimentation structure and of a fissured structure are described on both compression and shearing behaviour. A general structure shows an improving effect on the compression as well as the failure behaviour. However, a fissured structure makes it difficult to determine a clear yield point of the clay, making it challenging to determine a unique preconsolidation stress level. A fissured structure severely weakens the shear strength of a clay, as the clay is prone to shearing along pre-existent fissures.

The thesis is primarily based on five papers and a monograph section, and it is divided into three parts of different subjects. Part one is the determination of the general geotechnical properties of Søvind Marl, part two concerns the stiffness of Søvind Marl and part three deals with the strength determination of Søvind Marl.

Classification and index tests are made in cooperation with the engineering company Grontmij to gain a basic understanding of Søvind Marl. The plasticity of a clay has a great influence on the behaviour of the clay. Changes in the Eurocode dedicate the fall cone as the preferred method to determine the liquid limit. This method is found to yield liquid limits much lower than those found using the Casagrande cup for limits above 200%, rendering the fall cone with limited use on highly plastic clays. The plasticity of Søvind Marl is normally in the ranges of 100% to 250% with extreme values exceeding 300%. A clear correlation is found between the plasticity and the calcite content of Søvind Marl. The part presents cone penetration tests and field vane shear tests and the results shows a change in behaviour at similar depths. A change is also found in the plasticity and calcite content at the same depth. This is all an indication of the fact that a fundamental change occurs at a depth of approximately 25 m, despite no clear difference in the mesofabric of the clay.

Incremental and continuous loading oedometer tests are made to study the stiffness of Søvind Marl. Incremental loading oedometer tests are interpreted using the presented ANACONDA method. The fissured structure of Søvind Marl has an essential influence on the determination of the preconsolidation stresses. At relative low stress levels (600 kPa to 800 kPa), an apparent preconsolidation stress level is found; preconsolidation stress levels that are inconsistent with the geological history of the clay. The tests in this thesis are performed to higher stress levels than conventional tests, as these stress levels are more similar to the expected preconsolidation. Consequently, a second apparent preconsolidation stress level is found in the range of 6300 kPa to 8900 kPa, which is more similar to the geological history with millions of years of primary and secondary consolidation, whereas the lower preconsolidation is deemed to be a result of the fissured structure. During the continuous loading oedometer tests, the horizontal pressure acting on the oedometer ring is measured, enabling the earth pressure at rest to be determined. The normally consolidated earth pressure at rest is found to be independent of any known relation to the friction angle or plasticity of the clay. Overconsolidation ratios are often used in the estimation of the overconsolidated earth pressure at rest. The clay loses its "short-term" memory and OCR must be determined based on the previous maximum stresses in the test.

Undrained triaxial tests are made to determine the undrained shear strength of Søvind Marl. The samples are found to primarily shear along pre-existent fissures, indicating that the strength of fissured clays is significantly lower than that of a similar unfissured sample. The relation between the undrained shear strength and the field vane shear strength, μ, is, on modern undrained triaxial tests, confirmed to be 0.3 while the CPT corrected cone factor, N_{kt}, was found to be 20.

Resumé på dansk

I Danmark er der en stor tilstedeværelse af plastiske ler, som er lokaliseret nær overfladen i et smalt bånd tværs igennem landet samt flere steder under yngre aflejringer. Disse fede lerarter har et højt indhold af plastiske lermineraler, som resulterer i en betydelig evne til at absorbere store mængder vand. Dette medfører, at leret er tilbøjeligt til at svelle eller svinde. Et andet særligt kendetegn for disse lerarter er den sprækkede struktur, der har en stor indflydelse på lerets opførelse. Til trods for at disse plastiske lerarter har været kendt i årtier, er den videnskabelige viden om deres opførsel begrænset. I disse år er der en stor byggeaktivitet på lokaliteter, hvor undergrunden består af disse fede lerarter. Dette øger behovet for en bedre forståelse af disse plastiske lerarter.

Denne afhandling omhandler karakteregenskab og opførsel af den plastiske Eocæne ler Søvindmergel. Søvindmergel er studeret for at få en bedre forståelse for disse plastiske lerarters geotekniske egenskaber. Søvindmergel er en ekstremt plastisk og meget kalkholdig lerart, med et kalkindhold på helt op til 75% af den samlede lerprøve. Søvindmergels struktur er meget sprækket med sprækker løbende ustruktureret igennem hele leret. De benyttede lerprøver stammer alle fra to lokaliteter på Aarhus Havn, hvor Søvindmergel er til stede fra tæt på oversladen til store dybder.

Et litteraturstudie er udført for at få en forståelse for strukturens indflydelse på leret. Indflydelsen af en general post-sedimentation samt en sprækket struktur er beskrevet både på stivheden og styrken af leret. Tilstedeværelsen af en general struktur har en forbedrende effekt på såvel stivheden samt styrken mod brud. En sprækket struktur derimod besværliggører bestemmelsen af et flydepunkt, hvilket gør det vanskeligt at bestemme en entydig forbelastningsspænding. Desuden svækker en sprækket struktur styrken af ler, da brud sker i den svageste del af leret: de eksisterende sprækker.

Denne afhandling er primært baseret på fem artikler samt et monografafsnit og er delt i tre dele, som alle omhandler forskellige emner. Første del omhandler bestemmelsen af generelle geotekniske egenskaber, anden del omhandler bestemmelse af stivhedsegenskaber og tredje del omhandler bestemmelsen af styrkeegenskaber af Søvindmergel.

Klassifikation og indeks tests er lavet i samarbejde med ingeniørfirmaet Grontmij

for at få en grundviden om Søvindmergel. Lers opførsel er stærkt afhængig af dets plasticitet. Ændringer i Eurocode stipulerer, at faldkeglen er at foretrække når flydegrænses skal bestemmes. Faldkeglen giver betydeligt mindre flydegrænser i forhold til Casagrande-skålen for flydegrænser over 200%, hvilket gør faldkeglen usikker på lerarter med meget høj plasticitet. Plasticiteten af Søvindmergel er typisk i intervallet mellem 100% og 250%, men med ekstreme værdier over 300%. Der er fundet en tydelig sammenhæng mellem plasticiteten og kalkindholdet for Søvindmergel. Resultater fra CPT og vingeforsøg er præsenteret, og en ændring i udviklingen af resultaterne blev fundet i en dybde af ca. 25 m. Også i plasticiteten og kalkindholdet af Søvindmerglen er en markant ændring observeret i samme dybde. Alt dette indikerer en væsentlig ændring i leret i denne dybde, til trods for ingen ændring var synlig i leret.

Trinvis samt kontinuerlig belastede oedometerforsøg er udført for at undersøge stivheden af Søvindmergel. Trinvis lastede oedometerforsøg blev tolket ved hjælp af den beskrevede ANACONDA-metode. Den sprækkede struktur af Søvindmergel havde en betragtelig indflydelse på bestemmelsen af forbelastningsspændingen. Tilsyneladende forbelastninger er fundet ved relativt lave spændingsniveauer (600 kPa til 800 kPa), og disse spændinger er ikke samstemmende med lerets kendte geologiske historie. Forsøgene præsenteret i denne afhandling er kørt til større spændingsniveauer end normal praksis, da disse spændingsniveauer er bedre samstemende med de forventede forbelastninger. Dermed er der fundet en anden forbelastningsspænding i størrelsesorden 6300 kPa til 8900 kPa. Denne forbelastning stemmer bedre overens med den geologiske historie med millioner af år med konsolidering og krybning, hvorimod den lave forbelastning tillæges den sprækkede struktur. Under de kontinuerlig belastede oedometerforsøg blev de horisontale spændinger målt, dermed kan hviletrykskoefficienten bestemmes. Hviletrykskoefficienten for Søvindmergel bragt i et normal konsolideret niveau er bestemt til at være uafhængig af kendte korrelation til friktionsvinkle eller plasticitet. Hviletrykskoefficienten for overkonsolideret jord bestemmes oftest ved hjælp af overkonsolideringsgraden. Det er fundet, at leret mister sin "kortidshukommelse", og OCR skal bestemmes ud fra maksimale tidligere spændinger under forsøget.

Der er udført udrænet triaksialforsøg for at bestemme den udrænet forskydningsstyrke af Søvindmergel. Prøverne bryder primært i eksisterende sprækker, hvilket er en indikation af, at den målte udrænede forskydningsstyrke af den sprækkede ler er betydeligt mindre end styrken af en lignende usprækket ler. Forholdet mellem den målte udrænet forskydningsstyrke og vingestyrken, μ, er på moderne triaksialtests blevet bekræftet til 0.3 mens den korrigerede keglefaktor fra CPT'erne, N_{kt}, er bestemt til 20.

Contents

CHAPTER 1
Introduction

The subsoil in a large part of Denmark consists of Tertiary deposits, often very fat and highly plastic clays. This thesis focuses on the behaviour of one of these clays; the extremely plastic and highly fissured Eocene clay called Søvind Marl.

Clays are characterised based on their plasticity using the Casagrande's plasticity chart (Casagrande 1932). This defines very plastic clays as a clay with a plasticity index and liquid limit above 50% and 80%. The clay content of these clays is very high, above 80%, making these clays very prone to swelling. The swelling ability of these clays characterises them as expansive clays. A plastic clay with access to water will absorb the water and bind the water to its molecular structure, the more plastic a clay is. The more water it binds. As the volume of a clay is directly related to the water content, an unloaded clay swells when it has unlimited access to water.

The expansiveness of these clays combined with seasonal variations in the natural water content can cause great problems, in particular for shallow foundations where settlement or uplift can lead to large damages of the constructions (Knudsen 1985). During foundation of constructions in Denmark, the presence of plastic Tertiary clays automatically leads to restricted foundation class according to the Danish Standard, drastically increasing the price of the project. The seasonal changes are particularly evident near plants with deep roots. Knudsen (1993) described how a forest floor had height differences of up to 12 cm from summer to winter due to subsoil consisting of expansive clays. Damages caused by deep roots in plastic clays do not fully evolve until the trees have reached their full height, usually at the age of 20 - 30 years, causing damages long after planting.

Highly plastic Tertiary clays are most often fissured, which further complicates handling of the clay. The fissures can open up during unloading resulting in easier water penetration in greater depths. The water is absorbed due to the high plasticity. This results in a softening of the soil leading to weaker strength and larger deformations. Similar expansive soils are known to cause problems all over the world. Jones and Holtz (1973) estimated that expansive clays cause more damage to constructions than any other natural hazard.

1.1 Plastic clays in Denmark

Tertiary deposits can be found in most of Denmark, except the north-eastern part of Jutland, southern Zealand/northern Lolland Falster and Bornholm. In the southern, western and central part of Jutland, the Miocene deposits are located just below the till, and on northern Zealand along with Djurs and the lowest part of northern Jutland, the Danien Limestone is located below the till. However, the plastic Eocene and Oligocene clays are located just below the till or even topsoil in a narrow band across Jutland. The band covers from Thy in north-western part of Denmark, across Mors to Skive and Randers before reaching Aarhus and following the coast to the Little Belt region. From here it covers the eastern and southern part of Funen, across the sea bed to the southern part of Falster along with Samsø and the north-western part of Zealand. This is illustrated in Figure 1.1. The five main plastic clays in Denmark are: Røsnæs Clay, Little Belt Clay and Søvind Marl, Viborg Formation and Skive Septerian clay listed after decreasing age.

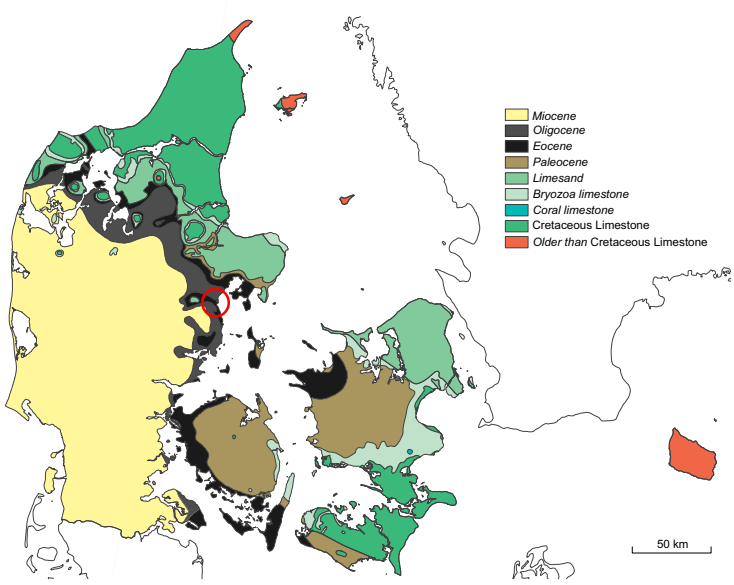

Figure 1.1 Plastic Eocene and Oligocene clays in Denmark marked by dark grey bands, ◯ marks Aarhus. Modified after Geocenter Danmark (2010b)

Eocene clays is particularly close to the ground surface in the eastern part of Jutland which includes Aarhus. The presence of plastic clays in Denmark has been known for many years, but the scientific knowledge is still limited due to the problematic and lengthy process of testing plastic clays. In the last decade, the research activity has increased significantly, all in the hope of gaining a better understanding of the behaviour of these clays. The Eocene clays are spread throughout Denmark and cover areas with

either finished, ongoing or planed extensive development activity. The high plasticity causes problems as large settlements can take place. Settlements in Eocene clay occur over long periods of time due to the low permeability and great depths. The Little Belt Bridge opened in 1935 and is founded directly on the plastic Little Belt Clay. It has to date suffered settlements of up to 0.7 m, which is still increasing. Among the most high-profile projects currently ongoing is the urban re-development of the former industrial harbour in Aarhus, which is located on great depths of Søvind Marl and the Fehmarn Belt connection between Falster in Denmark and Fehmarn in Germany; the bed of Fehmarn Belt consists of primarily Røsnæs Clay.

1.2 Location of studied Søvind Marl

The work done during this thesis has been made on Søvind Marl originating from two locations (LH and BS) at Aarhus Harbour, cf. Figure 1.2. Both locations have Søvind Marl in great depths, starting under a small layer of man-made fill laid during the construction of the original industrial harbour and a thin layer of glacial till. The boring logs from each location can be seen in Appendix F. The samples were collected in connection with the urban re-development of the two areas.

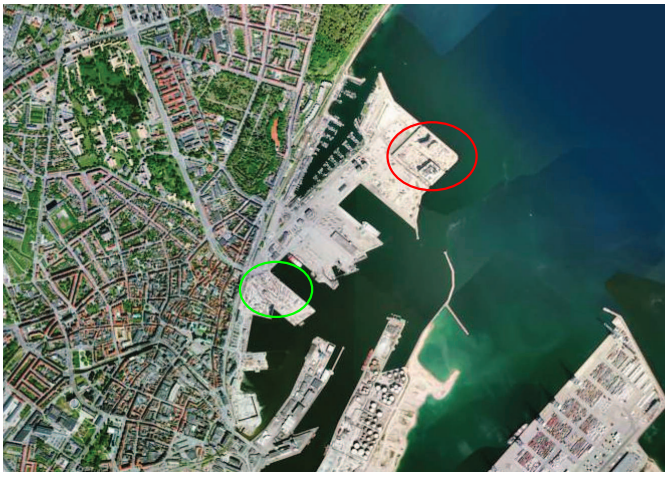

Figure 1.2 In situ location of tested Søvind Marl, ◯: LH samples and ◯: BS samples

5 borings from the LH location were used with depths ranging from 40 m to 69 m, and 5 sample tubes from the BS location were used all from the same depth of 11.5 m. All samples are remarkably similar in appearance, regardless of in situ depth. The only mesofabric difference is the colour, ranging from light grey to dark grey and olive green/brown. The difference in colour is dependent on the calcite content. BS

samples are from the younger part of the Søvind Marl Formation and has a higher lime content than LH samples, which originate from the older part of the formation. The most noteworthy physical feature of Søvind Marl is the fine net of unstructured fissures running throughout the layers.

Søvind Marl was first described by Andersen (1937), and is named after the small village of Søvind located by Horsens Fjord where the marl is visible in the now closed marl pit.

CHAPTER 2
Tertiary Geology in Denmark

The behaviour of a soil is highly dependent of the deposit geology and later history. The current Danish landscape is clearly defined by the glaciers that covered Denmark during the Quaternary period. But several places, just few meters below the surface, the soil is Tertiary or even older. Figure 2.1 presents the upper layers of soils older than Quaternary. The chapter is primarily based on Heilmann-Clausen *et al.* (1985), Larsen (1989), Heilmann-Clausen (1995) and Geocenter Danmark (2010b) with additional references in text.

65 million years ago an asteroid hit earth and drastically changed the global environment and climate; this event marks the transition between the Cretaceous period and the Tertiary period. The impact caused a few centimeter thick layer of clay containing cosmic particles to be spread across the globe. This layer can be seen at Stevn's Cliff in Denmark in the form of Fiske Clay. The Danish geology is tightly connected to that of the North Sea; however, this will not be described further.

Tertiary sediments mainly consists of limestone and fat clays which overlay the Cretaceous limestone, and are all marine deposited in the relative deep sea covering Denmark at that time. The Tertiary period is separated into two different time periods: The Palaeogene period and the Neogene period, which both are divided into different eras.

2.1 Palaeogene period

The Palaeogene period lasted from 65 million years to 23 million years ago and is divided in four eras: Danien, Paleocene, Eocene and Oligocene era. Figure 2.2 lists an outline of the most significant Danish Paleogene deposits.

2.1.1 Danien era

The first 5 million years of the Paleogene period is known as the Danien era. During the Danien era Denmark was still covered by a large ocean. The limestone sedimentation continued from the Cretaceous period as the climate had not yet changed

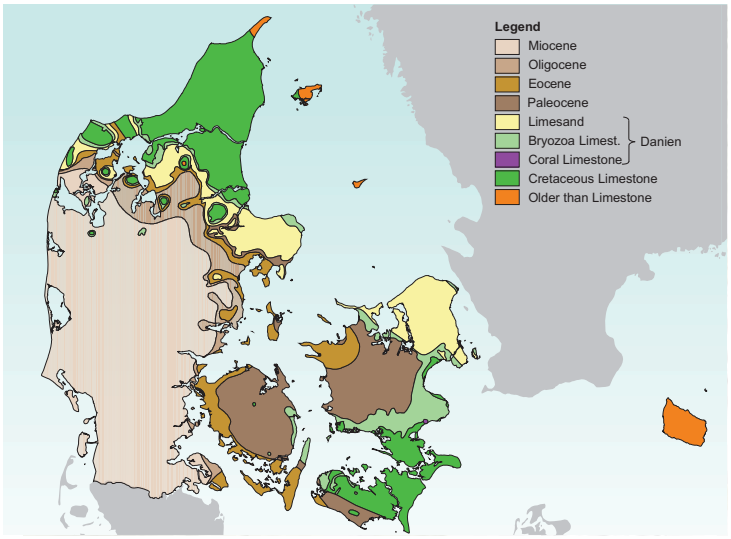

Figure 2.1 Sub-Quaternary surface of Denmark. Modified after Geocenter Danmark (2010b)

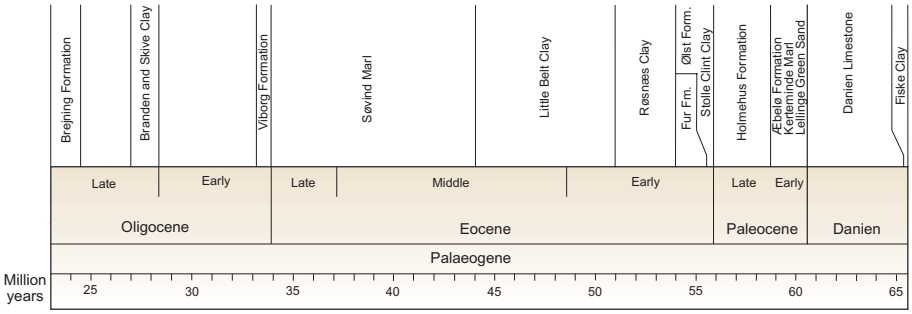

Figure 2.2 Geological time scale of the most prominent Danish Palaeogene deposits. Modified after Geocenter Danmark (2010b)

drastically. However, a small layer of Fiske Clay separates the two limestone formations. The main difference of the two limestone types is the presence of fossils in Danien limestone. The fossils originate from bryozos and corals living on the Danien ocean floor and shells from animals in the ocean. During the Danien earlier limestone formations eroded and re-sedimented in the Danien ocean; this type of limestone is known from the Copenhagen area. The depth of the Danien limestone varies greatly, with 100 m in eastern Zealand and more than 200 m in north-western Jutland (Thomsen 1995).

2.1.2 Paleocene era

As the temperature rose and the sediment type changed from limestone to fine grained clays, the Danien era were succeed by the Paleocene era. The changes was due to thermal rise of the British Isles as volcanic activity increased in the Icelandic area, creating the volcanic Thule land bridge, disconnecting the North Sea area from the warmer Tethys Ocean and Atlantic Ocean. The transit to clay sediments indicates that the main transportation method was via the rivers. The sedimentation originated from chemical weathering of the parts of Scandinavia not covered by the ocean.

In the late beginning of the Paleocene era, the land under the North Sea rose significantly, resulting in a significant erosion of the underlying limestone. This limestone was mixed with the clay sediments creating a highly calcareous clay with a high content of re-deposited limestone known as Kerteminde Marl. Through the middle and late Paleocene era the North Sea rose continuously, likely due to cooling of the subsoil as an effect of less volcanic activity at the Icelandic Hotspot. This introduced a cold and acidic environment, and sediments deposited under these circumstances belong to the Æbleø Formation, which is distinguished by being low-calcareous. In the late Paleocene era the depth of the North Sea reached up to 400 m. In this ocean, a finely grained clay was deposited; a clay rich on colour and consisting of almost only the highly plastic clay mineral smectite. This clay is Holmehus clay, which is abundant also in the current North Sea area.

2.1.3 Eocene era

At the transition time between the Paleocene and Eocene eras a massive increase in temperature occurred called the PETM (Paleocene-Eocene Thermal Maximum). PETM had a massive effect on the fauna, causing the ancestor of modern fauna to gain ground. PETM is believed to be initiated by a large increase in volcanic activity at the Islandic Hotspot, which also caused the subsoil to heat up and rise significantly. This caused parts of Denmark to be uncovered in the beginning of the Eocene era. During this early period of the Eocene era the lower part of the ocean above Denmark was deprived of oxygen and hereby bottom-dwelling animals, resulting in preservation of the initial fine layering of the non-calcareous Stolle Clint Clay, which can be found in the north and north-western parts of Jutland. The volcanic activity increased drastically after PETM, and several big volcanic eruptions took place, where Basalt ashes from the biggest spread over most of Northern and Central Europe. At the same time, continental drift opened the Atlantic Ocean between Norway and Greenland. 140 ash layers can be found in Denmark as evidences of an extensive geological activity during the Early Eocene. The sedimentation during this period was of altering layers of non-calcareous clay and ash, and can be found in the north-western part of Jutland as the Fur Formation (also known as Mo Clay), and the Ølst Formation can be found in the rest of Denmark. Organic material can be found in the Ølst formation, indicating sedimentation in salt or brackish water.

After an intense start of the Eocene era, the Icelandic Hotspot cooled leading to a land settlement and a drastic increase of water depth in the North Sea of up to 600 m to 1000 m. In this sea, almost no sediment originating from land areas was deposited in Denmark, evidence of great distances to any land area. All sediments are very fine grained plastic clays, originating from chemical weathering of volcanic materials. The deposits consist primarily of smectite, kaolinite and illit. The North Sea was still cut off from the warmer oceans to the south, causing almost non-calcareous clays to be deposited, but during the Eocene era the connection to warmer oceans was re-established resulting in calcareous clays to be deposited. Depths of more than 200 m of plastic clay were deposited during the middle and late Eocene era. These plastic Eocene clays are divided into three formations: Røsnes Clay, Little Belt Clay and Søvind Marl.

Røsnæs Clay

Røsnes Clay Formation is the oldest of the three plastic Eocene clays in Denmark, deposited in the middle of the Early Eocene era. It primarily has a reddish colour due to ferric compounds, but the colour varies from dark brown to pale grey and yellowish. Røsnæs Clay is divided into seven beds: the oldest Knudshoved member and R1 to R6. Figure 2.3 illustrates the bedding of Røsnæs Clay at Ølst and its characteristic. Few ash layers are to be found in beds R3 to R5, whereas beds R1 and R2 are glauconitic. The clay is mainly calcareous and bioturbated as an indication of a rich fauna during the time of deposit. There is trace of organic materials in only the Knudshoved member and R6. The colour, calcareous nature and lack of organic material indicates an oxygen rich deposit environment. Røsnæs Clay can be found in most of the North Sea and surrounding areas, and in most of Denmark except the north-western part of Jutland. The depth of Røsnæs Clay varies with 3 m at Ølst and up to 28 m at Boulstrup.

Little Belt Clay

Little Belt Clay Formation is located above the Røsnæs Clay Formation and is deposited in the late Early Eocene era to the middle of the Middle Eocene era. Little Belt Clay is mainly grey-greenish and non-calcareous. It is divided into six beds, L1 to L6. Figure 2.4 illustrates the bedding of Little Belt Clay at Hinge and its characteristic. Organic content is present in L1 to L4, indicating, along with the greenish colour, an oxygen deprived environment. In the upper beds of L5 and L6, the colour changes and the clay becomes slightly calcareous due to micro fossils, indicating an increase of oxygen at the ocean floor. Little Belt Clay can be found at the same location as Røsnæs Clay and has a depth of up to 100 m at the Danish-German border and 70 m at the Little Belt area.

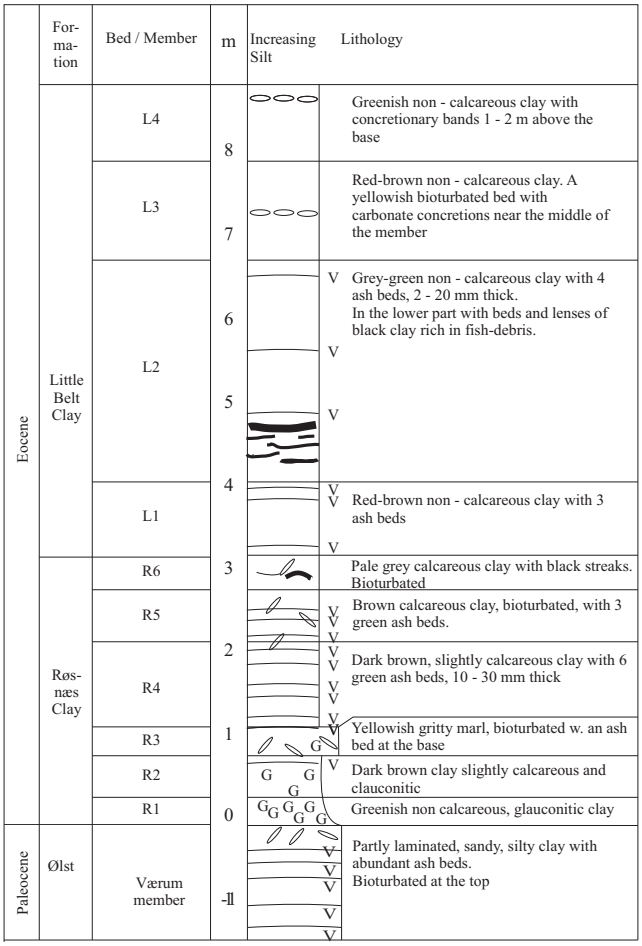

Figure 2.3 Bedding of Røsnæs Clay at Hinge. Modified after Heilmann-Clausen *et al.* (1985)

Søvind Marl

Søvind Marl Formation is located above the Little Belt Formation. Søvind Marl was deposited from the middle of the Middle Eocene era to late Eocene era, and is, thereby, the youngest of the plastic Eocene clays. Søvind Marl is mainly grey to almost white and is predominant highly calcareous with calcite ($CaCO_3$) content up to 70%, and occasionally glauconitic. The colour of the marl is highly dependent of calcite content and the less-calcareous clays can be almost black. The change in calcite content and thereby colour derives from the difference in the magnitude of coccoliths at the time of deposit due to difference in water temperature. Søvind Marl is highly bioturbated and has no clear bedding as the previous plastic Eocene clays. The presence of coccoliths enables a division of Søvind Marl into six NP zones. From the oldest Søvind Marl in

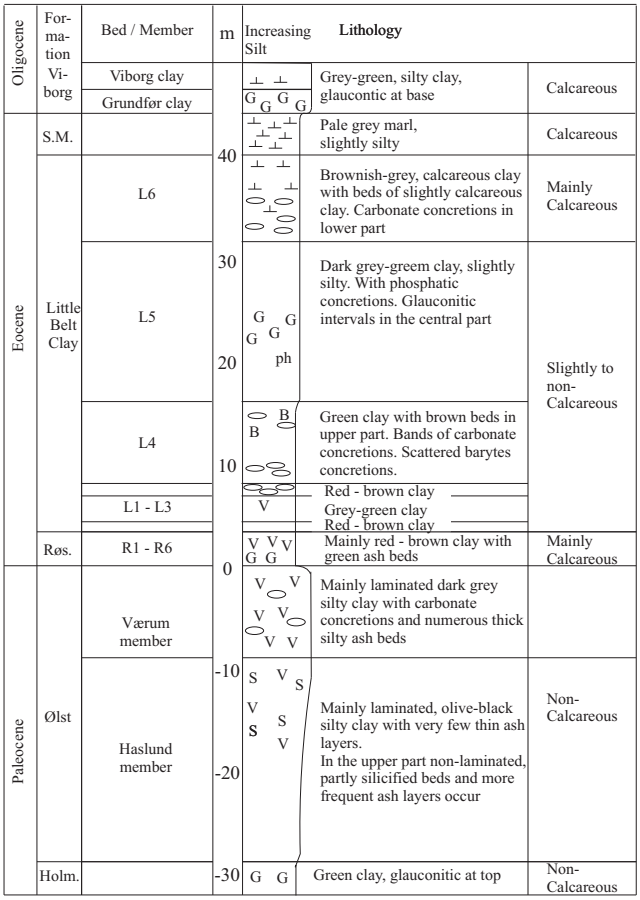

Figure 2.4 Bedding of Little Belt Clay at Ølst. Modified after Heilmann-Clausen *et al.* (1985)

NP zone 15 located just above the Little Belt Clay to the youngest in NP-zone 21 just below the Oligocene Viborg Formation. Figure 2.5 presents the NP zones and age of Søvind Marl. (Okkels and Juul 2008)

Søvind Marl is known in most of Denmark, but it is absent in the north-western part of Jutland as the remaining plastic Eocene clays. A large variation in depth of Søvind Marl can be found, with 4 m at Ølst, 60 m in Aarhus and up to 90 m at the Danish-German border.

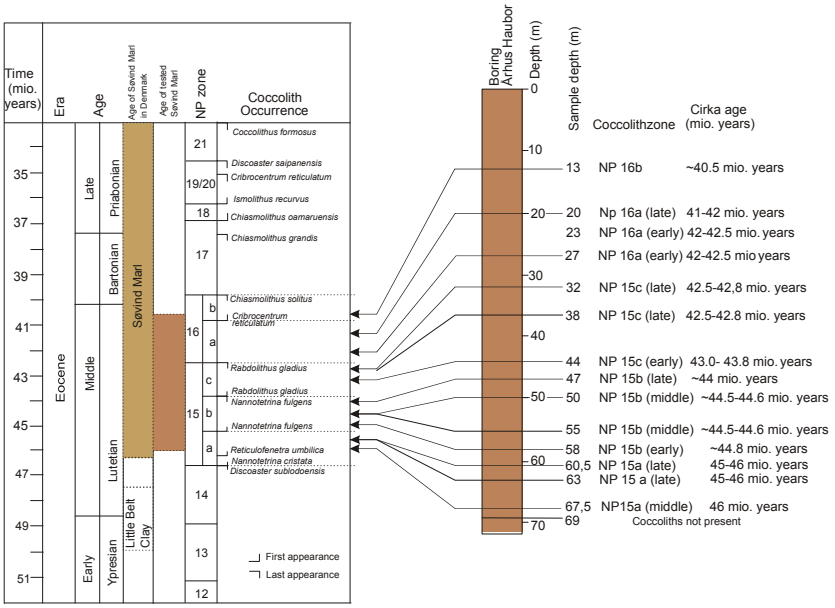

Figure 2.5 Coccoliths in Søvind Marl and age determination of Søvind Marl at Aarhus Harbour from NP zones.

2.1.4 Oligocene era

At the end of the Eocene era, the climate cooled, the ice cap formed at the Antarctica and the present climatic zones were formed. The land rose and the fine grained plastic clays deposits were succeed by thick mud and sand layers. The Viborg Formation was formed in the early Oligocene era and was gradually changing from plastic clay to also containing silt and sand materials. Due to the occasional exposure of land, most of the early Oligocene deposits eroded and are therefore not found in Denmark. The water depth increased during the late Oligocene era from where the calcareous and glauconitic Branden and Skive Clays can be found in Jutland and on Funen from the early period. The Vejle Fjord Formation is the last deposit from the Oligocene era and stretching into the Miocene era. It shows signs of land areas closing in on Denmark, as the deposits change from silty clay and clayey silt to increasing sand content.

2.2 Neogene period

The Neogene period (also known as the Later Tertiary period) lasted from 23 million years to 2.5 million years ago and covers two eras: The Miocene era and Pliocene era. No deposits from the upper Miocene era and the Pliocene era are found on land in Denmark, but they can be found in large quantities in the North Sea (Friis 1995) and (Geocenter Danmark 2010a).

The transition period between the Paleogene and Neogene periods was characterised by significant movement in the earth's crust with the formation of the Alps due to the collision between the European and African tectonic plates and the growth of the North Atlantic, causing what is now Norway and Sweden to rise. The climate was generally sub-tropical; however, a short cooling due to the buildup of ice caps on Antarctica caused the ocean depth to drop, leading to a clear and distinct difference in deposits from the two periods (Rasmussen *et al.* 2010).

2.2.1 Miocene and Pliocene era

Most of Denmark was covered by the North Sea in the Early Miocene era. Miocene deposits consist of alternating layers of sand deposited in river deltas and clay deposited at marine environments. As the mountains in Norway and Sweden eroded, particles from clay size to gravel size were transported south to the North Sea by rivers. Sand and gravel was deposited in the rivers, whereas organic rich clay was deposited at the river plains between the rivers. This caused the coast line to travel south and land to form where Denmark is located today (Geocenter Danmark 2010a). Miocene deposits can, therefore, only be found in central, western and south-western Jutland (Larsen 1989). The organic rich clay had a consistency of organic silt, which has since been lost during consolidation during the Quaternary period (Steenfelt *et al.* 2014). Significant characteristics of Miocene clay are the presence of brown coal, and in some places, light shimmering particles, giving these clays the nickname "Shimmer clay" ("Glimmerler" in Danish) (Steenfelt *et al.* 2014).

During the Middle Miocene era, the climate changed and Denmark was flooded as the North Sea area started to settle. This resulted in sedimentation of the fine grained glauconitic Ørnhøj Formation in the south - south-western part of Denmark. The North Sea continued to settle in the Late Miocene era causing the water depth to rise over Denmark and increasing the sedimentation of clay particles. Denmark was still flooded at the beginning of the Pliocene era. However, two million years to three million years ago as the climate cooled, Scandinavia started to rise, uncovering Denmark. No deposits from this period are found in Denmark (Geocenter Danmark 2010a)l possibly due to the erosion in the Quaternary period which also remoulded and altered the top layers of the remaining Tertiary deposits.

The Miocene deposits are divided into two groups: the Ribe Group consists of Early Miocene deposits of shallow water marine clay and river delta sand and the Måde Group from the Middle and Late Miocene era of primarily sands (Steenfelt *et al.* 2014).

2.3 The Quaternary period

The climate cooled during the last of the Tertiary period resulting in increasing ice caps at the poles, and snow and ice started to cover the high mountains in the Alps and Scandinavia. The beginning of the Quaternary period is marked by the expansion of the ice covered areas. Denmark has been covered by seven known Glacial periods, from which deposits from three are found in Denmark, as well as from three Inter Glacial periods (Larsen 1989). Glacial periods arise due to drastic climate changes, causing the temperature to drop, resulting in decreasing water depths causing Denmark to be connected to England by land (Geocenter Danmark 2005). During the Glacial periods, large glaciers covered Denmark, eroding large quantities of older deposits into the area now covered by the North Sea (Geocenter Danmark 2010a).

Deposits from the Glacial periods consist of till and melt water sediments. Till consists of particles from clay size to boulder size collected by the glacier and deposited under or where the glacier stopped. This is evident in several places in Denmark like Ølst in east Jutland where the glaciers have deformed the subjacent Miocene deposits and the till includes fat Miocene clay and at Odsherred in north-western Zealand. Melt water deposits consist of finely sorted particles carried by the melt water from the glacier. Melt water landscape are mainly found in central, western and south-western Jutland, as it was not covered by glaciers during the last Glacial period (Weichsel Glacial) (Larsen 1989).

2.4 The geology's influence on Søvind Marl

Søvind Marl is the last of the Eocene deposits and have therefore periodically been covered by younger deposits. The Søvind Marl samples analysed in this thesis originated from in the western part of Jutland, as described in section 1.2. Søvind Marl deposits at this location were over a period of about 20 million years covered by up to 1 km Oligocene and Miocene deposits (Geocenter Danmark 2010b), resulting in a substantial consolidation of the clay. As the overlaying layers eroded during the Quaternary period the Søvind Marl was unloaded; allowing it to swell. This swelling resulted in extensive tearing of the clay leading to a large presence of fissures and slickensides. During the Quaternary period at least seven ice ages and the associated glaciers covered the Søvind Marl location, resulting in further loading and unloading of the clay. Quaternary till deposits lies directly above Søvind Marl deposits at Aarhus Harbour and contains traces of Søvind Marl, while the upper most layers of Søvind Marl show clear signs of being disturbed during glacial thrusts.

CHAPTER 3
Influence of structure

The behaviour of a soil is highly dependent on the initial structure of the matrix (Amorosi and Rampello 1998). The structure is as important as the initial void ratio and the stress history when determining the behaviour of a clay (Leroueil and Vaughan 1990). The structure is defined as the combination of the fabric (e.g. mineralogy (microstructur), deposit history and fissures (macrostructure)) and the bonding (inter-particle forces, attraction between neighboring particles) (Lambe and Whitman 1969). Cotecchia and Chandler (2000) defined two different types of structure: 'Sedimentation structure' and 'Post-sedimentation structure'. Sedimentation structure is present in only normally consolidated soils and is a result of the sedimentation process and following an one-dimensional consolidation due to overlaying deposits. A normally consolidated reconstituted clay will have a sedimentation structure. Two clays with the same mineralogy do not necessarily have the same structure due to the difference in deposit history (as illustrated in Figure 3.1(a)). A post-sedimentation structure develops when a geological process following the one-dimensional consolidation intervenes with the sedimentation structure, such processes could be erosion of upper layers, unloading, secondary consolidation and general diagenesis. The natural structure of a clay collapses during high pressure consolidation (Banks *et al.* (1975), Leroueil and Vaughan (1990), Amorosi and Rampello (1998)). Leroueil and Vaughan (1990), later supported by Coop *et al.* (1995) and Saihi *et al.* (2002), showed that the presence of structure generally increases the stiffness and strength of a soil; however a fissured structure is an exceptions to this conclusion as presented later.

By comparing the location of the compression curve for a natural clay to the corresponding reconstituted compression line or intrinsic compression line (ICL) of a clay, the influence of the structure on the compression behaviour can be identified (Gasparre and Coop 2008). Burland *et al.* (1996) and Cotecchia and Chandler (2000) among others demonstrated the influence of the structure of a clay on the compression curve. Figure 3.1 demonstrated the influence using $e - \log(\sigma'_v)$ plane from Terzaghi (1941) - asterisk (*) denotes reconstituted properties as described by Burland (1990).

Figure 3.1(a) demonstrates the influence of the deposit history, which shows a normally consolidated natural clay and a reconstituted clay with identical mineralogy. A clay with a post-sedimentation structure arrived solely due to geological unloading (e.g. erosion of upper layers or rise in water table) will divert from clays with

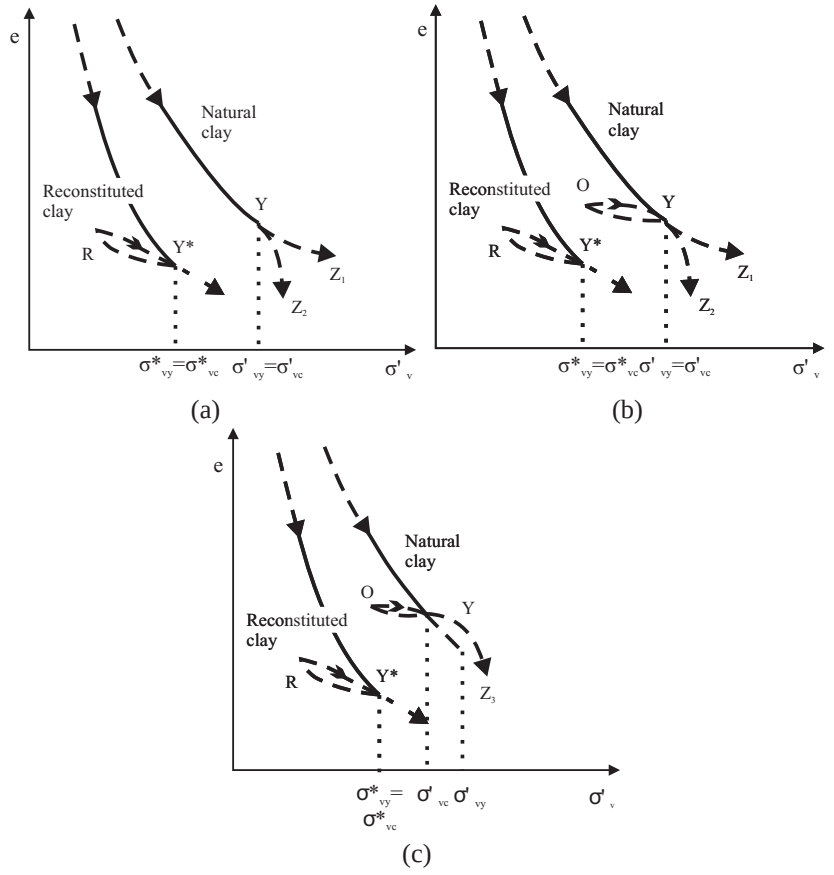

Figure 3.1 One-dimensional compression line. (a) Normally consolidated with a sedimentation structure, (b) simply overconsolidated and (c) overconsolidated with a post-sedimentation structure at gross yield. Drawn after Cotecchia and Chandler (2000).

a post-sedimentation structure due to other factors. Figure 3.1(b) shows that a clay with a post-sedimentation structure due to geological unloading will experience gross yield as it approaches the preconsolidation stresses, σ'_{pc}, during reloading, and return to the compression line of its sedimentation structure when reloaded past the preconsolidation stresses. The gross yield stresses, σ'_y, will as such coincide with the preconsolidation stresses ($\sigma'_y = \sigma'_{pc}$). The loading rate of the clays is rapid in laboratory testing compared to a natural loading rate. This is evident in the compression line in Figure 3.1(a) and (b) as a rapid loading rate will follow the $Y - Z_2$ path whereas a natural low loading rate will follow the $Y - Z_1$ path. An overconsolidated clay with a post-sedimentation structure due to factors other than geological unloading will experience a gross yield past the yield point of a simple overconsolidated clay, c.f. Figure 3.1(c). Also, the compression line will not necessarily aline with the sedimentation

compression line but rather follow the $Y - Z_3$ path shown in Figure 3.1(c). The behaviour should therefore be distinguished between a pre and post gross yield behaviour. This behaviour is also noted in Leroueil and Vanghan (1990), Amorosi and Rampello (1998) and Cotecchia and Chandler (1998). According to Burland (1990) and Cotecchia and Chandler (2000) and (1997), the gross yield stress of a strongly overconsolidated clay may be unrelated to the stress history as it is affected by factors such as secondary consolidation. The gross yield stresses are as a result higher than the preconsolidation stresses due to geological unloading ($\sigma'_y > \sigma'_{pc}$). The in situ state of a natural clay can as such be described using the yield stress ration (YSR), equation 3.1, as oppose to the overconsolidation ratio, OCR, equation 3.2, (Gasparre and Coop 2008).

$$YSR = \frac{\sigma'_y}{\sigma'_0} \tag{3.1}$$

$$OCR = \frac{\sigma'_{pc}}{\sigma'_0} \tag{3.2}$$

This is based on the assumption that the preconsolidation stresses originates solely from geological unloading $YSR > OCR$. However, if the effect of secondary consolidation, diagenesis and similar is assumed to be included in the preconsolidation stresses $YSR = OCR$. This assumption is made in the remaining of this thesis and the included papers.

A normal assumption is that the shear strength parameters of a soil are not affected by the initial microstructure at large deformations. However, Saihi *et al.* (2002) showed that the peak strength parameter located above the yield curve for destructured clay is highly dependent by the initial microstructure. Leroueil and Vaughan (1990) and Burland *et al.* (1996) tested and compared the strength in the in situ range of several different soils in both intact and destructured/remoulded state. They found that the general presence of structure in a soil, whether soft or stiff, enlarges the boundary state and results in increasing strengths, cf. Figure 3.2 and Figure 3.3. Jovičić *et al.* (2006) also showed this on a stiff North Sea clay at very high stress levels by, c.f. Figure 3.4.

Burland (1990) introduced the void index, I_v, in order to normalise the compression curves and, thus, compare the compression curve of a natural soil to its reconstituted counterpart. This allows for better determination of the influence of a post-sedimentation structure, e.g. fissures. However, it is not possible to distinguish between the different post-sedimentation elements, e.g. secondary consolidation or geological unloading.

$$I_v = \frac{e - e^*_{100}}{e^*_{100} - e^*_{1000}} = \frac{e - e^*_{100}}{C^*_c} \tag{3.3}$$

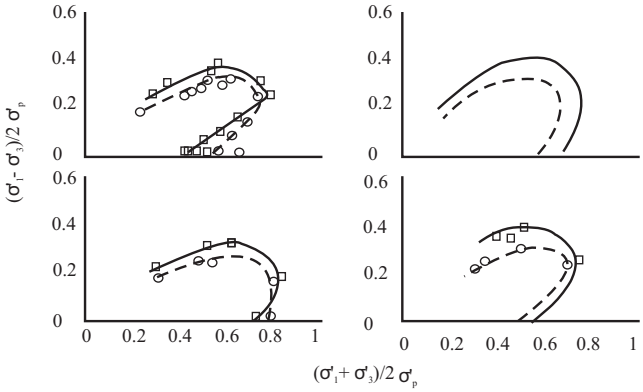

Figure 3.2 Yield curves for intact and destructured soft clays. □ and —: Intact and ○ and - - -: Destructured. Drawn after Leroueil and Vaughan (1990).

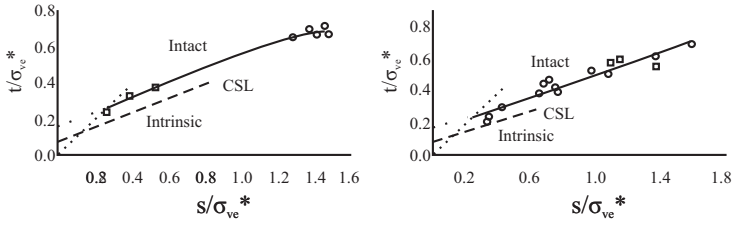

Figure 3.3 Comparison of intact and instrinsic Hvorslev strength envelops for different stiff clays, □: Drained and ○: Undrained. Drawn after Burland *et al.* (1996)

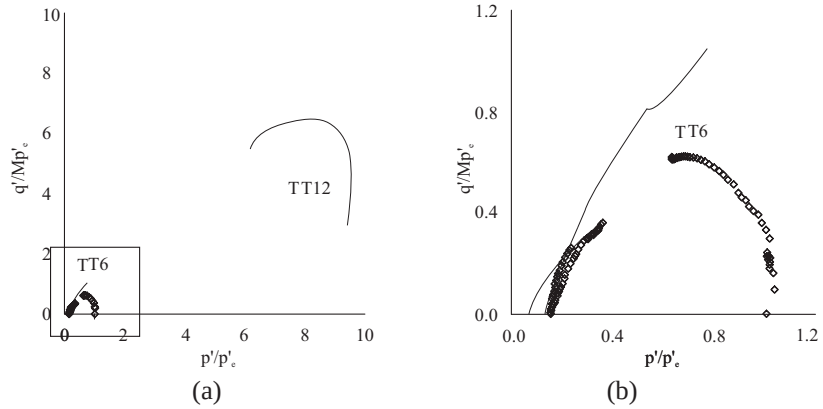

Figure 3.4 Normalised shearing data intact (–) and reconstituted (◊) stiff North Sea clay, framed part in (a) is enlarged in (b). Modified after Jovičić *et al.* (2006).

3.1 Influence of a fissured structure on stiffness

Bishop *et al.* (1965) determined that the fissured structure of London Clay had a significant influence on the behaviour. They felt that the effect of the fissures could not be determined based solely on the laboratory tests. This was due to the small size of the samples needed to enable full drainage of excess pore pressure during drained testing (e.g. oedometer tests). Bishop et. al (1965) stated that weak zones (fissures) would interfere with the small size of the sample and lead to complete separation of the sample, thus only allowing intact unfissured samples to be tested. They found that some of these "intact" samples would fail at stresses well below stresses of similar samples from same depth, concluding that a fine net of fissured was present in these samples, but with sufficient adhesion to enable preparation of fissured samples.

Gasparre and Coop (2008) quantified the effect of the structure of London Clay on the compressibility. The structure of London Clay is highly similar to that of Søvind Marl; with similar deposit environment and a highly fissured matrix. A significant difference is a notably higher plasticity of Søvind Marl. The tests by Gasparre and Coop (2008) were made on both natural intact and reconstituted samples in a conventional incremental loading oedometer apparatus. Figure 3.5 shows the compression curves for some of the samples.

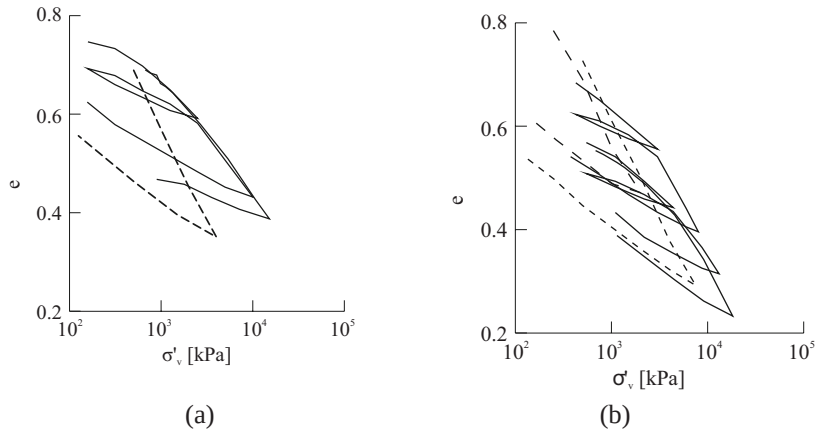

Figure 3.5 Compression curves for natural (–) and reconstituted (- -) London Clay samples. (a) Higher strata samples and (b) lower strata samples. Modified after Gasparre and Coop (2008).

The compression lines for all samples are fairly similar but dependent of the depth, and they cross all the reconstituted compression lines, indicating that the natural samples yield at a higher stress level than the reconstituted samples as a result of the natural structure. However, for the samples located at higher strata, the slope of the compression line does not yet follow the corresponding intrinsic curve. This indicates that the yield process is not yet completed regardless of the high stresses used in the

tests. For all samples, the yield process is slow and gradual, and the identification of a clear yield point is difficult. The increasing gradient of the swelling line as the stresses increase is clear evidence of the breakdown of the natural structure. To get a better understanding of influence of the structure, Burland's void ration (equation 3.3) is used in Figure 3.6. The influence of the structure is seen to lessen with increasing depth for London Clay. Cotecchia and Chandler (2000) found similar behaviour for other similar clays, cf. Figure 3.7. Bishop *et al.* (1965) found that the spacing between the fissures widens with depth (this is also noted by Skempton et. al (1969) and Chandler and Apted (1988)), indicating the fissured structure has a large influence of the stiffness of the clay.

To determine the gross yield stresses (preconsolidation stresses), Gasparre and Coop (2008) used the approach of Casagrande with the assumption that the samples would reach the compression line for the normally consolidated clay after exceeding the yield stresses. Figure 3.8 shows an example of the determination of the gross yield stresses.

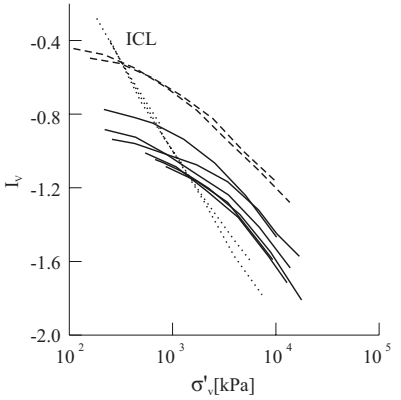

Figure 3.6 Void index normalisation of the compression curves of intact London Clay samples. · · ·: ICL, - - -: Upper strata samples, —: Lower strata samples. Modified after Gasparre and Coop (2008).

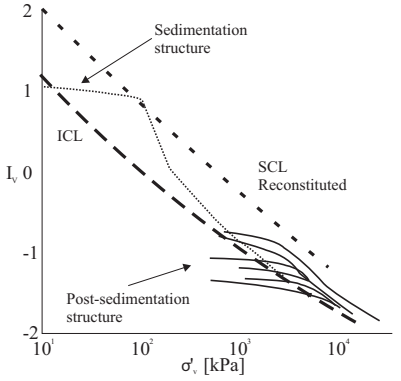

Figure 3.7 Void index normalisation of the compression curves of various intact samples with post-sedimentation structure and one sedimentation structure. Drawn after Cotecchia and Chandler (2000).

Gasparre and Coop (2008) believe that the gross yield stresses from Casagrande's method (σ'_{yl}) are a lower limit of the yield stresses. They determine the upper limit of the yield stresses (σ'_{yu}) to be the stresses occurring at the maximum rate of change in volumetric strains. A lower and upper limit of the yield stresses can be found for all London Clay samples with up to a factor of three in difference. The existence of the two values is a result of the highly fissured structure. Gasperre *et al.* (2008) also observed the presence of two yield stresses of London Clay using a hollow cylinder apparatus (HCA).

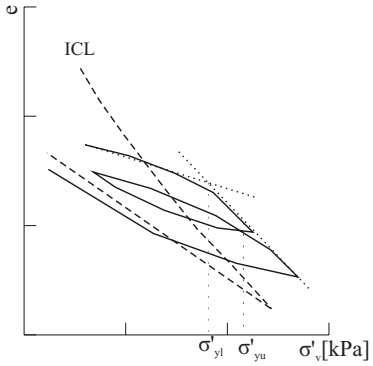

Figure 3.8 Construction for identification of the gross yield stresses and the gradient of the swelling lines. Modified after Gasparre and Coop (2008).

3.2 Influence of a fissured structure on shear strength

The shearing ability of clay is highly affected for a fissured structure. By comparing field shear test and undrained shear tests, Christensen and Hansen (1959) showed that due to the fissured nature of Skive Septarian Clay only one third of the in situ vane shear strength, C_{fv} could be used as the undrained shear strength, S_u, in relation to bearing capacity as illustrated in Figure 3.9.

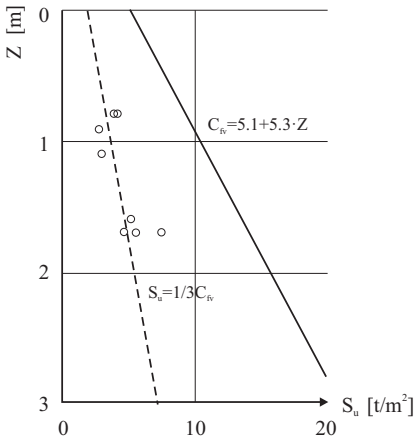

Figure 3.9 Mean value of undrained ("apparent") shear strength. ○: Measured S_u Drawn after Christensen and Hansen (1959).

Failure tends to occur at the weakest point in a clay, which for fissured clays is the

pre-existent fissures. This is shown in Figure 3.10 for a London Clay sample (Gasparre *et al.* 2008). Gasparre *et al.* (2008) compared the peak shear strength of samples of London Clay with and without pre-existent fissures. Figure 3.11 presents the peak shear strength envelops (excluding samples with pre-existent fissures) in normalised stresses. The effect of the fissures is clearly seen as all fissured samples have strengths well below the peak intact and even intrinsic, envelope. Vitone *et al.* (2013) found similar behaviour on fissured bentonite clay.

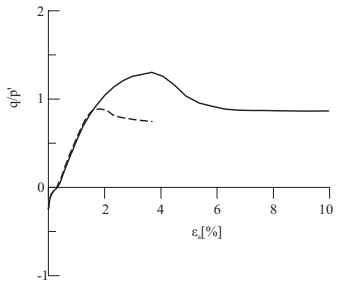

Figure 3.10 Typical stress-strain curve for undrained shearing in compression for a London Clay sample. Modified after Gasparre *et al.* (2008).

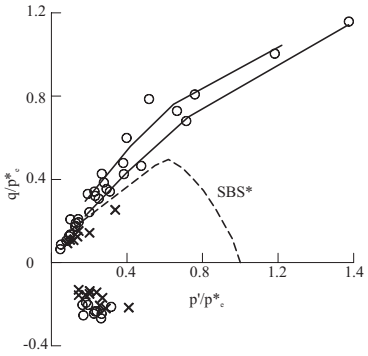

Figure 3.11 Peak states for London Clay samples in normalised stresses. ○: Intact samples, ×: Pre-existing fissurs, —: Intact boundary surface, - - - :SBS^* is the intrinsic State Boundary Surface. Modified after Gasparre *et al.* (2008).

Un-fissured London Clay samples were found to have strength well beyond the intrinsic strength, supporting the Leroueil and Vaughan (1990) statement that structure increases the strength of a clay. However, the relative weak strength of the fissured samples demonstrates that not all structure contributes to an increase of strength, as a fissured structure causes the strength to be located well below the intrinsic state boundary surface.

CHAPTER 4
Aim of thesis and research project

As described in section 1.1 in recent years large and prestigious developments have taken place on locations where the subsoil consists of highly fissure plastic clays. In order to optimise the use of the soil a much wider and specialised knowledge is needed in this area. This knowledge must be used to prevent devastating deformations and possible failure of the soil while minimising the construction cost. A key tool to understanding the behaviour of a soil is field and laboratory tests, which leads to a basic knowledge that can be used in relation to similar soils later on. The present project focuses on knowledge gained through extensive laboratory work.

4.1 Overall aim

The overall aim of the project is to improve the knowledge of Søvind Marl and, in secondary extension, other similar tertiary fissured clays. By improving the knowledge, the goal is to better estimate the behaviour of these soils and thus further optimise construction projects on these locations.

4.1.1 Specific aims

The PhD study includes three specific aims. The specific aims are to:

1. Gain a comprehensive understanding of the fundamental geotechnical properties of Søvind Marl and examine the applicability of the testing methods on Søvind Marl.
2. Analyse the stiffness of Søvind Marl and clarify the influence of the fissured matrix.
3. Study the strength parameters of Søvind Marl and determine the influences of the fissured matrix.

Aim one

Prior to advanced testing and construction on sites, it is of utmost importance to know the subsoil and its geotechnical properties. The geotechnical properties gives an indication of possible challenges when dealing with the soil. Often the geotechnical properties are also used to estimate advanced properties in order to minimise the need for more advanced tests. Development of new test methods is often made regarding soils with standard properties without consideration of the usability on soils with more extreme properties.

Aim two

A key geotechnical tool is the determination of a soil though oedometer testing and hereby determination of key parameters such as preconsolidation stresses, stiffness parameters and earth pressure at rest. However, all correlations and interpretation methods are developed on unfissured, often soft, soils with geotechnical properties in a particular range. The objective of this aim is to clarify the use of existent methods on Søvind Marl, and determine how the soil behaves during one-dimensional loading and identify the influence of the fissured matrix.

Aim three

Estimation of the strength parameters of a soil is a crucial requirement, and several different methods can be used. The most common methods are the use of triaxial tests in the laboratory and Cone Penetration Tests and in situ Vane shear tests in the field. However, the strength parameters of a soil are also affected by the matrix, and limited knowledge and prior tests are the base for current methods. The objective of this aim is to clarify the strength parameters of Søvind Marl and disclose the influence of the fissured matrix.

4.2 Research project

In order to reach the aim of the study, the research conducted is divided into three parts, all linking to the three specific aims listed in section 4.1.1. The research parts are:

- Part 1 - Geotechnical classification

  The part deals with the geotechnical classification of Søvind Marl and consists of two papers: Paper 1 and Paper 2. These papers are meant to give an insight into and basic knowledge of Søvind Marl.

- Part 2 - Stiffness parameters

  The part concerns the stiffness of Søvind Marl and is made up of three papers: Paper 3, Paper 4 and Paper 5. These papers deal with oedometer tests conducted on Søvind Marl. They clarify the interpretation methods used and the preconsolidation stresses as well as the earth pressure at rest. This part comprises the main part of the focus of the research.

- Part 3 - Strength parameters

  This part describes the determination of the strength parameters of Søvind Marl, and due to time restriction, this is made up as a monograph. It focuses on triaxial tests made in order to determine the undrained strength of Søvind Marl, as well as correlations between strength parameters found in the field (CPT and Shear Vane tests) and in the laboratory so as to illuminate the influence of the fissured structure on the measured strength parameters.

The following chapters (Chapter 5 to Chapter 7) each concerns a separate part of the research project and consists of a description of the experimental programme used in the research part, background information, summaries of the included papers (not part 3), main conclusions and any additional information. The papers are included in the Appendix with a specific reference in each summary. Figure 4.1 shows an graphical overview of the research project.

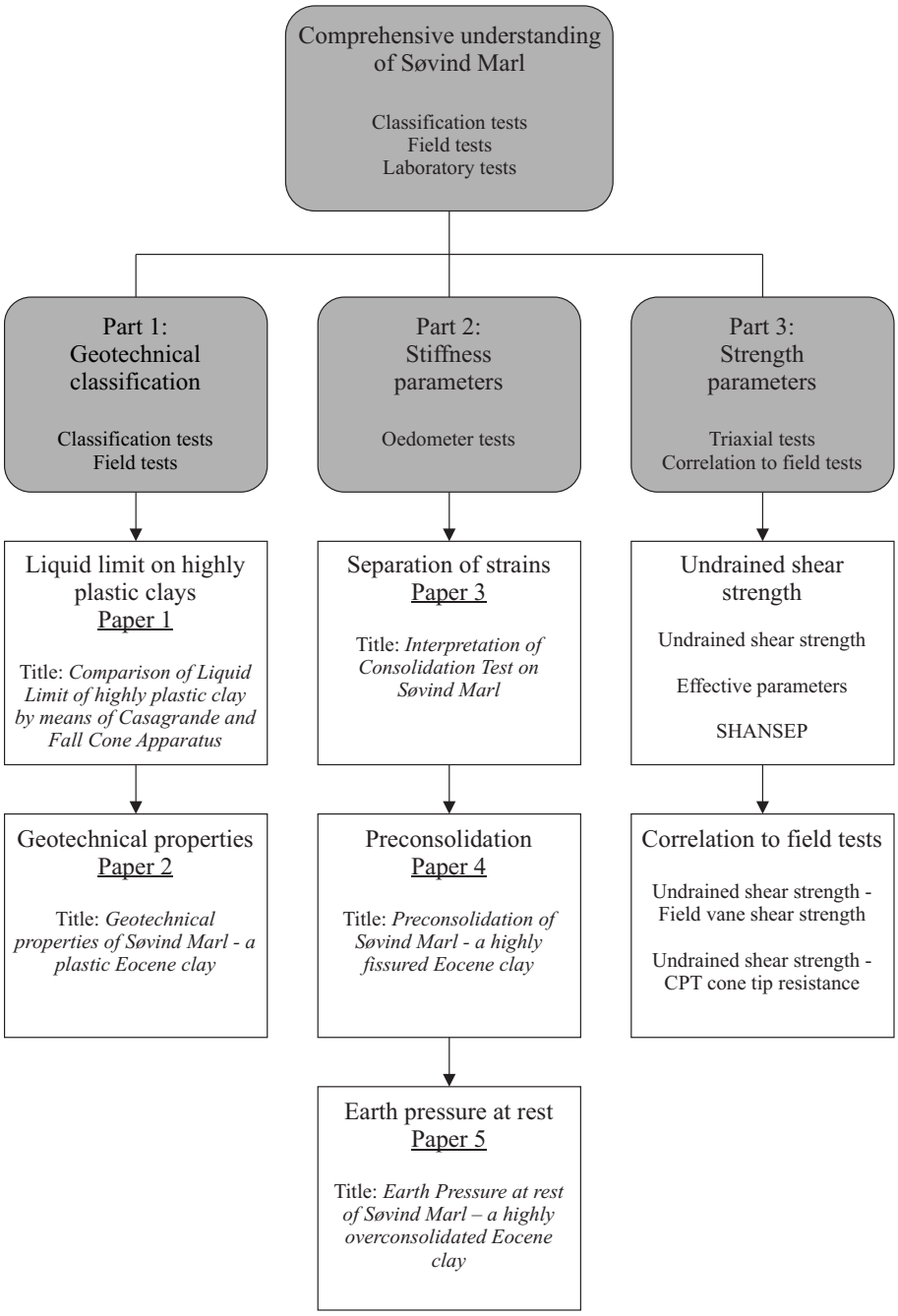

Figure 4.1 Overview of the research project and included papers.

CHAPTER 5
Part 1 - Geotechnical classification

This part concerns the geotechnical classification of Søvind Marl. The knowledge of the characteristics and properties of Søvind Marl is very limited, making Søvind Marl a "new" material despite its very old age. In order to get a comprehensive understanding of a material, basic knowledge of the geotechnical properties and indices is needed. Part 1 contains a description of the experimental programme and a summary of two papers: one regarding the test methods used in the determination of liquid limit of Søvind Marl and the range hereof (Paper 1), and one regarding the general geotechnical classification and properties of Søvind Marl (Paper 2). Figure 5.1 illustrates the overview of Part 1.

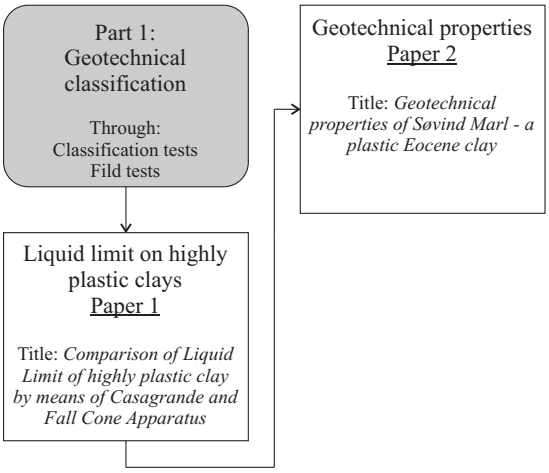

Figure 5.1 Overview of part 1.

5.1 Experimental programme

The experimental programme describes the preparation and tests which lies ahead of the papers. The tests were made on disturbed samples from several different depths; all from the same five downwards boreholes. The samples were collected and stored in sealed bags at a temperature of 8 °C until the time of testing.

5.1.1 Paper 1

The tests were performed on 33 samples from the same downwards borehole, 13 of which only the liquid limit was determined and 20 where both the liquid and plastic limit were found. The samples were all found to be homogenous in appearance with no visible differences except colour. Tests on the same sample was made simultaneously on Casagrande cup and fall cone.

Work process

1. Homogenising of the total sample as shown in Figure 5.2 to Figure 5.4
2. Removal of subsample for determination of plastic limit
3. Determination of numbers of strokes in Casagrande cup
   - Determination of water content in partial sample
4. Determination of numbers of fall depth in fall cone
   - Determination of water content in partial sample
5. Water added to sample and homogenising
6. Waiting 15 min and starting from point 3 until sample is clearly liquid
7. Determination of plastic limit on subsample

5.1.2 Paper 2

The tests were performed at Aalborg University (AAU) or the engineering company Grontmij|Carl Bro (now Grontmij). Three test types were made: Field, Index and classification and oedometer tests.

Figure 5.2 Grating the clay to maximise the surface.

Figure 5.3 Pugging the clay through a 0.42 sieve.

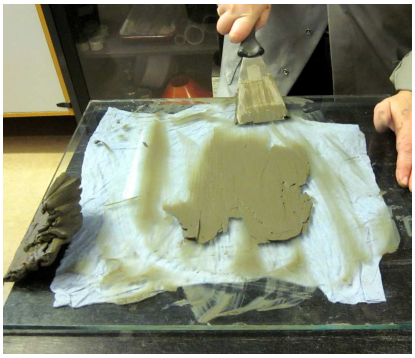

Figure 5.4 Spackling the clay until fully homogenised.

Field tests

- Cone Penetration Test (CPT)
- In situ shear vane test

Index and classification

- Mineral composition
- Natural water content
- Liquid and plastic limits
- Calcite composition
- pH of pore water
- Chloride (cl^-) content of pore water

Oedometer test

- Chapter 6 describes the experimental programme for oedometer tests.

In addition to the results presented in Paper 2, the following classification tests were found on five BS and two LH samples: natural water content, liquid and plastic limit, relative density, grain size distribution and pH and Cl^- of the pore water. The results of these tests are listed in appendix G.

5.2 Paper 1

Title:
Comparison of Liquid Limit of highly plastic clay by means of Casagrande and Fall Cone Apparatus

Authors:
Gitte Lyng Grønbech, Benjaminn Nordahl Nielsen and Lars Bo Ibsen

Published in:
Symposium Proceedings: 64th Canadian Geotechnical Conference and the 14th Pan-American Conference on Soil Mechanics and Engineering. 5th Pan-American Conference on Teaching and Learning of Geotechnical Engineering. October 2nd to 6th, 2011. Toronto, Canada.

Year of publication:
2011

Background:
The Atterberg limits are an essential geotechnical tool in the assessment of properties of a clay. Traditionally, these correlations are made with liquid limits found using the Casagrande cup. Resent changes in the standard states that it should be preferred to determine the liquid limit using the fall cone over the Casagrande cup.

"The fall-cone method is the preferred method of determining the liquid limit of a soil"
(DS 2004b)

A fine correlation between the results of the two results have been established for clays of plasticities below 100%. However, the correlation is not established for clays with very high liquid limits of more than 100%, like Søvind Marl. The aim of this paper is to document whether such a correlation exists for Søvind Marl.

Summary:
Atterberg limits play an important role in the assessment of a clay and in the estimation of its properties. Therefore, an accurate determination is of high importance. The Atterberg limits consists of the liquid limit and the plastic limit, where the plasticity index is defined as the difference between the two. Traditionally the liquid limit is determined using the Casagrande cup, which was developed by Arthur Casagrande in 1932 (Casagrande 1932). This method is highly dependent on the user of the cup, which can result in some uncertainties concerning the reproducibility and accuracy of the results. Wroth and Wood (1978) found that the liquid limit of a clay could be found using the fall cone apparatus; a method that eliminates some of the uncertainties associated with the Casagrande cup. Wasti (1987) found a near linear correlation between the liquid limit of clays found using the two methods in the range between 27% and 110%. However, this range does not nearly cover the plasticity of Søvind

Marl, which has liquid limits beyond 350%.
The two methods used, Casagrande cup and fall cone, are described as well as the homogenisation process. The homogenisation process was found to be of utmost importance, as an incomplete homogenisation would yield lower water content. Tests were made with increasing water content. The high plasticity of Søvind Marl resulted in a high absorption time. Tests done immediately after increasing the water content did not result in a noticeable change in the number of strokes/fall depth, whereas tests done 15 min after the increase of water content showed a change in strokes/fall depth. Tests used for the comparison are all done 15 min after increasing the water content.
The comparison of the two test methods showed a fine correlation for liquid limits in the range of 85% to 200%. However, for a liquid limit above 200%, the fall cone yield significantly lower liquid limits compared to the Casagrande cup (Figure 5.5.a). Since the correlation is weak at best, the method used to determine the liquid limit should be stated for Søvind Marl and similar highly plastic clays.
The plasticity of Søvind Marl is significantly higher than the plasticity cover by the standard Casagrande Chart (I_P up to 60% and w_L up to 100%), so an expansion of the plasticity chart is proposed in order to include the plasticity of Søvind Marl and other highly plastic clays. This expansion includes two new USC categories; Super High Plasticity Clay (CS) and Extremely High Plasticity Clay (CE), with liquid limits in the ranges of 100% to 200% and 200% to 350%, respectively. Figure 5.5.b shows the updated plasticity chart.
The paper can be found in Appendix A.

Main Points:

- The liquid limit found using Casagrande cup and the fall cone does not correlate after a liquid limit of 200%
- Homogenisation is an important process with a significant influence on the results, cf. section 5.2
- An expansion of Casagrande's plasticity chart was suggested to include the plasticity of Søvind Marl and two new USC categories were introduced
  - Super high plasticity clay (CS) with liquid limits from 100% to 200%
  - Extremely high plasticity clay (CE) liquid limits from 200% to 350%

Homogenisation

The homogenisation process of Søvind Marl was proven to be a very time-consuming process and the importance of which easily could be underrated. The thoroughness during the homogenisation process proved to have a large influence on the result of the tests. During initial testing, tests with different levels of homogenisation were made. Even small lumps of unhomogenised clay had an influence on the result, as the liquid limit decreased with lower degrees of homogenisation. Unhomogenised lumps

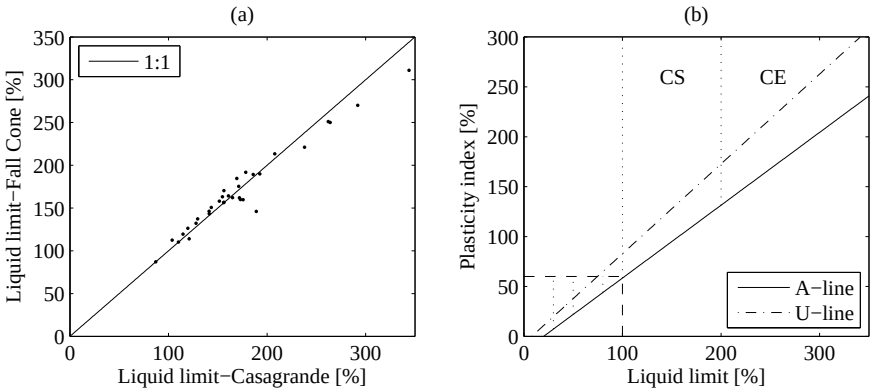

Figure 5.5 (a) Correlation between liquid limit found using Casagrande cup and fall cone (b) The updated Casagrande chart with two new categories (CS and CE).

of clay would have a water content near the natural water content (usually 40% - 50%) and as the liquid limit of Søvind Marl is in the normal range of 100% to 250%. These lumps of lower water content would significantly influence the measured water content during testing.

5.3 Paper 2

Title:
Geotechnical properties of Søvind Marl - a plastic Eocene clay

Authors:
Gitte Lyng Grønbech, Benjaminn Nordahl Nielsen, Lars Bo Ibsen and Peter Stockmarr

Published in:
Canadian Geotechnical Journal, Volume 52

Year of publication:
2015

Background:
The general knowledge of the unique geotechnical properties of Søvind Marl is fairly unknown. When dealing with a "new" soil, like Søvind Marl, it is important to get a fundamental knowledge of the soil through basic geotechnical properties and characteristics. This is done in order to evaluate which soils a comparison could be made to and to clarify any potential problem areas.

Summary:
Søvind Marl is an Eocene deposit found in Denmark, and is part of several tertiary deposits found various places throughout Denmark. The samples analysed in the paper all originates from the Søvind Marl formation found at Aarhus Harbour. All samples comes from five boreholes with varying depths of up to 69 m and are dated to be between 40.5 million years and 46 million years old. The appearance of the samples is remarkably uniform considering the large period of deposit. The only mesofabric difference in the samples is the difference in colour, which depends on the environmental circumstance during the time of deposit. An important mesofabric feature of Søvind Marl is the fissured matrix, which can cause great difficulties both when working with intact samples in the laboratory and estimating the intact load bearing capacity. The mineral composition of Søvind Marl showed that a large part of the clay minerals is of the highly plastic clay mineral smectite. General geotechnical properties and classification parameters are presented in the paper, as well as results from CPTs, shear vane tests and oedometer tests.
A noteworthy property of Søvind Marl is the extremely high plasticity, with plasticity index in the normal range of 150% to 250% and extreme values of more than 300%, which makes the plasticity of Søvind Marl much higher than similar soils and thus complicating comparisons and the use of known correlations. A high calcite ($CaCO_3$)content of 5% to 65 % was found with large variation over small distances. A clear inverse correlation between the plasticity and the calcite content was found. The correlation weakens slightly with a lower calcite content, indicating that the plasticity of the clay particles begins to have a larger influence on the plasticity. In general many of the measured parameters show a change in behaviour at a depth of around

25 m. This is evident in plasticity, calcite content, vane shear strength, cone tip resistance and sleeve friction. This pronounced change suggests a significant change in the macro behaviour although no mesofabric changes are evident. This indicates that the calcite content plays an important role in the behaviour of Søvind Marl.
CPTs were found to quickly build up a large excess pore pressure, resulting in limited use of the tests below 25 m. Furthermore, traditionally CPT classification charts was found to be useless on Søvind Marl as the high degree of overconsolidation causes a miscategorisation of the clay as silt.
The oedometer test revealed that two apparent values can be interpreted as the preconsolidation stresses due to the fissured matrix of the soil. Where the lower value was found to be a fraction of the higher values. The lower value at around 700 kPa to 800 kPa was deemed to be due to the collapse of the fissures, whereas the higher value at 6000 kPa to 7000 kPa was found to be due to previous consolidation and secondary consolidation. Known correlations between the in situ vane shear strength and the preconsolidation stresses was found not to be valid on Søvind Marl.
The paper can be found in Appendix B.

Main Points:

- Søvind Marl has a very uniform appearance with a high presence of fissures
- The plasticity of Søvind Marl was in the normal range of 150% to 250%
  - The extreme value of 306%
- Søvind Marl has a clear inverse correlation between the plasticity and calcite content, cf. Figure 5.6 and equation 5.1
- A change in the macro behaviour occurs at a depth of 25 m
- CPT are of limited use on Søvind Marl due to the high overconsolidation ratio
- No correlation between in situ vane strength and the preconsolidation stresses

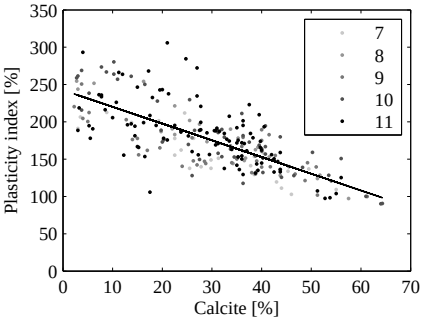

Figure 5.6 The correlation between the plasticity and calcite content.

$$I_P = 242.5 - 2.24 \cdot Calcite[\%] \qquad (5.1)$$

5.3.1 CPT classification charts

Paper 2 explains that CPT charts give a misclassification of Søvind Marl which is shown graphically here. CPT classification charts give a highly inaccurate description of Søvind Marl due to the high degree of overconsolidation, which most common CPT classification charts do not take into account. The most frequently used classification charts are based on the pore pressure ration and the corrected cone resistance or on the friction ratio and corrected cone resistance. These parameters can be seen in section 6 in the article in appendix B. Only data to a depth of 37 meters is used since the pore pressure is highly unreliable at lower depths. The classification charts are presented in Figure 5.7.

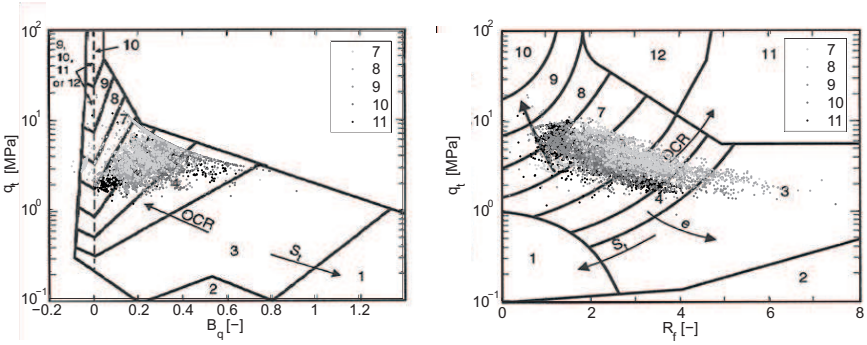

Figure 5.7 Søvind Marl samples in CPT classification charts, (a) $B_q - q_t$ and (b) $R_f - q_t$.

Both classification charts misclassify the Søvind Marl as a silty clay to a sandy silt, which does not correlate with the facts that Søvind Marl is a very high plasticity clay. As stated in the article, this is due to the very high degree of overconsolidation. Based on this, it is recommended not to use CPTs to classify highly overconsolidated clays, like Søvind Marl.

CHAPTER 6
Part 2 - Stiffness

This part concerns the stiffness and interpretation of oedometer tests (also called consolidation tests) on Søvind Marl. As described in chapter 5, Søvind Marl has a highly fissure matrix. The general influence of a fissure structure on the behaviour of a clay is discussed in section 3. Part 2 consists of a description of the experimental programme and a summary of three papers: Separation of strains following an oedometer test (Paper 3), the determination of the preconsolidation stresses, σ'_{pc}, and the influence which the fissured structure of Søvind Marl has hereon (Paper 4) and the behaviour of earth pressure at rest, K_0, (Paper 5). Figure 6.1 shows an overview of part 2.

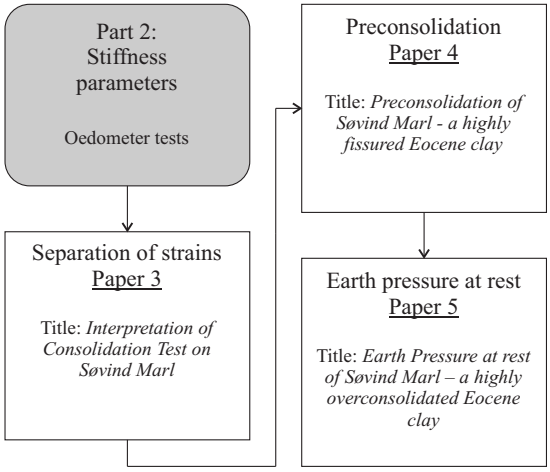

Figure 6.1 Overview of part 2.

6.1 Experimental programme

The experimental programme describes the preparation and tests which lies ahead of the papers. All Incremental Loading Oedometer (ILO) tests were made in the Danish

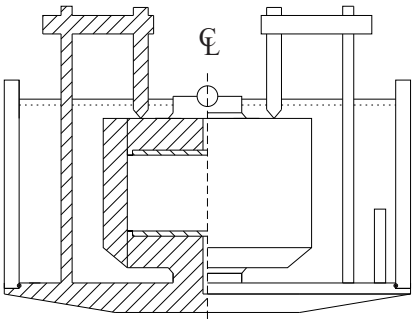

Figure 6.2 Illustration of the Danish incremental loading oedometer apparatus. Not to scale.

Figure 6.3 Danish incremental loading oedometer apparatus.

oedometer apparatus (Figure 6.2 and Figure 6.3), and all Continuous Loading Oedometer (CLO) tests were performed in the continuous loading oedometer apparatus (Figure 6.4 and Figure 6.5), both apparatus are described in Paper 4. The samples all had a diameter of 35 mm in order to reach the high stress levels required in the tests. Additionally, the samples had an initial height of 35 mm and 30 mm for ILO tests and CLO tests, respectively. All samples were fitted and levelled to the intended height by hand, Figure 6.6. Tests used in Paper 4 are numbered after: Test type (ILO tests are 1-4 and CLO tests are 5-8), location (LH first then BS) and finally in situ depth (the higher strata, the lower the number). Tests used in Paper 5 are listed after design of load programme: Purely loading (1 and 2), reloading à la ILO tests (3 and 4) and reloading à la preconsolidation (5 and 6). Test numbers and general information about the tests are listed in Table 6.1 and Table 6.2. In following text and in Appendix H and Appendix I the tests are numbered as in Paper 4, and the two additional CLO tests are numbered 9 and 10.

6.1.1 Incremental Loading Oedometer tests

The ILO tests were all made after a pre-planned load programme in the Danish oedometer apparatus. The load programme for tests 2 and 3 is listed in Table 6.3. It was found that the normal approach of doubling the load at each step ($1 = \frac{\Delta\sigma'}{\sigma'}$) yielded a much too coarse description of the behaviour of the soil. Therefore, a new load

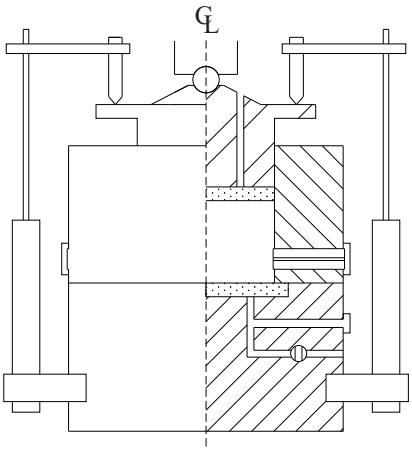

Figure 6.4 Illustration of the Danish continuous loading oedometer apparatus. Not to scale.

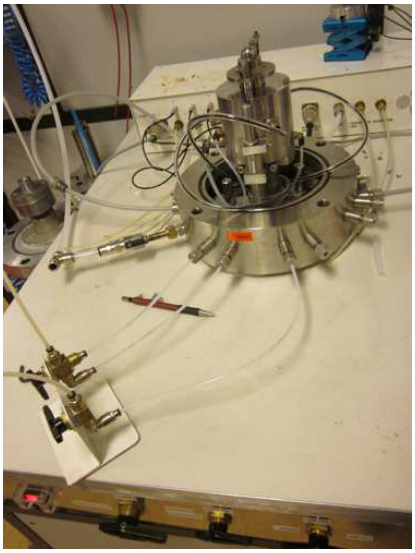

Figure 6.5 Danish continuous loading oedometer apparatus.

Figure 6.6 A levelled sample, the variation in colour is evident.

programme was used in the remaining ILO tests; this load programme can be seen in Table 6.4. This load programme was found to give a better description of the behaviour of the soil and, thereby, the preconsolidation stresses. Results and graphs for each test are presented in Appendix H.

In addition to the ILO tests used in Paper 3 and Paper 4, three loading and re-loading tests were made on material from same test tube as the presented tests and with a samples diameter of 70 mm. These tests are only used in this thesis to study the influence of the smaller diameter used in the ILO tests presented in the papers. The load programme, zero point measurements and raw data are presented in Appendix H.

Table 6.1 Incremental loading oedometer tests used in Paper 3 (marked with *), Paper 4 and Paper 5. c_{fv} not measured on BS samples.

Sample Metric	Sample			
No. Paper 4	1	2 *	3	4
No. Paper 5	-	-	-	-
Test type	ILO	ILO	ILO	ILO
Location	LH815	LH840	LH840	BS3
Depth [m]	29	39	39	11.5
σ'_{v0} [kPa]	255	350	350	110
γ [kN/m^3]	18.4	18.6	18.4	17.9
w_{nat} [%]	40.2	34.6	36.0	41.5
w_L [%]	187.0	203.8	203.8	78.8
c_{fv} [kPa]	786	829	829	-
$Calcite$ [%]	43.3	39.8	39.8	62.0
Cl^- [%]	0.7	0.6	0.6	1.7
pH [-]	9.30	9.30	9.30	8.3

Table 6.2 Continuous loading oedometer tests used in Paper 4 and Paper 5. c_{fv} not measured on BS samples.

Sample Metric	Sample					
No. Paper 4	5	6	7	8	(9)	(10)
No. Paper 5	4	1	2	3	5	6
Test type	CLO	CLO	CLO	CLO	CLO	CLO
Location	LH825	LH860	BS4	BS4	LH800	BS4
Depth [m]	33	47	11.5	11.5	23.5	11.5
σ'_{v0} [kPa]	285	400	110	110	210	110
γ [kN/m^3]	18.1	17.9	17.5	17.7	17.5	17.9
w_{nat} [%]	38.8	40.7	40.0	39.8	39.7	40.7
w_L [%]	253.0	239.8	75.6	75.6	134.0	75.6
c_{fv} [kPa]	744	>1000	-	-	615	-
$Calcite$ [%]	10.0	36.3	64.5	64.5	55.0	64.5
Cl^- [%]	0.5	0.6	1.7	1.7	0.9	1.7
pH [-]	9.25	9.15	8.4	8.4	9.2	8.4

6.1.2 Continuous Loading Oedometer tests

The CLO tests were planned to resemble the ILO tests and made in the Danish Continuous loading oedometer. The load programme is listed in Table 6.5 and Table 6.6.

Prior to every tests, the samples are trimmed by hand to fit in the oedometer cell. The oedometer cell with the sample is placed in a triaxial apparatus, where a load of 10 kg was applied via the load pistol. Hereafter, load pistol was stopped and test water was applied at a pressure of 200 kPa. Since deformation of the sample was not possi-

Table 6.3 ILO load programme for tests 2 and 3.

Step	Load [kg]	σ'_V [kPa]
1	0.5	52
2	1	104
3	2	208
4	4	416
5	8	832
6	15	1559
7	30	3118
8	60	6236
9	120	12473
10	180	18709
11	240	24945

Table 6.4 ILO load programme for tests 1 and 4.

Step	Load [kg]	σ'_V [kPa]
1	0,5	52
2	1	104
3	2	208
4	4	416
5	8	832
6	15	1559
7	25	2598
8	50	5197
9	75	7795
10	100	10394
11	130	13512
12	160	16630
13	200	20788
14	250	25985

ble in neither a horizontal nor a vertical direction, the swell pressure could hereby be measured as the pressure the sample applied to the load pistol. After full saturation of the sample, the load was increased to simulate the vertical in situ stresses, and then the load was decreased to just above the swell pressure. From here, the load programmes presented in Table 6.5 were used. Please note that the load is the input value, and not the actual load applied to the sample as they are not corrected for zero point measurements (listed in Appendix I). The CLO system was controlled by the commercial programme Catman Pro.

Table 6.5 CLO load programme Test 5 to Test 7.

Test 5		Test 6		Test 7	
Load [kg]	σ'_V [kPa]	Load [kg]	σ'_V [kPa]	Load [kg]	σ'_V [kPa]
393	3190	547	4750	789	7260
155	780	838	7650	1339	12860
393	3190	1352	12730	2000	19600
118	400	-	-	-	-
393	3190	-	-	-	-
100	200	-	-	-	-
828	7630	-	-	-	-

Table 6.6 CLO load programme Test 8 to Test 10.

Test 8		Test 9		Test 10	
σ'_V [kg]	Load [kPa]	σ'_V [kg]	Load [kPa]	σ'_V [kg]	[kPa]
393	3140	138	630	140	690
157	770	98	230	80	70
393	3130	562	4930	705	6450
118	4390	98	240	80	80
383	3010	705	6350	1034	9800
100	180	98	240	-	-
1049	9590	945	8760	-	-
1289	12930	-	-	-	-

6.2 Paper 3

Title:
Interpretation of Consolidation Test on Søvind Marl

Authors:
Gitte Lyng Grønbech, Lars Bo Ibsen and Benjaminn Nordahl Nielsen

Published in:
Proceedings of the 16th Nordic Geotechnical Meeting. May 9th to 12th, 2012. Copenhagen, Denmark.

Year of publication:
2012

Background:
When consolidation (oedometer) tests are performed the total deformation of the soil is measured. However, it is only the consolidation strains that are of interest. Many methods are used to separate the consolidation and secondary consolidation strains. Traditionally, in Denmark, Brinch Hansen's method $\sqrt{\mathrm{t}} - \log(\mathrm{t})$ (Brinch Hansen 1961) is used. This method does assumes that the secondary consolidation process does not begin until the primary consolidation is completed. This is likely not the case, which, consequently, overestimates the primary consolidation. The ANACONDA method described in the paper considers the fact that the primary and secondary consolidation happens simultaneously.

Summary:
The article describes three different methods to separate consolidation and secondary consolidation (also known as creep): $\sqrt{\mathrm{t}} - \log(\mathrm{t})$ method, ANACONDA method and 24-hour method. The article focuses on the ANACONDA method. The different methods are demonstrated on a Søvind Marl sample.
The ANACONDA method factors in that the primary and secondary consolidation processes are two separate processes that run simultaneously and independently of each other, whereas the $\sqrt{\mathrm{t}} - \log(\mathrm{t})$ method assumes that secondary consolidation does not begin until the primary consolidation is completed. The 24-hour method does not separate the strains, but uses the total strain after 24 hours as the consolidation strain.
The ANACONDA method assumes the primary consolidation to be momentary and over at the time $t = 0$, the consolidation process can hereafter been viewed as a delay of strains. By studying the secondary consolidation isochrones, a strain state can be reached by either preconsolidation or secondary consolidation. The isochrones give the theoretical time past before the secondary consolidation start, t_A, and are used to estimate the increase in secondary consolidation strains. As the secondary consolidation is constant under constant stress level, the increase in secondary consolidation strains can be subtracted from the total strain to obtain the primary consolidation

strains.
An essential detail when using the ANACONDA method is to ensure sufficient secondary consolidation of each load step in order to make sure the increase in secondary consolidation is found correctly. As the primary and secondary consolidation is two separate processes, the ANACONDA method gives a more accurate description of the secondary consolidation for soils which has a large secondary compression index.
The consolidation test on Søvind Marl was conducted at high stresses and, consequently, a high strain level. The difference between natural and engineering strain was found to be significant at high stresses, with a difference of 2.5% point at 24500 kPa.
The output parameters of consolidation tests are minimally affected by the method of separation of the strains, but they are affected by the method used to analyse the consolidation strains subsequently in order to find the preconsolidation stresses, where several different methods are needed to get an accurate determination of the preconsolidation stresses.
The paper can be found in Appendix C.

Main Points:

- ANACONDA method takes into account primary and secondary consolidation happening simultaneously
  - ANACONDA method is to be preferred if the secondary consolidation is large
- The method used to separate strains have little influence on the preconsolidation stresses
- There is a large difference on the different method used to determine the preconsolidation stresses

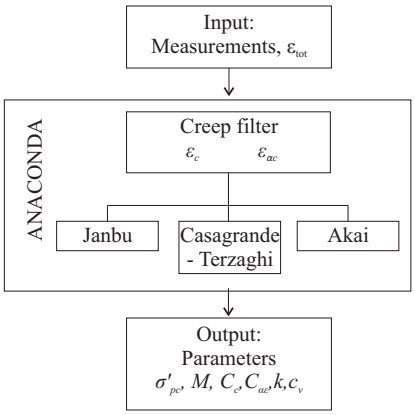

Figure 6.7 Flow chart using the ANACONDA method.

6.2.1 Use of ANACONDA method

The total strain, ε_{tot}, of a load step in a consolidation test consists of primary consolidation strains, ε_c, and secondary consolidation strains, $\varepsilon_{\alpha c}$. At the end of each load step, all deformation is assumed to be secondary consolidation. By identifying these strains and assuming them to develop constant under constant loading, the primary consolidation strains can be found. The increase in secondary consolidation strains can be described as:

$$\Delta\varepsilon_{\alpha\varepsilon} \approx C_{\alpha\varepsilon} \log\left(1 + \frac{t}{t_A}\right) \tag{6.1}$$

The time, t, is known from the load step. The best way to find t_A is as the value that transforms equation 6.1 into a straight line in a semi-logarithmic depiction when added to t, where $C_{\alpha\varepsilon}$ (secondary compression index) is the inclination, equation 6.2. To do this, the end of the load step should be observed where the primary consolidation is done, c.f. Figure 6.8. The flow chart in Figure 6.9 is used to determine whether t_A and $C_{\alpha\varepsilon}$ are estimated correctly. Hereafter the increase in secondary consolidation strains can be found through equation 6.1, and thereby also the primary consolidation strains by equation 6.3 and equation 6.4.

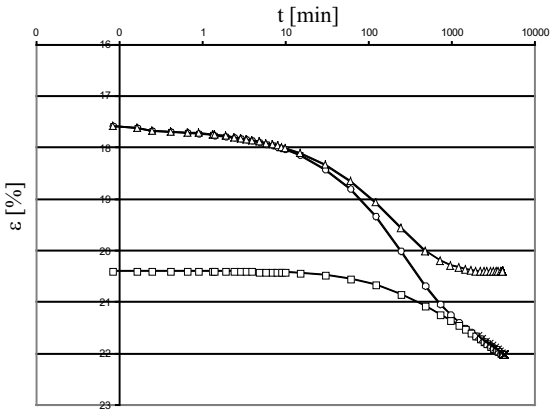

Figure 6.8 ANACONDA method used on a load step. ○: Total strains, □: Secondary consolidation strains, △: Primary consolidation strains and ×: $t + t_A$

$$C_{\alpha\varepsilon} = \text{slope of}(t^{end} + t_A; \varepsilon_{tot}^{end}) \tag{6.2}$$

$$\varepsilon_{con} = \varepsilon_{tot}^{end} - \Delta\varepsilon_{\alpha\varepsilon} \tag{6.3}$$

$$\varepsilon_c = \text{mean}(\varepsilon_{con}) \tag{6.4}$$

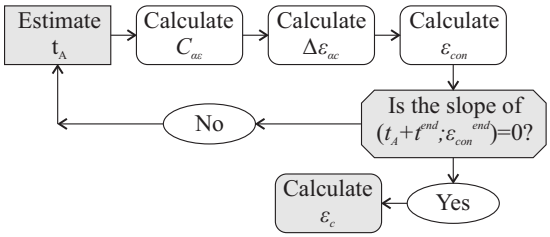

Figure 6.9 ANACONDA flow chart. ^{end} denotes the data point from the beginning of t_A at the end of the load step.

6.3 Paper 4

Title:
Preconsolidation of Søvind Marl - a highly fissured Eocene clay

Authors:
Gitte Lyng Grønbech, Lars Bo Ibsen and Benjaminn Nordahl Nielsen

Accepted with changes at:
Geotechnical Testing Journal

Time of acceptances:
Accepted with changes, December 2014, changes submitted January 2015

Background:
Oedometer tests are a key geotechnical tool used to determine the stiffness and preconsolidation stresses of a soil. Previous tests on Søvind Marl in 70 mm oedometer cells have shown that the samples are affected by the fissures in the soil. This necessitates a study of the influence of the fissures on the interpretation of the preconsolidation stresses.

Summary:
Gasparre and Coop (2008) showed the determination of preconsolidation stresses of a fissure clay is highly difficult, as a unique yield point is not clearly defined and an upper and lower bound of the preconsolidation stresses can be found. However, Krogsbøl *et al.* (2012) suggested that these high plasticity clays lose their stress memory and, hereby, their preconsolidation stresses.
Two different oedometer apparatus are used to determine the preconsolidation stresses of Søvind Marl: Incremental Loading Oedometer (ILO) and Continuous Loading Oedometer (CLO). Both apparatus are described to give an insight in the application of the test methods. The ILO tests were found highly dependent on the load programme, and the analysis of the test was significantly affected by it, whereas CLO tests give a continuous description of the test resulting in a more accurate determination of the preconsolidation stresses. All samples had a diameter of 35 mm during testing to enable high stresses in the samples to better simulate the geological history of Søvind Marl. The smaller diameter, as compared to the 70 mm which is standard in Danish engineering practice, was shown to have a limited influence on the found preconsolidation stresses. However, the smaller diameter should only be used when high stresses are an absolute necessity.
The analysis of the tests shows that the interpretation of the preconsolidation stresses was affected by the fissures in the soil, cf. Figure 6.10. This is evident as two apparent values can be interpreted as the preconsolidation stresses, cf. Figure 6.11 and Figure 6.12. The lower boundaries of the preconsolidation stresses were found in the range of 600 kPa to 800 kPa in depth from 29 m to 47 m, which is only two to three times the in situ stresses, and hereby deemed to be a result of the fissured matrix collapsing.

The upper boundaries of the preconsolidation stresses were found in the range of 6300 kPa to 8900 kPa in the same depth (the preconsolidation stresses are listed in Table 6.7). These values are in agreement with the geological history with extensive previous consolidation and secondary consolidation through millions of years; the stress memory is thereby not forgotten. While only the upper bound is related to the geological preconsolidation, it is, however, the lower bound which is useful for geotechnical engineering purposes.
The paper can be found in Appendix D.

Main Points:

- The fissured structure has a large influence on the determination of the preconsolidation stresses
- Two apparent values can be determined as the preconsolidation stresses
  - Lower bound is deemed to be caused by the collapse of the fissured matrix
  - Upper bound is found to the result of preconsolidation and secondary consolidation
- The lower bound is useful in geotechnical engineering, while the upper bound is interesting to geology engineering
- High stresses are a necessity in order to get a comprehensive description of the stiffness of Søvind Marl
- CLO tests give a more comprehensive description of the results as compared to ILO tests

6.3.1 Stiffness parameters through known emperical correlations

Through the years, many correlations have been made between geotechnical properties and various stiffness parameters.
In 1975 Mesri made a correlation between the undrained shear strength and the preconsolidation stresses, equation 6.5. (Mesri 1975)

$$S_u = 0.22 \cdot \sigma'_{pc} \tag{6.5}$$

Paper 2 (appendix B) showed that utilising Bjerrum's (Bjerrum 1973) factor, μ, between the in situ vane shear strength (listed in Table 6.1 and Table 6.2) and mobilised undrained shear strength, $S_u(mob)$, in equation 6.5 does not yield a satisfactory resemblance to neither the lower nor upper bound of the preconsolidation stresses found in Paper 4, cf. Table 6.7.

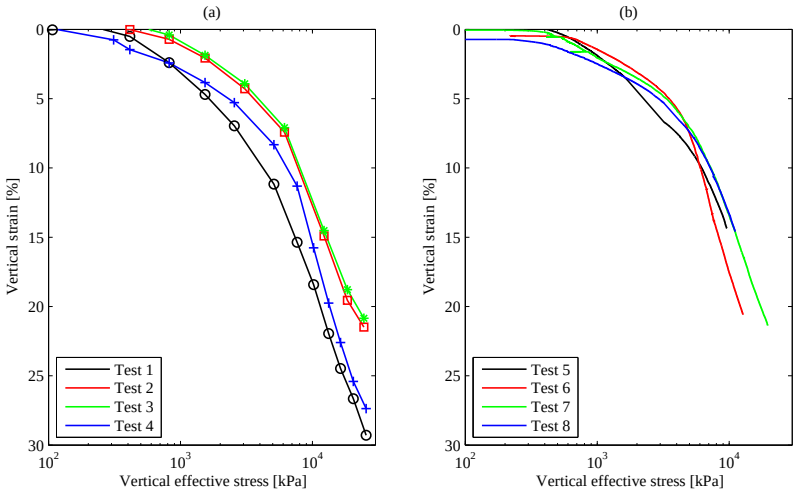

Figure 6.10 Stress-strain curves from the oedometer tests. (a) ILO tests and (b) cCLO tests.

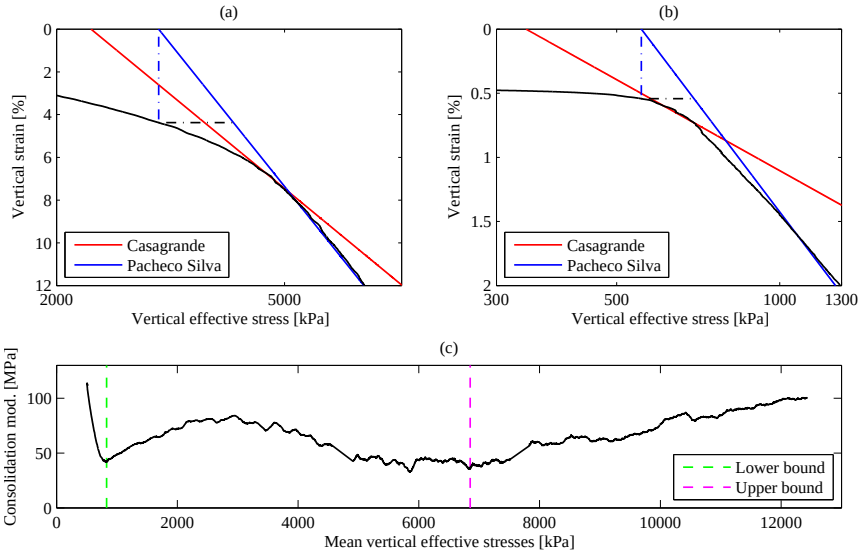

Figure 6.11 Illustration used to determine the preconsolidation stresses from CLO test 6. (a) Upper bound found according to Casagrande (1936) and Pacheco Silva (1970) methods, (b) lower bound found via Casagrande (1936) and Pacheco Silva (1970) methods and (c) upper and lower bounds found via the (1970) method.

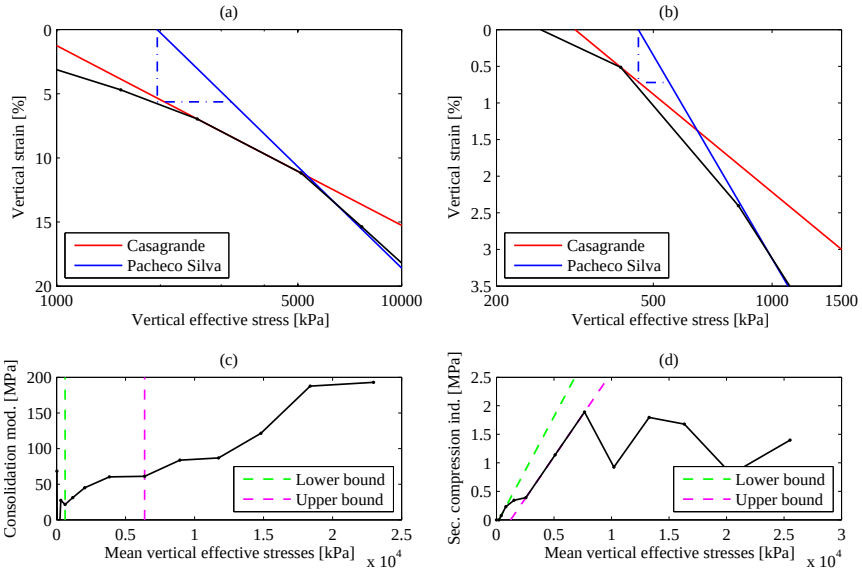

Figure 6.12 Illustration used to determine the preconsolidation stresses from ILO test 1. (a) Upper bound found according to Casagrande (1936) and Pacheco Silva (1970) methods, (b) lower bound found via Casagrande (1936) and Pacheco Silva (1970) methods, (c) upper and lower bounds found via the Janbu (1970) method and (d) upper and lower bounds found via the Akai (1960) method.

Table 6.7 Empirical correlation for σ'_{pc} used on Søvind Marl.

	Test				
	1	2	3	5	6
Lower σ'_{pc}	700	1200	1200	700	800
Upper σ'_{pc}	6300	9200	9200	6500	6800
Mesri (c_{fv})	1072	1130	1130	1015	1364

The compression index, C_c, is often correlated to the liquid limit or the natural water content. Terzaghi *et al.* (1996) suggested a correlation between the liquid limit (listed in Table 6.1 and Table 6.2) and the secondary compression index.

$$C_c = 0.009 \cdot (w_L - 10) \tag{6.6}$$

As shown in Table 6.8, also this correlation yields a non-existing correlation between the compression index and the liquid limit. This is a result of the extremely high liquid limit of Søvind Marl. Azzouz *et al.* (1976) presented several correlations to the compression index, one in relation to the natural water content is shown in equation 6.7.

$$C_c = 0.01 \cdot (w_{nat} - 5) \tag{6.7}$$

Equation 6.7 also results in fairly poor and slightly too high compression index (Table 6.8).

Table 6.8 Empirical correlation for C_c used on Søvind Marl.

	Test							
	1	2	3	4	5	6	7	8
Lower C_c	9.2	8.9	6.2	5.8	7.2	5.6	5.3	4.3
Upper C_c	26.3	25.4	24.5	33.3	24.2	33.5	27.0	23.0
Terzaghi	159.3	174.4	174.4	61.9	218.7	206.8	59.0	59.0
Azzouz	35.2	29.6	31.0	35.5	33.8	35.7	35.0	34.8

None of the existing and often used empirical correlations are usable on Søvind Marl due to the extreme properties. This emphasises the importance of correctly and carefully planned and executed oedometer tests when dealing with Søvind Marl.

6.4 Paper 5

Title:
Earth pressure at rest of Søvind Marl - a highly overconsolidated Eocene clay

Authors:
Gitte Lyng Grønbech, Lars Bo Ibsen and Benjaminn Nordahl Nielsen

Submitted for peer-review at:
Engineering Geology

Year of submission:
2015

Background:
The behaviour of a soil is highly dependent on the stresses present in the soil. Estimation of horizontal stresses are often based on experience which is lacking for highly overconsolidated plastic clays, such as Søvind Marl.

Summary:
Six continuous loading oedometer tests with a constant rate of strain were performed on Søvind Marl (three LH samples and three BS samples) to evaluate the development of earth pressure at rest, K_0, during loading and reloading. An advance of CLO testing is the continuous nature of the results. $K_0(nc)$ was found to be 0.68 and 0.42 for LH and BS samples, respectively and found to be affected by the unloading and reloading process, as the earth pressure at rest in the normally consolidated range for reloading samples was 0.89 - 0.96 and 0.62 - 0.81 for the two different sample types. Estimations of the friction angle of the material based on Jaky's relation (1944): $K_0(nc) = 1 - \sin(\varphi)$ yields unrealistic values of the friction angle indicating no use for the relation on Søvind Marl. This makes the friction angle useless in the estimation of $K_0(nc)$. The measured earth pressure at rest during reloading reached high values of more than 10, and values in the range of 6 - 8 at in situ stress levels. The measured $K_0(nc)$ for both the loading and reloading tests were used to fit Meyerhof's (1976) relation for overconsolidated soils: $K_0(oc) = K_0(nc) \cdot OCR^{\alpha}$. The relation yields poor fits and shows a tendency to weaken significantly as OCR increases, regardless of whether the loading or reloading $K_0(nc)$ was used. As determination of $K_0(nc)$ for the loading tests shows (Figure 6.13), the upper bound of the preconsolidation stresses is remembered. However, the poor fit indicates a loss of "short-term" memory. This results in "new" preconsolidation stresses set during testing as the maximum previous load in the test, redefining OCR as $OCR_{lab} = \sigma'_{unload}/\sigma'_v$, as suggested by Krogsbøl *et al.* (2012). The use of OCR_{lab} in Meyerhof's relation gave better fits to the measured K_0. The best fit was found when $K_0(nc)$ for the loading branch was used, with an α value approximately 1.05 (cf. Figure 6.15), regardless of whether the sample was from LH or BS, (equation 6.8 and equation 6.9).
The paper can be found in Appendix E.

Main Points:

- $K_0(nc)$ increases if found after reloading cycles.
- Jaky's relation cannot be used on these highly plastic clays.
  - Consequently, the friction angle cannot be used in estimation of $K_0(nc)$.
- Earth pressure at rest of Søvind Marl reaches high values of between 6 and 8 in the in situ stress range.
- $K_0(oc) = K_0(nc) \cdot OCR^{\alpha}$ yield bad fits to the measured K_0.
- While the preconsolidation stresses are remembered, the "short-term" memory of the reloading stresses is lost.
  - The maximum previous stresses, σ'_{unload}, in the test were used in OCR_{lab}.
  - $OCR_{lab} = \sigma'_{unload}/\sigma'_v$.
- Relation using OCR_{lab} and initial loading $K_0(nc)$ yields good relations, cf. equation 6.8 and equation 6.9.
- High α values found to be 1.04 and 1.05 for LH and BS samples, respectively.

Best fit for LH samples:

$$K_0(oc) = 0.68 \cdot OCR_{lab}^{1.04} \tag{6.8}$$

Best fit for BS samples:

$$K_0(oc) = 0.42 \cdot OCR_{lab}^{1.05} \tag{6.9}$$

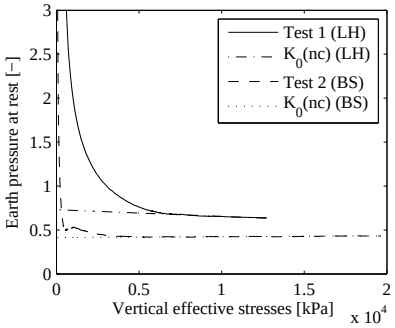

Figure 6.13 Determination of normally consolidated earth pressure at rest for loading tests.

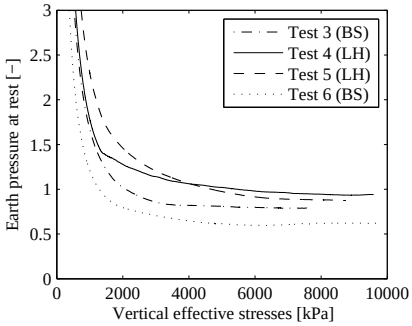

Figure 6.14 Determination of normally consolidated earth pressure at rest for reloading tests.

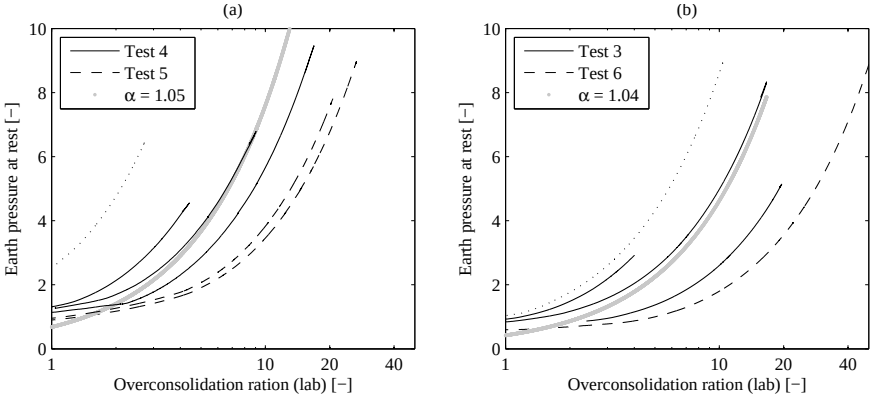

Figure 6.15 Best $K_0 \cdot OCR_{lab}^{\alpha}$ fit. (a) SM samples and (b) BS samples.

CHAPTER 7
Part 3 - Strength parameters

This part concerns the determination of strength parameters of Søvind Marl. As mentioned in Chapter 3, the undrained shear strength of Søvind Marl is influenced by the fissured structure as failure occurs at the weakest part of the clay structure: the pre-existent fissures. Part 3 consists of a description of the experimental laboratory programme, the determination of strength parameters and correlations to field tests. Figure 7.1 shows an overview of part 3.

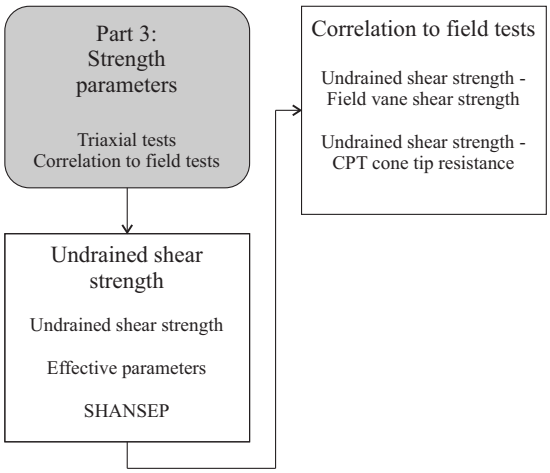

Figure 7.1 Overview of part 3.

7.1 Experimental laboratory programme

The tests were all made in the triaxial apparatus at the geotechnical laboratory at Aalborg University. Figure 7.2 shows an illustration of the apparatus (numbers in brackets [ ] in the following text refer to numbers in the figure).

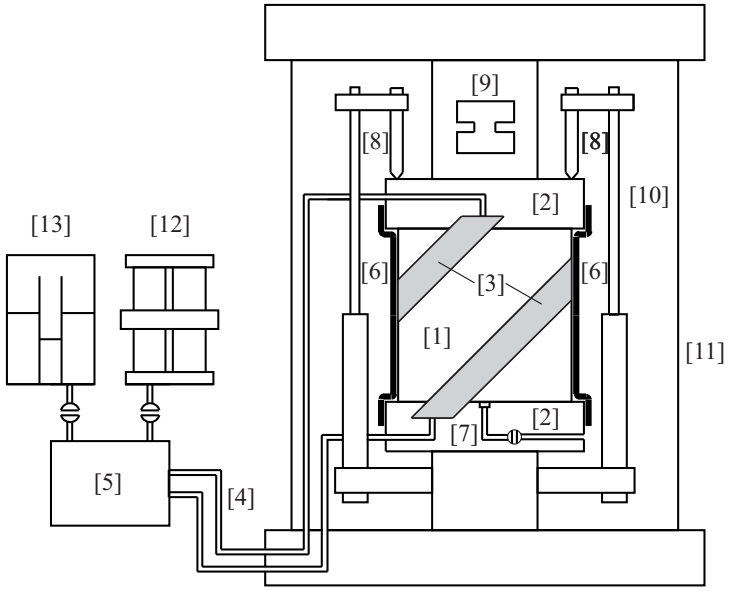

Figure 7.2 Illustration of the triaxial apparatus. Not to scale.

All test samples were trimmed by hand to ensure a height of 70 mm (1 $\times$ diameter), cf. Figure 7.3. After trimming, the samples [1] were installed in the triaxial apparatus. The upper and lower pressure heads [2] have smooth end plates in order to eliminate friction between the sample and end plates. Felt drains [3] run from top to bottom at an angle of 45°, which drains the sample and transports pore water to the drain pipes [4] which runs to the control board [5]. The samples were hereafter covered with two latex membranes [6] separated by a layer of high vacuum silicone grease to ensure water tightness of the sample and eliminate shear stresses at the surface of the sample. The pore pressure in the sample is measured by a 7-bar pressure transducer [7] placed in the lower pressure head. Axial deformations are measured by two displacement transducers [8] placed opposite of the upper pressure head. The total deviatoric stresses are measured by the load pistol [9]. Total radial stresses are equal to the cell pressure applied by the water surrounding cell water [10], which is encased in a Plexiglas cylinder [11]. The sample is saturated through the back pressure system [12], which, during the consolidation process, measures the volumetric strains of the sample through differential pressure measurements. The volume of the sample is keep constant throughout the undrained shearing tests via the volume control [13], which adjust the cell pressure if the sample consolidates or swell.

Saturation of the samples were made with test water resembling the salinity and pH of the pore water to minimise osmotic influence of the test results. Paper 2 describes the salinity and pH of the samples ($cl^- = 0.6$ and pH 9.2 cf. Appendix B). All tests were

Figure 7.3 Hand trimming of sample.

applied a back pressure of 200 kPa during saturation of the sample and the testing. All samples were prior to the shear test re-consolidated. Due to physical limitations of the triaxial apparatus, the samples were only re-consolidated to the lower bound of the preconsolidation stresses ($\sigma'_{pc} = 750$ kPa cf. Paper 4, section 6.3). Hereafter, the stresses were reduced to the intended stresses at which undrained shearing should be made (cf. σ'_{su} in Table 7.1).

All shearing tests were made undrained with a constant rate of strain of 0.5 $\%/h$ (minimum deformation rate of the unaltered triaxial apparatus) while controlling the cell pressure acting on the sample to keep a constant volume of the sample. This testing method is chosen as the main purpose of the tests was to determine the undrained shear strength. If the estimation of the effective parameters was the main purpose, the tests should have been run at a lower strain rate. This would require an alteration of the triaxial apparatus and significantly increase the testing time by at least a factor of five.

7.1.1 Samples

A total of seven undrained triaxial tests were made, all on LH samples. Four tests were made from in situ stresses (Test 1 - Test 4), and three tests from $0.5 \times \sigma'_{pc}$, $1 \times \sigma'_{pc}$ and $1.5 \times \sigma'_{pc}$ (Test 5 - Test 7). Information on the samples is listed in Table 7.1.

Table 7.1 Sample classification for undrained triaxial tests. c_{fv} estimated based on Paper 2 (Appendix B), * extended correlation as samples are located in depth without field vane tests, - symbolises shear test made from other stresses than the in situ stresses and ^{x} excess pore pressure in CPT is above 2 MPa.

Sample Metric	Sample						
Test	1	2	3	4	5	6	7
Lab. number	130607	130608	130609	130610	130611	130612	130613
Depth [m]	35	23	43	63	27	27	27
σ'_{v0} [kPa]	300	210	370	525	240	240	240
γ [kN/m^3]	18.0	18.4	18.5	18.0	18.0	18.2	18.5
w_{nat} [%]	42.7	36.7	37.6	44.0	38.4	38.5	38.7
I_P [%]	143.6	103.2	131.6		188.7	188.7	188.7
c_{fv} [kPa]	724*	583	818*	1053*	-	-	-
q_t [kPa]	5060^{x}	6960	6070^{x}	7270^{x}	-	-	-
σ'_{su} [kPa]	300	210	370	525	375	750	1125

Figure 7.4 to Figure 7.9 presents the physical appearance of the samples immediately after testing; unfortunately, no photo was taken of Test 1. The light stripes running diagonally across all the samples are marks after the felt drains and have no influence on the test results.

Tests 5, 6 and 7 all have shearing patterns in a very similar trend, with two shear plains originating at the top of the sample going down and outwards. Test 3 has a one shear plain going downwards across the sample. Test 2 has developed a small shear band, but seems to have failed based on horizontal deformation. Test 4 has likely failed at an existent fissure, as the sample has divided into two pieces where the rest of the sample seems relative undisturbed.

7.2 Strength parameters

Both the undrained and the effective parameters were attempted to be found through undrained triaxial tests, but with the main focus on determining the undrained shear strengths. Data from the re-consolidation and shearing steps is presented in Appendix J.

Figure 7.4 Test 2 after shearing.

Figure 7.5 Test 3 after shearing.

Figure 7.6 Test 4 after shearing.

Figure 7.7 Test 5 after shearing.

7.2.1 Undrained shear strength

The strength of an undrained soil is solely dependent on the undrained shear strength, $\tau = S_u$, and is given as the radius of Mohr's circle at failure:

Figure 7.8 Test 6 after shearing.

Figure 7.9 Test 7 after shearing.

$$S_u = 0.5 \cdot (\sigma_1 - \sigma_3)_{max} = 0.5 \cdot q_{max} \tag{7.1}$$

The undrained shear strength is given by the deviatoric stresses. The deviatoric forces are measured directly by the load pistol and are distributed over the actual area to yield the stresses. Figure 7.10 presents the stress-strain curve of each test.

The stress strain curve clearly shows which tests were isotropic consolidated (Test 1 to Test 5) and which tests were an-isotropic consolidated (Test 6 to Test 7), as the stress curves for the latter start at a deviatoric stress level different from zero. However, this does not affect the results of the tests. Test 4 peaks at around 2% for the stresses to become stable until they start increasing at around 5.5%. This is clear evidence of the fact that the measured peak strength at 2% is a result of a pre-existent fissure and the total strength of the sample was not fully reached.

Table 7.2 lists the resulting undrained shear strength using equation 7.1 for each test.

Table 7.2 Undrained shear strength of seven Søvind Marl samples.

Sample Metric	Sample						
Test	1	2	3	4	5	6	7
S_u [kPa]	188	378	280	188	297	421	425

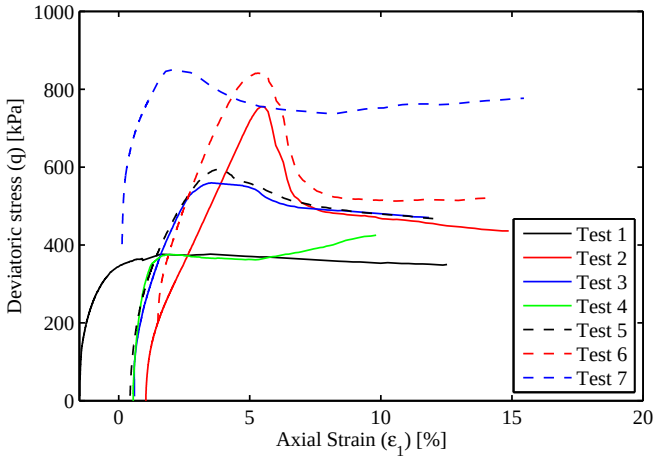

Figure 7.10 Stress-strain curve of the seven undrained triaxial tests.

The undrained shear strength is generally seen to increase with rising shearing stresses. However, Test 2 gives a very high undrained shear strength close to the field vane shear strength listed in Table 7.1, indicating the measured strength is not significantly influenced by the fissured structure, cf. Figure 7.4. Test 4, on the other hand, yields a very low undrained shear strength at initial failure. Figure7.6 shows a very distinct slickenside along which the failure has occurred. The measured shear strength is likely a residual strength in the fissure and not an expression of the strength of the clay. These tests are consequently not included in any further fit or correlations.

To give a better base for correlations based on the undrained shear strength, prior tests made on Søvind Marl by Madsen *et al.* (2008) at Aalborg University are included in the following (Section 7.3 to Section 7.4.2). Table 7.3 lists the data from these tests. These tests were also performed as undrained triaxial tests with test water resembling the pore water. Shearing tests on all sdditional samples are made from in situ stresses.

Figure 7.11 presents all undrained shear strengths as a function of the shearing stresses.

7.2.2 Effective parameters

The strength of a drained soil is determined by the effective parameter consisting of the effective friction angle, φ', and the effective cohesion, c', $\tau = c' + \sigma_v \cdot \tan(\varphi')$. Thøgersen (2001b) found the effective friction angle to be between 14° and 19° for the Danish Eocene clay Little Belt Clay, found using a strain rate of 0.1 $\%/h$. The effective parameters at failure are dependent on the deviatoric and effective mean stresses at the time of shear:

Table 7.3 Prior tests performed on Søvind Marl. c_{fv} estimated based on Paper 2 (Appendix B), * extended correlation as samples are located in depth without field vane tests and ^{x} excess pore pressure in CPT exceeded 2 MPa.

Sample Metric	Sample			
Test	8	9	10	11
Depth [m]	17	31	59	67
σ'_{v0} [kPa]	158	270	494	558
S_u [kPa]	105	213	239	413
c_{fv} [kPa]	427	677	1 006*	1 100*
q_t [kPa]	3070	4570^x	7990^x	9490^x

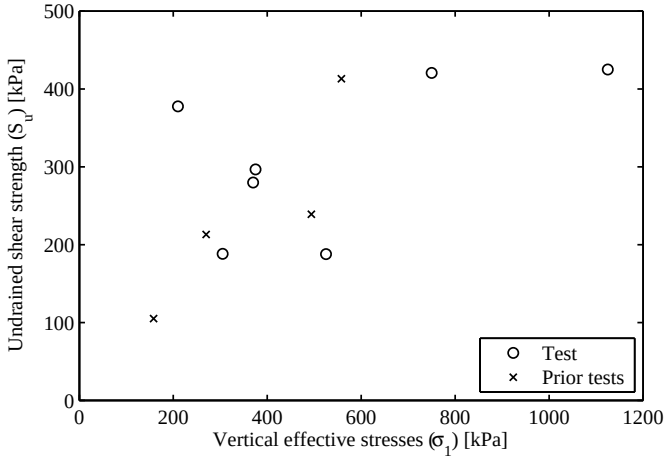

Figure 7.11 Undrained shear strength as a function of shearing stresses.

$$q = \frac{6 \cdot \sin(\varphi')}{3 - \sin(\varphi')} \cdot p' \tag{7.2}$$

The effective parameters are independent of the shearing stresses and, therefore, based on all tests. Figure 7.12 shows the effective stress paths of each test based on the pore pressure. Table 7.4 lists the resulting effective parameters.

The pore pressure is very high in some of the samples. This results in negative mean effective stresses for Test 2 (the pore pressure was measured to be higher than the cell pressure cf. Figure J.10 and Figure J.12 in Appendix J). Test 7 has mean effective stresses smaller than Test 6, despite being run from $1.5 \times \sigma'_{pc}$ and $1 \times \sigma'_{pc}$, respectively. Tests 2, 4 and 7 were as a result excluded from the estimation of the effective parameters listed in Table 7.4. There is generally a poor fit to the stress curves. Both the friction angle and the effective cohesion are considered too high to be realistic for

Søvind Marl, making the parameters of little use. In the attempt to eliminate the effect of the large pore pressure, the back pressure was used instead of the pore pressure when determining the effective stresses and parameters (Figure 7.13).

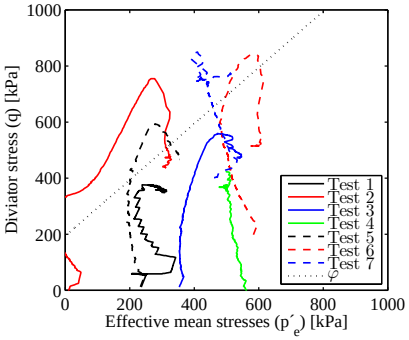

Figure 7.12 The determination of the effective parameters using the pore pressure in determination of the effective stresses.

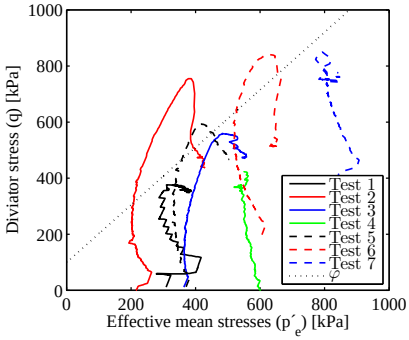

Figure 7.13 The determination of the effective parameters using the back pressure in determination of the effective stresses.

Table 7.4 lists the estimation of the effective parameters based on the back pressure which are also considered unrealistic. In this estimation, Test 2 and 4 are excluded as prior explained.

Table 7.4 Effective parameters based on the stress paths.

Sample Metric	Pore pressure	Back pressure
φ' [°]	25.4	26.0
c' [kPa]	193.5	99.1

The effective parameters estimated based on each individual test are usually related to large uncertainties, but this is attempted, in order to see if acceptable results are obtained. In the near proximity of the point of shear, the stress curve is approximately linear; this part of the curve is used to estimate the effective parameters. Figure 7.14 and Figure 7.15 shows the estimation of the effective parameters, which are listed in Table 7.5.

Also, these effective parameters are unrealistic. The effective friction angles are generally much too high, and the effective cohesions are either much too high or negative (a physical impossibility). As a rule of thumb, the effective cohesion should not be more than 10% of S_u. If this guideline is applied to the tests, the effective friction angle increases making them even more unrealistic as this only leads to a substantial increase in the friction angle. cf. Table 7.6.

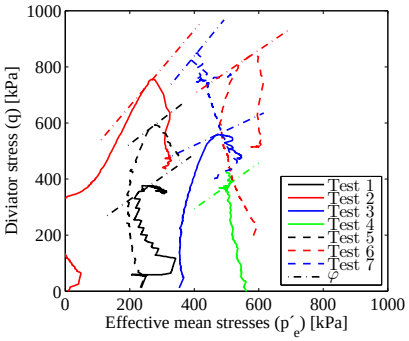

Figure 7.14 The determination of the effective parameters for each individual test using the pore pressure in determination of effective stresses.

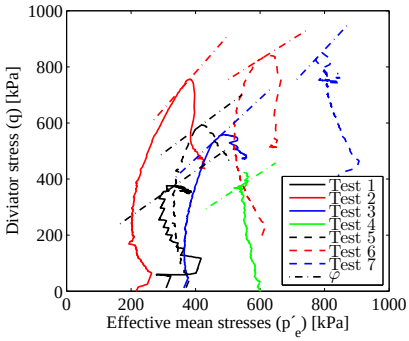

Figure 7.15 The determination of the effective parameters for each individual test using the back pressure in determination of effective stresses.

Table 7.5 Effective parameters based on each individual test.

Sample Metric	Sample - Pore pressure						
Test	1	2	3	4	5	6	7
φ' [kPa]	20.9	33.5	14.2	21.1	22.6	20.2	34.6
c' [kPa]	164.0	390.0	305.7	-33.1	347.6	392.4	278.3
Sample Metric	Sample - Back pressure pressure						
Test	1	2	3	4	5	6	7
φ' [kPa]	20.8	32.5	27.0	19.6	21.9	18.8	30.7
c' [kPa]	107.1	256.4	45.3	-33.5	237.0	393.3	-123.0

Mohr's Circles are used as a final attempt to determining the effective parameters, using Mohr–Coulomb's failure criterion for determination of the effective parameters in Figure 7.16 and Figure 7.17. The same tests are eliminated in this estimation as in the estimation based on the stress paths.

Table 7.6 Effective parameters based on each individual test with $c' = 0.1 \times S_u$.

Sample Metric	Sample - Pore pressure						
Test	1	2	3	4	5	6	7
φ' [kPa]	34.0	64.7	28.2	18.6	49.2	34.0	47.8
c' [kPa]	18.8	37.8	28.0	18.8	29.7	42.1	42.5
Sample Metric	Sample - Back pressure pressure						
Test	1	2	3	4	5	6	7
φ' [kPa]	27.2	45.1	27.6	17.3	33.3	31.8	25.8
c' [kPa]	18.8	37.8	28.0	18.8	29.7	42.1	42.5

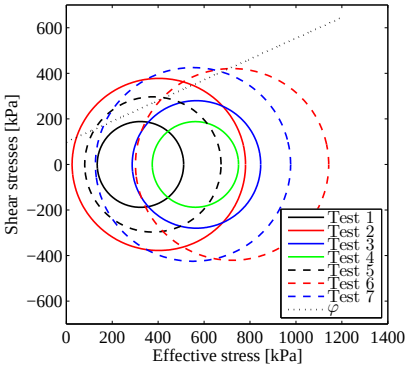

Figure 7.16 Mohr's circles, effective stresses based on the pore pressure.

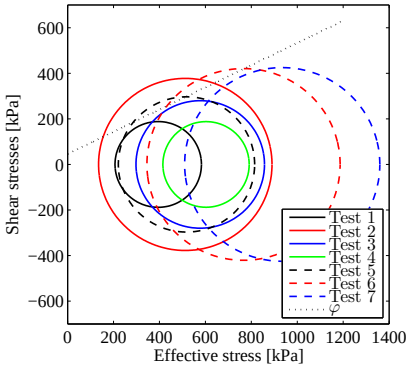

Figure 7.17 Mohr's circles, effective stresses based on the back pressure.

The best estimation of the failure line crosses than one of Mohr's circles in both cases, a physical impossibility, and overestimates the failure line for others Mohr's circles. Table 7.7 lists the effective parameters. Also, this method yields much too high values of the effective parameters.

Table 7.7 Effective parameters based on Mohr's Circles.

Sample Metric	Pore pressure	Back pressure
φ' [°]	24.5	26.0
c' [kPa]	98.0	46.1

All methods have poor fit and yield either an unrealistically high effective friction angle and/or effective cohesion. Søvind Marl has a very low permeability resulting in very large excess pore pressure present in the sample, even though the shearing tests were performed at tha slowest possible deformation rate of the unaltered triaxial apparatus. The high excess pore pressure leads to a very uncertain determination of the effective parameters. To better estimate the effective parameters, a slower deformation rate similar to that used in the CLO tests or as suggested by Thøgersen (2001b) should have been used. This optimises the determination of the effective parameters at the expense of a much larger testing time.

7.3 SHANSEP

Ladd *et al.* (1977) presented SHANSEP (Stress History And Normalized Soil Engineering Properties) as a way to normalise the undrained shear strength to the in situ stresses in relation to the overconsolidation ratio, equation 7.3.

$$\frac{S_u}{\sigma'_{V0}} = S \cdot OCR^m \tag{7.3}$$

According to Ladd *et al.* (1977), Mayne (1988) and Augustesen *et al.* (2005), the parameters S and m are usually in the following interval for undrained triaxial tests on various clays:

$0.25 \leq S \leq 0.55$
$0.7 \leq m \leq 0.8$

Test 2 and Test 4 are not included in the correlation due to reasons described earlier. The re-consolidation pressure equal to the lower bound of the preconsolidation stresses is used to determine OCR. The best fit is presented in Figure 7.18 and the resulting values of S and m are listed in Table 7.8.

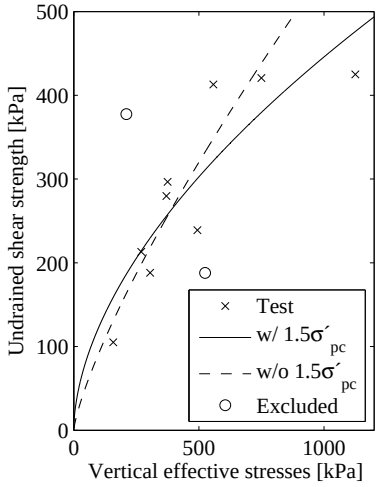

Figure 7.18 SHANSEP, OCR found using the lower bound of the preconsolidation stresses.

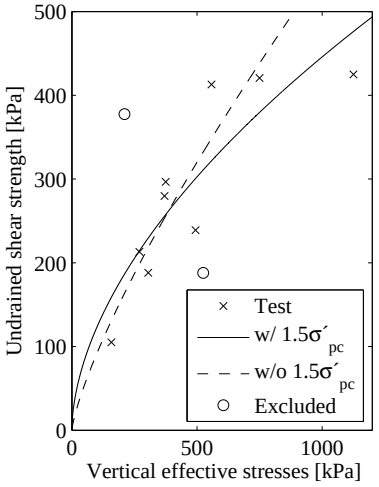

Figure 7.19 SHANSEP, OCR found using the upper bound of the preconsolidation stresses.

Including Test 7 ($1.5 \times \sigma'_{pc}$) in the fit significantly weakens the fit of SHANSEP to the measured undrained shear strength: SHANSEP overestimates the undrained shear strength at high stress levels, where the shear strength is measured to be virtually unchanged from the lower bound of the preconsolidation stresses. The improvement to the fit by excluding Test 7 can also be noted if the upper bound of the preconsolidation stresses are used to determine OCR (Figure 7.19). Table 7.8 shows that the parameter m is not affected by the preconsolidation stresses, as it remains constant between the two boundaries. The SHANSEP curves are identical between the two boundaries of the preconsolidation stresses as the larger S for the lower bound makes up for the

smaller values of OCR.

Table 7.8 SHANSEP parameters and the coefficient of determination (R^2) for both the lower and upper bound of the preconsolidation stresses.

	Lower bound			Upper bound		
	S	m	R^2	S	m	R^2
W/ $1.5 \times \sigma'_{pc}$	0.51	0.44	0.78	0.20	0.44	0.78
W/O $1.5 \times \sigma'_{pc}$	0.58	0.22	0.82	0.36	0.22	0.82

Using the lower bound of the preconsolidation stresses S is found to be in the high end of the interval mentioned earlier, whereas m is found to be significantly lower. This is due to the almost linear development of S_u up to the lower bound of the preconsolidation stresses, which was also used as the re-consolidation stresses. This is yet another indication that fissured structure determines the lower bound of the preconsolidation stresses.

7.4 Correlations

Advanced undrained triaxial tests are time-consuming and thereby costly, making estimations of the undrained shear strength based on other parameters crucial. Field vane shear tests and CPTs are often used for this purpose.

7.4.1 Field vane shear strength - μ

Field vane shear strength, c_{fv}, found via field vane tests are often used to assess the undrained shear strength, S_u. However, as stated in section 3 the fissured structure of Søvind Marl causes the strength to be significantly lessened compared to that of a similar unfissured clay. The strength is reduced by a factor μ:

$$\frac{S_u}{c_{fv}} = \mu \tag{7.4}$$

Christensen and Hansen (1959) determined μ to be one third on Skive Septarian Clay (a Danish highly fissured overconsolidated tertiary clay). The relation between the field vane shear strength for Søvind Marl and the undrained shear strength found in the undrained triaxial tests and using SHANSEP parameters are compared in Figure 7.20. c_{fv} is determined based on the linear correlation presented in Paper 2 (Appendix B), as it is believed to give the most accurate determination. Field vane shear tests were only carried out to a depth of 42 m, c_{fv} at lower depths are estimated by extending the linear correlation.

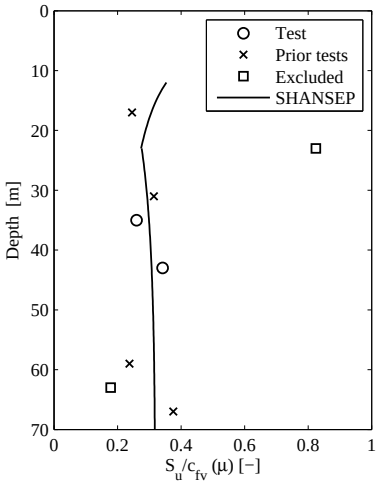

Figure 7.20 Comparison of the measured undrained shear strength and fiend vane shear strength to determine μ.

μ found using the measured undrained shear strength falls in the interval between 0.2 and 0.4 which is in great agreement of the findings by Christen and Hansen (1959). If the undrained shear strength is determined using the SHANSEP parameters found earlier, μ is found to decrease from 0.4 to 0.3 in the first 10 m of Søvind Marl due to the high increase in the field vane shear strength in these depths. Hereafter, μ becomes constant at 0.3 throughout the depth.

The determination and use of μ have often been discussed in the Danish geotechnical community, as it is a vital and commonly used parameter. The previous knowledge has been based solely on the tests performed by Christensen and Hansen (1959) (Illustrated in Figure 3.9). The test methods used differ from modern triaxial tests, making μ untested in regards to undrained triaxial tests on highly fissured tertiary clays. The undrained triaxial tests presented in this chapter confirm the relation between the undrained shear strength and the field vane shear strength to be 0.3.

7.4.2 Cone tip resistance - N_{kt}

The corrected cone tip resistance from CPT is also a useful tool to estimate the undrained shear strength, using the cone tip resistance factor, N_{kt}.

$$N_{kt} = \frac{q_t - \sigma_{v0}}{S_u} \tag{7.5}$$

Rad and Lunne (1988) found N_{kt} to vary between 8 and 29 and being dependent on OCR. Whereas Aas *et al.* (1988) and Powell and Quarterman (1988) found N_{kt} to be dependent on the plasticity, with N_{kt} increasing with plasticity. Powell and Quarterman (1988) found N_{kt} in the range of 10 to 30 when scale effects were considered.

The measured undrained shear strength is compared to the corrected cone tip resistance presented in Paper 2 (Appendix B). As stated in Paper 2, the corrected CPT data becomes unreliable at a depth of 25 m due to unmeasurable high pore pressure. Nonetheless, the correlation is made for the whole depth but is uncertain below depths of 25 m. Figure 7.21 and Figure 7.22 shows the determination of N_{kt} through the depth for the measured S_u and SHANSEP, respectively.

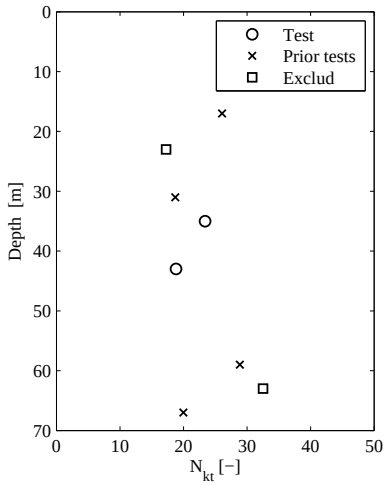

Figure 7.21 Comparison of undrained shear strength and corrected cone tip resistance to determine N_{kt}.

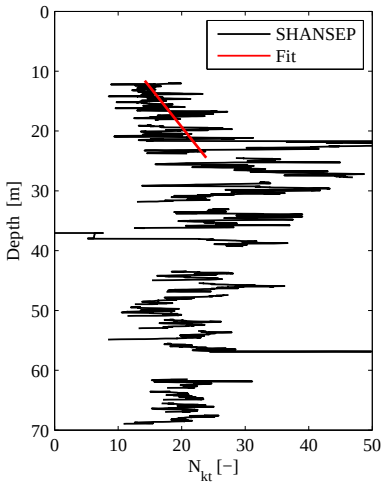

Figure 7.22 Comparison of undrained shear strength found via SHANSEP and corrected cone tip resistance to determine N_{kt}.

N_{kt} is for the measured samples in the interval between 20 and 30, which are in fine agreement with the intervals mentioned earlier, considering the high degree of overconsolidation and the very high plasticity of the samples. N_{kt} found using SHANSEP yields values in the same interval at lower depths where the CPTs are unreliable and slightly lower with values increasing from 15 to 22 at higher strata, in which the excess pore pressure was in the measurable range during the CPT (fit presented in Figure 7.22). This is relative low and not in correlation with the finding of Powell and Quarterman (1988), considering the very high plasticities in these strata (I_P between 100% and 250%). However, the results are likely more affected by the high overconsolidation ratio than the plasticity; an affect that was clear in the misclassification in the CPT classification charts (section 5.3.1). A N_{kt} value of 20 seems to be a likely estimate

of the cone tip resistance factor.

7.5 Recapitulation

The undrained shear strength is found for seven samples of Søvind Marl at different stress levels. SHANSEP parameters were found to be $S = 0.58$ and $m = 0.22$ and are used to describe the undrained strength through the depth. Furthermore, correlation factors to field vane shear strength and corrected cone tip resistance are found to be $\mu = 0.3$ and $N_{kt} = 20$, respectively. Figure 7.23 and Figure 7.24 present the undrained shear strength through the depth found by undrained triaxial tests, field vane shear tests and cone penetration tests.

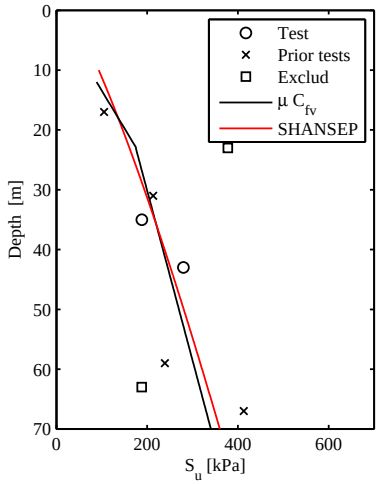

Figure 7.23 Estimations of the undrained shear strength through depth via field vane shear strength and SHANSEP.

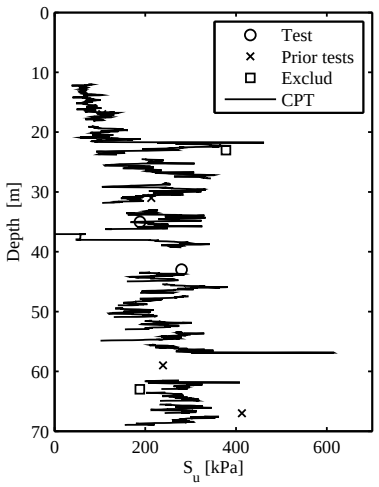

Figure 7.24 Estimations of the undrained shear strength through depth via corrected cone tip resistance.

The main purpose of the triaxial tests was to determine the undrained parameters of Søvind Marl. Furthermore, several methods were used in the attempt to determine the effective parameters of Søvind Marl. All methods yield unrealistic high parameters due to too high excess pore pressure. To determine the effective parameters, the deformation rate at the shearing step should be much lower than the 0.5 $\%/h$ used, extending the testing time significantly.

The undrained shear strength is often estimated based on field tests. For years, the relation between the undrained shear strength and the field vane shear strength has been estimated to one third based on few tests made by Christensen and Hansen (1959).

Through the undrained triaxial tests presented, the relation was confirmed to be approximately $\mu = 0.3$. The relation between the CPT corrected cone tip resistance and the undrained shear strength was determined to be approximately $N_{kt} = 20$.

Main points:

- The undrained shear strength is determined at various stress levels.
- The effective parameters are indeterminable due to a large pore pressure.
  - The shearing speed should be kept at 0.1 $\%/h$ for Søvind Marl due to the very low permeability.
- Best SHANSEP fit is obtained when only shear strengths at or below the lower bound of the preconsolidation stresses are used.
  - $S = 0.58$
  - $m = 0.22$
- The undrained shear strength was found to be 0.3 times the field vane shear strength ($\mu = 0.3$).
  - $S_u = 0.3 \cdot c_{fv}$
- The CPT cone tip resistance factor to the undrained shear strength was found to be 20 ($N_{kt} = 20$).
  - $S_u = \frac{q_t - \sigma_{v0}}{20}$

CHAPTER 8
Conclusion

The work presented in the present Ph.D. thesis was made to expand the knowledge of the behaviour of Søvind Marl, a highly plastic and fissured Eocene clay. This chapter gives an overview of the findings and main points of the studies leading to this Ph.D. thesis.

Søvind Marl has a post-sedimentation fissured structure. A literature study showed the influence of structure on the stiffness and shearing behaviour of a clay. The presence of a structure was found to generally have an increasing effect on both the stiffness and the shear failure envelope. However, a fissured structure had a very distinct influence on the behaviour. A post-sedimentation structure complicates a clear definition of the preconsolidation stresses for a heavily overconsolidated clay, and the presence of fissures would further complicate the determination as it gives a gradual change in the behaviour during closure of the fissures. This leads to the appearance of a lower and upper bound of the preconsolidation stresses. The undrained shear strength of a fissured clay was also described to be significantly lower than that of an unfissured clay, as failure occurs at the weakest part of the clay: the pre-existent fissures.

Part one of the thesis concerned the geotechnical description and properties of Søvind Marl. Tests were made to compare the liquid limit of Søvind Marl found using the Casagrande cup and fall cone, because the Eurocode states the fall cone as the preferred method over the traditional Casagrande cup. However, it was found that the fall cone yield values of the liquid limit increasingly lower than those of the Casagrande cup for liquid limits above 200%. This makes the usability of the fall cone limited on highly plastic clays. Visual description, general classification and field tests on Søvind Marl were presented to give a general knowledge of Søvind Marl. The used samples were between 40.5 million years and 46 million years old and all had a visual similar appearance with a highly fissured structure and only slight changes in colour. A notable property of Søvind Marl was a very high plasticity with plasticity index in the normal range of 100% to 250%, with extreme values over 300%. Søvind Marl was found to be very calcareous, with calcite content up to 65%. An inversely proportional connection between the plasticity and the calcite content was found. CPTs were found to quickly become unreliable due to an excess pore pressure too large to measure. Also CPT classification chart was found to mis-classify Søvind Marl as a silt or even sand

due to the high degree of overconsolidation of the clay. A pronounced change in the behaviour of many properties like plasticity, calcite content, shear vane strength and CPT cone tip resistance occurred at a depth of around 25 m. This suggested a substantial change in the macro behaviour despite no mesofabric change was evident in the appearance of the samples.

Part two of the thesis dealt with the stiffness of Søvind Marl found through different oedometer tests and analysing methods. This part presents the ANACONDA method for separating primary and secondary consolidation strains following oedometer tests, and introduces the method on highly plastic clays with high secondary consolidation index. It takes into account the consolidation and secondary consolidation process occur simultaneously. This is preferred when the secondary consolidation index is high, as is the case for Søvind Marl. The ANACONDA method is used to separate strains in all incremental oedometer tests presented in the thesis. Both incremental and continuous loading oedometer tests were made to determine the preconsolidation stresses of Søvind Marl. Two apparent values of the preconsolidation stresses were found at each sample independent of the testing or interpretation method used. The lower bound of the preconsolidation stresses was found to be between 600 kPa and 800 kPa, which was only two to three times the in situ stresses and not in agreement with the geological history of an Eocene clay. This was deemed to be a result of the fissured structure. The upper bound of the preconsolidation stresses was found in the range of 6300 kPa to 8900 kPa and is in agreement of the geological history of primary and secondary consolidation through millions of years. Continuous loading oedometer tests were found to give a much more accurate and detailed description of the behaviour of the sample during increasing testing. All oedometer tests were made on samples with a diameter of 35 mm to enable high stress levels in the sample. The reduction of the diameter from the standard 70 mm had very limited to no influence on the test results. During continuous loading oedometer tests, the horizontal pressure exercised by the sample was measured in order to determine the earth pressure at rest. High earth pressure at rest was found with values around 6 to 8 in the in situ stress range. The normally consolidated earth pressure at rest was determined to be independent of the friction angle, making Jaky's relation ($K_0(nc) = 1 - \sin(\varphi)$) of no use on highly plastic clays, like Søvind Marl. The normally consolidated earth pressure at rest should be determined through testing, since no existent relation yields useful values. The development of the earth pressure at rest is generally assumed dependent of the overconsolidation ration. However, Søvind marl was in this thesis found to lose its "short-term" memory even though the memory of the preconsolidation stresses was intact. The loss of memory results in a "new" preconsolidation set during testing, which should be used in the estimation of the overconsolidation ratio.

Part three of the thesis concerned the undrained triaxial tests and the determination of the strength parameters of Søvind Marl. Undrained shear strengths were found on seven samples and generally found to increase with increasing stresses. The samples were found to shear at pre-existent fissures, indicating that the strength of fissured clays is significantly lower than that of a similar un-fissured sample. The SHANSEP

parameters S and m were found to 0.58 and 0.22, respectively, when using undrained shear strengths found for stresses lower than the lower bound of the preconsolidation stresses. The lower bound was also used as the re-consolidation stresses and in the determination of OCR in relation to SHANSEP. The undrained triaxial tests were made to determine the undrained shear strength. However, it was attempted to estimate the effective parameters, but based on high excess pore pressure it proved difficult. Slower strain rates in the range of 0.1 $\%/h$ are expected to be needed if the effective parameters are the objective of the tests. The relation between the undrained shear strength and the field vane shear strength, μ, is in Danish geotechnical practice usually determined to be one third based on few field tests made by Christensen and Hansen (1959). In this thesis, the relation was confirmed for the first time on Søvind Marl using undrained triaxial tests to be $\mu = 0.3$ on Søvind Marl, while the CPT corrected cone factor was determined to be $N_{kt} = 20$.

8.1 Recommendations for future work

Recommendations for future work related, directly or indirectly, to this study are given to further expand the knowledge of plastic fissured clays.

General:

- Reconstituted samples
  The effect of the fissured structure should further be analysed. It is recommended to do this with reconstituted samples of Søvind Marl with focus on deformations at high stresses.

- Empirical correlation
  Typically, empirical correlations are made on clays with much lower plasticity and degrees of overconsolidation than Søvind Marl and similar clays. Unique correlations valid for clays with very high plasticity and a high degree of overconsolidation should be made and tested on several different clays.

- Influence of calcite
  The influence of calcite should be tested on parameters such as friction angle, earth pressure at rest and compressibility.

- Field tests
  Analysis of field tests results, like CPT, on overconsolidated clays in order to utilise tests results to e.g. classification of the soil.

- Database on plastic clays
  As the behaviour and properties of plastic clays are studied, the general knowledge increases. This knowledge should be compiled into a database consisting of research and commercial information, leading to a more comprehensive understanding.

Oedometer:

- Influence of strain rate
  Strain rate in CLO tests is chosen in order to minimise build-up of excess pore pressure. Analysis should be done on the influence of high excess pore pressure on test results compared to the influence of secondary consolidation on soil with high secondary consolidation index and low permeability.

- Consolidation modulus in CLO tests
  When analysing CLO tests, the chosen $\Delta\varepsilon$ or $\Delta\sigma$ have a significant influence on the consolidation modulus. The influence that this has on the determination of the preconsolidation stresses should be studied further, and a clear recommendation should be made. This is not only the case for plastic clays, but for CLO tests made on clays in general.

- Normally consolidated earth pressure at rest
  Clarifying whether or not a correlation of various parameters to $K_0(nc)$ exists on highly plastic clays.

Triaxial:

- Triaxial tests
  Establish testing procedure for undrained triaxial tests on highly plastic clays with low permeability in order to make determination of effective parameters possible.

CHAPTER 9
List of Symbols

Greek Symbols

α	Coefficient to determine the earth pressure at rest
γ	Bulk unit weight
γ_w	Unit weight of water
$\Delta\varepsilon_{\alpha c}$	Increase in secondary consolidation strains
$\Delta\varepsilon_c$	Increase in consolidation strains
$\Delta\sigma'$	Increase in effective stresses
Δu	Excess pore pressure
ε^E	Engineering strains
ε^N	Natural strains
$\varepsilon_{\alpha c}$	Secondary consolidation strains / creep
ε_c	Consolidation strains
ε_{tot}	Total vertical strain
μ	Field vane shear strength factor
σ_1	Maximum total principal stresses
σ_3	Minimum total principal stresses
σ'_κ	Reference stresses
σ'_H	Horizontal effective stresses
σ_H	Horizontal total stresses
σ'_{pc}	Preconsolidation stresses
σ'_{unload}	Unloading stresses

σ'_v	Vertical effective stresses
σ'_{v0}	Vertical effective in situ stresses
σ_{v0}	Vertical total in situ stresses
σ'_{vc}	Vertical effective consolidation stresses
σ'_y	Effective yield stresses
σ'_{vy}	Vertical effective yield stresses
σ'_{yl}	Lower boundary of the yield stresses
σ'_{yu}	Upper boundary of the yield stresses
φ	Friction angle

Latin Symbols

A_c	Activity
B_q	Pore pressure ratio
c'	Effective cohesion
C_c	Compression index
$C_{\alpha c}$	Secondary compression index
c_{fv}	Field vane shear strength
c_{fvr}	Remoulded field vane shear strength
c_v	Coefficient of consolidation
CF	Clay fraction
Cl^-	Chloride content
e	Void ratio
f_s	Sleeve friction
G_s	Specific gravity
H_0	Initial sample height
H_D	Drainage path
I_L	Liquidity index
I_P	Plasticity index

I_v	Void index
ICL	Intrinsic compression line
k	Coefficient of permeability
K_0	Earth pressure at rest
$K_0(nc)$	Normally consolidated earth pressure at rest
$K_0(oc)$	Overconsolidated earth pressure at rest
M	Consolidation modulus
m	SHANSEP parameter
N_{kt}	Corrected cone tip resistance factor
OCR	Overconsolidation ratio
OCR_{lab}	Overconsolidation ratio based on laboratory tests
p	Vertical mean total stresses
p'	Vertical mean effective stresses
q	Deviatoric stresses
q_c	Cone tip resistance
q_t	Corrected cone tip resistance
R^2	Coefficient of determination
R_f	Friction ratio
S	SHANSEP parameter
S_t	Sensitivity
S_u	Undrained shear strength
$S_u(mob)$	Mobilised undrained shear strength
SCL	Sedimentation compression line
T	Dimensionless time
t	Time
t_{50}	Time passed when 50% of the consolidation has occured
t_A	Characteristic time pasted before secondary consolidation started in the point A'

t_b	Characteristic time
U	Degree of consolidation
u	Deformation of sample
u_0	Hydrostatic pressure
u_0	Test water pressure
u_1	Pore pressure
u_2	Pore pressure
YCR	Yield stress ratio
Z	Depth
w	Natural water content
w_L	Liquid limit
w_{nat}	Natural water content
w_P	Plastic limit

Bibliography

Aas, G., LaCasse, S., Lunne, T., and Høeg, K (1988). Use of in situ tests for foundation design on clay. *Proceedimgs of the ASCE Specialty Conference In Situ '86: Use of In Situ Tests in Geotechnical Engineering*, 1–30. Blacksburg, American Society of Engineers (ASCE).

Abdelhamid, M.S. and Krizek, R.J. (1976). At rest lateral earth pressures of a consolidating clay. *ASCE Journal of Geotechnical Engineering Division* **102**(7), 721–738.

Akai, K. (1960). De strukturellen eigenschaften von schluft mitteilugen (in german). *Die Technische Hochschule Aachen*, Heft 22.

Amorosi, A. and Rampello, S. (1998). The influence of natural soil structure on the mechanical behavior of a stiff clay. *Proceedings of the 2nd International Symposium of Hard Soils, Soft Rocks*. 12th-14th of October 1998. Naples, Italy.

Andersen, S.A. (1937). Oligocænet ved aas. *Meddelser fra Dansk Geologisk Forening (in Danish)* **9**(2), 218–223.

Andrawes, K.Z. and El-Sohby, M.A. (1973). Factors affecting coefficient of earth pressure k_0. *Journal of the Soil Mechanics and Foundation Division ASCE* **99**(7), 527–539.

Armour Jr., D.W. and Drnevish, V.P. (1986). Improved techniques for the constant-rate-of-strain consolidation test. *Consolidation of soils: testing and evaluation, ASTM SPT 892*.

ASTM (2011). Standard practice for classification of soils for engineering purposes (unified soil classification system). *ASTM standard D2487. American Society for Testing and Material*. West Conshohocken, Pa. doi:10.1520/D2487-11.

ASTM (2012). Standard test method for one-dimensional consolidation properties of saturated cohesive soils using controlled-strain loading. *ASTM Standard: D4186-06*.

Augustesen, A., Andersen, L., and Sørensenl, C. S. (2005). *Time Function for Driven Piles in Clay*. Department of Civil Engineering, Aalborg University. ISBN:1398-6465.

Azzouz, A., Krizek, R., and Corotis, R.B. (1976). Regression analysis of soil compressibility. *Soils and Foundations Japanese Society of Soil Mechanics and Foundation Engineering*.

Balic-Žunić, T. (2008). *X-ray diffraction, Århus Harbor (Personal comminication)*. University of Copenhagen.

Banks, D.C., Strohm, W.E., De Angulo, M., and Lutton, R.J. (1975). *Study of clay-shale slopes along the Panama Canall*. US Army Engineers Waterways Expermint station, Vicksburg, Mississippi. Technical report S-70-9.

Bishop, A.W., Ewbb, D.L., and Lewin, P.I. (1965). Undisturbed samples of london clay from the ashford common shaft: Strength-effective stress relationships. *Geótechnique* **15**(1), 1–31.

Bjerrum, L. (1973). Problems of soil mechanics and construction on soft clays. *Proceeding 8th international conference on Soil Mechanics and Foundation Engineering* **3**, 111 – 159. 6th – 11th August 1973, Moscow.

Brinch Hansen, J. (1961). A model law for simultaneous primary and secondary consolidation. *Bulletin No. 13. The Danish Geotechnical Institute*.

Brooker, E.W. and Ireland, H.O. (1965). Earth pressure at rest related to stress history. *Canadian Geotechnical Journal* **2**(1), 1–15.

Burland, J.B. (1990). On the compressibility and shear strength of natural soils. 30th rankine lecture. *Geótechnique* **40**(3), 329–378.

Burland, J.B., Rampello, S., Georgiannou, V.N., and Calabresi, G. (1996). A laboratory study of the strength of four stiff clays. *Geótechnique* **46**(3), 491–514.

Casagrande, A. (1932). Research on the atterberg limits of soils. *Public Roads* **13**(8), 121 – 136.

Casagrande, A. (1936). The determination of the preconsolidation load and its practical significance. *International conference on soil mechanics and foundation engineering*. 22nd-26th of June 1936, Cambridge, Massachusetts, USA.

Chandler, R.J. and Apted, J.P. (1988). The effects of weathering on the strength of london clay. *Quarterly Journal of Engineering Geology & Hydrogeology* **21**(1), 59–68.

Christensen, N.H. and Hansen, B. (1959). Shear strength properties of skive septarian clay. *Bulletin No. 7. The Danish Geotechnical Institute*.

Clementino, Renato V. (2005). Discussion o f'an oedometer test study on the preconsolidation stress of glaciomarine clays'. *Canadian Geotechnical Journal* **42**, 972–974.

Coop, M.R., Atkinson, J.H., and Taylor, R.N. (1995). Strength and stiffness of structured and unstructured soils. *Proceedings of the11th European Conference on Soil Mechanics and Foundation Engineering, DGF-Bulletin 11* **1**, 1.55–1.62. 28th of May - 1st June 1995, Copenhagen , Denmark.

Cotecchia, F. and Chandler, R.J. (1997). The influence of structure on the pre-failure behaviour of a natural clay. *Geótechnique* **47**, 523–544.

Cotecchia, F. and Chandler, R.J. (1998). One-dimensional comperssion of a natural clay: Structural changes and mechanical effects. 12th-14th of October 1998. Naples, Italy.

Cotecchia, F. and Chandler, R.J. (2000). A general framework for the mechanical behaviour of clays. *Geótechnique* **50**(4), 431–447.

Crawford, C.B. (1986). State of the art: Evaluation and interpretation of soil consolidation tests. *ASTM STP 892. American Society for Testing and Materials*, 71–103.

Davison, L.R. (1989). *Continuous loading consolidation tests on soil*. Bristol Polytechnic. Ph.D. Thesis (CNAA).

DGF (1999). *Reference test procedure for field vane tests*. Danish Geotechnical Society - Field Committee.

Dobak, P. (2003). Loading velocity in consolidation analysis. *Geological Quarterly* **47**(1), 13–20.

Donath, A. (1891). Untersuchungen über den erddruk auf stützwände (in german). *Zeitschrift für Bauwesen* **41**, 491–518.

DS (2004a). *Geotechnical investigation and testing - Laboratory testing of soil - Part 1: Determination of water content*. Danish Standards Association. DS/CEN ISO/TS 17892-1.

DS (2004b). *Geotechnical investigation and testing - Laboratory testing of soil - Part 12: Determination of Atterberg limits*. Danish Standards Association. DS/CEN ISO/TS 17892-12.

DS (2004c). *Geotechnical investigation and testing - Laboratory testing of soil - Part 2: Determination of density of fine grained soil*. Danish Standards Association. DS/CEN ISO/TS 17892-2.

DS (2004d). *Geotechnical investigation and testing - Laboratory testing of soil - Part 3: Determination of particle density – Pycnometer method*. Danish Standards Association. DS/CEN ISO/TS 17892-3.

DS (2004e). *Geotechnical investigation and testing - Laboratory testing of soil - Part 5: Incremental loading oedometer test*. Danish Standards Association. DS/CEN ISO/TS 17892-5.

DS (2009). *Ground investigation and testing - Field testing - Part 9: Field vane test*. Danish Standards Association. DS/EN ISO 22476-9.

DS (2012). *Geotechnical investigation and testing - Field testing - Part 1: Electrical cone and piezocone penetration test*. Danish Standards Association. DS/EN ISO 22476-1.

Ducasse, P., Mieussens, C., Moreau, M., and Soyez, B. (1986). Oedometric testing in laboratories de ponts et chaussees, france. *ASTM STP 982. Consolidation of Spils: Testing and Evaluation*, 282–298.

Friis, H. (1995). Neogene aflejringer (in danish). *Department of Geology, Aarhus Univeristy*, 115–127.

Gasparre, A. and Coop, M.R (2008). Quantification of the effects of structure on the compression of a stiff clay. *Canadian Geotechnical Journal* **45**, 1324–1334.

Gasparre, A., Nishimura, S., Coop, M.R., and Jardine, R.J. (2008). The influence of structure on the behaviour of london clay. *Geótechnique* **57**(1), 19–31.

Gasparre, A., Nishimura, S., Minh, N.A., Coop, M.R., and Jardine, R.J. (2008). The stiffness of natural london clay. *Geótechnique* **57**(1), 33–47.

Geocenter Danmark (2005). De seneste 150.000 år i danmark (in danish). *Geoviden 2*. ISSN 1604-8172.

Geocenter Danmark (2010a). Neogen - da danmark streg op af havet (in danish). *Geoviden 3*. ISSN 1604-8172.

Geocenter Danmark (2010b). Palæogen - fra drivhus til kølehus (in danish). *Geoviden 3*. ISSN 1604-8172.

Gorman, C.T., Hopkins, T.C., Deen, R.C., and Drnevich, V.P. (1978). Constant-rate-of-strain and controlled-gradient testing. *Geotechnical Testing Journal* **1**, 3–15.

Grønbech, G.L., Ibsen, L.B., and Nielsen, B.N. (2010). *Chloride concentration and pHs influence on the Atterberg limits of Søvind Marl*. Department of Civil Engineering, Aalborg University, Denmark. DCE Technical Reports no. 088, ISSN 1901-726x.

Grønbech, G.L., Ibsen, L.B., and Nielsen, B.N. (2014). Preconsolidation of søvind marl - a highly fissured eocene clay. *Accepted with changes in Geotechnical Testing Journal*. Submitted for peer-review.

Grønbech, G.L., Nielsen, B.N., and Ibsen, L.B. (2011). Comparison of liquid limit of highly plastic clay by means of casagrande and fall cone apparatus. *Proceedings of 2011 Pan-Am CGS Geotechnical Conference. Toronto, Ontario, Canada*, Paper no. 1100.

Grønbech, G.L., Nielsen, B.N., and Ibsen, L.B. (2012a). Geotechnical classification of søvind marl. *NGM 2012, Nordisk Geoteknikermøde Bulletin No. 27* **1/2**, 95–102. 9th-12th of May 2012. Copenhagen, Denmark. ISBN 978-87-89833-27-9.

Grønbech, G.L., Nielsen, B.N., and Ibsen, L.B. (2012b). Interpretation of consolidation test on søvind marl. *NGM 2012, Nordisk Geoteknikermøde Bulletin No. 27* **1/2**, 85–93. 9th-12th of May 2012. Copenhagen, Denmark. ISBN 978-87-89833-27-9.

Grønbech, G.L., Nielsen, B.N., Ibsen, L.B., and Stockmarr, P. (2015). Geotechnical properties of søvind marl - a plastic eocene clay. *Canadian Geotechnical Journal* **52**. To be published at time of print of thesis.

Grontmij | Carl Bro (2008). *Geotechnical site investigation at Århus Harbor*. Grontmij | Carl Bro.

Hamilton, J.J. and Crawford, C.B. (1959). Improved determination of preconsolidation pressure of sensitive clay. *ASTM STP 254. American Society for Testing and Materials*, 254–271.

Hamouch, K., Leroueil, S., Roy, M., and Lutenegger, A.J. (1995). In situ evaluation of k_0 in eastern canada clays. *Canadian Geotechnical Journal* **32**(4), 677–688.

Hansbo, S. (1957). A new approach on the determination of shear strength of clay by fall cone test. *Royal Swedish Geotechnical Institute, Proceedings no.* **14**.

Head, K.H. (2006). *Manual of soil laboratory testing* (3 ed.). Whitles Publishing.

Heilmann-Clausen, C. (1995). Palæogene aflejringer over danskekalken (in danish). *Department of Geology, Aarhus Univeristy*, 69–114.

Heilmann-Clausen, C., Nielsen, O.B., and Gersner, F. (1985). Lithostratigraphy and depositional enviroments in the upper paleocen and eocene of denmark. *Bulletin of the Geological Society of Denmark, Copenhagen, Denmark*, 287–323.

Holt, R.D., Kovacs, W.D., and Sheahan, T.C. (2011). *An introduction to Geotechnical Engineering* (2 ed.). Pearson.

Holts, R.D. and Jamiolkowski, M.B. (1985). Discussion of time dependence of lateral earth pressure. *ASCE Journal of Geotechnical Engineering* **111**(10), 1239–1242.

Jacobsen, M. (1992a). Bestemmelse af forbelastningstryk i laboratoriet (in danish). *NGM-92, Nordisk Geoteknikermøde Bulletin No.9* **2/3**. 28th-30th of May 1992. Aalborg, Denmark. ISBN 87-983058-7-5.

Jacobsen, M. (1992b). Karakteristiske belastningstilstande for moræneler (in danish). *NGM-92, Nordisk Geoteknikermøde Bulletin No.9* **2/3**. 28th-30th of May 1992. Aalborg, Denmark. ISBN 87-983058-7-5.

Jaky, J. (1944). The coefficient of earth pressure at rest. *Journal for Society of Hungarian Architects and Engineers*, 355–358.

Janbu, N. (1970). *Grunnlag i Geoteknikk (in Norwegian)*. Tapir forlag.

Janbu, N., Tokheim, O., and Senneset, K. (1981). Consolidation tests with continuous loading. *Proceeding of: X International Conference on Soil Mechanics and Foundation Engineering, Stockholm, Sweden* **1**, 645–654.

Jones, D.E.J. and Holtz, W.G. (1973). Expansive soils - the hidden disaster. *Civil Enigneering* **43**(8).

Jovičić, V., Coop, M., and Simpson, B. (2006). Interpretation and modelling of deformation characteristics of a stiff north sea clay. *Canadian Geotechnical Journal* **43**, 341–354.

Karlsson, R. (1977). *Consistency Limits*. Swedish Council for Building Research in coorperation with the Laboratory Committee of the Swedish Geotechnical Society.

King, C. (1981). The stratigraphy of the london clay and associated deposits. *Tertiary Research Special Paper*, Paper no. 6. Rotterdam: Backhuys.

Knudsen, B. (1985). Problems concerning clays of very high plasticity in denmark. *Proceedings of the Eleventh International Conference on Soil Mechanics and Foundation Engineering* **4**, 2427–2429. San Francisco, 12th-16th of August 1985.

Knudsen, B. (1993). Plastisk ler- geotekniske problemer. *Geologisk Nyt* (1), 9–11.

Krogsbøl, A., Hededal, O., and Foged, N. (2012). Deformation properties of highly plastic fissured palaeogene clay – lack of stress memory? *NGM 2012, Nordisk Geoteknikermøde Bulletin No. 27* **1/2**, 133–140. 9th-12th of May 2012. Copenhagen, Denmark. ISBN 978-87-89833-27-9.

Lacasse, S. and Lunne, T. (1982). Penetration testing in two norwegian clays. *Penetration testing* **2**, 607–613. Balkema, Rotterdan, The Netherlands.

Ladd, C.C., Foott, R., Ishihara, K., Schlosser, F., and Poulos, H. G. (1977). Stress-deformation and strength characteristics. *Proceedings of: International Conference on Soil Mechanics and Foundation Engineering, 9th, 1977, Tokyo, Japan*.

Ladd, R.S. (1965). *Use of electrical pressure transducers to measure soil pressure*. Massachusetts Institute of Technology Research Report R65-48. No. 180.

Lambe, T.W. and Whitman, R.V. (1969). *Soil Mechanics*. John Wiley & Sons Inc., New York.

Lancellotta, R. (1993). *Geotecnica*. Zanichelli, II ed., Bologna.

Larsen, G. (1989). *Træk af Danmarks geologi (in Danish)*. DGF-Bulletin 3 - Danish Geotechnical Society.

Larsson, L. and Sällfors, G. (1986). Automatic continuous consolidation testing in sweden. *ASTM STP 982. Consolidation of Spils: Testing and Evaluation*, 299–328.

Lefebvre, G., Bozozuk, M., Philibert, A., and Hornych, P. (1991). Evaluating k_0 in champlain clays with hydraulic fracture tests. *Canadian Geotechnical Journal* **28**(3), 365–377.

Lefebvre, G. and Philibert, A. (1979). Measurement of lateral pressures in the one-dimensional consolidation of a structured clay. *In proceedings of the 32nd Canadian Geotechnical Conference, Québec, Canada. September*, 2.61–2.75.

Leroueil, S. and Vaughan, P.R. (1990). The general and congruent effects of structure in natural soils and weak rocks. *Geótechnique* **40**(3), 467–488.

Lunne, T., Robertson, P.K., and Powell, J.J. (1997). *Cone penetration testing in geotechnical practice*. Spon Press. ISBN: 0-419-23750-x.

Madsen, J.V., Johannesen, C.L., and Vestergaard, K.T. (2008). *Geotekniske egenskaber for tertiært ler ved Light*House*. Department of Civil Engineering, Aalborg University, Denmark. Masters Thesis.

Massarsch, K.R. (1979). Lateral earth pressure in normally consolidated clay. *Proceedings of the Seventh European Conference on Soil Mechanics and Foundation Engineering, Brighton, England* **2**, 245–250.

Mayne, P.W. (1988). Determining ocr in clays from laboratory strength. *J. Geotech. Engng. Div. Am. Soc. Civ. Engrs. 108, GT6*,, 75–92.

Mayne, P.W. and Kulhawy, F.H. (1982). k_0-ocr relationship in soil. *Journal of the Geotechnical Enigeering Devision, ASCE* **108**, 851–872.

Mesri, G. (1975). New design procedure for stability of soft clayclay, discussion. *Journal of Geotechnical Engineering, ASCE* **101**(4), 409–412.

Mesri, G. and Hayat, T.M. (1993). The coefficient of earth pressure at rest. *Canadian Geotechnical Journal* **30**, 647–666.

Meyerhof, G.G. (1976). Bearing capacity and settlement of pile foundations. *J. Geotech. Eng. Div. ASCE, No. CT3* **102**, 197–228. 11th Terzaghi Lecture.

NS (1993). *Geotechnical testing - Laboratory methods - Determination of one-dimensional consolidation properties by oedometer testing - Method using continuous loading (In Norwegian)*. Norsk Standard. NS 8018:1993.

Okkels, N. and Juul, K. (2008). Søvindmergel (in danish). *Danich Geological Society*.

Pacheco Silva, F. (1970). A new graphical construction for determination of the preconsolidation stress of a soil sample (in portuguese). *In Proceedings of the 4th Brazilian Conference on Soil Mechanics and Foundation Engineering* **2**(1), 225–121. August 1970. Rio de Janeiro.

Pantelidou, H. and Simpsoni, B. (2007). Geotechnical variation of london clay across central london. *Geótechnique* **57**(1), 101–112.

Powel, J.J.M. and Quarterman, R.S.T. (1988). The interpretation of cone penetration tests in clays, with particular reference to rate effects. *Proceedimgs of the International Symposium on Penetration Testing* **2**, 903–910. ISOPT-1, Orlando, Balkema Pub., Rotterdam.

Praastrup, U., Jakobsen, K.P., and Ibsen, L.B. (1999). Two theoretically consistent methods for analysing triaxial tests. *Computers and Geotechnics* **25**, 157–170.

Prakasha, K. and Sridharan, A. (2002). Determination of liquid limit from equilibrium sediment volume. *Geótechnique* **52**(9).

Rad, N.S. and Lunne, T. (1988). Direct correlations between piezocone test results and undrained shear strength of clay. *Proceedimgs of the International Symposium on Penetration Testing* **2**, 911–917. ISOPT-1, Orlando, Balkema Pub., Rotterdam.

Rasmussen, E.S., Dybkjær, K., and Piasecki, S. (2010). Lithostratigraphy of the upper oligocene - miocene succession of denmark. *Bulletin 22, Geological survey of Denmark and Greenland*.

Rosenqvist, I.T. (1953). Consideration on the sensitivity of norwegian quick clay. *Geótechnique* **3**(5), 22–52.

Rowe, P.W. (1954). A stress-strain theory for cohesionless soil with applications to earth pressure at rest and moving walls. *Géotechnique* **4**(1), 70–88.

Rowe, P.W. (1958). General report on papers in section i. *Proceedings of a Conference on Earth Pressure Problems, Brussels, Belgium. September* **3**, 25–30.

Rowe, P.W. and Barden, L. (1966). A new consolidation cell. *Géotechnique* **16**, 162–170.

Sahih, F., Leroueil, S., Rochelle, P., and French, I. (2002). Behaviour of the stiff and sensitive saint-jean-vianney clay in intact, destructured, and remoulded conditions. *Canadian Geotechnical Journal* **39**, 1075–1087.

Sheahan, T.C. and Watters, P.J. (1997). Experimental verification of crs consolidation theory. *Journal of geotechnical and geoenvironmental engineering* **125**(5), 430–437.

Skempton, A.W. (1953). The colloidal activity of clay. *Proceedings of the Third International Conference on Soil Mechanics and Foundation Engineering* **1**, 57–61. Zürich, Switzerland.

Skempton, A.W., Schuster, R.L., and Petley, D.J. (1969). Joints and fissures in the london clay at wraysbury and edgware. *Géotechnique* **19**(2), 205–217.

Smith, R. and Wahls, H. (1969). Consolidation under constant rate of strain. *Journal of the Soil Mechanics and Foundation Division ASCE* **90**, 519–538.

Standard Norge (1993). *Geoteknisk prøving Laboratoriemetoder Bestemmesle av endimensjonale konsolidaeringegenskaper ved ødometerprøving Metode med kontinuerlig belastning NS 8018 (in Norwegian)*. Standard Norge.

Steenfelt, J.S., Jakobsen, L., Frederiksen, J.K., and Christensen, H.F. (2014). Neogent ler (in danish). *Dansk Geoteknisk Forening*. Consultation edition.

Terzaghi, K. (1941). *Undisturbed Clay Samples and Undisturbed Clays*. Harvard University.

Terzaghi, K. (1944). Ends and means in soil mechanics. *Engineering Journal of Canada* **27**.

Terzaghi, K., Peck, R.B., and Mesri, G. (1996). *Soil Mechanics in Engineering Pratice, 3rd edition*. Wiley, New York. ISBN: 978-0-471-08658-1.

Thøgersen, L. (2001a). *Continuous Loading Oedometer Tests with measurement of Horizontal Pressure carried out on the Tertiary Little Belt Clay*. AAU Geotechnical Engineering Papers. Laboratory Testing paper. Aalborg University, Denmark.

Thøgersen, L. (2001b). *Effects of experimental techniques and osmotic pressure on the measured behaviour of tertiary expansive clay*, Volume 1. Soil Mechanics Laboratory, Aalborg University, Denmark. Ph.D. Thesis, ISSN: 1398-6465 R 2016.

Thomsen, Erik (1995). Kalk og kridt i den danske undergrund (in danish). *Department of Geology, Aarhus Univeristy*, 31–67.

Thomsen, E. (2008). *Coccolith-Stratigrafiske undersøgelser af boringer i Århus havn (Personal comminication)*. Geological Institute, Aarhus University.

Vitone, C., Cotecchia, F., Viggiani, G., and Hall, S.A. (2013). Strain fields and mechanical resopnse of a highly to medium fissured bentonite clay. *International Journal for Numerical and Analytical Methods in Geomechanics* **37**, 1510–1534.

Wasti, Y. (1987). Liquid and plastic limits as determined from fall cone and the casagrande methods. *Geotechnical Testing Journal* **10**(1).

Wissa, A.E.Z., Christian, J.T., Davis, E.H, and Heiberg, S (1971). Consolidation testing at constant rate of strain. *Journal of Soil Mechanics Foundation Division ASCE* **97**(10), 1393–1413.

Wroth, C.P. (1984). The interpretation of in situ soil tests. *Geótechnique* **34**(4), 449–489.

Wroth, C.P. and Wood, D.M. (1978). The correlation of index properties with some basic engineering properties. *Canadian Geotechnical Journal* **15**(2).

Appendix

APPENDIX A
Comparison of Liquid Limit of highly plastic clay by means of Casagrande and Fall Cone Apparatus

Authors:
Gitte Lyng Grønbech, Benjaminn Nordahl Nielsen and Lars Bo Ibsen

Published in:
Symposium Proceedings: 64th Canadian Geotechnical Conference and the 14th Pan-American Conference on Soil Mechanics and Engineering. 5th Pan-American Conference on Teaching and Learning of Geotechnical Engineering. October 2nd to 6th, 2011. Toronto, Canada.

Year of publication:
2011

A.1 Author's Right

Gitte Lyng Groenbech

Fra: CGS Administration - Wayne Gibson
Sendt: 27. september 2014 02:14
Til: Gitte Lyng Groenbech
Emne: RE: Author's Right

Dear Gitte,

The CGS conference does not ask authors to transfer copyright to us in order to be published in our proceedings – our release just seeks an author's permission for CGS to publish the paper and states that copyright remains with the author.

So, please include your paper as you have the rights to it. Please feel free to mention that is was first published in the proceedings of the 2011 Pan-Am CGS Geotechnical Conference.

Good luck with your Ph.D. thesis and defence.

Best regards,

Wayne Gibson, Administrator
The Canadian Geotechnical Society
La Société canadienne de géotechnique

http://www.cgs.ca

From: Gitte Lyng Groenbech
Sent: September-24-14 2:01 AM
To:
Subject: Author's Right

Dear Sir,

The Canadian Geotechnical Society hosted the 2011 Pan-Am CGS Geotechnical Conference in Toronto, Canada in October 2011. I attend with the paper "Comparison of Liquid Limit of highly plastic clay by means of Casagrande and Fall Cone Apparatus", which I would like to include in my Ph.D. thesis. I would like to ask for your permission to do so.

Sincerely /Venlig Hilsen

Gitte Lyng Grønbech
Ph.D. student
Geotechnical Engineering

AALBORG UNIVERSITY
DENMARK

Department of Civil Engineering
Sofiendalsvej 11
Lokale 9.109
DK-9000 Aalborg

Comparison of Liquid Limit of highly plastic clay by means of Casagrande and Fall Cone Apparatus

Gitte Lyng Grønbech, Benjaminn Nordahl Nielsen & Lars Bo Ibsen
Department of Civil Engineering – Aalborg University, Aalborg, Denmark

2011 Pan-Am CGS Geotechnical Conference

ABSTRACT
The connection between the Liquid Limit found using the Casagrande and the Fall Cone Apparatus is tested for the Danish Eocene Clay that has Liquid Limits up to 350% and Plasticity Index up to 300%, which is well outside the normal range of Casagrande's Plasticity Chart. Based on the high plasticity of the Danish Eocene Clay two new classification categories are introduces to the Plasticity Chart in order to fully describe the clay; super high plasticity Clay (CS) and extremely high plasticity clay (CE), covering the range up to Liquid Limits up to 200% and 350% respectively. A correlation between the Liquid Limit from the Casagrande and the Fall Cone Apparatus is for super high plasticity clay. For extremely high plasticity clay it was found that the Fall Cone method underestimated the Liquid Limit with up to 43 percentage points, making the Fall Cone an unreliable method of finding the Liquid Limit for extremely high plasticity clay

PRESENTACIONES TÉCNICAS
La relación entre el limite liquido es obtenida usando los métodos de Casagrande y el Cono de caída, ensayados para arcillas Danesas del Eoceno las cuales alcanzan limites líquidos de hasta 350% e índices plásticos de hasta 300%, lo cual está muy alejado del rango contemplado en la gráfica de Casagrande. Basándose en la alta plasticidad de las arcillas Danesas del Eoceno, dos nuevas categorías de clasificación son introducidas en el diagrama de plasticidad, de manera que la arcilla queda completamente descrita; arcillas súper plásticas (CS) y arcillas extremadamente plásticas (CE), de tal modo, que el limite liquido superior de 200% y 350% respectivamente queda completamente cubierto. Una correlación entre el limite líquido por Casagrande y el cono de Caída es hallada para arcillas súper plásticas. Para arcillas extremadamente plásticas, se halló que el método del Cono de caída infravalora el limite liquido hasta con un 43 por ciento, lo cual hace del Cono de caída un método poco fiable para determinar el limite liquido de arcillas extremadamente plásticas.

1 INTRODUCTION

The Atterberg Limits play a great role in assessing and classifying clay. Atterberg divided the behavior of clay into types, depended on the water content of the clay, the Atterberg Limits. The plasticity of clay is a property in clay that allows wet clay to be molded into a given shape when pressure is applied, and sustain the shape when pressure is released. The Plastic Limit, w_P, is the water content, at which the clays consistency changes from semi-solid to plastic. The Liquid Limit, w_L is the water content at which the consistency changes from plastic to liquid. The Plasticity Index, I_P, is given as the difference between the Liquid Limit and the Plastic Limit. The definition of the Atterberg Limits can be seen in Figure 1.

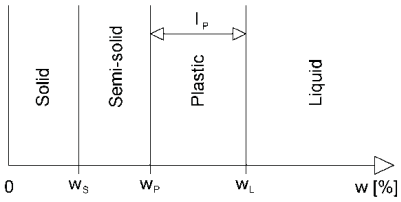

Figure 1. Atterberg Limits.

Classification of clay is done by Casagrande's Plasticity Chart (Casagrand, 1932), which covers a Liquid Limit up to 100% and a Plasticity Index up to 60%. The highly plastic Danish Eocene Clay has Liquid Limits up to 350%, making the normal plasticity chart useless to classify the Danish Eocene Clay. The Plasticity Chart for the Danish Eocene Clay can be seen in Figure 6.

The Liquid Limit is traditionally been determined by use of the Casagrande percussion cup method. This method is however very dependent on the apparatus and the person operating it, possibly resulting in variations of the results of each individual sample. Hansbo (1957) showed through a series of tests, that the Fall Cone Apparatus could be used as a quick and easy way to find the shear strength of soils. Wroth and Wood (1978) found that the Liquid Limit test establishes the water content, at which the clay has a certain undrained shear strength. They suggested, based on series of tests, that the Liquid Limit corresponds to a fall depth of 10 mm, when using a cone weighing 60 grams and having an angle of 60°.

Wasti (1987) compared Liquid Limits in the range between 27% and 110%, found by using the Casagrande and the Fall Cone method, of 15 soils from different locations in Turkey. The correlation found was given by:

$$w_{L(FC)} = 1.0056 \cdot w_{L(C)} + 4.92 \quad [1]$$

where $w_{L(FC)}$ and $w_{L(C)}$ is the Liquid Limit found by respectively the Fall Cone and the Casagrande method, most of these tests were covered by the Plasticity Chart. The correlation between the two methods becomes more

unclear, due to lack of data, for clay with extremely high Liquid Limits, like the Danish Eocene Clay. Head (2006) and Karlsson (1977) shoved that the Fall Cone tends to underestimate the Liquid Limit for clay which exceed the normal range of the Plasticity Chart.

The plastic properties of clay are, among other things, dependent on its ability to bind water to the crystal structure; this ability depends on the mineral composition of the clay. A description of the clay minerals in the tested Danish Eocene Clay can be seen in section 2.1.

In recent years the Fall Cone penetration method has however started to become the preferred method of determining the Liquid Limit compared to the Casagrande Apparatus method. It is wanted to find if this comparability of the two methods also applies to clays with an extremely high Liquid Limit, such as the Danish Eocene Clay.

In this paper the correlation between Liquid Limit found by the Fall Cone and the Casagrande method is assessed for highly plastic clays with Liquid Limits up to 350%, and a modification of Casagrande's Plasticity Chart is considered.

2 DESCRIPTION OF THE DANISH EOCENE CLAY

The climate of the Eocene period was in Northern Europe tropical or subtropical, and the sediments of the period are all deposited in the ocean of the time. The changes in the characteristic of the sediments are due to the changes in the water level and the degree of living organisms of the time. The sediments changes from limestone in the earlier deposits to clays and silt in the latest deposits. Through the Eocene layers around 180 layers of ashes from volcanic eruption can be found, evidence of a great and long lasting geological change. Above the layers of ashes large quantities of plastic clay is found. In Århus, Denmark the Danish Eocene Clay is located to depths of more than 70 meters and has a very high concentration of lime. The lime concentration varies from very light, 1 %, to highly limy, 65 % (Grontmij | Carl Bro 2008). The lime originates from coccoliths that lived when the Danish Eocene Clay was deposited.

Based on the coccoliths the age of the Danish Eocene Clay from a location in Århus, Denmark is determined. The coccoliths are all from NP zone 15 and 16, estimating the age of the Danish Eocene Clay to be between 40.5 and 46 million years old. It was determined that all the samples were from the Middle Eocene age, and the formations are located in a correct stratigraphic order, with no overlapping. (Thomsen, 2008)

2.1 Mineralogy

An analysis of the composition of the clay minerals in the Danish Eocene Clay has been made by Balic-Žunić (2008), it showed a very large percentage, up to 95%, of the clay have a grain diameter less than 2 μm. The composition of the clay minerals can be seen in Table 1.

The Clay mineralogy is the primary factor controlling the physical and chemical properties of clay. There are big differences on the behavior of each mineral type, and how big an influence it has on the plasticity. The clay mineral Smectite has a very large influence on the swelling of clay, since it has a big tendency to expand when it comes in contact with water. As can be seen in Table 1, almost half of the clay particles are Smectite, making the Danish Eocene Clay a very expansive clay, capable of absorbing large amounts of water.

Table 1. The composition of the clay minerals in the Danish Eocene Clay. The percentage of each clay mineral is in relation to the clay portion of the soil, and not the total soil sample. (Balic-Žunić, T. 2008.)

Depth (m)	15	30	45	60
Clay (%)	95.6	72.8	76.4	74.0
Kaolinite (%)	19	12	14	15
Illite (%)	33	15	12	17
Smectite (%)	44	34	42	33
Calcite (%)	2	25	30	34
Quartz (%)	2	1	1	1
Siderite (%)	-	7	1	-
Rhodochrosite (%)	-	6	-	-

2.2 Geotechnical properties

During and after boring a number of classification test was made on the Danish Eocene Clay and the pore water in the clay, the geotechnical properties can be seen in Table 2. Classification tests were made by Grontmij | Carl Bro (2008).

Table 2. Information and geotechnical properties of the Danish Eocene Clay. (Grontmij | Carl Bro 2008)

Age (mil. Years)	-	40.5 - 46
Depth[1] (m)	-	10 - 70
Water Content (%)	w	20 - 55
Liquid Limit (%)	w_L	87– 350
Plastic Limit (%)	w_P	31 – 60
Plasticity Index (%)	I_P	55– 285
Unit weight (kN/m^3)	γ	16.7 – 18.1
Vane strength (kPa)	c_v	280 - >715
Angle of friction (^{o})	φ'	12 - 25
Lime content (%)	-	1 - 65
pH	-	8.6 – 9.6
Cl^- content (%)	-	0.5 – 1.6

[1] The depth of which the Danish Eocene Clay is present.

The natural water content of the samples is similar to the Plastic Limit of the clay, meaning the soil in its natural state is semi-solid to only just plastic, cf. Figure 1. The pH and the Chloride concentration of the sample is measured in pore water extracted from the soil.

3 METHODS

Two methods have been use to determine the Plasticity Index of the Danish Eocene Clay, and there are found pro and cons with both.

3.1 Casagrande

The Casagrande Apparatus tests are carried out on an apparatus with a base of bakelite and a brass cup with a manual handle, Figure 2. A similar apparatus, but with an automatic handle, was also used for a portion of the tests, and the tests gave identical results independent of the

apparatus used, the measured water content and the resulting Liquid Limit.

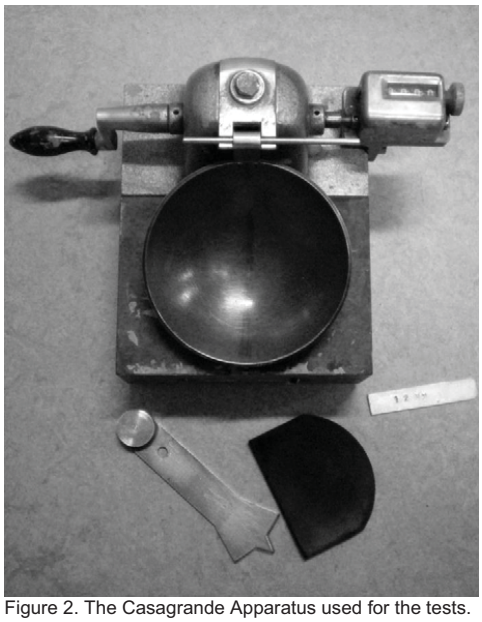

Figure 2. The Casagrande Apparatus used for the tests.

When using a Casagrande Apparatus, the Liquid Limit is defined as the water content at which the groove closes over a distance of 12 mm after 25 strokes at a rate of 2 strokes per second.

The results obtained by the Casagrande Apparatus method is however very dependent on the person operation the Casagrande Apparatus, thus making it hard to replicate the results when the same test is carried out on the same material, but by a different person. The factors dependent on the operator includes the rate at which the cup is dropped, judgment on when the sample is touching over a distance of 12mm, the placement of the sample in the cup and the making of the groove. Small variations in the height of the vertical drop of the cup also have a large influence in the number of strokes used to close the groove. Other factors that might influence the results are the material and state of the base and the cup, the fundaments stability and the grooving tool. (Prakasha et al., 2002)

3.2 Fall Cone

The Fall Cone tests are carried out on a Geonor Fall Cone Apparatus with a 60 grams / 60^{o} cone, Figure 3. The water content corresponding to a fall depth of 10 mm 5 seconds after release of the cone is described as the Liquid Limit.

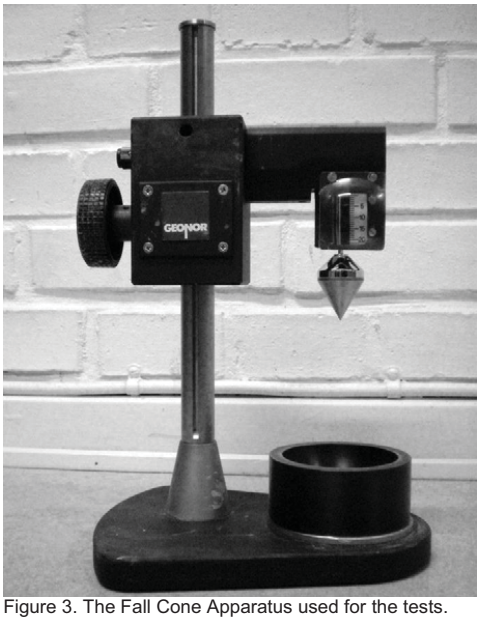

Figure 3. The Fall Cone Apparatus used for the tests.

The Fall Cone is widely known throughout the world, and the accepted standard for finding the Liquid Limit in many countries. The Fall Cone has the advantage over the Casagrande Apparatus that the operation of the apparatus is not affected by the operator, and the results are thereby comparable independent of the user. When using the Fall Cone Apparatus, one should be aware of the state of the cone, since a worn cone can affect the fall depth, and thereby the results of the Liquid Limit. Air pockets trapped in the clay around the point of impact can also influence the measured fall depth.

3.3 Plastic Limit

The Plastic Limit is found by rolling the clay on a glass plate into stings with a diameter of 3 mm, until they just do not crumble. Air drying is used to decrease the water content in the material. This is done to avoid a dry crust on the material that can occur when drying is done by slowly heating the material.

3.4 Homogenizing

For both the Casagrande cup and the Fall Cone method, the clay should be homogenize and the water content brought to a level close to yet under the Liquid Limit, which is a time-consuming process. The homogenizing of the clay is a very important part of finding the Liquid Limit, and should be done carefully. Not homogenizing the clay sufficient or mixing air in the clay can have a great influence on the outcome of the Liquid Limit.

The tests are made while gradually adding more de-ionized water. The tests are carried out simultaneously on both apparatus on the same material.

Through the tests, it became evident that the homogenization process has a great influence on the results of the tests, making it highly important to be meticulous.

Based on the high plasticity of the clay, a special homogenizing process was used. The material was first grated to small pieces with a maximum length of 1.5 cm and a thickness of 1-2 mm. The pieces were gathered in a plastic bag and added de-ionized water. The material was left over night to fully absorb the water. Hereafter the material was gently massaged through a sieve with a mesh aperture of 0.42 mm to discard any larger particles and to reduce any lumps of clay. There were no particles left at the sieve in any of the samples of the Danish Eocene Clay. The material was then placed in small portions at a glass plate, and a large spatula was used to further homogenize the material, Figure 4.

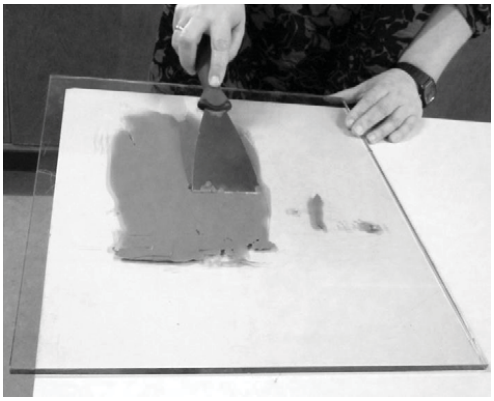

Figure 4. The material being homogenized on a glass plate.

The homogenizing was continued until no visual imperfections were left and the material had a glossy surface. This was done to all the material, and the material was finally collected in a bowl, where the material was molded together until it appeared as a uniform mass.

The homogenizing process is hard and time consuming, making it a costly process. At least two hours were used to sift and homogenize each sample prior to the tests, before an acceptable homogenization of the material was obtained.

During the tests when de-ionized was added to increase the water content of the material, homogenization was also proven to be important. A significant amount of water could be added to the material without an influence on the number of stroke or fall depth. If, however, the material was covered by a damp cloth and left to absorb the water for 15 min, there was a clear difference in the results of the tests. The effect of the absorption time was particularly clear for clay with an extremely high plasticity.

The lengthy duration of the homogenization before and during the test, one test could easily last up to 6 hours. This causes for a need to simplify or automate the homogenization process saving valuable man power.

4 RESULTS

The plasticity of the Danish Eocene Clay is found for 33 samples, for depth up to 69 meters under the surface. The results from both the Casagrande and Fall Cone Apparatus can be seen in Table 3.

Table 3. The measured Liquid and Plastic Limits for the samples of the Danish Eocene Clay. (C) marks results from the Casagrande Apparatus and (FC) marks the results from the Fall Cone Apparatus. - symbolize that the test was not preformed.

Sample No.	Depth (m)	w_P (%)	w_L (C) (%)	I_P (C) (%)	w_L (FC) (%)	I_P (FC) (%)
1	15.5	-	154.7	-	163.1	-
2	19.5	-	141.1	-	146.2	-
3	31.5	-	151.6	-	158.0	-
4	33.5	-	160.8	-	164.2	-
5	37.5	-	103.7	-	112.5	-
6	39.5	-	143.5	-	150.7	-
7	43.5	-	129.6	-	137.4	-
8	47.5	-	127.9	-	132.2	-
9	51.25	-	178.4	-	191.8	-
10	51.5	-	186.0	-	189.2	-
11	63.5	-	207.7	-	213.4	-
12	67.5	-	156.2	-	170.4	-
13	69.25	-	169.3	-	184.6	-
14	13	49.7	192.6	142.9	190.0	140.3
15	17	44.6	172,6	128.0	161.5	116.9
16	17	48.4	237.5	189.2	221.2	172.9
17	17	40.8	171.2	130.4	175.3	134.5
18	21	32.8	110.2	77.4	110.3	77.5
19	20	43.2	264.1	220.9	250.1	206.9
20	22	51.6	292.1	240.6	270.4	218.9
21	24	44.4	262.1	217.6	250.8	206.4
22	25	31.3	87.0	55.7	87.1	55.8
23	25	35.3	120.8	85.5	114.4	79.1
24	29	32.1	119.6	87.5	126.3	94.2
25	33	35.3	141.4	106.1	143.4	108.1
26	33	42.2	173.2	130.8	160.4	118.0
27	33	36.3	175.6	139.3	159.8	123.5
28	37	33.9	165.0	131.1	162.2	128.3
29	41	31.6	114.7	83.1	119.4	87.9
30	41	33.9	189.0	155.1	145.6	111.7
31	45	31.5	156.2	124.7	156.6	125.1
32	49	32.3	155.9	123.6	156.4	124.1
33	49	60.2	344.9	284.7	311.1	250.9

To see if there is a direct connection between the Liquid Limit from the two methods, the results from each sample is drawn in a chart with the Liquid Limit found using the Casagrande Apparatus at the abscissa axes and the Liquid Limit found using the Fall Cone Apparatus at the ordinate axes, the chart can be Figure 5.

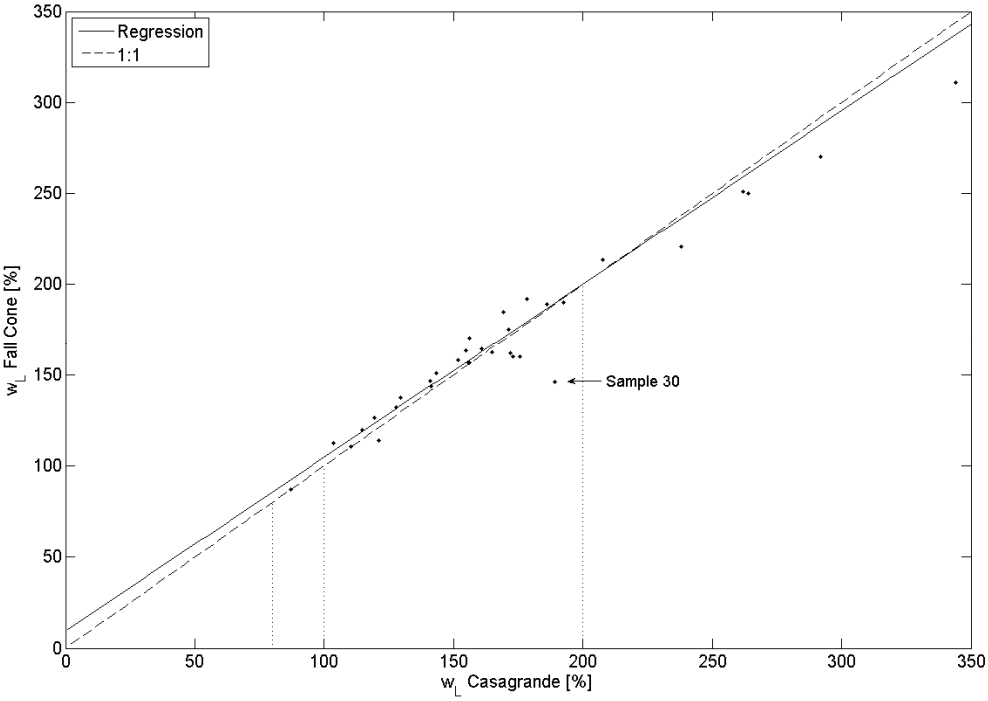

Figure 5. The relation between the Liquid Limit of the Danish Eocene Clay found using the Casagrande and Fall Cone Apparatus respectively.

The results appear to be approximately identical regardless of the methods used until a Liquid Limit of roughly 200%. Here after the results from the Fall Cone consistently gives smaller values for the Liquid Limit. This suggests that results can be divided into two groups, with a Liquid Limit of 200% as the separation point. The relation between the Liquid Limit of the Danish Eocene Clay in the range of 85% to 200% found by the two methods in Figure 5 can by using linear regression analysis using the least squares method be described as:

$$w_L(FC) = 0.95 \cdot w_L(C) + 9.4 \quad [2]$$

For the relation in Equation 2 sample No. 30 is not included since this is believed to give a false description of the relation. This relation correlates well with the relation found by Wasti (1987) in Equation 1 for up to very high plasticity clays.

The relation in Equation 2 shows that the Fall Cone gives slightly larger results for Liquid Limits up to 200%, which is also the limit for the valid range of the relation, and the Fall Cone results starts to significantly differ from the Casagrande results.

The Plasticity Index of sample no. 14-33 is plotted against the Liquid Limit in a plasticity chart for both methods, which can be seen Figure 6 and Figure 7 for Casagrande and Fall Cone respectively. The A-line in both figures is described by:

$$I_P = 0.73 \cdot (w_L - 20) \quad [3]$$

Casagrande defined the U-line (Upper Limit Line) as the limit for which results located beyond this line the Plasticity Index is too large for the corresponding Liquid Limit, and no sample can be located above this line, without an indication of an error in the results (Casagrande, as described in Holtz et al., 2011). The U-line is described by:

$$I_P = 0.9 \cdot (w_L - 8) \quad [4]$$

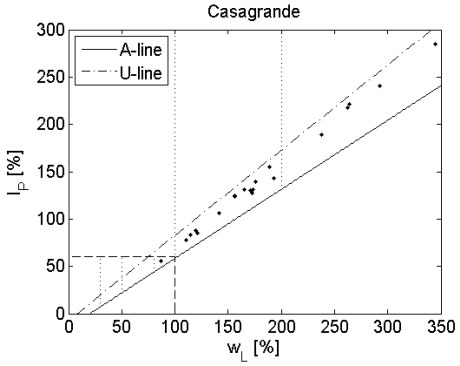

Figure 6. Plasticity Chart for the Danish Eocene Clay using the Casagrande Apparatus. The normal range of the Plasticity Chart is marked with the dashed lines.

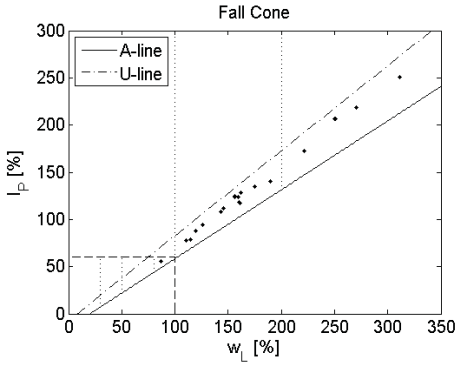

Figure 7. Plasticity Chart for the Danish Eocene Clay using the Fall Cone Apparatus. The normal range of the Plasticity Chart is marked with the dashed lines.

From Table 3 and Figure 6 and Figure 7, it is seen that all but one sample of the Danish Eocene Clay falls outside the normal range of the Plasticity chart, but still well above the A-line (Equation 3) and under the U-line (Equation 4), indicating that it is an exceptional plastic clay. This gives a need to expand the Plasticity Chart in order to include the Danish Eocene Clay. Based on the results found in Figure 5, two new classification categories are introduced; first a category for super high plasticity clay (CS) with a Liquid Limit of 100% to 200%, which is the range in which the results from the two methods correlated, succeed by a category for extremely high plasticity clay (CE) from 200% till 350% where there were no correlation between the results.

The very high concentration of clay particles of between 73 – 95% of the total soil sample, has large influence on the plasticity, and gives super and extremely high plasticity clay. By comparison of Table 1 and Table 3 it is noticed that the extreme high plasticity clay is primary located in depths with a high content of more than 40% of the clay mineral Smectite, which causes a highly expansive clay. The clay mineral composition has an influence on the Liquid Limit and for clays with large content of expansive minerals, like Smectite, the Fall Cone method is unreliable to use for Liquid Limit tests.

5 CONCLUSION

The plasticity and Liquid Limit of Danish Eocene Clay were discussed in this paper. The Danish Eocene Clay has a plasticity which has seldom been seen before, with Liquid Limits up to 350%. The main focus of this paper was to study the relation between Liquid Limit test preformed on the Casagrande and Fall Cone Apparatus.

In order to include the Danish Eocene Clay it has been necessary to modify the Casagrande Plasticity Chart. Only one sample of the Danish Eocene Clay could be described as a very high plasticity clay (CV), whereas the rest laid beyond the normal range of the Plasticity Chart. Two new categories were added; super high plasticity clay (CS) for clays with Liquid Limits between 100% and 200% and extremely high plasticity clay (CE) for clays with Liquid Limits between 200% and 300%. The updated plasticity chart can be seen in Figure 8.

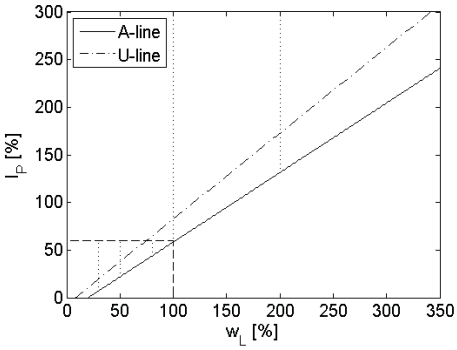

Figure 8. The Plasticity Chart adapted to include the Liquid Limits covered by the Danish Eocene Clay. The normal range of the Plasticity Chart is marked with the dashed line.

The classification of clay based on the Liquid Limit can be seen in Table 4.

Table 4. Classification of Clay.

	w_L (%)	USC-system
Low Plasticity Clay	<30	CL
Medium Plasticity Clay	30-50	CM
High Plasticity Clay	50-80	CH
Very High Plasticity Clay	80-100	CV
Super High Plasticity Clay	100-200	CS
Extremely High Plasticity Clay	200-350	CE

The behavior of the clay during the test varied dependent on the Liquid Limit, and a significant change happened around a Liquid Limit of 200%. For super high

plasticity clays (CS) it was found through Equation 2 that there was a good correlation between the results from the two methods making Equation 5 a valid approximation for Danish Eocene Clays with a Liquid Limit up to 200%.

$$w_L(FC) \cong w_L(C) \quad [5]$$

For extremely high plasticity clay (CE) there was found no correlation between the two methods for Danish Eocene Clays, and the Fall Cone largely underestimated the Liquid Limit, making this method unfit for extremely high plasticity clays.

On basis of the present tests the Fall Cone Apparatus only has a limited usability on the Danish Eocene Clay, and thus the results should be used with caution and clear specification on the test method used.

ACKNOWLEDGEMENTS

The project is funded by The Danish National Advanced Technology Foundation project “Cost-effective deep water foundations for large offshore wind turbines”. The funding is sincerely acknowledged.

REFERENCES

Balic-Žunić, T. 2008. X-ray diffraction, Århus Harbor, University of Copenhagen

Casagrande, A. 1932. *Research on the Atterberg Limits of Soils*. Public Roads, Vol 13. No 8. pp 121 - 136

Grontmij | Carl Bro. 2008. Geotechnical Site Investigation at Århus Harbor.

Hansbo, Sven. 1957. *A New approach on the determination of shear strength of clay by Fall Cone test.* Royal Swedish Geotechnical Institute. Proceedings no. 14

Head, K.H. 2006. *Manual of soil Laboratory testing*. 3rd edition. Whitles Publishing. 416 p

Holt, R.D., Kovacs, W.D. and Sheahan, T.C. 2011, *An Introduction to Geotechnical Engineering*. 2nd edition, International Edition, Pearson, 62 p

Karlsson, R.. *Consistency Limits* in cooperation with the Laboratory Committee of the Swedish Geotechnical Society, Swedish Council for Building Research, Document D&.. 40 p

Prakasha, K . and Sridharan, A. 2002. Determination of Liquid Limit from equilibrium sediment volume. *Geótechnique 52*. No. 9

Thomsen, Erik. 2008. Coccolith-Stratigrafiske undersøgelser af boringer I Århus havn. Geological Institute Aarhus University

Wasti, Yildiz. 1987. Liquid and Plastic Limits as Determined from the Fall Cone and the Casagrande Methods. *Geotechnical Testing Journal*. Volmune 10. Number 1

Wroth, C.P. and Wood, D.M. 1978. The correlation of index properties with some basic engineering properties of soil. *Canadian Geotechnical jounal.* Vol. 15 No. 2

APPENDIX B
Geotechnical properties of Søvind Marl - a plastic Eocene clay

Authors:
Gitte Lyng Grønbech, Benjaminn Nordahl Nielsen, Lars Bo Ibsen and Peter Stockmarr

Published in:
Canadian Geotechnical Journal Volume 52, 2015

Time of Acceptance:
September 2014

B.1 Author's Right

Authors' rights

As of 2009, copyright in all articles in NRC Research Press journals remains with the authors. All articles published previously are copyright Canadian Science Publishing (which operates as NRC Research Press) or its licensors (also see our Copyright information).

Under the terms of the license granted to NRC Research Press, authors retain the following rights:

1. To post a copy of their submitted manuscript (pre-print) on their own Web site, an institutional repository, a preprint server, or their funding body's designated archive (no embargo period).
2. To post a copy of their accepted manuscript (post-print) on their own Web site, an institutional repository, a preprint server, or their funding body's designated archive (no embargo period). Authors who archive or self-archive accepted articles are asked to provide a hyperlink from the manuscript to the Journal's Web site.
3. Authors, and any academic institution where they work at the time, may reproduce their manuscript for the purpose of course teaching.
4. Authors may reuse all or part of their manuscript in other works created by them for noncommercial purposes, provided the original publication in an NRC Research Press journal is acknowledged through a note or citation.

These authors' rights ensure that NRC Research Press journals are compliant with open access policies of research funding agencies, including the Canadian Institutes of Health Research, US National Institutes of Health, the Wellcome Trust, the UK Medical Research Council, the Institut national de la santé et de la recherche médicale in France, and others.

In support of authors who wish or need to sponsor open access to their published research articles, NRC Research Press also offers an OpenArticle option.

The above rights do not extend to copying or reproduction of the full article for commercial purposes. Authorization to do so may be obtained by clicking on the "Reprints & Permissions" link in the Article Tools box of the article in question or under license by Access©. The Article Tools box is accessible through the full-text article or abstract page.

http://www.nrcresearchpress.com/page/authors/information/rights

i. Title of the paper

Geotechnical properties of Søvind Marl - a plastic Eocene clay

ii. Authors

1. Gitte Lyng Grønbech
2. Benjaminn Nordahl Nielsen
3. Lars Bo Ibsen
4. Peter Stockmarr

iii. Affiliations

1. Ph.D. student, Aalborg University, Sofiendalsvej 9, 9200 Aalborg SV, Denmark, email: glg@civil.aau.dk
2. Associate Professor, Aalborg University, Sofiendalsvej 9, 9200 Aalborg SV, Denmark, email: bnn@civil.aau.dk
3. Professor, Aalborg University, Sofiendalsvej 9, 9200 Aalborg SV, Denmark email: lbi@civil.aau.dk
4. Senior geologist, Grontmij AS, Kokbjerg 5, 6000 Kolding, Denmark, email: Peter.Stockmarr@grontmij.dk

iv. Address

1. Gitte Lyng Grønbech, Sofiendalsvej 9, 9200 Aalborg SV, Denmark, Phone: (+45) 40 85 19 43, Fax (+45) 99 40 85 52, E-mail: glg@civil.aau.dk

Abstract, English

Results are presented of the analyses of the geotechnical properties of a fissured and highly plastic Danish tertiary clay: Søvind Marl. The analyses demonstrate the difficulties that can arise when dealing with this particular clay due to its unique characteristics. To characterise Søvind Marl and its pore water, samples were collected at multiple depths from five different borings located at the same site at Aarhus Harbour, Denmark, and all encountering the same Søvind Marl strata. Although Søvind Marl was deposited under circumstances very similar to those of London Clay, its properties show a poor resemblance to London Clay or other known clays. One of the key properties of Søvind Marl was found to be its extremely high plasticity, which can exceed 300%. Søvind Marl has high concentrations (up to 95%) of clay minerals, with a particularly large portion of smectite. Several key index parameters are presented and dissued including natural water content, Atterberg Limits (plasticity in the typical range of 100-250%), and calcite content (up to 65%). Results of vane shear tests and cone penetration tests are also presented. Oedometer tests yield two very different values for the preconsolidation stress level, although only one of these is correct. The dual calculation is associated with the fissured nature of Søvind Marl, which may confound traditional interpretation of test results, but must be taken into account for understanding of test results leading to proper classification of the material.

Key words: Fissured clay, Tertiary clay, High plasticity, Soil Classification, Site investigation, Overconsolidated clay

1 INTRODUCTION

Søvind Marl is an extremely plastic and highly overconsolidated Danish tertiary clay. It is part of a group of plastic clays found in Denmark, including Lillebælt Clay, Røsnæs Clay and others. Although the engineering challenges posed by these clays have hampered construction projects since the early 19th century, no comprehensive detailed study of this group has been completed.

Narrow bands of these clays run across Denmark in several areas and intersect locations where extensive construction activity occurs. One of the most prominent projects is the redevelopment of Aarhus Harbour from an industrial zone to an urban area. This redevelopment plan includes a variety of features, one of which is the tallest building in Denmark. At this location, Søvind Marl is found down to depths greater than 70 meters, a fact that must be taken into consideration when designing effective building foundations. The high plasticity and expansiveness of the clay can cause very large deformations both during the construction phase and over the lifespan of the construction. These problems are known from the Little Belt Bridge (Lillebælts broen), which opened in 1935. The foundation of this bridge has settled approximately 0.7 m to date.

The appearance and deposition environment of Søvind Marl is very similar to that of London Clay. However, Søvind Marl has several unique properties, thus limiting the utility of London Clay information when designing projects affected by Søvind Marl. Extremely high plasticity is one of the most prominent properties of this clay, with plasticity indices in the general range of 150% to 200%, and some as high as 300%. Søvind Marl is highly fissured with an elevated presence of slickensides, which can compromise the shear strength of the clay. In addition, the fissured structure makes the Søvind Marl sensitive to water penetration, and thereby possible swelling, in the event of excavation. This paper focuses on the geotechnical properties of Søvind Marl from Aarhus Harbour, which has been quantified through laboratory, index and field tests of collected samples.

2 GEOLOGICAL DESCRIPTION

Søvind Marl is a tertiary clay sediment deposited during the middle to late Eocene period. The clay deposit is found on top of the older Eocene Lillebælt Formation and below the Oligocene Viborg Formation. More than 60 m of Søvind Marl has been recorded at Aarhus Harbour.

Most tertiary sediments in Denmark are highly plastic clays, which are, in general, strongly fissured and additionally characterized by frequent slickensides. The formation of fissures and slickensides occurred due to consolidation, swelling, and glacial disturbance during the Eocene and into the Quaternary period. Søvind Marl was deposited in a relatively deep ancient seafloor, although the depth of the clay layers decreases from the underlying Lillebælt Formation and further decreases in the overlying Viborg Formation deposits. Søvind Marl was covered by up to 1 km of Oligocene and Miocene deposits over a period of about 20 million years (Geocenter Danmark 2010). These deposits have since eroded and are now located west of Denmark in the North Sea. At Aarhus Harbour, Søvind Marl is found under a small layer of glacial till and 10 m of man-made fill, primarily sand. Differences in the deposits may be related to climatic change factors, such as sea level, temperature, and marine biomass, which can impact the amount of calcite in the water and sediments. Current data indicate that Søvind Marl was deposited at about the same time as the first glaciation was occurring in Antarctica, even though Denmark itself had a tropical-subtropical environment during the Eocene. Elevated climatic variability can be interpreted from the highly layered calcite content of the marl; these conditions appear similar to the depositional environment leading to London Clay (King 1981).

Søvind Marl is the youngest Eocene Formation in Denmark and occurs at the western extent of the Danish Eocene deposits. Figure 1 illustrates the Eocene deposits found in Denmark. Present as a narrow band throughout the country, the deposits begin along the northwest coast at the island of Mors and run southeast in a sinuous pattern across Jutland to Aarhus (circled in Figure 1). From there the deposits cover the Little Belt area, the western and southern parts of Funen, and extend along the seabed to the southern coast of Lolland-Falster. Eocene deposits are also found in the north-western part of Zealand.

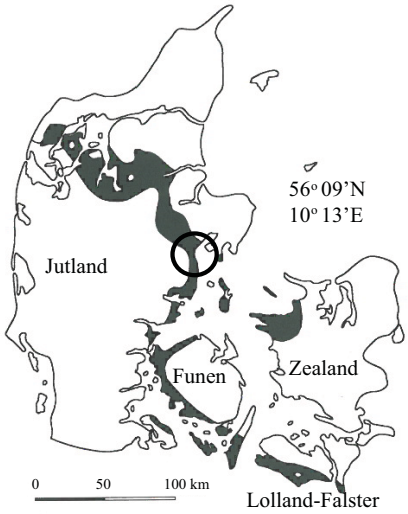

Figure 1: Locations of plastic Eocene deposits in Denmark (marked with a dark band). Listed coordinates are for the city of Aarhus, indicated by the circle.

As with any other marl, Søvind Marl has a very high calcite content. In Søvind Marl this calcite originates from the shells of coccolith fossils, which have been dated to estimate the age of deposits at Aarhus Harbour. The coccoliths found are all from the NP zones 15a to 16b (Figure 2). Based on these data Søvind Marl at Aarhus Harbour is between 40.5 and 46 million years old, placing it within the lower Søvind Marl Formation dating to the middle Eocene. Based on the coccolith stratigraphy presented in Figure 2, it was concluded that the Søvind Marl at Aarhus Harbour occurs in the stratigraphical order that reflects older material in deeper layers and progressively more recent deposition in the upper strata. This pattern indicates that very little or no disturbance or folding has taken place (Thomsen 2008).

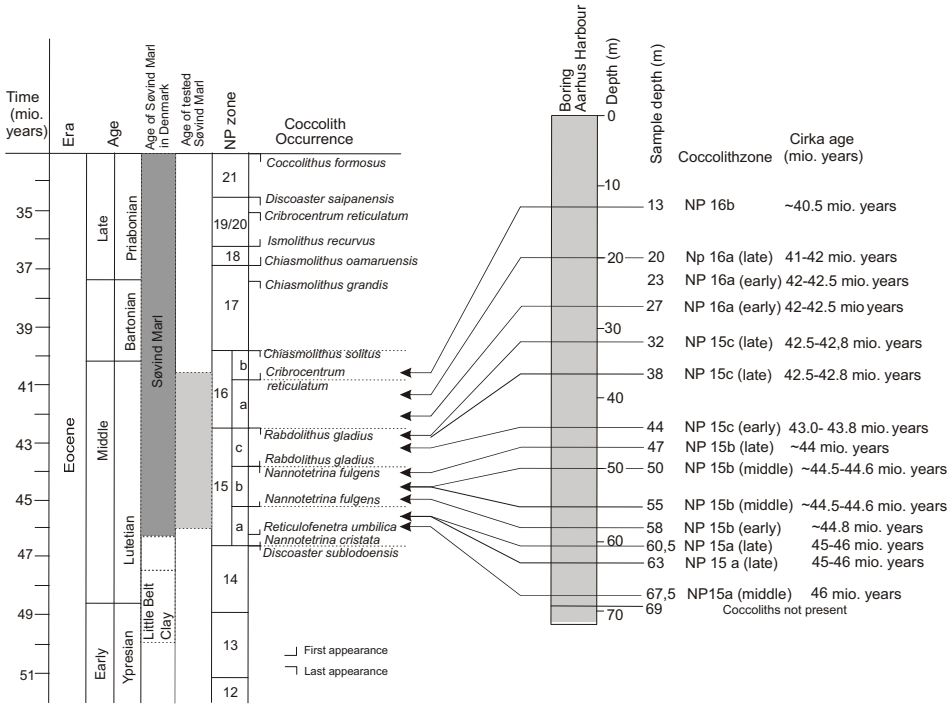

Figure 2: Geological stratigraphy and age determination. Modified after Thomsen (2008). Mio., million

3 CLAY MINERALOGY

The properties and behaviour of clay are highly dependent on the quantity and composition of the minerals present. Balić-Žunić (2008) determined the clay mineral composition of the same Søvind Marl that is the subject of the current study. The analysis of mineral composition, conducted on samples from four different depths of boring 11, was completed using X-ray powder diffraction employing the Rietveld refinement method and clay mineral preparation. The analysis showed that at a depth of 15 m, more than 95% of the soil particles have a grain size of less than 2 μm, as shown in Table 1. Between 15 and 30 m in depth the total soil composition changes, primarily due to a large increase in calcite.

Table 1: Clay composition of the Søvind Marl. After Balić-Žunić (2008)

Sample Metric *	Depth [m]			
	15	30	45	60
Clay size [%]	95.6	72.8	76.4	74.0
Kaolinite [%]	19/20	12/17	14/18	15/21
Illite [%]	33/34	15/21	12/16	17/23
Smectite [%]	44/45	34/46	42/55	33/44
Quartz [%]	2/1	1/1	1/1	1/<1
Calcite [%]	2/-	25/15	30/10	34/12
Siderite [%]	-/-	7/-	1/-	-/-
Rhodochrosite [%]	-/-	6/-	-/-	-/-
Total carbonat [%]	2/-	38/15	30/10	34/12

*With the exception of Clay size, values for all parameters are presented as mineral percentage of the total sample/percentage of the clay size fraction. Siderite and rhodochrosite are iron carbonate and manganese carbonate respectively.

Smectite is the primary clay mineral in Søvind Marl, accounting for 35–45% of the total sediment sample at every depth, which corresponds to 45–55% of the clay-sized fraction. The high smectite composition makes Søvind Marl a highly expansive clay. Kaolinite and illite are also relatively abundant at every depth, making Søvind Marl sensitive to environmental changes. At a depth of 30 m, nearly one-third of the sediment consists of calcite ($CaCO_3$). Figure 6 shows the calcite composition to be approximately 30% through the depth; however, a large fluctuation is evident. This indicates that the low calcite composition at 15 m (Table 1) is not representative of this stratum.

4 CLAY PROPERTIES

Characterization of Søvind Marl and its pore water was conducted by Aalborg University and the engineering company Grontmij AS. For the tests, five different borings (labelled 7, 8, 9, 10, and 11) were made, all situated approximately 15 m apart at Aarhus Harbour. The depth of the borings varied from 40 to 69 m, but all encountered Søvind Marl at a depth of 11–12 m. Data shown here from the borings begins at a depth of 10 m. All tests were performed according to current Danish Standards unless otherwise noted.

4.1 Visual Description

Søvind Marl appears very uniform throughout all the layers, with no visible particles. The fissures and slickensides that characterize Søvind Marl run in unstructured directions throughout the material. The fissures developed during the loading and unloading of the clay that occurred over millions of years and during at least seven known ice ages. During unloading periods, for example during glacial melt and erosion, clay swelled vertically, resulting in tearing and fissure formation. Figure 3 shows that the surfaces of the clay, fissures and slickensides have a shiny appearance, which is indicative of high plasticity. The structure of Søvind Marl is similar to the structure known from formations such as London Clay.

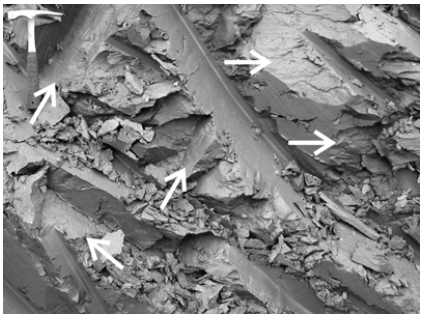

Figure 3: Fissured surface of Søvind Marl; slickensides are evident.

The colour of the Søvind Marl ranges from light grey to dark grey, as well as olive brown-green. The greatest influence on colour is the proportion of calcite, with a lighter colour resulting from higher calcite levels.

4.2 Unit Weight and Specific Gravity

The bulk unit weight, γ, of Søvind Marl is between 16.7 and 18.1 kN/m^3. This is a relatively low bulk unit weight, which is caused by the high natural water content. The presence of large numbers of hollow coccoliths results in many cavities in which the water can be stored. The bulk unit weight was determined according to DS/CEN ISO/TS 17892-2 (DS 2004b). The specific gravity, G_s, was found to be relatively high with values between 2.7 and 2.8. The specific gravity was determined according to DS/CEN ISO/TS 17892-3 (DS 2004c).

4.3 Atterberg Limits and Natural Water Content

The Atterberg limits consist of the plastic limit, w_P, and liquid limit, w_L. The plastic limit is found by rolling the clay to a thickness of 3 mm and the liquid limit is found using the Casagrande cup (Casagrande, 1932). The material was homogenized with de-ionized or distilled water according to standard procedures, and the tests are performed within 24 h. Using de-ionized water has a leaching effect of approximately 10% on Søvind Marl Atterberg limits (Grønbech et al. 2010), resulting in a higher value relative to those determined using a natural saline test water. If the Atterberg limits are to be used in empirical correlations, it is important to note whether a saline solution is the preferred water. The plastic and liquid limits and natural water content determinationswere performed as described in DS/CEN ISO/TS 17892-12 (DS 2004e) and DS/CEN ISO/TS 17892-1 (DS 2004a), respectively. The Atterberg limits and natural water content, w, of Søvind Marl are presented in Figure 4.

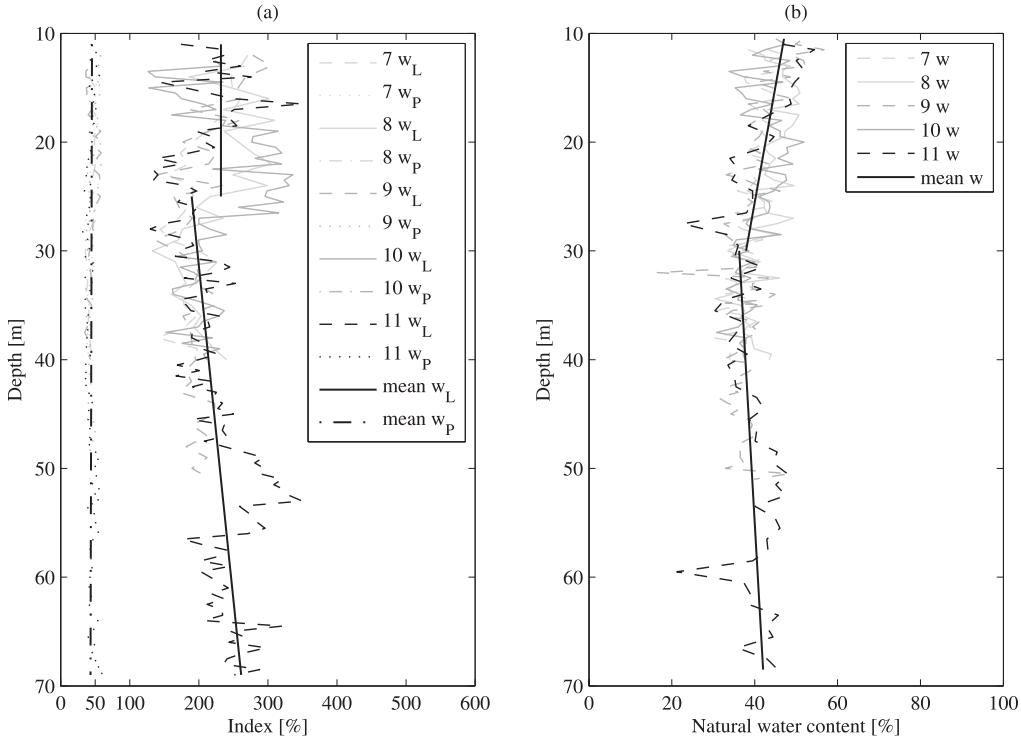

Figure 4: Characteristics of Søvind Marl, (a) Atterberg limits and (b) natural water content.

The plastic limit of Søvind Marl was found to be roughly constant regardless of depth with a value of around 50%. There was, however, notable variability in the liquid limit. To a depth of approximately 25 m, the liquid limit varied between 150% and 300%, with a mean value of 230% and some values as high as 350%. From 25 m downward, the liquid limit was just over 200%, increasing slightly with depth to 250%, and with peak values of 350%.

The natural water content varied with depth. In the upper strata, Søvind Marl had a relatively high water content of around 50% for all borings. Increasing depth resulted in a slight but steady decrease in water content reaching approximately 35% at 30 m, where it remained as the depth increased further.

The Søvind Marl plasticity index, I_P, which is the difference between the liquid and plastic limits, varied with depth, particularly between 12 and 25 m. Within this depth interval, the plasticity index typically ranged between 100% and 250%, with extreme values as high as 300%. At greater depths, the plasticity index was approximately 150%, once again demonstrating a slight increase with increasing depth. At

306%, Søvind Marl has the highest measured plasticity index of any soil in Denmark. The liquidity index, I_L, was found to vary between -0.05 and 0.05, a range that suggests a consistent ability to shift between semi-solid and plastic states, with a plastic state most often occurring in the upper strata.

The high plasticity of Søvind Marl is driven primarily by several different clay minerals, comprising about two-thirds of the clay, one-third of which (50% of the total clay component) is smectite. Spatial variability in plasticity of Søvind Marl with depth is due to differences in the composition and amount of clay minerals as well as nonplastic materials, primarily calcite, which can "dilute" the clay.

Casagrande (1932) introduced the plasticity chart to classify soils based on the liquid limit and plasticity index. The original and most often used plasticity chart has maximum liquid limit and plasticity index of 100% and 60%, respectively. However, this is too restrictive for an adequate description of Søvind Marl plasticity where liquid limits may be as high as 350%. Grønbech et al. (2011) proposed an updated version of the plasticity chart, which extends the range to account for the plasticity of Søvind Marl, and introduces two new Unified Soil Classification categories System (USCS; ASTM 2011): super high plasticity clay (CS) and extremely high plasticity clay (CE). Figure 5 presents the data from the Søvind Marl samples, and shows that it easily falls into these categories, with the majority of samples extending into the CE range.

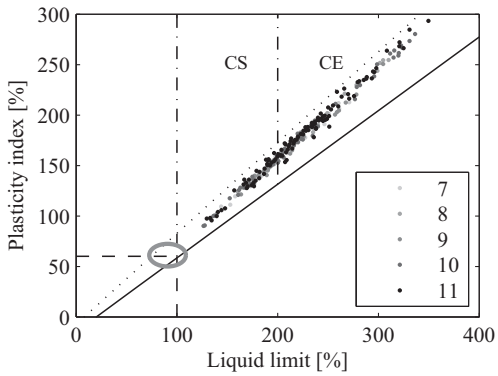

Figure 5: Plasticity chart with extended ranges to accommodate Søvind Marl. Dotted lines mark the area of the original chart. Dashed-dotted lines mark the new USCS categories proposed by Grønbech et al. (2011). Grey oval marks the location of London Clay (Pantelidou and Simpson, 2007).

4.4 Calcite Composition

Because calcite is generally found in high concentrations in marl, it is not surprising that calcite is abundant in Søvind Marl. Figure 6 shows that the downhole calcite levels vary significantly, even over small distances. These variations are a result of environmental fluctuations at the time of deposit. In the first 15 m of Søvind Marl, in four of the borings, calcite percentage was measured at 5–30%. However, in boring 10 the percentage of calcite was nearly 65% in the first 10 m of Søvind Marl, after which calcite percentage declined to approximately 5–20%. This amount corresponds to the calcite content presented in Table 1. Beyond 25 m calcite levels continue to fluctuate, with a slight increasing tendency to 40% at 50 m. It is not surprising, given calcite's non-plastic nature, that increasing calcite levels are associated with decreasing plasticity, which is clearly evident when calcite percentage is plotted against the plasticity index in Figure 7.

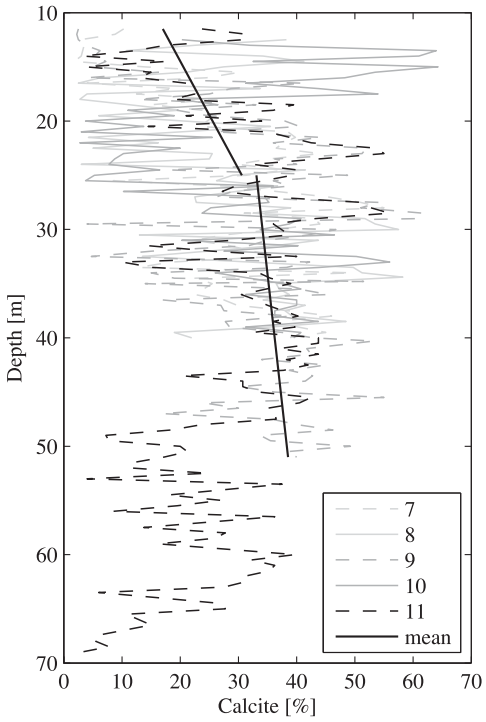

Figure 6: Calcite content of Søvind Marl.

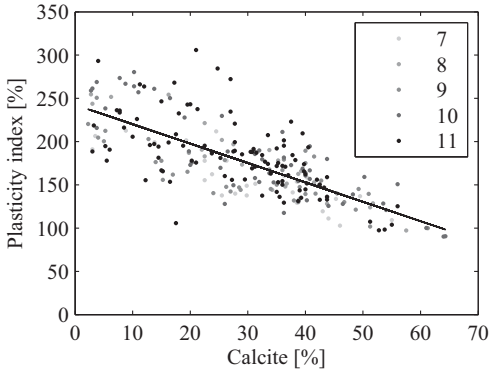

Figure 7: Relationship between plasticity index and calcite content in samples of Søvind Marl collected at multiple depths.

The effect of calcite concentrations on the plasticity of Søvind Marl is more predictable at higher calcite levels, with a substantial decrease in variability around the trend line, as shown in Figure 7. As the calcite level decreases, its effect on plasticity lessens, the correlation weakens and the data are more variable. At these lower calcite concentrations the plasticity of the clay minerals becomes increasingly significant. The increasing importance of high concentrations of calcite is evident in the following equation, which expresses the calcite plasticity index correlation:

$$I_P = 242.5 - 2.24 \cdot (Calcite[\%]) \qquad [1]$$

4.5 Clay Size Fraction and Activity

The activity, A_C, as defined by Skempton (1953) of Søvind Marl was determined in four samples, corresponding to the depths shown in Table 2; all samples are from boring 11. Søvind Marl was found to have a very high activity between 1.74 and 2.74, which is related to a high amount of smectite, which itself has an activity between 1 and 7. An increase in activity occurs below a depth of 30 m, where Smectite concentrations also rose.

Table 2: Activity of the Søvind Marlin boring 11.

Sample Metric	Depth [m]			
	15	30	45	60
I_p [%]	167*	130	208	174
CF[%]	96	73	76	74
Activity (-)	1.74	1.78	2.74	2.35

*I_P found at a depth of 15.5 m

4.6 Vane Shear Strength

In situ vane shear tests were completed simultaneously with the borings. All in situ vane tests were run according to current European standard DS/EN ISO 22476-9 (DS 2009) with regard to the Danish

engineering practice (DGF 1999). A deep vane, V4, was used with a height of 80 mm and a diameter of 40 mm; the torque was measured by a 50 kg dial indicator spring. Both the undisturbed, c_{fv}, and remoulded, c_{fvr}, vane shear strengths were measured. The tests were conducted to a depth of 42 m in each of the borings, and are presented in Figure 8.

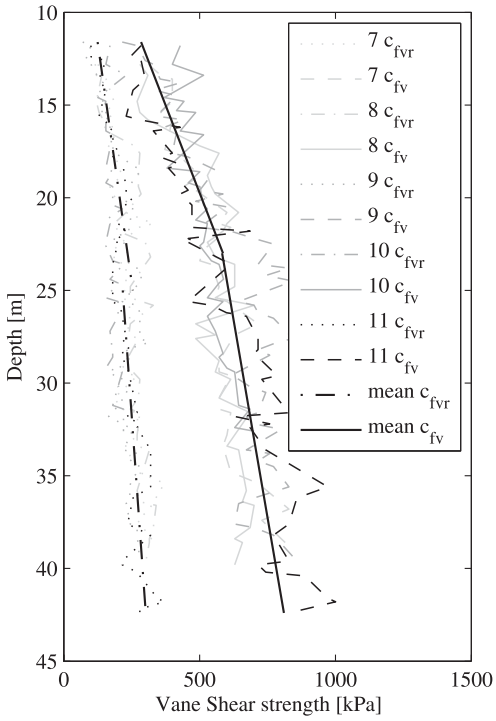

Figure 8: Undisturbed, c_{fv}, and remoulded, c_{fvr}, vane shear strength of Søvind Marl.

Vane shear strengths in each boring were very similar at every depth. The undisturbed vane shear strength of Søvind Marl increased with depth in all borings in a relatively linear trend, from approximately 300 kPa at 12 m to 600 kPa at approximately 25 m. The rate of increase of vane shear strength slowed after 25 m and reached a maximum of approximately 850 kPa 42 m. The high vane shear strength values are due to the very high degree of overconsolidation in Søvind Marl. The remoulded vane shear strength also increased with greater depth, although the rise in values was less pronounced than for

undisturbed vane shear strength. Remoulded vane shear strength increased from 100 kPa to about 350 kPa at 42 m. The rate of increase of remoulded vane shear strength also slowed at approximately 25 m, which is roughly the depth where calcite concentration dropped, as seen in Figure 6. It is unclear whether this phenomenon is a direct, indirect or coincidental occurrence, although the data indicate that multiple parameters are clearly interrelated, with fluctuations in one precipitating concurrent alterations in others

The fissured nature of Søvind Marl affects the shear strength, S_u, with respect to load-bearing capacity. Because load failure occurs at the weakest point, failure in Søvind Marl tends to run along the fissures. Christensen and Hansen (1959) showed that in highly fissured tertiary clays only one-quarter to one-third of the vane shear strength can be used as an estimate of the bearing capacity.

Terzaghi (1944) described sensitivity, S_t, as an indicator of the loss of shear strength of a soil when remoulded. Sensitivity is the ratio between the undisturbed and the remoulded shear strengths. In the current study sensitivity varies between 1.6 and 4 with a slight increase with depth, making Søvind Marl a medium sensitive clay, as it loses a great part of its strength when remoulded (Rosenqvist 1953). No correlation was found between the sensitivity or vane shear strength and plasticity or calcite content.

5 PORE WATER CHARACTERISTICS

Søvind Marl is a marine deposit and consequently the pore water is saline. The chemical properties of pore water play an important role in the behaviour of the clay and its response to external and internal forces. It is important to understand the composition of pore water prior to performing advanced analyses. The more the test water resembles the natural pore water, the less the water composition influences test results (Thøgersen 2001). The chloride concentration of the pore water was measured by dispersing the clay in de-ionized water and measuring chloride in the extracted water mixture. Chloride was measured in samples from boring 11. Figure 9 shows the chloride concentration and pH of Søvind Marl.

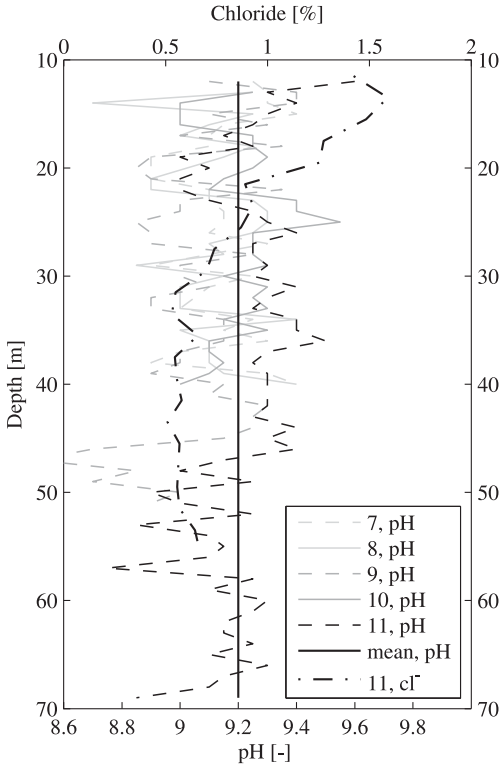

Figure 9: pH of pore water in Søvind Marl, and chloride concentration of pore water from boring 11.

The chloride concentration decreased from a high concentration of 1.5% (15 g/L) at a depth of 12 m to around 0.5% (5 g/L) at a depth of 27 m after where the concentration stabilized. The pH varied from 8.9 to 9.4 for all measured samples with an average value of 9.2. The pH was not correlated with depth or any index parameter. As the clay minerals kaolinite and illite are very dependent on environmental pH, it is important during testing and analysis that the natural ambient pH of the test water be maintained in order to avoid a negative charge in the clay. Failure to do so will result in inaccurate test results.

6 CONE PENETRATION TESTS

Cone penetration tests (CPTs) were performed on all five borings to depths of 40 to 69 m. The cone used was an ENVI Memocone corded CPT (Environmental Mechanics AB, Alingsås, Sweden), with a cone

diameter of 36 mm. The tests were performed and interpreted according to European standard DS/EN ISO 22476-1 (DS 2012). The tests were performed as standard CPTs with a penetration rate of 20 mm/s. Measurements were made every 2 cm. The CPTs on Søvind Marl start at a depth of 12 m.

6.1 Measured Uncorrected Parameters

During the test, three parameters were measured: cone tip resistance, q_c, sleeve friction, f_s, and pore pressure, u_2. These three uncorrected parameters plus vertical effective in situ stresses, σ'_{v0} and hydrostatic pressure, u_0, are illustrated in Figure 10. During testing, it was necessary to drill at several depths, which is evident in Figure 10 by sudden leaps in the values.

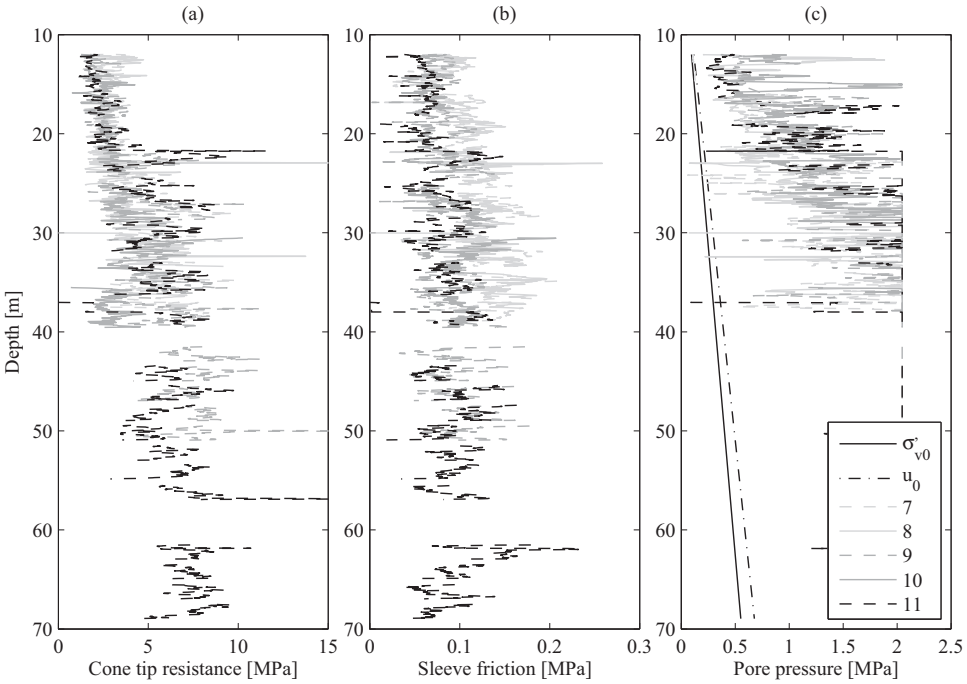

Figure 10: Uncorrected CPT data: (a) uncorrected cone tip resistance, (b) sleeve friction and (c) pore pressure. Vertical effective in situ stress and hydrostatic pressure are also shown in (c).

Cone tip resistance was very uniform in all of the borings up to a depth of just over 20 m, at that point cone tip resistance increased slightly from 1.5 to 3 MPa. After 22 m the cone tip resistance increased at a higher rate and reached about 7 MPa at 40 m, after which it stabilized. In this interval, there is a large variation of the cone tip resistance. Overconsolidated clays tend to have very high cone tip resistance, due to the high degree of overconsolidation, which for Søvind Marl is approximately 25 (Table 3). Sleeve friction increased slightly in the first 10 m, from 60 to 100 kPa, before becoming relatively constant. Pore pressures were found to be very high compared to the hydrostatic pressure. The pore pressure increased from 0.3 MPa at 12 m to over 2 MPa at 25 m. The high excess pore pressure, Δu, consequently carried a large portion of the applied load. This phenomenon indicates soil with very low permeability, making it unable to adequately drain during the standard test. The CPT apparatus can only measure pore pressures up to 2 MPa, resulting in a sharp right edge to the graphed pore pressure from a depth of 25 m.

6.2 Derived Parameters

Several useful parameters can be derived from the measured CPT parameters, including corrected cone tip resistance, q_t, friction ratio, R_f, and pore pressure ratio, B_q (e.g. Lunne et al., 1997). All derived parameters are dependent on the pore pressure, which becomes unreliable at a depth of approximately 25 m. The derived parameters are therefore only considered accurate and reliable down to 25 m, which is presented in Figure 11.

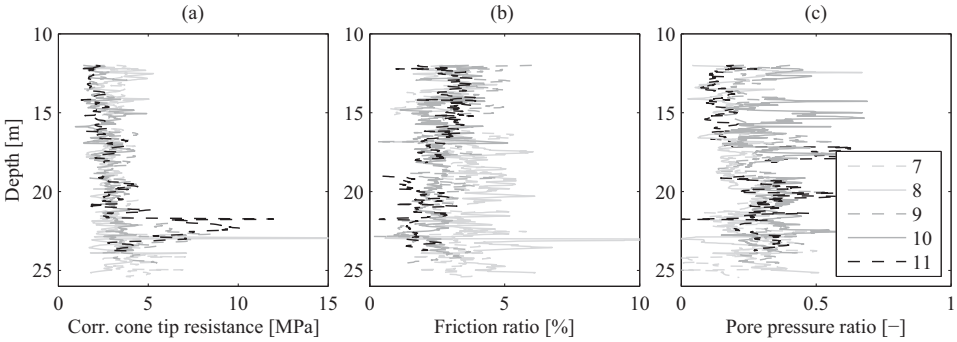

Figure 11: Derived parameters of the CPT: (a) corrected cone tip resistance, (b) friction ratio and (c) pore pressure ratio.

Corrected cone tip resistance measured in the downhole sample showed a pattern very similar to measured cone tip resistance, as it increased from 1.5 to 4.5 MPa in a depth of 25 m. Friction ratio is constant around 2-3% at every depth. Pore pressure ratio increased in the first 10 m of measurements, from 0.1 to 0.3, after which the ratio stabilized with little change, indicating that up to almost one-third of the applied pressure was carried by the excess pore pressure.

The most frequently used soil classification charts are based on B_q and q_t or on R_f and q_t. However, these classification charts do not account for the overconsolidation ratio (OCR), which is very high in Søvind Marl (Table 3). Lacasse and Lunne (1982) and Wroth (1984) showed that B_q tends to decrease as OCR (or q_t) increases. This leads to a misinterpretation of the data and misclassification of Søvind Marl as silty clay to sandy silt, rather that the extremely high-plasticity clay which it is known to be. The utility of the classification is therefore greatly diminished for Søvind Marl and other highly overconsolidated tertiary clays.

7 PRECONSOLIDATION

Søvind Marl is up to 46 million years old and has previously been covered by deposits up to 1 km thick. As a result, Søvind Marl experienced very high consolidation pressures. Furthermore, Søvind Marl has undergone a secondary consolidation with secondary compression index, $C_{\alpha\varepsilon}$, of up to 1% over millions

of years (Grønbech et al., 2012). Given these historical events the preconsolidation stress level, σ'_{pc}, of Søvind Marl would be expected to have a quite high value. Eight oedometer tests were conducted to determine the preconsolidation stress level of Søvind Marl. Five tests on the material discussed directly in this paper, as well as three tests on a younger Søvind Marl deposit from a different location (also at Aarhus Harbour), were evaluated and are presented here.

Both incremental and continuous loading oedometer tests were completed. The incremental loading oedometer (ILO) tests were performed in the Danish Oedometer Apparatus, made at Aalborg University, Denmark. The apparatus has a stiff floating ring, and is completely surrounded by test water, with a salinity and pH matching that of the pore water in the clay specimen. The samples have a diameter and height of 35 mm, allowing determination of deformations at high stress levels. Load steps are applied when full consolidation and sufficient secondary consolidation of the previous step is observed. The tests were performed according to DS/CEN ISO/TS 17892-5 (DS 2004d). Consolidation strains, ε, were calculated using the ANACONDA method described by Grønbech et al. (2012). The continuous loading oedometer (CLO) tests were conducted in the CLO-apparatus developed at Aalborg University, Denmark. The CLO-apparatus consists of a stiff fixed ring. The ring, as well as all transducers, is completely surrounded by test water similar to that of the incremental loading test. The test water is applied at a pressure of 200 kPa to better enable saturation and drainage of the sample. The samples have a diameter of 35 mm and a height of 30 mm. The rate of deformation is selectable and set at 0.05 %/h, as this rate was found to minimize the build-up of excess pore pressure. The tests were performed according to Norwegian standard NS 8018:1993 (NS 1993). All samples were collected in a 72 mm tube and trimmed by hand to ensure the best possible fit to the oedometer ring. The resulting stress-strain curves are presented in Figure 12, which shows that the curves generated by the two methods are very similar. All curves are located in the same band and demonstrate the same behaviour, with two apparent local maximum curvatures.

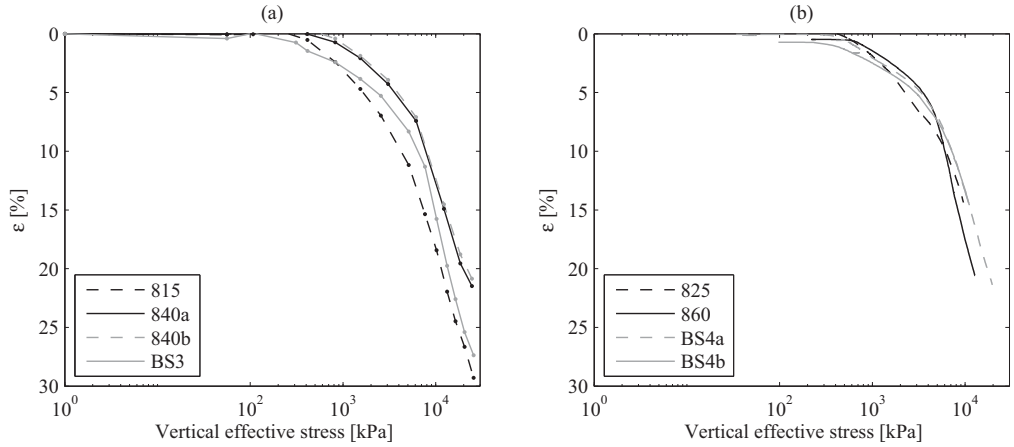

Figure 12: Stress-strain curves determined from oedometer tests performed on Søvind Marl: (a) ILO-tests and (b) CLO-tests.

Accurate determination of the preconsolidation stress level can prove to be difficult when working with highly fissured, overconsolidated clays due to the physical structure of the matrix (Gasparre and Coop 2008). This is also the case with Søvind Marl, where each investigatory method will yield two possible values, as also indicated by the two maximum curvatures of the stress-strain curves. Of the two suggested outcomes, only the higher of the two values should be considered as representative of primary and secondary consolidation. The low value that is obtained represents only about twice the in situ stresses and is not a result of millions of years of primary and secondary consolidation, as evidence by the geological history. This behaviour has also been noted in the compression curves of other highly overconsolidated fissured clays (Cotecchia and Chandler 1997; Gasparre and Coop 2008). Gasparre and Coop (2008) concluded that the lower value for preconsolidation stress must arise from other factors, such as the fissured structure of the clay. All interpreted values, along with OCR, can be seen in Table 3, where the preconsolidation stress level is referred to as the 'true' value, while the low value is called the 'false' value, as the latter is not related to preconsolidation events. The preconsolidation stress level, false value, and effective in situ stress level at each depth are shown in Figure 13.

Table 3: 'False' and 'true' stress level values, as well as an estimate on the preconsolidation stress level and OCR.

Sample Metric	Sample							
	815	825	840a	840b	860	BS1	BS2	BS3
Depth [m]	29	33	39	39	47	11.5	11.5	11.5
σ'_{vo} [kPa]	255	290	335	335	400	110	110	110
Test type	ILO	CLO	ILO	ILO	CLO	ILO	CLO	CLO
Method	False values							
False value	700	700	1200	1200	800	620	620	570
False OCR	2.7	2.4	3.6	3.6	2	5.6	5.6	5.2
	True values							
σ'_{pc} [kPa]	6300	6600	9100	9100	6850	8900	6400	5900
OCR	25	23	27	27	17	80	58	54

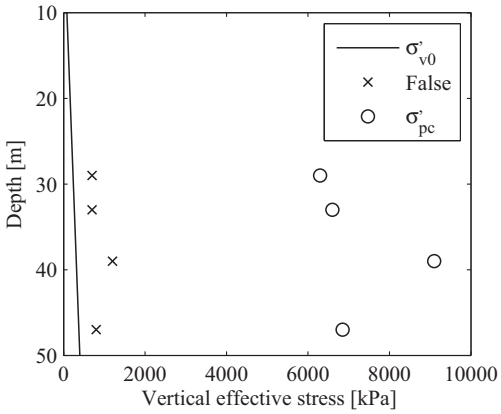

Figure 13: Preconsolidation stress level through depth, as well as false values and effective in situ stresses.

Preconsolidation stress levels increased with depth at a rate that roughly corresponded to in situ stress changes. Because the load program for 840a/b has larger incremental steps, the data are "coarser" and the results less precise. For the remaining ILO tests, a different load program was developed to yield higher resolution of the data, and therefore a better estimate of the preconsolidation stress level. However, it was found that the CLO tests provide a better description of the deformation of the sample due to the continuous nature of the results.

Mesri (1975) suggested shear strength as an indicator of the preconsolidation stress level. Bjerrum (1973) developed a correlation between the undrained shear strength, S_u, and the in situ vane shear strength, as shown in equation 2:

$$S_u = \mu \cdot c_{fv} \qquad [2]$$

Using μ=0.3 for Søvind Marl due to the fissured structure, as suggested by Christensen and Hansen (1959). Mesri's (1975) correlation between the undrained shear strength and the preconsolidation stress level is shown in equation 3:

$$S_u = 0.22 \cdot \sigma'_{pc} = \mu \cdot c_{fv} \qquad [3]$$

By utilizing these correlations, values for Søvind Marl were calculated and are presented in Table 4.

Table 4: Mesris (1975) correlation between c_{fv} and σ'_{pc}, as well as the measured values.

Sample	Sample				
Metric	815	825	840a	840b	860
c_{fv} [kPa]	786	744	826	826	>1000
$\sigma'_{pc,mesri}$[kPa]	1072	1014	1126	1126	>1363
σ'_{pc} [kPa]	6300	6600	9100	9100	6850
σ'_{false}[kPa]	700	700	1 200	1 200	800

It is very clear that the correlation does not apply to Søvind Marl, as the preconsolidation stress level is severely underestimated. Because the correlation is not applicable for effective calculation of the

preconsolidation stress level of Søvind Marl, it is important that accurate estimates be determined through direct use of oedometer tests.

8 CONCLUSION

Søvind Marl is a tertiary clay common in certain regions of Denmark, with an elevated occurrence of fissures and slickensides. The plasticity of Søvind Marl is extremely high with plasticity indices of up to 250% and higher. This and other characteristics make it difficult to make direct, constructive comparisons of Søvind Marl properties to other soil matrices, as many Søvind Marl metrics easily exceed values utilized in correlations for various clays. A summary of the typical range of values for parameters presented in this paper is presented in Table 5.

Table 5: Summary of the range of typical values of classification parameters of the Søvind Marl presented in this paper.

Parameter		Range	Parameter		Range
Age [milion Years]	-	40.5 – 46	Remoulded vane shear strength [kPa]	c_{fvr}	100 – 350
NP-zone	-	15a – 16b	Sensitivity [-]	-	1.6 – 4
Depth [m]	d	11 – >70	pH of pore water [-]	-	8.6 – 9.6
Clay fraction [%]	-	72.8 – 95.6	Cl^- content of pore water [%]	-	0.5 – 1.6
Bulk unit weight [kN/m^3]	γ	16.7 – 18.1	Cone resistance [MPa]	q_c	1.5 – 8
Specific gravity [-]	G_s	2.7 – 2.8	Sleeve friction [kPa]	f_s	60 – 100
Natural water content	w	35 – 50	Pore Pressure [MPa]	u_2	0.3 – >2
Liquid limit [%]	w_L	150 – 300	Hydrostatic pressure [MPa]	u_0	0.1 – 0.7
Plastic limit [%]	w_P	35 – 55	Corrected cone resistance [MPa]	q_t	1.5 – 8
Plasticity Index [%]	I_P	100 – 250	Friction ratio [%]	R_f	2 – 3.7
Liquidity index [-]	I_C	-0.05 – 0.05	Pore pressure ratio [-]	B_q	0.05 – 0.30
Calcite content [%]	-	5 – 65	Effective in situ stresses [kPa]	σ'_{v0}	100 - 560
Activity [-]	-	1.57 – 2.72	Preconsolidation stress level [kPa]	σ'_{pc}	6000 - 7000
Vane shear strength [kPa]	c_{fv}	300 – 900	Degree of overconsolidation [-]	OCR	17 - 25

It was noted that many of the measured parameters demonstrated substantial changes at approximately the same depth of around 25 m. There was, for example, a clear correlation between the plasticity and the calcites composition of the clay. The rate at which shear vane strength increased shifted noticeably downward at about 25 m. Conversely, cone tip resistance measured in the CPT began to increase at a higher rate at 25 m and sleeve friction became almost constant. These multiple shifts suggest a significant change in the macro behavior and physical nature of Søvind Marl at this depth, even though

there was no noticeable alteration in the sample appearance. While the strong correlation between plasticity index and the calcite content was clearly evident, it is possible that the shift in calcite composition of the clay also may have impacted other properties as well, either directly or indirectly. These data suggest that calcite plays a very important and governing role in the macro behaviour of Søvind Marl. The concentration of calcite should be considered as a key metric and potential independent variable when developing correlations to other parameters such as friction angle, φ, or earth pressure at rest, K_0.

Another important consideration is the manner in which CPTs are interpreted. Commonly used classification charts provide generally incorrect or incomplete descriptions of the soil type due to the very high cone tip resistance that occurs because of overconsolidation of the soil matrix. Using CPTs, therefore, to classify highly overconsolidated clays like Søvind Marl could be problematic and lead to miscategorization.

Oedometer tests show some interesting results, apparently unique to overconsolidated fissured clays. While two different interpretations of the data are possible with regard to preconsolidation stress level, it is physically impossible for a soil to have more than one preconsolidation stress level. Only one of the interpreted values originates from previous consolidation, whereas the other, and significantly lower, interpreted value is caused by the fissured structure of Søvind Marl. The preconsolidation stress level of Søvind Marl is estimated to be between 6 000 and 7 000 kPa, resulting in OCRs of approximately 25. Due to the difficulties that are encountered in determining the preconsolidation stress level, it is important to pay close attention to the individual date and structure of the clay matrix to ensure that an accurate and realistic stress level determination is made. It is also clear based on collected data that the correlation between in situ vane shear strength and the preconsolidation stress level, while applicable to other matrix types, is not valid for Søvind Marl, and would underestimate the preconsolidation value.

REFERENCES

ASTM. 2011. Standard practice for classification of soils for engineering purposes (Unified Soil Classification System). ASTM standard D2487. American Society for Testing and Materials, West Conshohocken, Pa. doi:10.1520/D2487-11.

Balić-Žunić, D.T. 2008. Xray-diffraction, Århus Havn (Personal communication in Danish). University of Copenhagen

Bjerrum, L. 1973, Problems of soil mechanics and construction on soft clays, Proceeding 8th international conference on Soil Mechanics and Foundation Engineering, 6th – 11th August 1973, Moscow, **3**, 111-159

Casagrande, A., 1932. Research on the Atterberg Limits of Soils. Public Roads, 13(8). 121 – 136

Christensen, N.H. and Hansen, B.1959. Shear strength properties of Skive septarian clay. Bulletin No. 7. The Danish Geotechnical Institute.

Cotecchia, F., and Chandler, R.J. 1997. The influence of structure on the pre-failure behaviour of a natural clay. Geótechnique, **47**: 523–544.

Gasparre, A. and Coop, M.R.. 2008. Quantification of the effects of structure on the compression of a stiff clay. Canadian Geotechnical Journal, **45**: 1324–1334

DGF, 1999, Reference test procedure for field vane tests. Danish Geotechnical Society - Field Committee

DS. 2004a. Geotechnical investigation and testing – Laboratory testing of soil – Part 1: Determination of water content. DS/CEN ISO/TS 17892-1. Danish Standard Association. Nordhavn, DK

DS. 2004b. Geotechnical investigation and testing – Laboratory testing of soil – Part 2: Determination of density of fine grained soil. DS/CEN ISO/TS 17892-2. Danish Standard Association. Charlottenlund, DK

DS. 2004c. Geotechnical investigation and testing – Laboratory testing of soil – Part 3: Determination of particle density – Pycnometer method. DS/CEN ISO/TS 17892-3. Danish Standard Association. Nordhavn, DK

DS. 2004d. Geotechnical investigation and testing – Laboratory testing of soil – Part 5: Incremental loading oedometer test. DS/CEN ISO/TS 17892-5. Danish Standard Association. Nordhavn, DK

DS. 2004e. Geotechnical investigation and testing – Laboratory testing of soil – Part 12: Determination of Atterberg limits. DS/CEN ISO/TS 17892-12. Danish Standard Association. Nordhavn, DK

DS. 2009. Ground investigation and testing - Field testing - Part 9: Field vane test. DS/EN ISO 22476-9. Danish Standard Association. Nordhavn, DK

DS. 2012. Geotechnical investigation and testing - Field testing - Part 1: Electrical cone and piezocone penetration test. DS/EN ISO 22476-1. Danish Standard Association. Nordhavn, DK

Geocenter Danmark (2010). Geoviden 3, ISSN 1604-8172

Grønbech, G. L., Ibsen, L. B. and Nielsen, B. N. (2010). Chloride concentration and pHs influence on the Atterberg limits of Søvind Marl. DCE Technical Reports no. 088. Department of Civil Engineering, Aalborg University, Denmark. ISSN 1901-726X

Grønbech, G. L., Nielsen, B. N. and Ibsen, L. B. 2011. Comparison of liquid limit of highly plastic clay by means of Casagrande and Fall Cone Apparatus. Proceedings of 2011 Pan-Am CGS Geotechnical Conference., Toronto, Ontario, Canada. Paper no. 1100

Grønbech, G.L., Nielsen, Benjaminn N. and Ibsen, Lars B. (2012). Interpretation of Consolidation Test on Søvind Marl. NGM 2012, Nordisk Geoteknikermøde. 9th-12th of May 2012. Copenhagen, Denmark.

King, C. 1981. The stratigraphy of the London Clay and associated deposits. Tertiary Research Special Paper, No. 6. Rotterdam: Backhuys.

Lacasse, S. and Lunne, T. 1982, Penetration testing in two Norwegian clays, Penetration testing, Vol. 2, Balkema, Rotterdan, The Netherlands, 607-613,

Lunne, T., Robertsin, P.K. and Powell, J. J. M. 1997. Cone penetration testing in geotechnical practice. Spon Press. ISBN: 0-419-23750-x

Mesri, G. 1975, New design procedure for stability of soft clay, Discussion. Journal of Geotechnical Engineering, ASCE, **101**(4). 409-412

NS. 1993. Geotechnical testing - Laboratory methods - Determination of one-dimensional consolidation properties by oedometer testing - Method using continuous loading (In Norwegian). NS 8018:1993. Standard Norge. Lysaker, NO

Pantelidou, H. and Simpson, B. 2007. Geotechnical variation of London Clay across central London. Géotechnique **57**(1). 101–112

Rosenqvist, I. Th. (1953). Consideration on the sensitivity of Norwegian quick clay. Géotechnique. **3** (5). 195-200

Skempton, A.W. (1953). The colloidal activity of clay, Proceedings of the Third International Conference on Soil Mechanics and Foundation Engineering, Zürich, **1**,.57-61.

Terzaghi, K. 1944. Ends and means in soil mechanics, Engineering Journal of Canada, **27**. 608

Thomsen, E. 2008. Coccolith-stratigrafiske undersøgelser af boringer i Århus Havn (Personal communication in Danish), Århus University, Denmark

Thøgersen, L. 2001, Effects of experimental techniques and osmotic pressure on the measured behaviour of tertiary expansive clay, Vol. 1. Ph.D. Thesis, Soil Mechanics Laboratory, Aalborg University, Denmark, ISSN: 1398-6465 R 2016

Wroth, C. P. 1984. The interpretation of in situ soil tests, Geótechnique, **34**(4). 449–489.

APPENDIX C
Interpretation of Consolidation Test on Søvind Marl

Authors:
Gitte Lyng Grønbech, Lars Bo Ibsen and Benjaminn Nordahl Nielsen

Published in:
Proceedings of the 16th Nordic Geotechnical Meeting. May 9th to 12th, 2012. Copenhagen, Denmark.

Year of publication:
2011

C.1 Author's Right

Fra: Jan Dannemand Andersen
Sendt: 5. november 2014 09:50
Til: Gitte Lyng Groenbech
Emne: SV: Author's Right

Hej Gitte.

Tilladelse er hermed givet (Premission hereby granted - Translated by Author)

Med venlig hilsen/Kind Regards
Jan Dannemand Andersen

Senior Project Manager

Geo | Sødalsparken 12 | DK-8220 Brabrand | CVR-nr. 59781812 | www.geo.dk

Fra: Gitte Lyng Groenbech [_____]
Sendt: 5. november 2014 09:48
Til: Jan Dannemand Andersen (JDA)
Emne: Author's Right

Dear Sir,

I write to you because of your function as the president of The Danish Geotechnical Society. The Danish Geotechnical Society hosted the 16th Nordic Geotechnical Meeting in Copenhagen, Denmark in May 2012. I attend with the paper "Interpretation of Consolidation Test on Søvind Marl", which I would like to include in my Ph.D. thesis. I would like to ask for your permission to do so.

Sincerely /Venlig Hilsen

Gitte Lyng Grønbech
Ph.D. student
Geotechnical Engineering

Interpretation of Consolidation Test on Søvind Marl

Gitte Lyng Grønbech
Aalborg University, Denmark, glg@civil.aau.dk

Lars Bo Ibsen and Benjaminn Nordahl Nielsen
Aalborg University, Denmark

ABSTRACT

The article deals with the interpretation of consolidation test in order to determine the preconsolidation stress; this is done by reviewing different methods. A main point in the article is the interaction between the consolidation and the secondary consolidation strains, and the methods used to separate the two strain types. This is in Denmark traditionally done by a √(t)-log(t) description, where the secondary consolidation first starts when the consolidation process is over. This assumption gives an uncertain description of the strain process, since the two processes in reality run simultaneously. By use of the ANACONDA-method the two processes are assumed to run simultaneously. The method gives a more accurate description of the strain process, and thereby a better determination of the deformation properties. The methods for determining clay properties are demonstrated on Søvind Marl and the difference in results are shown.

Keywords: Consolidation, Creep, Deformation, Expansive Soils, Laboratory tests

1 INTRODUCTION

The estimation of deformations in a clay when the stress level increases is of great importance. For some clays, like the Søvind Marl, the secondary consolidation, also called creep, has a very large influence on the deformation. It is therefore important to be able to give an accurate description of both the consolidation and secondary consolidation process, which is traditionally done with the use of consolidation tests.

Following a consolidation test, separating the consolidation and the secondary consolidation (also called creep) strains is an important step. In Denmark traditionally done by using Brinch Hansens method in a $\sqrt{t}$-log(t) graph, which assumes the primary and the secondary consolidation process are two separate processes. However, the two processes are not separate and run simultaneously as suggested by Bjerrum in 1967, which the ANACONDA-method (Analysis of consolidation test data) takes into account when filtering the strains [Jacobsen, 1992].

The different theories described in the paper will be used on consolidation tests conducted on Søvind Marl. Classification and properties of the Søvind Marl can be found in Grønbech et al. (2012). The sample tested in this paper come from a depth of 39 meters and has a plasticity index, I_P (%), of 132%, a unit weight, γ (kN/m^3), of 18.1 kN/m^3 and an effective in situ stress level, $\sigma'_{in\ situ}$, of approximately 350 kPa.

2 SEPERATING STRAINS

Three methods to separate the total strains, ε_{tot}, into consolidation strains, ε_c, and secondary consolidation strains, ε_{ac}, are described here; the $\sqrt{t}$-log(t) method, the ANACONDA-creep filter and the 24 hour measurement method.

2.1 Traditional √t-log(t) method

In Denmark the traditional method to separate the consolidation and secondary consolidation strains is by using a $\sqrt{t}$-log(t) graph as described by Brinch Hansen (1961). The method assumes the consolidation strains are linear in a $\sqrt{t}$-ε graph and the secondary

consolidation strains are linear in a log(t)- ε graph, an example can be seen in Figure 1.

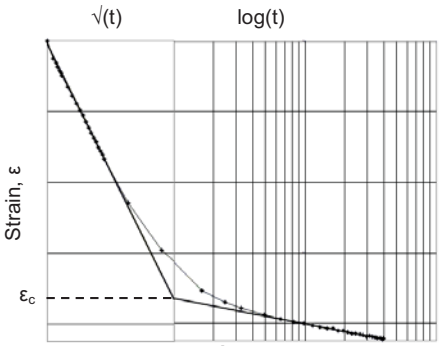

Figure 1: Traditional √(t)-log(t) graph.

The consolidation strains, ε_c, are found as the strain level at the intersection point of the two lines.

2.2 ANACONDA-Creep Filter

As mentioned earlier the consolidation and secondary consolidation strains are two separate processes that run simultaneously. By considering the consolidation process as an instant process, the secondary consolidation process can be estimated. Hereafter can the consolidation be regarded as a delay of deformation. The secondary consolidation occurring while the consolidation process is happening will thereby not be included in the consolidation strains. This process is called the ANACONDA-creep filter, and is her described. A flow chart of the entire ANACONDA-method can be seen in Figure 2.

Slightly preconsolidated clay is approximately described by Bjerrums theory, and is used to describe the creep filter.

The relation between stresses and strains can for the curved virgin curve be described as:

$$\varepsilon_c = C_c \log\left(1 + \frac{\sigma'}{\sigma'_\kappa}\right) \qquad (1)$$

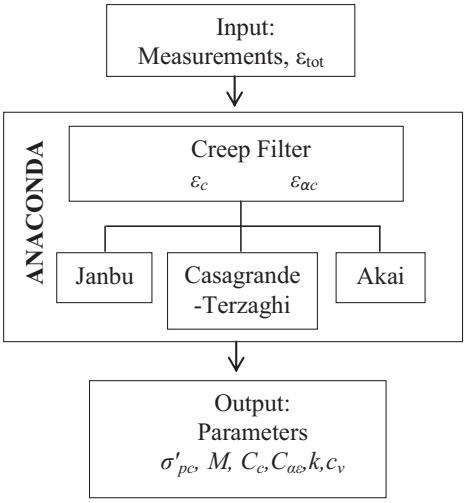

Figure 2: Flow chart using the ANACONDA-method.

where ε_c (%) is the consolidation strains, C_c (%) is the compression index and σ' (kPa) is the effective stresses and σ'_κ (kPa) is a characteristic stress.

Since the consolidation strains are assumed to happen instantly, the strains in equation (1) are not dependent on the time. σ'_κ is relative small for a slightly preconsolidated clay and equation (1) can be simplified to:

$$\varepsilon_c \approx C_c \log\left(\frac{\sigma'}{\sigma'_\kappa}\right) \qquad (2)$$

It is an assumption that the primary consolidation process is completed at the time $t = 0$, in reality the process last until $t >> 0$, and the normally consolidated state is a theoretical limit state that will never occur.

Under constant stress level, the secondary consolidation process can be described as:

$$\varepsilon_{\alpha c} = \varepsilon_s \log\left(1 + \frac{t_r}{t_b}\right) \qquad (3)$$

where $\varepsilon_{\alpha c}$ (%) is the secondary consolidation strain, t_r (sek) is the real time, t_b (sek) is a characteristic time governing the instant compression curve placement, corresponding to $t = 0$ and ε_s (%) is the secondary compression index, a constant for the individual secondary consolidation curve. For

a slightly preconsolidated clay, ε_s is assumed to be equal to $C_{\alpha\varepsilon}$ for every secondary consolidation curve, and that $\varepsilon_s = C_{\alpha\varepsilon} = \alpha C_c$, α is a constant for the given clay. By combining equation (2) and (3), the total strain is given by:

$$\varepsilon_{tot} = C_c \log\left(\frac{\sigma'}{\sigma'_\kappa}\right) + C_{\alpha\epsilon} \log\left(1 + \frac{t_r}{t_b}\right) \quad (4)$$

The strain distribution described in equation (4) describes curves parallel to the instant compression curve (t = 0) for similar values of t_r, these curves is called secondary consolidation isochrones which can be seen in Figure 3. C_c determines the slope of the isochrones and α determines the distance between the isochrones.

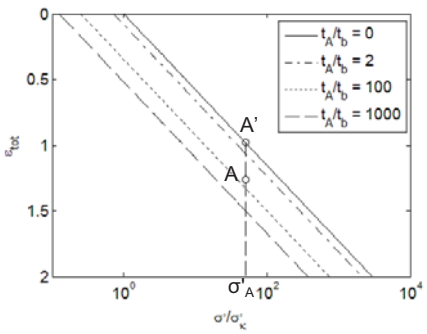

Figure 3: Instant compression curve (t = 0) and secondary consolidation isochrones.

The solid line in Figure 3 is the instant compression curve and the rest are secondary consolidation isochrones dependent on the characteristic time, t_b, and describes strains that can be achieved by either unloading from a higher stress level or secondary consolidation under constant stress.

If a given stress-strain level *A*, Figure 3, is reached by secondary consolidation from the stress-strain level *A'*, the secondary consolidation time, *t* (sek), is given by

$$t = t_r - t_A \quad (5)$$

where t_A is the time pasted before the secondary consolidation started in the point *A'*.

The increase in strains originated from secondary consolidation is:

$$\Delta\varepsilon_{\alpha c} = \varepsilon_A - \varepsilon_{A'} = C_{\alpha\epsilon} \log\left(\frac{t + t_A + t_b}{t_A + t_b}\right) \quad (6)$$

Since $t_b << t_A$ equation (6) can be approximated to:

$$\Delta\varepsilon_{\alpha c} \approx C_{\alpha\epsilon} \log\left(1 + \frac{t}{t_A}\right) \quad (7)$$

Equation (7) can be used to find t_A and α, if sufficient time curves are available. The time t_A is easiest determined as the addition to the time t that transforms the log(t+t_A)-ε curve to a straight line as illustrated in Figure 4.

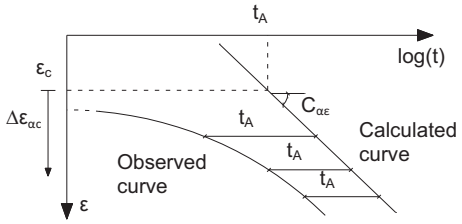

Figure 4: Creep curves and the delay of time, t_A.

The secondary consolidation isochrones illustrated in Figure 3 can as mentioned be obtained by both secondary consolidation as shown, and unloading to σ'_A from the preconsolidated stress, σ'_{pc}. This shows that secondary consolidation in a clay under constant stress will increase the preconsolidated stress level to a higher level than any earlier load.

2.3 24 Hour Measurement

The consolidation process is often finished after 24 hours. In inferior engineering practice it is suggested that the 24 hour measurement of the strains is used as the consolidation strains, ε_c. This method completely disregards the secondary consolidation, and can only be used to estimate the preconsolidated stress level, σ'_{pc}.

3 DETERMINATION OF DEFORMATION PARAMETRES

Some of the most significant deformations parameters obtained from consolidation tests will briefly be covered here.

3.1 Consolidation Modulus

The consolidation modulus, M (kPa), is a stiffness parameter given by:

$$M = \frac{\Delta\sigma'}{\Delta\varepsilon_c} \qquad (8)$$

where $\Delta\sigma'$ and $\Delta\varepsilon_c$ is the change in correlated effective stresses and consolidation strains respectively. The primary consolidation strains are separated from the secondary consolidation strains by either method mentioned in section 2.

3.2 Coefficient of Consolidation and Permeability

The coefficient of consolidation, c_v (m^2/sek) and the coefficient of permeability, k (m/s), are both dependent of the dimensionless time T (-) which is given by:

$$T = \frac{c_v}{H_D^2}t = \frac{kM}{\gamma_w H_D^2}t \qquad (9)$$

where H_D (m) is the drainage path and t (sek) is the passed time.

The degree of consolidation, U (-), is dependent of T and is given by:

$$U^{-6} = 1 + \tfrac{1}{2}T^{-3} \qquad (10)$$

If the consolidation process is halfway done, U=0.5, it is found that T=0.2. By rewriting equation (9) the coefficient of consolidation is given by:

$$c_v = \frac{TH_D^2}{t} = 0.2\frac{H_D^2}{t_{50}} \qquad (11)$$

where t_{50} (min) is the time when the consolidation process is halfway done.

The coefficient of permeability, k (m/s), is dependent on the coefficient of consolidation, unit weight of water, γ_w (kN/m^3) and consolidation modulus, M (kPa), and can also be derived from equation (9):

$$k = \frac{c_v\gamma_w}{M} \qquad (12)$$

4 PRECONSOLIDATION STRESS

Being able to determine a clay stress history, and thereby the largest stresses the clay has been exposed to, is of great importance. When the preconsolidated stress level, σ'_{pc} is exceeded a large increase of secondary consolidation takes place and a drastic drop in the consolidation modulus, M, occurs.

The following methods to determine the preconsolidation stress level is included in the ANACONDA-method, Figure 2, but can also be used if other methods have been used to separate the strains.

4.1 Casagrande-Terzaghi Method

The Casagrande-Terzaghi method seek to determine σ'_κ used in equation (2). σ'_κ can be determined as the stress level that gives the curved virgin curve the best linear description in a logarithmic depiction as illustrated in Figure 5. The preconsolidated stress level, σ'_{pc}, can be found to be given by Jacobsen (1992) as:

$$\sigma'_{pc} = 2 \cdot \sigma'_\kappa \qquad (13)$$

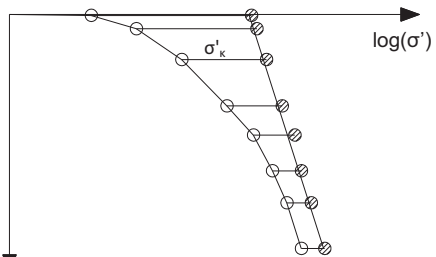

Figure 5: Casagrande-Terzaghi's method to determine σ'_κ.

4.2 Akai

One of the characteristic for clay is the increase in the degree of secondary consolidation that happens when the stress level approaches the preconsolidated stress level, σ'_{pc}. Akai (1960) used this knowledge to determine the preconsolidation stress level based on the secondary compression index, $C_{\alpha\varepsilon}$. The secondary consolidation is assumed logartichmic dependent on the time, t, in respect to the secondary compression index. Akai found that the secondary compression increased porportionally with the stress level, when this was below the preconsolidated stress level, and that the secondary compression index increased porportionally to the logaritchmic stress level when this was above the preconsolidated stress level. The preconsolidated stress level can be determined as the interval where the σ' - $C_{\alpha\varepsilon}$ curve breaks and starts to flatten, as illustrated in Figure 6.

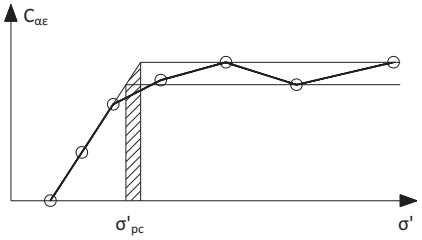

Figure 6: Akai's method to determine the preconsolidated stress level based on the secondary compression index.

4.3 Janbu

Janbu (1970) studied the correlation between the consolidation modulus, M, and the vertical effective stresses, σ', in a series of drained consolidation tests. It was found that a drastic change occurs in the consolidation modulus when the preconsolidated stress level was exceeded. This is due to the fact that the stiffness of the clay decreases when the preconsolidation stresses are exceeded, since a change in the structure of the clay take place. The preconsolidated stress level can now be determined as the stress level where a drop in the consolidation modulus occurs, as illustrated in Figure 7.

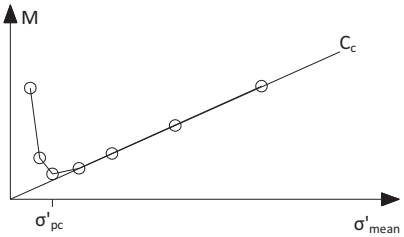

Figure 7: Janbu's method to determine the preconsolidated stress level based on the consolidation modulus

When the stress level in the clay becomes greater than the preconsolidated stress level, the consolidation modulus approximately increases by a straight line dependent on the effective stresses. Knowing the consolidation modulus is given by equation (8), it can be found that the relation for the straight line is given by:

$$M = \frac{\log(10)}{C_c}\sigma'_{mean} \qquad (14)$$

The consolidation modulus is here shown to be dependent of the compression index, C_c (%).

5 RESULTS

The methods mentioned above are used on consolidation test made on Søvind Marl. The consolidation tests are made on two different diameters, 35 mm and 70 mm. The tests used to determine the deformation properties described in section 3 have a diameter of 70 mm, and the tests used to determine the preconsolidated stress level (section 4) have a diameter of 35 mm. The optimal is to have a diameter as large as possible, to reduce the influence of the boundary condition (friction between the ring and sample), but small enough to be able to obtain high enough stress levels in the sample to determine the preconsolidated stress level. The 35 mm diameter sample is a strictly loading test, whereas on the 70 mm diameter sample unloading-reloading branches were made.

5.1 Determination of strains

The most commonly used engineering strains, ε^E, are defined by:

$$\epsilon^E = \frac{u}{H_0} \qquad (15)$$

where u (mm) is the deformation and H_0 (mm) is the initial height of the sample. engineering strains uses a constant linear relation between deformations and strains, which is valid for small deformations. To describe larger deformations the non-linear natural strains, ε^N, gives a better description of the strains. Natural strains are defined by:

$$\epsilon^N = \ln\left(\frac{H_0}{H_0 - u}\right) \qquad (16)$$

A discussion on the two strain types can be found in Praastrup et al. (1999).

The two methods to calculate the total strains are used on tests performed on the Søvind Marl and the methods mentioned in section 2 are the used to determine the consolidation strains. The in total 6 stress-strain curves can be seen in Figure 8, where the black curves are calculated using engineering strains and the red curves are calculated using natural strains.

From Figure 8 the difference in the two strain types are clear. Already at a strain level of 5% a difference in notable. At the highest stress level, 24,500 kPa, the difference is very significant from 21.5% to 24% for respectively engineering and natural strains. At the stress-strain curves a bend in the virgin compression curve occurs at the last load step, this bend is due to insufficiency in the theory. The bend is however less significant for the natural strains, which better handles larges strains.

Based on the significant difference in results of the two strains types, the further handling of results will be based on natural strains, for both the 35 mm and 70 mm diameter sample.

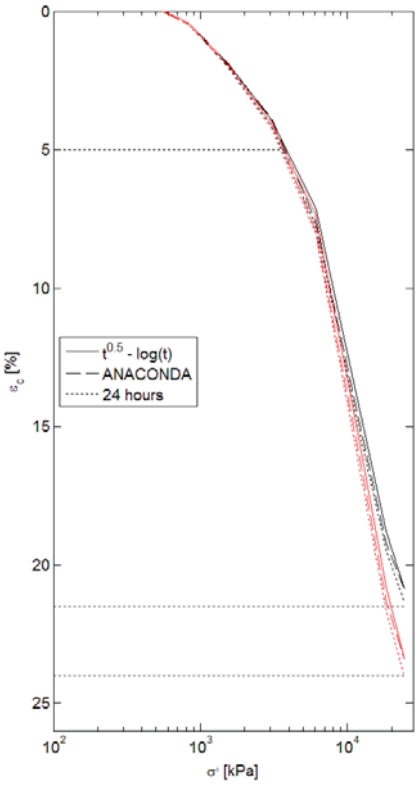

Figure 8: Stress-strain curves for Søvind Marl. Black curves represent engineering strains and red curves represent natural strains.

5.2 Consolidation Modulus

The consolidation modulus, *M*, is found using equation (8). The results are shown in Figure 9.

The consolidation modulus' for the primary load curve are between 50 and 100 MPa, whereas for the reloading curves the consolidation modulus' are between 150 and 900 MPa. The $\sqrt{t}$-log(t) method gives consistently higher modulus' and the lowest modulus' originates from the 24 hour measurements.

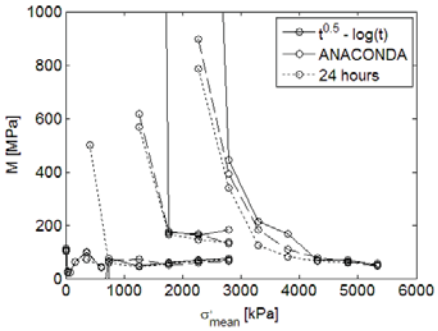

Figure 9: Consolidation modulus, M.

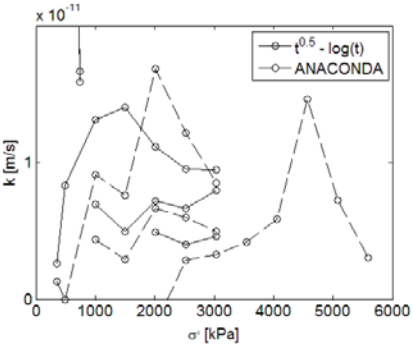

Figure 11: Coefficient of permeability, k.

5.3 Coefficient of Consolidation

The coefficient of consolidation, c_v, is found using equation (11). The results are shown in Figure 10.

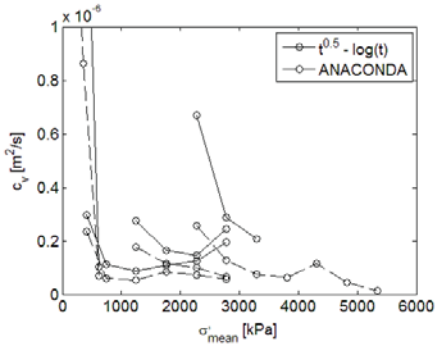

Figure 10: Coefficient of consolidation, c_v.

After approximately 500 kPa the coefficient of consolidation is between 0.05 and 0.15 x 10^{-6} m^2/s, with a slightly higher value for the reloading branches. The √t-log(t) method gives consistently higher values then the ANACONDA-method.

5.4 Coefficient of Permeability

The coefficient of permeability, *k*, is found using equation (12) and can be seen in Figure 11.

The coefficient of permeability is generally highest for the primary loading branch, and are located between 0.3 and 1.5 x 10^{-11} m/s. Results from the √*t*-log(*t*) method gives slightly higher results then the ANACONDA-method.

5.5 Secondary Compression Index

The secondary compression index, $C_{\alpha\varepsilon}$, is found using equation (*7*) for the ANACONDA-method, and the slope of the secondary consolidation curve for the √*t*-log(*t*) method. The index can be seen in Figure 12.

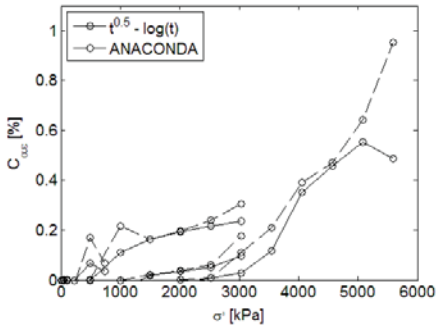

Figure 12: Secondary compression index, $C_{\alpha\varepsilon}$.

The index is constantly rising for the primary compression branch, whereas it is fairly constant around 0.05-0.1% for the reloading branches. The ANACONDA-method gives consistently higher secondary compression indexes than the √*t*-log(*t*) method.

5.6 Preconsolidated stress

5.6.1 Casagrande-Terzaghi Method

To determine the preconsolidated stress level, σ'_{pc}, it is first need to determine σ'_{κ}, as illustrated in Figure 5, the curves can be seen

in Figure 13 and σ'_κ are listed in Table 1 for the three separation methods.

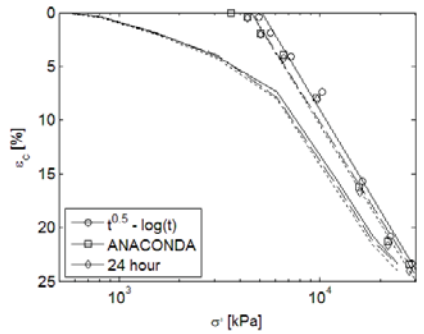

Figure 13: σ_κ found using Casagrande-Terzaghis method

Table 1: σ'_κ from Casagrande-Terzaghis Method.

Method	**σ'_κ [kPa]**
$\sqrt{t}$-log(t)	4138
ANACONDA	3541
24 hour	3546

Equation (13) is hereafter used to determine the preconsolidated stress level listed in Table 2.

5.6.2 Akai

To determine the preconsolidated stress level, the secondary compression index, $C_{\alpha\varepsilon}$, is plotted against the effective stress level, as illustrated in Figure 6. The plot can be seen in Figure 14.

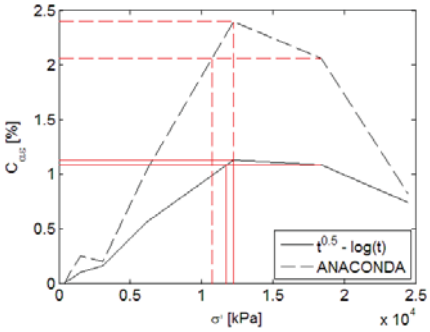

Figure 14: Preconsolidated stress level based on Akais method.

The preconsolidated stress level interval is marked with red in Figure 14 and can be seen in Table 2.

5.6.3 Janbu

The preconsolidated stress level is found based on the changes in the consolidation modulus, M, as described in Figure 7. The curves for the test can be seen in Figure 15.

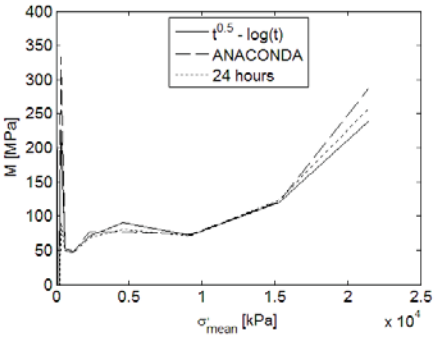

Figure 15: Preconsolidated stress level based on Janbus method.

The three strain methods give very similar results, all with clear drops in the consolidation modulus. A drop appears to occurs twice on each curve. The first drop happens when the fissured structure in the clay collapses, decreasing the stiffness of the clay, the second drop is due to the exceeding of the preconsolidated stress level as described by Janbus theory. The preconsolidated stress level can be seen in Table 2.

The interval of the preconsolidated stress level found using the three methods can be seen in Table 2. Casagrande-Terzaghi methods gives the lowest preconsolidated stress level and Akais method gives the highest preconsolidated stress level interval.

Janbus method is based on results from each load increment, which is why the results based on this method are equal independent of the method used to separate the strains. To get a finer description, the consolidation tests need to be performed with smaller load steps.

Table 2: Preconsolidated stress level based on the discussed methods.

Method	$\sqrt{t}$-log(t)	ANA-CONDA	24 hour
Casagrande-Terzaghi	8276	7082	7092
Akai	11743-12253	10726-12253	-
Janbu	9191	9191	9191

6 DISCUSSION

The natural strains are used in this paper since they give a more accurate description of the strains for large deformations compared to engineering strains, as seen in Figure 8.

Significant differences are found in the secondary compression index, $C_{\alpha\varepsilon}$, dependent on the method used to separate the strains. From Figure 12 and Figure 14 it is evident that the ANACONDA-method gives consistently higher secondary consolidation indexes. If secondary consolidation is suspected to be a main component, the ANACONDA-creep filter should be used to filter the strains.

The lower consolidation modulus, M, derived from 24 hour measurements compared to the other two measurements suggest that part of the secondary consolidation is included in the results, and thereby underestimates the stiffness of the clay.

The method used to separate the strains only has little influence on the determined preconsolidated stress level, with the ANACONDA-method giving slightly lower results than the other methods. The methods used to determine the preconsolidated stress level have however great influence, with a difference of more than 5000 kPa in the found preconsolidated stress level of the sample as seen in Table 2.

7 REFERENCES

Akai, K. (1960). De strukturellen Eigenschaften von Schluft Mitteilugen (in German). Heft 22. Die Technische Hochschule Aachen

Brinch Hansen, J. (1961). A Model Law for Simultaneous Primary and Secondary Consolidation. Bulletin No. 13. The Danish Geotechnical Institute. Copenhagen

Grønbech, G.L., Nielsen, B.N. and Ibsen, L.B. (2012). Geotechnical Classification of Søvind Marl. NGM 2012, Nordisk Geoteknikermøde. 9th-12th of May 2012. Copenhagen, Denmark.

Jacobsen, H.M. (1992). Karakteristiske belastningstilstande for moræneler (in Danish). NGM-92 11. Nordiske Geoteknikermøde dgf-Bulletin 9 Vol 2/3. 28th-30th of May 1992. Aalborg, Denmark. ISBN 87-983058-7-5

Janbu, Nilmar (1970). Grunnlag i Geoteknikk (in Norwegian). Tapir forlag

Praastrup, U., Jakobsen, K.P. and Ibsen, L.B. (1999). Two Theoretically Consistent Methods for Analysing Triaxial Tests. Computers and Geotechnics. Vol 25, pp. 257-170

APPENDIX D
Preconsolidation of Søvind Marl - a highly fissured Eocene clay

Authors:
Gitte Lyng Grønbech, Lars Bo Ibsen and Benjaminn Nordahl Nielsen

Submitted to:
Geotechnical Testing Journal

Time of acceptance:
Accepted with changes, December2014, changes submitted January 2015

D.1 Author's Right

Gitte Lyng Groenbech

Fra:
Sendt: 8. december 2014 20:50
Til: Gitte Lyng Groenbech
Emne: RE: Regarding Manuscript ID GTJ-2014-0246 - Geotechnical Testing Journal

Dear Gitte,

Thank you for your email. Because your manuscript has not yet been accepted for publication, you cannot cite the Geotechnical Testing Journal in your thesis. Ideally, the paper would be accepted prior to submitting your thesis, but having your paper in your thesis would not be considered dual publication. Please don't hesitate to contact me if you have any further questions or concerns.

Best Wishes,
Sara Welliver
GTJ Editorial Office

-------- Original Message --------
Subject: Regarding Manuscript ID GTJ-2014-0246 - Geotechnical Testing Journal
From: Gitte Lyng Groenbech <>
Date: Mon, December 08, 2014 4:55 am
To:

Dear Geotechnical Testing Journal editors

I have a paper with preliminary acceptance at Geotechnical Testing Journal (Manuscript ID GTJ-2014-0246). I would like to ask for permission to include the paper in the appendix for my PhD thesis. The thesis will be printed in approximately 25 copies intended primary for the Danish marked, after defense of the thesis it will be published as an e-book at Aalborg University research portal. Full reference will be giving to Geotechnical Testing Journal in the thesis.

Sincerely /Venlig Hilsen

Gitte Lyng Grønbech
Ph.D. student
Geotechnical Engineering

[Page #]

i. Title of the paper

Preconsolidation of Søvind Marl - a highly fissured Eocene clay

ii. Authors

1. Ms. Gitte L. Grønbech
2. Prof. Lars B. Ibsen
3. Mr. Benjaminn N. Nielsen

iii. Affiliations and designations

1. Ph.D. student, Department of Civil Engineering, Aalborg University, Sofiendalsvej 9, 9200 Aalborg SV, Denmark, e-mail: glg@civil.aau.dk, telephone number: (+45) 99 40 85 74, area of expertise: Geotechnical classification, fissured clay and laboratory testing
2. Professor, Department of Civil Engineering, Aalborg University, Sofiendalsvej 9, 9200 Aalborg SV, Denmark e-mail: lbi@civil.aau.dk, telephone number: (+45) 99 40 84 58, area of expertise: Geoetchnical testing, foundation design and off shore engineering
3. Associate Professor, Department of Civil Engineering, Aalborg University, Sofiendalsvej 9, 9200 Aalborg SV, Denmark e-mail: bnn@civil.aau.dk, telephone number: (+45) 99 40 84 59, area of expertise: Geoetchnical testing, foundation design and geotechnical classification

Abstract, English

Determination of the preconsolidation stresses is a key tool in geotechnical engineering used to evaluate and estimate the behavior of soils. However, it has proven difficult to accurately estimate these stresses in highly fissured, overconsolidated clays, due to the influence of the fissured structure. In the current study, oedometer tests were performed on Søvind Marl, a plastic Eocene clay containing a large number of fissures and slickensides. Four incremental loading oedometer tests and four continuous loading oedometer tests were performed in order to determine the preconsolidation stresses. Multiple assessment methods were used to assess preconsolidation stresses based on the oedometer test data, results of which are presented and discussed on this paper. All of the test and interpretation methods yielded very similar results, with two possible values calculated as the preconsolidation stresses. However, only the upper stress bound is actually identified as being associated with preconsolidation; and the lower bound is generated as a result of the collapse of the fissured structure in response to increasing stresses that were applied during testing. The upper bounds of the preconsolidation stresses of Søvind Marl were between 6,300 and 8,900 kPa, whereas the lower were between of 600 and 800 kPa.

Key words: Consolidation,stiffness, clays, fabric/structure of soils, laboratory equipment, laboratory tests

NOTATIONS

C_c	Compression index	%
$C_{\alpha\varepsilon}$	Secondary compression index	%
I_P	Plasticity index	%
OCR	Overconsolidation ratio	-
w_{nat}	Natural water content	%
γ	Bulk unit weight	kN/m^3
ε	Strain	%
σ_H	Total horizontal stresses	kPa
σ'_{pc}	Preconsolidation stresses	kPa
σ'_{v0}	Effective vertical in situ stresses	kPa
σ'_y	Yield stresses	kPa
σ'_κ	Reference stresses	kPa

1 INTRODUCTION

This article examine the preconsolidation stresses, σ'_{pc}, of a highly fissured, overconsolidated tertiary clay called Søvind Marl. The very low permeability found in Søvind Marl, as well as similar tertiary clays like Little Belt clay and London Clay, is problematic for many advanced characterization tests, causing them to be both time consuming and expensive. Because of these limitations, data on the stress history of these highly overconsolidated clays are often lacking at high stress levels. Casagrande (1936) found that the stress history, and therefore the preconsolidated stresses, of a soil sample can be determined using oedometer tests. This is accomplished based on the assumption that the natural structure of the soil decays after preconsolidation stresses are reached and the rate of strain increase is relatively slower at higher stress levels. In the current study, preconsolidation stresses were identified in several samples of Søvind Marl from two different locations in the city of Aarhus, Denmark. Two different oedometer test methods were used and described here: Incremental Loading Oedometer (ILO) tests and Continuous Loading Oedometer (CLO) tests with a constant rate of strain. Crawford (1986) reported a good correlation between the two test methods as long as the pore pressure ratio does not exceed 50% in CLO-tests. The test data were analyzed using several recognized methods to determine the preconsolidation stresses.

1.1 Influence of structure

The structure of a clay is due to a combination of its fabric (e.g., mineralogy, deposit history and fissures) and bonding (inter-particle forces). Cotecchia and Chandler (2000) defined the structure of an overconsolidated, stiff clay as a post-sedimentation structure, meaning that the main structure of the clay arises from events which have taken place after initial sedimentation, such as glacial disturbance or consolidation and swelling from overlaying deposits, which have later eroded. For many tertiary deposits, these events have resulted in a stiff and highly fissured matrix, which is also the case for Søvind Marl. Cotecchia and Chandler (2000) described how the yield point, σ'_y, of a clay with a post-sedimentation structure will occur outside the sedimentation compression line, and will therefore be greater than the

preconsolidation stresses ($\sigma'_y > \sigma'_{pc}$). Several studies have reported that the yield stresses may not be related to the geological history (Burland 1990, Cotecchia and Chandler 1997, 2000). In the present paper the term "preconsolidation stresses" is used to describe both yield and preconsolidation stresses.

The fissured structure of some clays complicates the determination of preconsolidation stresses since a clear yield point is not evident, and the lower and higher bounds of the yield stress can be determined based on the compression curve (Gasparre and Coop 2008). The influence of structure has previously been tested on tertiary clays such as London Clay (Gasparre et al. 2007a, 2007b; Gasparre and Coop 2008) and Vallericca Clay (Amorosi and Rampello 1998). These studies found that two stress levels can be defined based on an uncertain yield point.

Krogsbøll et al. (2012) suggest that fissured, highly plastic tertiary clays, like Søvind Marl, lose their stress memory when unloaded and are unable to recall their previous consolidation. The authors suggest that this is due to the high content of smectite, a very plastic clay mineral, which they propose erases the stress memory of a clay when unloaded. This results in interpreted preconsolidation stresses as low as a few hundred kilopascals, which is only a fraction of the expected stresses based on the geological history of these tertiary clays. However, these tests are often conducted at a maximum stress level of only 5 000 to 7 000 kPa, and have not been sufficiently elevated past the expected preconsolidation level based on the geological history. As a result, there is an insufficient description of the stress history at high stresses. Previous tests on Søvind Marl conducted by Grønbech et al. (2012) indicate the stress history of Søvind Marl is not forgotten; preconsolidation stresses can be found which approximately correspond to the known level of previous effective stresses.

2 SØVIND MARL

Søvind Marl is a plastic highly fissured Eocene deposit. Søvind Marl and other similar clays are found in various places throughout Denmark. Analysis shows the age of Søvind Marl to be between 46 million years and 34 million years old. The deposits haves a very high clay content. Between 60% and 95% of the material

is consistent with clay particles, of which between 44% and 55% is smectite. The high plasticity of Søvind Marl is evidence by a typical plasticity index in the range of 100% to 250%, and extreme values of more than 300%. Additionally, Søvind Marl has a very high calcite content (up to approximately 65% of the total sample). Grønbech et al. (2014) gives a detailed description of the geotechnical properties and characteristics of Søvind Marl.

The samples used in this study were all from Søvind Marl deposits located at two different locations at Aarhus Harbor in Aarhus, Denmark. These locations are named LH and BS. The only significant difference between these two locations is the age of the samples, where LH samples are of the older part of the Søvind Marl formation and BS samples are from a younger part of the same formation. All LH samples originated from the same borehole, whereas BS samples were from the same depth, but from two different boreholes located 5 m apart. At these locations Søvind Marl reaches thicknesses of more than 60 m and is covered by 10 m of primarily man-made fill (sand) and glacial till. After deposition Søvind Marl was covered by up to 1 km of Oligocene and Miocene deposits (Geocenter Danmark 2010), which caused a comprehensive consolidation. These deposits have now eroded and are located in the North Sea west of Denmark, resulting in an unloading of the Søvind Marl. The visual appearance of Søvind Marl is very uniform, despite the extended depositional period. The only mesofabric difference in the samples is the color which depends on the calcite content. Field and laboratory work revealed that a very fine net of fissures runs through Søvind Marl in different directions with no apparent origin. This characteristic proves problematic when fitting samples to, for example oedometer rings. The fissures originated from millions of years of consolidation, swelling and glacial, which have resulted in tearing of the clay. The surfaces of the fissures have a very clean cut and shiny appearance. Figure 1 shows the fissures in a Søvind Marl sample directly out of a sample tube.

Figure 1: Fissured structure of a Søvind Marl sample. Sample diameter is 72 mm.

Table 1 shows some significant classification parameters of the samples presented in this paper. Sample numbers in Table 1 correspond to legends in the subsequent figures.

Table 1: Classification of utilized samples.

Sample Metric	Sample							
	1	2	3	4	5	6	7	8
Test type	ILO	ILO	ILO	ILO	CLO	CLO	CLO	CLO
Location	LH	LH	LH	BS	LH	LH	BS	BS
Depth [m]	29	39	39	11.5	33	47	11.5	11.5
σ'_{v0} [kPa]	255	350	350	110	285	400	110	110
γ [kN/m^3]	18.4	18.6	18.4	17.9	18.1	17.9	17.5	17.7
w_{nat} [%]	40.2	34.6	36.0	41.5	38.8	40.7	40.0	39.8
I_P [%]	150.2	132.2	132.2	47.2	205.6	195.2	43.6	43.6
Calcite content [%]	43.3	39.8	39.8	62.0	10.0	36.3	64.5	64.5
Chloride content [%]	0.7	0.6	0.6	1.7	0.5	0.6	1.7	1.7
pH [-]	9.30	9.30	9.30	8.3	9.25	9.15	8.4	8.4

3 TEST METHODS

The preconsolidation stresses of Søvind Marl were found using two different oedometer tests: Incremental Loading Oedometer test (ILO) and Continuous Loading Oedometer test (CLO). When determining preconsolidation stresses of a highly overconsolidated soil, one of the main goals is to ensure the presence of sufficiently high stress levels in the samples in order to guarantee the preconsolidation stresses are exceeded. To obtain this during the tests within the limitations of the test apparatus, sample diameter was set to 35 mm, which is within the size requirements of standards. The standard diameter in Danish engineering practice is 70 mm. Using a smaller diameter samples did not adversely affect the tests; additional detail on the effect of sample size is presented in Section 7. Samples were collected in a 72 mm rotary tube and hand trimmed to ensure the best possible fit to the oedometer ring. Stresses of almost 25 MPa could be obtained by applying a maximum of 2.5 metric tons.

In both methods, the oedometer ring is surrounded by test water to ensure full saturation of the sample. Thøgersen (2001) showed that the chemical composition of test water greatly influences the test results, as an incorrect chemical composition or pH of the test water will cause internal forces in the sample to yield inaccurate results. To prevent potential errors, the water used in all tests must reflect resemble the salinity and pH of the sample pore water.

3.1 Incremental loading oedometer

All ILO tests were completed in a Danish consolidation apparatus at Aalborg University, Denmark. The tests were performed according to Danish standard DS/CEN ISO/TS 17892-5. The Danish consolidation apparatus is illustrated in Figure 2; numbers in parentheses () in the following text refer to numbers in the figure.

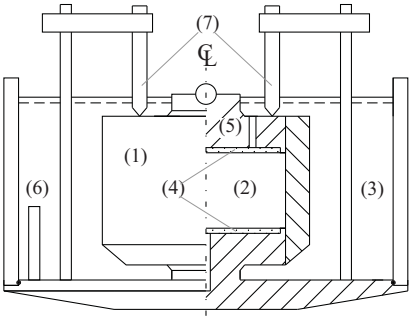

1: Floating oedometer ring
2: Soil sample
3: Test water
4: Porous bronze filter stones
5: Upper pressure head
6: Lower drain pipe
7: Displacement transducer

Figure 2: Illustration of the Danish incremental loading oedometer apparatus. Figure not to scale.

The consolidation apparatus consists of a rigid ring (1), in which the soil specimen (2) is placed. The soil specimen has a height of 35 mm. The rigid ring hinders horizontal deformation of the soil and maintains a constant cross-sectional area of the sample, thus ensuring all deformations to be one-dimensional. The ring floats, being held in place only by the cohesion between ring and sample, minimizes boundary conditions between the two. The entire consolidation cell is covered by test water at all times (3). Porous bronze filter stones (4) are placed in the upper (5) and lower pressure heads to allow double-sided drainage of excess pore water. The pressure heads are carefully fitted to allow free vertical movement, while preventing rotation of the pressure heads. The pore size of the filter is chosen to ensure free water flow while retaining soil particles. The top drain and lower drain pipes (6) are cover by test water at all times. The vertical one-dimensional deformation is measured by two displacement transducers (7), with a measuring range of 20 mm. The transducers are placed at opposite sides of the upper pressure head to ensure measurement of the mean displacement of the sample. Load is applied by placing weights on a lever arm, which transfers the load to the sample via a steel ball placed at the upper pressure head. The steel ball enables the load to be applied centrally and vertically to the sample. Load steps are applied when full consolidation and sufficient

secondary consolidation of the previous step are observed. Displacements and time elapsed since initiating the load step are measured at a set interval by a connected computer (not depictured in Figure 2).

A loading schedule was used to determine the load increments. After the first two tests (tests 2 and 3), the loading schedule was found to be too coarse, resulting in an imprecise description of the deformations and, consequently, an inaccurate estimate of the preconsolidation stresses. A new, finer schedule was thereafter used, yielding greater differences in the determined preconsolidation stresses presented in section 5.

Consolidation strains were identified and separated from secondary consolidation strains using the ANACONDA method described by Grønbech et al. (2012), which takes into account the simultaneous occurrence of the primary and secondary consolidations during the consolidation process. At the end of each consolidation step all strains were due to secondary consolidation, providing the secondary compression index. The secondary consolidation was assumed constant during each individual load step, enabling back calculation of secondary consolidation strains occurring since the beginning of each step. These back calculated secondary strains are subtracted from the total strain to obtain the consolidation strains.

3.2 Continuous loading oedometer

The CLO tests were all completed in a Danish continuous loading oedometer apparatus as Constant-Rate-of-Strain tests. The apparatus was developed at Aalborg University. The tests were performed according to Norwegian standard NS 8018:1993. The Danish continuous loading oedometer apparatus is illustrated in Figure 3; numbers in brackets [] in the following text refer to numbers in the figure.

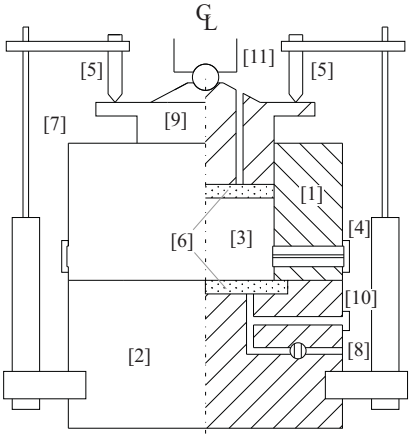

1: Oedometer ring
2: CLO base
3: Soil sample
4: Horizontal pressure gauge
5: Displacement transducer
6: Porous bronze filter stones
7: Test water
8: Drainage path
9: Upper pressure head
10: Pore pressure transducer
11: Load cell

Figure 3: Illustration of the Danish continuous loading apparatus. Figure not to scale.

The apparatus consists of a rigid ring [1], bolted to the CLO-base [2], and an O-ring sealing the joint. The soil specimen [3], with a height of 30 mm, is placed in the rigid ring, which prevents horizontal displacement, making it possible to measure the horizontal pressure, σ'_H, exerted by the soil sample. The horizontal pressure is measured by three, 20 bar pressure gauges [4] placed evenly in the ring with an internal spacing angle of 120º. The pressure gauges each have a diameter of 7.6 mm and are placed to ensure full contact with the soil specimen at all times. The vertical one-dimensional deformation of the soil specimen is measured by two, 20 mm displacement transducers [5] placed at opposite sides of the upper pressure head, measuring the mean displacement. Porous bronze filter stones [6] are placed at the top and bottom of the sample, giving the soil specimen access to the test water surrounding the apparatus. The test water [7] is applied at a pressure of 200 kPa to better enable saturation and drainage of the sample. Drainage paths [8] are placed in the upper pressure head [9] and the CLO base. The drainage paths in the CLO base

are closed during testing allowing the sample to only drain single-sided. Excess pore pressure built up in the sample is measured by a 7 bar pore pressure transducer [10] placed in the CLO base. The load is measured continuously by a two metric ton load cell [11] to a steel ball placed on the upper pressure head. The CLO apparatus and all the measuring components are surrounded by the pressurized test water and enclosed in a Plexiglas cylinder. The rate of deformation is selectable and set to 0.015 mm/h, corresponding to an initial rate of 0.05 %/h. This rate was chosen to minimize the build-up of excess pore pressure in the sample.

All measurements, consisting of two displacements, one pore pressure, one load (effective vertical stress), three total horizontal pressures, one test water pressure and the time, were recorded using a linked computer (not shown in Figure 3) at a rate of 0.1 Hz. This rate was chosen in order to assemble a comprehensive description of what is happening in the sample as well as to limit the amount of data to an acceptable quantity.

The tests were conducted with stresses from the swell pressure of the individual soil sample to the lower maximum capacity of either the horizontal pressure transducer or load cell.

3.3 Interpretation methods

Casagrande (1936) suggested that the consolidation test could be used to determine the preconsolidation stresses. Several other methods have been suggested as useful in interpreting the results of consolidation tests. All methods are empirical, based on observation of plots of various test results. Five different methods were used to determine the preconsolidation stresses in this study; further information on the interpretation methods can be found in the referenced literature.

Casagrande (1936) used the compression curve in a semi-logarithmic depiction to determine the preconsolidation stresses. The method is based on the point of maximum curvature of the compression curve and the virgin branch. The virgin branch is described as:

$$\varepsilon = C_c \times \log(1 + \frac{\sigma'}{\sigma'_\kappa}) \qquad \text{[eq. 1]}$$

where ε is the vertical strain, C_c is the compression index, σ' is the effective vertical stress and σ'_κ is a reference stress corresponding to the point of the maximum curvature of the compression curve. Pacheco Silva (1970) (As mentioned in Clementino 2005) presented another method based on Casagrande's depiction of the compression curve. Jacobsen (1992) defined the preconsolidation stresses as two times the reference stress corresponding to the point of the maximum curvature σ'_κ. Akai (1960) and Janbu (1970) used the change in secondary compression index, $C_{\alpha\varepsilon}$, and consolidation modulus, M, respectively, to determine the preconsolidation stresses.

4 RESULTS

Eight oedometer tests (four ILO and four CLO tests) were performed to obtain a comprehensive description of the deformation behavior of Søvind Marl under increasing stress levels (Figure 4). All of the curves show similar behavior, and all are located in the same narrow band. A significant feature of all the curves is the presence of two maximum curvatures and two approximately straight sections of the compression curves following these curvatures. These two features are typically present only once for unfissured clays and usually indicate of a clay with characteristics that approach a normal consolidated state. The fact that these trends (maximum curvatures and straight sections) occur more than once is reflective of the macrostructure of Søvind Marl. The fissures substantially influence the stiffness of the clay at lower stresses, as the increased stresses force the fissures to close and the stiffness of the intact clay begins to dictate the behavior of the soil sample.

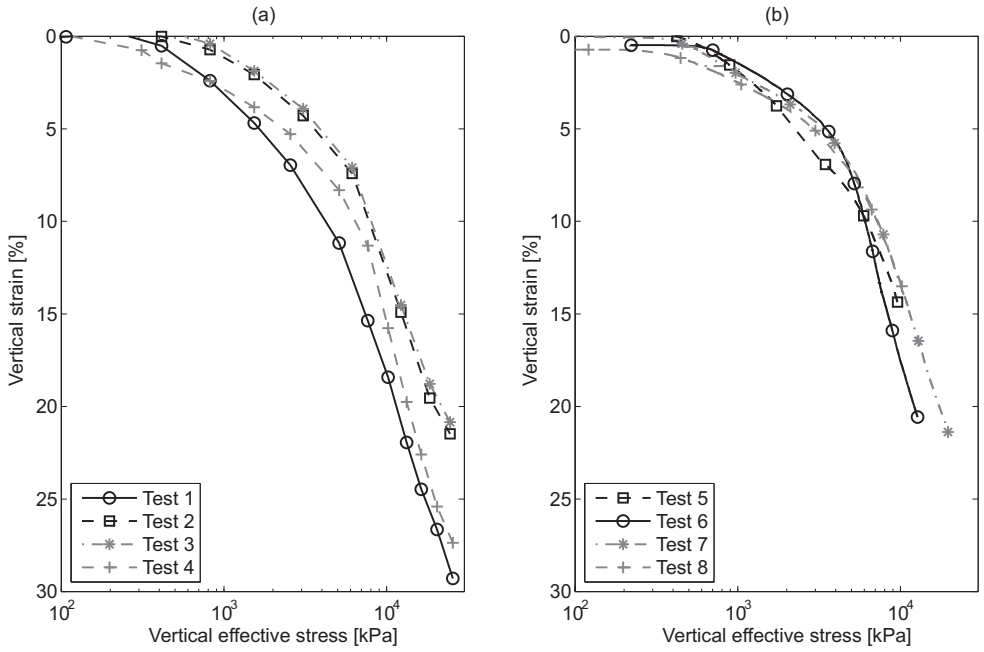

Figure 4: Compression curves: (a) ILO tests (b) CLO tests.

The results of the oedometer tests were analyzed using the methods described in section 4. The Akai (1960) method, however, was only applied on the ILO tests, since the secondary consolidation index was not determined during the CLO tests. While only results from ILO test 1 and CLO test 6 are graphically presented in Figures 5 and 6, respectively, the graphs of all tests follow the same patterns. Table 2 presents the result of all tests and interpretation methods. The compression curves for tests 1 and 6 are marked with fully drawn lines in Figure 4, Figure 5 (a) and (b) and Figure 6 (a) and (b).

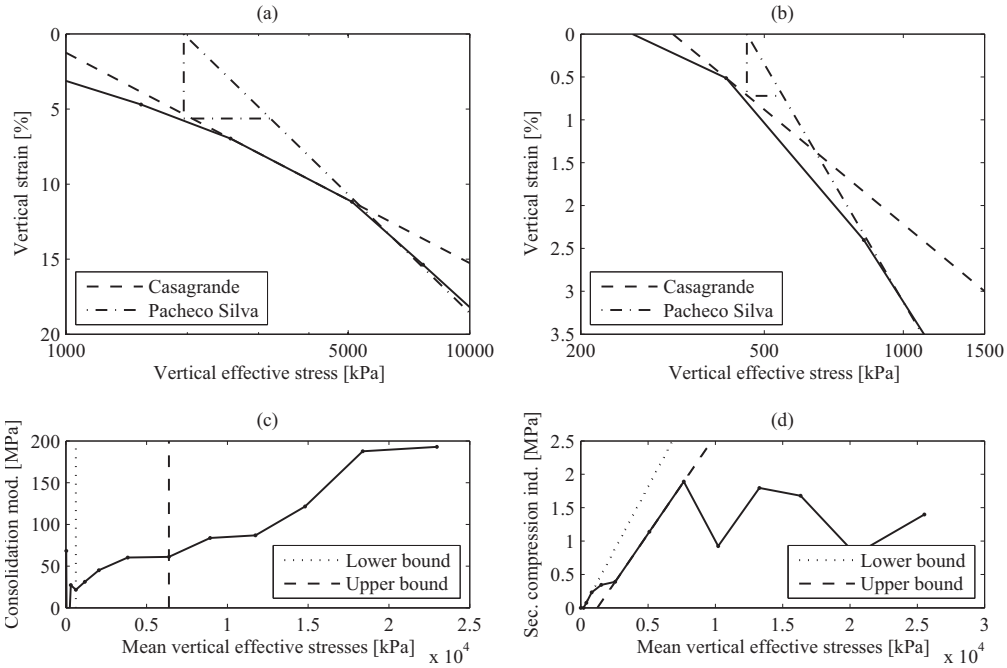
(a)
Vertical strain [%]
Vertical effective stress [kPa]
Casagrande
Pacheco Silva
(b)
Vertical strain [%]
Vertical effective stress [kPa]
Casagrande
Pacheco Silva
(c)
Consolidation mod. [MPa]
Mean vertical effective stresses [kPa]
x 10^4
Lower bound
Upper bound
(d)
Sec. compression ind. [MPa]
Mean vertical effective stresses [kPa]
x 10^4
Lower bound
Upper bound

Figure 5:

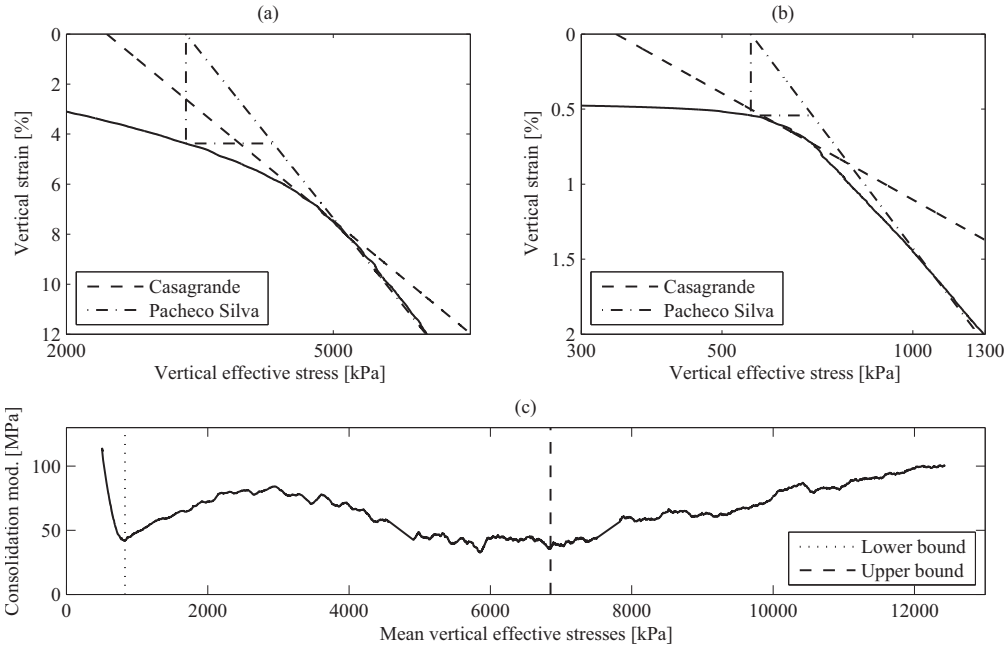

Figure 6: Illustration used to determine the preconsolidation stresses from CLO test 6. (a) Upper bound found according to Casagrande (1936) and Pacheco Silva (1970) methods, (b) lower bound found via Casagrande (1936) and Pacheco Silva (1970) methods and (c) upper and lower bounds found via the Janbu (1970) method.

As expected, based on the fissured matrix of the clay, a clearly defined single preconsolidation stress is not evident. Regardless of whether the data are from an ILO or CLO test, all methods yields two values for all samples which could both be interpreted as the preconsolidation stresses. As two preconsolidation stresses are a physical impossibility, the lower bound is deemed to arise from the fissured matrix as suggested by Gasparre and Coop (2008).

A significant change in the behavior of the samples occurs twice, as shown in Figures 5 and 6. Also, the high stresses generated for these tests were necessary in order to obtain an adequate description of the total behavior and with this the full description of the preconsolidation stresses. Further alterations at even higher

stresses have not been evaluated and therefore cannot be ruled out. However, as the effect of the fissures was eliminated in these tests, it seems unlikely that any further changes are likely to occur.

Both the ILO and CLO tests yield similar results. However, a comparison of Figures 5 and 6 make it clear that the CLO tests provide a more detailed description of sample deformations. Due to the continuous nature of the CLO tests, a description of all the behavioral changes is generated whereas ILO tests only describe the changes at increasing intervals. The additional information provided in the CLO tests lends itself to increased accuracy, a more thorough description and the best estimate of the preconsolidation stresses.

5 PRECONSOLIDATION

Table 2 lists an estimate on the two possible interpreted values (upper and lower bounds), the appurtenant values of the overconsolidation ratio, *OCR*, and the compression index, C_c.

Table 2: The upper and lower bounds, as well as an estimate on the preconsolidation stress level and OCR.

Sample Metric	Sample							
	1	2	3	4	5	6	7	8
Depth [m]	29	39	39	11.5	33	47	11.5	11.5
σ'_{vo} [kPa]	255	350	350	110	285	400	110	110
Location	LH	LH	LH	BS	LH	LH	BS	BS
Test type	ILO	ILO	ILO	ILO	CLO	CLO	CLO	CLO
Method	Lower bound [kPa]							
Casagrande	530	1,150	850	450	580	750	480	480
Pacheco Silva	550	1,190	790	440	610	690	450	390
Jacobsen	830	1,640	1,650	620	930	1,300	860	810
Janbu	620	1,180	1,180	620	710	840	620	550
Akai	1,000	3,200	3,300	850	–	–	–	–
Lower σ'_{pc} [kPa]	700	1,200	1,200	620	700	800	620	550
Lower OCR [-]	2.7	3.4	3.4	5.6	2.5	2.0	5.6	5.0
Lower C_c [%]	9.2	8.9	6.2	5.8	7.2	5.6	5.3	4.3
Method	Upper bound [kPa]							
Casagrande	4,340	5,340	5,280	6,140	5,080	4,840	4,860	4,160
Pacheco Silva	3,210	4,660	4,580	5,350	4,050	4,070	4,740	4,260
Jacobsen	7,670	9,200	9,200	10,220	8,130	9,410	6,780	4,010
Janbu	6,380	9,200	9,200	8,940	6,660	6,850	8,500	5,920
Akai	6,330	10,720	10,040	8,050	–	–	–	–
Upper σ'_{pc} [kPa]	6,300	9,200	9,200	8,900	6,500	6,800	6,700	4,700
Upper OCR [-]	24.7	26.3	26.3	80.1	22.8	17.0	60.9	42.7
Upper C_c [%]	26.3	25.4	24.5	33.3	24.2	33.5	27.0	23.0

The lower bounds are only two to three times the vertical effective in situ stresses, σ'_{v0}, resulting in very low *OCR*s. Results such as these are highly unlikely for preconsolidation of a tertiary clay, since it is known to previously have been covered by up to 1 km of sediment deposits and endured several ice ages and the associated ice sheets. The lower compression index was also found to be very low and dissimilar to values which could be expected of an overconsolidated clay. These results demonstrate the significant influence of the fissured matrix on the stiffness behavior of Søvind Marl.

The impact of the geological history of the Søvind Marl is evident in the preconsolidation. The upper bounds are significantly higher than the lower bounds and, consequently, the *OCR*s are significantly higher. The compression index is elevated for Søvind Marl, corresponding to the very high plasticity of up to 250%. The values from tests 2 and 3 are significantly higher than the other values from the LH location (1, 5 and 6). This is due to a coarser load program, which consequently leads to a higher and less precise preconsolidation stress values. This illustrates the importance of a detailed and carefully planned load program.

The lower and upper bounds of the preconsolidation stresses are unrelated, as only the upper bound is associated with preconsolidation, while the lower is related to the structure of the clay. As the upper bound is significantly higher than any realistic stresses following an engineering project, the upper bound is mainly interesting from an engineering geology point of view, as it provides valuable information on the clay history. The lower bound, while being independent of the preconsolidation, can be used as a benchmark for preconsolidation stresses in designing of geotechnical engineering projects.

The interpretation methods that were used in this study yielded very different results on the same tests, cf. Table 2. The difference between the methods can be as high as a factor of two. Akai's method, and occasionally Jacobsen's method, often produced values that are significantly higher than found using the remaining methods. Because of these method-specific differences, it is important to use several different methods when determining the preconsolidation stresses. The preconsolidation stresses found in Table 2 are estimated based on all methods.

Preconsolidation stresses and *OCR* measured at increasing formation depth are shown in Figure 7. Only preconsolidation stresses from the older part of the Søvind Marl formation (LH) are illustrated since the

samples from the younger part of the formation (BS) were collected from a different location, and the depths could not be directly compared.

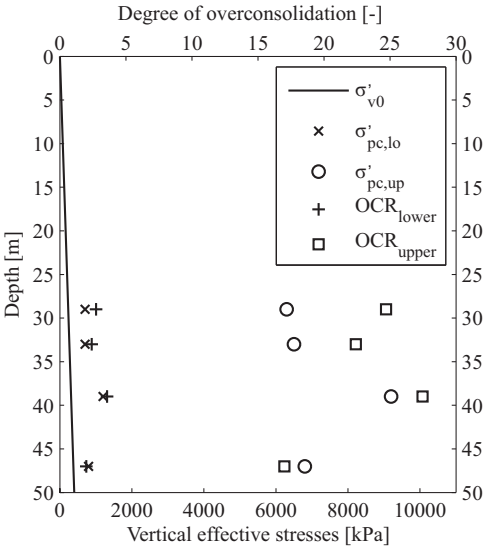

Figure 7: Interpreted value as well as in situ stresses at different depths.

Both the upper and lower bounds (not including tests 2 and 3) increased with depth at a rate that roughly corresponds to the rise in the in situ stresses. Conversely, *OCR*s decreased with increasing depth because of the diminishing influence of the previous clay consolidation compared to the in situ stresses.

6 INFLUENCE OF SOIL SAMPLE DIAMETER

The standard diameter of a soil sample in the Danish consolidation apparatus is 70 mm. Reducing the sample core diameter to 35 mm, as needed for this study quadruple the applied stresses, while also increasing the influence of the boundary conditions between the ring and the sample. This influence is further enhanced by the fact that the height/diameter ratio is not keep constant. It was deemed important, therefore, to further evaluate the effect of the smaller sample diameter on the results of this study. In order to do so, incremental

oedometer tests using both 35 and 70 mm sizes were conducted on samples from the same test tubes as the ILO tests presented in this paper. Figure 8 shows the comparison of the compression curves from those tests.

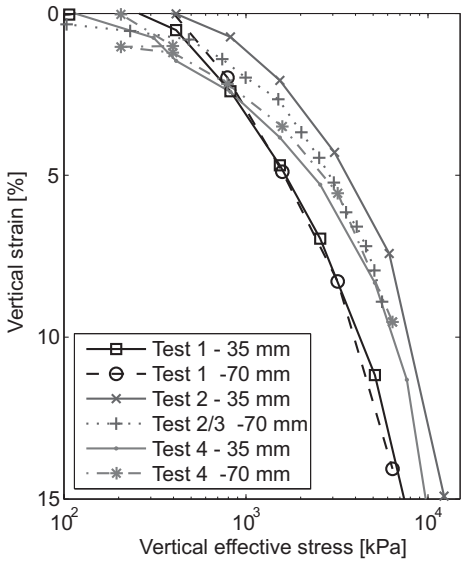

Figure 8: Comparison of compression curves for different sample diameters.

The comparisons for test 1 and 4 show no effect of the smaller diameter, as the compression curves are coincident and all show the same behavior at the various stress levels. For test 2, a small effect of the boundary conditions is apparent, with a parallel displacement of about 1% in strain present at every stress level. However, the shape of the two curves is identical, with maximum curvatures at similar stresses. The upward displacement of the curve derived from the 35 mm sample diameter has a limited, to essentially no, effect on the preconsolidation stresses, compared to the effect of the large load increments in this test.

The importance of the high stresses in the sample is apparent in Figure 8, as the second maximum curvature was found only at the very end of the 70 mm compression curve. While the smaller sample size was essential

to the current studies where high stress levels were evaluated, use of the smaller diameter in tests requiring only lower stresses is not recommended.

7 CONCLUSION

Eight oedometer tests (four ILO tests and four CLO tests) were performed on a highly fissured Danish tertiary clay called Søvind Marl. The samples originated from two different locations in Arhus, Denmark, LH and BS, both with large quantities of Søvind Marl. The samples used are up to 46 million years old and have previously been covered by up to 1 km of Oligocene and Miocene deposits, and were overlain by glaciers from seven known ice ages. Because of these events, it was expected preconsolidation stresses would be high.

The geological history of Søvind Marl is known, providing a priori insight into the previous stresses the clay has sustained. In order to reproduce these high stresses, a sample diameter of 35 mm was used, rather than the 70 mm sample typically used in Danish engineering practice. The sample diameter should be as large as possible, while still prioritizing the goal of achieving the required stresses. This should be done in order to minimize the influence of boundary condition. In this study, the smaller diameter did not noticeably the affect the results. One main concern when determining the preconsolidation stresses of Søvind Marl is ensuring that adequate stresses in the sample are reached so as to exceed the stresses which can be expected based on the geological history.

As stated by Gasparre et al. (2007a, 2007b) among others, the preconsolidation stresses are difficult to clearly determine in a fissured overconsolidated clay, due to the structure of the clay. The fissures influence the stiffness of the soil and, consequently, also the determination of the preconsolidation stresses. Consequently, two apparent values can be determined as the preconsolidation stresses based on several recognized methods. This is also the case with Søvind Marl, with lower and upper bounds identified in all eight tests. The lower bounds were between 600 and 800 kPa at depths from 29 m to 47 m, which corresponds to only two to three time the effective in situ stresses. This does not correlate with the known

geological history and is deemed to be a result of the fissured structure. The upper bounds are more likely a result of the previous consolidation as well as secondary consolidation. The preconsolidation stresses range from 6 300 to 8 900 kPa at the same depth interval. While the upper bound is deemed to represent the 'true' preconsolidation stresses, this is only useful from an engineering geology point of view. In contrast, the lower bound, despite being independent of the previous consolidation, can be used in the design of geotechnical engineering projects.

Both ILO and CLO tests yielded data that could be used to describe the deformation of the soil at varying stresses. However, the continuous nature of the CLO tests yields a more detailed description of the deformations, compared to ILO tests. Consequently, the CLO test enables a more accurate estimate of the preconsolidation stresses, since it does not rely on increasing load steps, as does the ILO test. The design of the load program for ILO tests proved to be important. There was a large difference in the results of ILO tests 2 and 3 compared to the other tests performed on LH-material. Tests 2 and 3 were performed by doubling the effective stresses in the samples at each load step. This process resulted in deformation descriptions that were too coarse because of the small diameter of the samples. Adjusting the load program to smaller load steps improved the deformation description. Based on these observations, CLO tests are preferred over the traditional ILO tests.

REFERENCES

Akai, K., 1960, De strukturellen Eigenschaften von Schluft Mitteilugen (in German). Heft 22. Die Technische Hochschule Aachen

Amorosi, A. and Rampello, S., 1998, "The Influence of Natural Soil Structure on the Mechanical Behavior of a Stiff Clay," Proceedings of the 2nd International Symposium of Hard Soils, Soft Rocks. 12th-14th of October 1998. Naples, Italy.

Burland, J.B., 1990, "On the Compressibility and Shear Strength of Natural Soils," *Geótechnique*, Vol. 40, pp. 329-378.

Casagrande, A., 1936, "The Determination of the Preconsolidation Load and its Practical Significance," *International Conference on Soil Mechanics and Foundation Engineering*, Cambridge, Massachusetts, USA, June 22-26, 1936.

Clementino, R.V. 2005, "Discussion of "An oedometer test study on the preconsolidation stress of glaciomarine clays"". *Can. Geotech. J.*, Vol. 42, pp. 972-974

Cotecchia, F. and Chandler, R.J., 1997, "The Influence of Structure on the Pre-Failure Behaviour of a Natural Clay," *Geótechnique*, Vol. 47**,** pp. 523–544.

Cotecchia, F. and Chandler, R. J., 2000, "A General Framework for the Mechanical Behaviour of Clays," *Géotechnique*, Vol. 50, pp. 431–447.

Crawford, C.B., 1986, "State of the Art: Evaluation and Interpretation of Soil Consolidation Tests," *Consolidation of Soils: Testing and Evaluation, ASTM STP 892*, American Society for Testing and Materials, Conshohocken, PA, pp. 71-103.

Gasparre, A., Nishimura, S., Coop, M.R. and Jardine, R.J., 2007a, "The Influence of Structure on the Behaviour of London Clay," *Geótechnique*, Vol. 57, pp. 19–31.

Gasparre, A., Nishimura, S., Minh, N.A., Coop, M.R. and Jardine, R.J., 2007b, "The Stiffness of Natural London Clay," *Geótechnique*, Vol. 57, pp. 33-47.

Gasparre, A. and Coop, M.R., 2008, "Quantification of the Effects of Structure on the Compression of a Stiff Clay," *Can. Geotech. J.*, Vol. 45**,** pp**.** 1324–1334.

Geocenter Danmark, 2010,. Geoviden 3, ISSN 1604-8172

Grønbech, G.L., Nielsen, B.N. and Ibsen, Lars B., 2012, "Interpretation of Consolidation Test on Søvind Marl," NGM 2012, *Nordic geotechnical meeting*, Copenhagen, Denmark, May 9-12, 2012, Vol. ½, pp. 85-93. Grønbech, G.L., Nielsen, B.N., Ibsen, Lars B. and Stockmarr, P., 2014, "Geotechnical Properties of Søvind Marl - a Plastic Eocene Clay. *Can. Geotech. J*., Accepted for publication

Jacobsen, M., 1992, "Bestemmelse af Forbelastningstryk i Laboratoriet (in Danish). *NGM 1992 Nordic geotechnical meeting*, Aalborg, Denmark, May 28-30, 1992, Vol. 2/3.

Janbu, N., 1970, Grunnlag i Geoteknikk (in Norwegian). Tapir forlag

Krogsbøl, A., Hededal, O. and Foged, N., 2012, "Deformation Properties of Highly Plastic Fissured Palaeogene Clay – Lack of Stress Memory?" *NGM 2012, Nordic geotechnical meeting*, Copenhagen, Denmark, May 9-12, 2012, Vol. ½, pp.133-140.

Pacheco Silva, F., 1970, "A New Graphical Construction for Determination of the Preconsolidation Stress of a Soil Sample, (in Portuguese)" *Fourth Brazilian Conference on Soil Mechanics and Foundation Engineering*, Rio de Janeiro, Brazil, August 3-8 1970. Vol. 2, op. 225-121.

Thøgersen, L., 2001, "Effects of Experimental Techniques and Osmotic Pressure on the Measured Behaviour of Tertiary Expansive Clay," Vol. 1. Ph.D. Thesis. Soil Mechanics Laboratory. Aalborg University, Denmark. ISSN: 1398-6465 R 2016

APPENDIX E

Earthe Pressure at Rest of Søvind Marl - a highly overconsolidated Eocene clay

Authors:
Gitte Lyng Grønbech, Lars Bo Ibsen and Benjaminn Nordahl Nielsen

Submitted to:
Engineering Geology

Year of submission:
2015

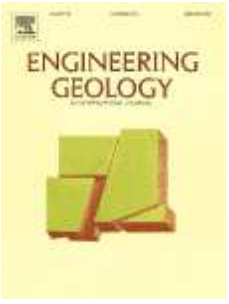

E.1 Author's Right

Author Rights

Elsevier supports the need for authors to share, disseminate and maximize the impact of their research. We take our responsibility as stewards of the online record seriously, and work to ensure our policies and procedures help to protect the integrity of scholarly works.

Author's rights to reuse and post their own articles published by Elsevier are defined by Elsevier's copyright policy. For our proprietary titles, the type of copyright agreement used depends on the author's choice of publication:

For subscription articles: These rights are determined by a copyright transfer, where authors retain scholarly rights to post and use their articles.

For open access articles: These rights are determined by an exclusive license agreement, which applies to all our open access content.

In both cases, the fundamental rights needed to publish and distribute an article remain the same and Elsevier authors will be able to use their articles for a wide range of scholarly purposes.

Details on how authors can reuse and post their own articles are provided below.

Help and support
For reuse and posting not detailed below, please see our posting policy, or for authors who would like to:

- Include material from other sources in your work being published by Elsevier, please visit: Permission seeking guidelines for Elsevier authors.
- Obtain permission to re-use material from Elsevier books, journals, databases, or other products, please visit: Obtaining permission to reuse Elsevier material
- Or if you are an Elsevier author and are contacted by a requestor who wishes to re-use all or part of your article or chapter, please also refer them to our Obtaining Permission to Re-Use Elsevier Material page.
- See our FAQ on posting and copyright queries.
- Contact us directly, please email our Permissions Help Desk.

http://www.elsevier.com/journal-authors/author-rights-and-responsibilities

i. Title of the paper

Earth Pressure at rest of Søvind Marl – a highly overconsolidated Eocene clay

ii. Authors

1. Gitte Lyng Grønbech
2. Lars Bo Ibsen
3. Benjaminn Nordahl Nielsen

iii. Affiliations and designations

1. Ph.D. student, Department of Civil Engineering, Aalborg University, Sofiendalsvej 9, 9200 Aalborg SV, Denmark, e-mail: glg@civil.aau.dk, telephone number: (+45) 99 40 85 74
2. Professor, Department of Civil Engineering, Aalborg University, Sofiendalsvej 9, 9200 Aalborg SV, Denmark e-mail: lbi@civil.aau.dk, telephone number: (+45) 99 40 84 58
3. Associate Professor, Department of Civil Engineering, Aalborg University, Sofiendalsvej 9, 9200 Aalborg SV, Denmark e-mail: bnn@civil.aau.dk, telephone number: (+45) 99 40 84 59

Abstract, English

The present study evaluated earth pressure at rest, K_0, in highly overconsolidated Eocene clay called Søvind Marl, which exhibits extremely high plasticity indices of up to 300%, a highly fissured structure, and preconsolidation stresses up to 6,800 kPa. Continuous Loading Oedometer (CLO) tests with a constant rate of strain were conducted on Søvind Marl in the Danish Continuous Loading Oedometer Apparatus, which enables test water to be applied at 200 kPa, and measures the horizontal stresses via pressure gauges placed in a stiff oedometer ring. The horizontal and vertical stresses were measured from in situ stresses to various stress levels to estimate continuous K_0 development in this highly overconsolidated clay. The normally consolidated earth pressure at rest was found for two different sample ages of Søvind Marl to be between 0.42 and 0.68. Results indicated the overconsolidated K_0 reached values as high as 6 to 8 in the in situ stress range. Meyerhof's (1976) reported correlation between $K_{0(oc)}$ and OCR was found inconsistent with $K_{0(oc)}$ development of in Søvind Marl. However, the development of OCR_{lab} dependent on previous test stresses, as an alternative to preconsolidation stresses, showed congruent results using $\alpha = 1.05$ independent of sample age.

Key words: Earth pressure at rest, Overconsolidated clay, Constant rate of strain, Plastic clay

1 INTRODUCTION

Current stresses are the governing factors determining soil behavior. The initial stress state is essential, an integral element to properties. Donath (1891) first introduced the concept of a stationary pressure of unlimited ground. The in situ vertical effective stresses, σ'_{V0} can be easily estimated based on the weight of soils located at higher levels in the soil column and soil pore. However, the horizontal effective stresses, σ'_{H0}, are more difficult to estimate, and are often determined based on prior experience and knowledge. The relationship between horizontal effective and vertical stresses in the in situ state, when horizontal displacement is not permitted in a homogeneous natural soil deposit is known as the earth pressure at rest, K_0, and the coefficient is a constant given by:

$$K_0 = \frac{\sigma'_H}{\sigma'_V} \tag{1}$$

The earth pressure at rest coefficient is often used to estimate horizontal stresses on structures in soils, including but not limited to piles, sheet pile walls, and underground tunnels.

Several methods are known to estimate $K_0(nc)$ based on, for example the plasticity index shown in Eq. 2 (Brooker and Ireland 1965 and Massarsch 1979) or the friction angle indicated by Eq. 3 (Jaky 1944):

$$K_0(nc) = 0.44 + 0.42(I_P/100) \tag{2}$$

$$K_0(nc) = 1 - \sin(\varphi) \tag{3}$$

$K_0(oc)$ is then estimated by the overconsolidation ratio, OCR, Eq. 4 by Meyerhof (1976) and Eq. 5 by Mayne and Kulhawy (1982):

$$K_0(oc) = K_0(nc) \times OCR^{\alpha} \tag{4}$$

$$K_0(oc) = K_0(nc) \times OCR^{\sin\varphi} \tag{5}$$

where $K_{0(nc)}$ is derived from Eq. 3, and based on Meyerhof (1976), α in Eq. 4 is 0.50.46 $\pm$ 0.06 according to Lancellotta (1993); and Lefebvre et al (1991) and Hamouche et al (1995) found α as high as 1.0 for sensitive clays. Krogsbøl et al. (2012) determined α at approximately 0.6 – 0.7 for Røsnæs Clay and Little Belt Clay, which are Danish Tertiary clays from the same geological period as Søvind Marl. However, these results were calculated based on much smaller preconsolidation stress values; and thereby OCR.

In the present study, K_0 for the Danish Tertiary clay Søvind Marl was examined.

This article describes the Constant Rate of Strain (CRS) tests performed in a Continuous Loading Oedometer (CLO) apparatus on Søvind Marl and the subsequent data analyses and interpretation. The purpose of this study was to determine how the earth pressure at rests, specifically of Søvind Marl a Danish Tertiary clay, behaves during high stress levels.

2 SØVIND MARL

Søvind Marl is a Danish tertiary clay, which is found distributed in various geographic locations throughout Denmark. The formation age is determined between 46 million years and 36 million years old. Søvind Marl is characterized by a very high plasticity index of a nominal range up to 250%, with maximum values exceeding 300%. The extreme plasticity results from a relatively high content of different clay minerals, and specifically, increased plastic Smectite (approximately 50% of the clay minerals). Søvind Marl was determined a sensitive clay. An additional characteristic is the highly fissured clay structure. Søvind Marl exhibits a very uniform visual appearance, despite the long deposit period. The only noteworthy mesofabric difference is sample color. While working with the material, a fine net of fissures and slickensides were clearly defined. The fissures ran in unstructured directions through the deposit. Grønbech et al. (2015a) provided a thorough description of Søvind Marl, including the geotechnical properties and characteristics.

Samples from two locations (named LH and BS) located approximately 1.3 km from each other at Aarhus Harbor in Denmark were examined in this study, Søvind Marl from both locals was found at great depths of more than 70 m, and the only notable difference between the two locations was the Søvind Marl age. LH

samples originated from an older portion of the formation, whereas BS samples originate from a younger part of the same formation. LH samples were derived from different depths in the same downward borehole, and all BS samples were from the same depth but at two different boreholes situated approximately 5 m apart.

2.1 Preconsolidation stresses

Structure has an effect on fissured clays behavior. Gasparre and Coop (2008) found structure particularly influential in determining preconsolidation stresses, giving an appearance of an upper and lower bound of preconsolidation stresses. Krogsbøl et al. (2012) reported Eocene clays lose stress memory due to its high plasticity, and the lower bound of the preconsolidation stresses were the only preconsolidation stresses resulting in much smaller OCR values. However, these tests were only conducted to stress levels between 1,000 kPa and 4,000 kPa, and therefore not near the upper bound of the preconsolidation stress (up to 9,000 kPa). Grønbech et al. (2015b) examined Søvind Marl preconsolidation stresses and found the clay was highly affected by its fissured structure, as two values were be interpreted as the preconsolidation stresses. The lower bound was between 550 kPa and 800 kPa, only two to three times the in situ stress values. This result was not consistent with Søvind Marl's geological history and millions of years of secondary consolidation. It was therefore determined the lower bound of the preconsolidation stresses resulted from the fissured structure collapse. The upper bound of the preconsolidation stresses was between 5,000 kPa and 9,000 kPa, which were congruent with the geological history of Søvind Marl.

Relevant classification properties and preconsolidation stresses of study samples are listed in Table 1.

Table 1: Classification of study samples. *Represents estimates as no tests were conducted to directly determine the preconsolidation stresses.

Sample Metric	Sample					
	1	2	3	4	5	6
Location	LH	BS	BS	LH	LH	BS
Depth [m]	47	11.5	11.5	33	23.5	11.5
σ'_{v0} [kPa]	400	110	110	285	210	110
Upper σ'_{pc}[kPa]	6,800	6,700	4,700	6,500	6,200*	4,700*
Lower σ'_{pc}[kPa]	800	620	550	700	680*	550*
γ [kN/m^3]	17.9	17.5	17.7	18.1	17.5	17.9
w_{nat} [%]	40.7	40.0	39.8	38.8	39.7	40.7
I_P [%]	195.2	43.6	43.6	205.6	95.7	43.6
Calcite content [%]	36.3	64.5	64.5	10.0	55.0	64.5
Chloride content [%]	0.6	1.7	1.7	0.5	0.9	1.7
pH [-]	9.15	8.4	8.4	9.25	9.2	8.4

3 CONTINUOS LOADING OEDOMETER

Hamilton and Crawford (1959) first introduced the continuous loading oedometer (CLO) method as a fast and easy approach to determine soil preconsolidated stress level, σ'_{pc}. The setup and boundary conditions were similar to an incremental oedometer test (ILO), with the exception of a single sided drain placed on top, allowing the excess pore pressure to be measured in the bottom of the sample (Larsson and Sällfors 1986). Back pressure was later applied to increase sample saturation (Lowe et al. 1964 and Ducasse et al. 1986). The primary difference between the conventional ILO and CLO tests is the manner in which the load is

applied to the sample. The load in ILO tests is applied in increasing increments, resulting in an incremental description of the sample stiffness, whereas the load is applied continuously in CLO tests, which therefore yields a continuous description of sample deformation and stiffness of the sample. The strain rate should be chosen to reduce substantial excess pore pressure in the soil sample. The entire applied load is therefore a direct increase in effective stresses to the sample. Gorman et al. (1977) suggested the strain rate should be chosen based on the liquidity index; this method is used to determine strain rate in the ASTM (2012) standard. Lowe at al. (1969) varied the strain rate to maintain a constant excess pore pressure, whereas Janbu et al. (1981) maintained a constant excess pore pressure ratio compared to the applied load. Both methods require careful test monitoring to vary the strain rate. Hamilton and Crawford (1959) reported CLO tests yielded results comparable to ILO tests, under the requirement that strain rate was maintained at a rate that minimized the excess pore pressure. Traditionally, CLO tests were conducted in rigid oedometer cells placed in modified triaxial frames (Larsson and Sällfors 1986, Smith and Wahls (1969), Wissa et al. 1971, Gorman et al. 1977, Grønbech et. al 2015b). The rigid ring is the method used by the American (ASTM 2012), and Norwegian (Standard Norge 1993) standards. Alternatively, a Rowe cell with a motorized piston can be employed (Rowe and Barden 1966, Davison 1989).

CLO tests advantages include continuous results, yielding more accurate determinations. For example, compression curves and preconsolidation stresses, and the possibility for slow strain rates make CLO tests ideal for very plastic clays, including Søvind Marl. Amour and Drnevich (1986) reported the two of the most notable disadvantages of CLO tests. The first was the challenging determination of secondary compression indices, significant in Søvind Marl. . The second, excess pore pressure build up was dependent on strain rate and soil permeability, which is very low in Søvind Marl. Therefore, the strain rate should be chosen carefully to minimize the pore pressure accumulation. (Sheahan and Watters 1997, Dobak 2003).

4 METHOD

CLO tests exhibit the potential advantage of achieving a clear and continuous description of the earth's pressure at rest. A modification of the oedometer and placement of the pressure transducers in the rigid ring (Figure 1) allows the total horizontal pressure to be measured (Ladd 1965, Abdelhamid and Krizek 1976, Lefebvre and Philibert 1979, Thøgersen 2001). Measurement of horizontal pressure in a rigid ring prevents of horizontal movement, hence all deformation is one-dimensional. This is at the cost of friction between the rigid ring and soil sample. Side friction can be reduced by using a semi-rigid ring, where strain gauges measure lateral movement, which is subsequently prevented by applying pressure to surrounding oil, corresponding to horizontal pressure incurred by the soil sample (Mesri and Hayat 1993). Side friction influence can be avoided by measuring horizontal pressure in a triaxial apparatus, where the sample is enclosed by a flexible membrane and horizontal movement is controlled by applying pressure to surrounding water, much like the semi-rigid ring; however, a feedback system is required to control the water pressure (Andrawes and El-Sohby 1973).

4.1 Testing method

The CLO apparatus at Aalborg University was used to conduct all soil tests in this study. Pressure was applied to the test water in the triaxial cell, which better enabled sample saturation and drainage. The apparatus is composed of a stiff ring with three horizontal pressure gauges placed evenly around the ring. Two displacement transducers positioned at opposite sides of the sample measured vertical deformation. The sample diameter was set to 35 mm to obtain sufficient stresses that exceeded the preconsolidation stresses (listed in Table 1) within the physical limitation of the 2 metric ton load pistol. Samples were collected in situ in a 72 mm tube and hand trimmed to the required diameter and height. The sample was drained single-sided and the sample pore pressure was measured at the sample bottom. Test water with pore water pH and

salinity was applied at 200 kPa. Deformation rate was adjustable and set to 0.015 mm/h, corresponding to an initial deformation rate of 0.05 %/h with an initial height of 30 mm. This rate was chosen to minimize excess pore pressure build up in the sample. The tests were performed according to Norwegian standard NS 8018:1993 (NS 1993).Grønbech et al. (2015b) provided a more comprehensive physical description of the apparatus, and an illustration is provided in Figure 1.

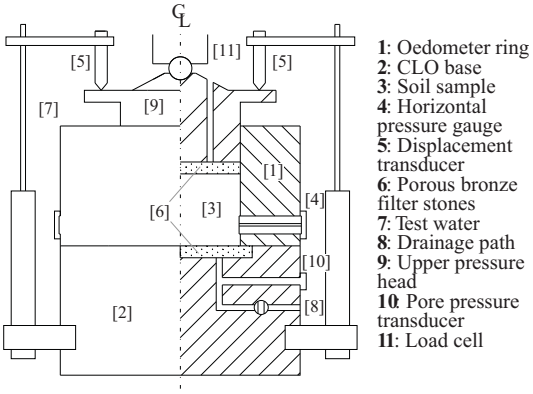

Figure 1: Schematic of Continuous Loading Oedometer apparatus developed at Aalborg University. Not to scale.

Three different test programs were used to examine the behavior of the earth pressure at rest under different conditions. Two tests (on LH and BS materials) were performed with each test program. The test programs were as follows: i) Strictly loading (tests 1 and 2) from sample swell pressure to the maximum load the apparatus could sustain to estimate earth pressure at rest for normally consolidated Søvind Marl, ii) unloading and reloading from three predetermined stresses (tests 3 and 4) and iii) unloading and reloading from lower and upper bounds of the preconsolidation stresses (tests 5 and 6) to estimate the earth pressure at rest under different conditions.

The vertical effective stresses, σ'_V, test water pressure, u_0, pore pressure, u_1, and sample deformation were measured directly and need little correction. However, measured horizontal pressure is total horizontal pressure, and therefor needs a correction to take into account the pore pressure. The excess pore pressure is

zero at the top of the sample (as it is allowed to drain freely), and is measured at the bottom of the sample. The excess pore pressure is assumed to take the shape of a parabola and 2/3 of the excess pore pressure acts on the horizontal pressure gauges. The effective horizontal pressure is therefore calculated as follows:

$$\sigma'_H = \sigma_H - \tfrac{2}{3}u_1 \quad (6)$$

5 RESULTS

The compression curves derived from the six tests and the vertical and horizontal pressures from each test are respectively presented in Figure 2 and Figure 3.

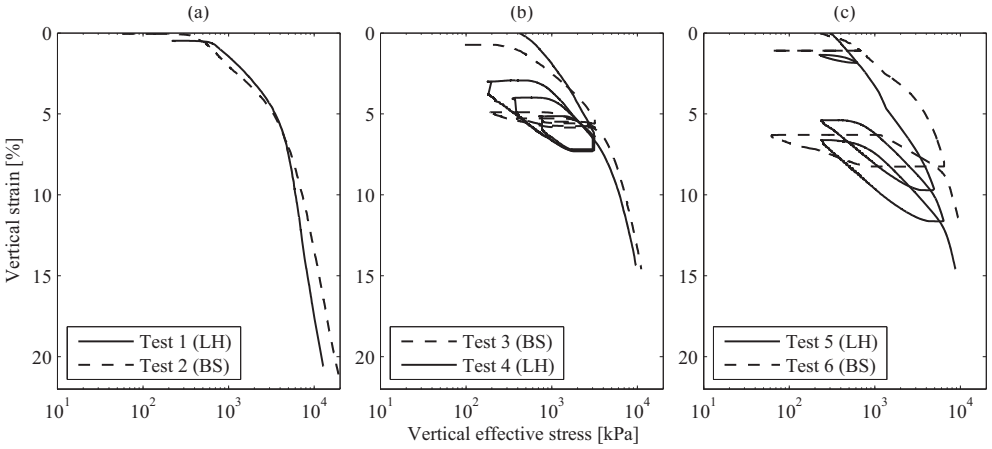

Figure 3: Compression curves. (a) Strictly loading; (b) Reloading from predetermined stresses; and (c) Reloading from preconsolidation stresses.

The unloading/reloading compression curves show similar behaviors within the sample group; the LH samples, which exhibited increased plasticity, showed more expansive behavior than the less plastic BS samples, resulting in substantially steeper unloading/reloading curves.

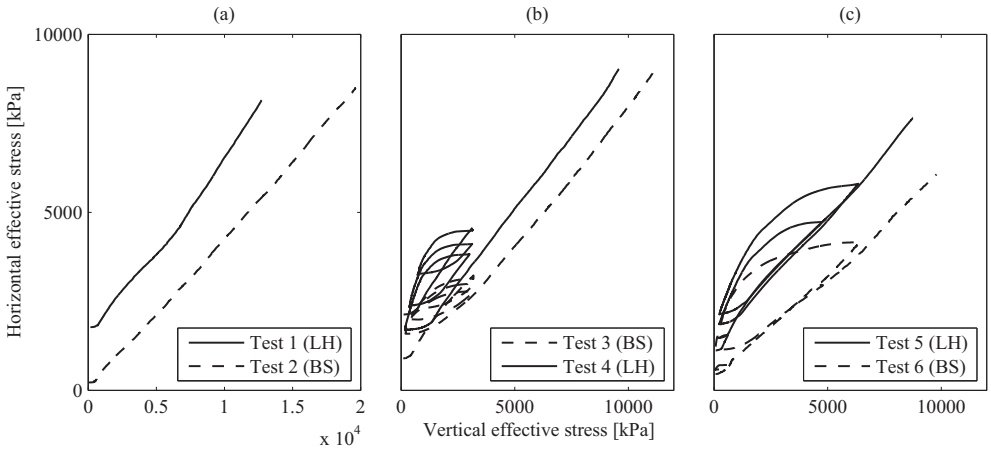

Figure 3: Vertical vs. horizontal stresses. (a) Strictly loading; (b) Reloading from predetermined stresses; and (c) Reloading from preconsolidation stresses.

The initial horizontal pressure (after saturation) of LH vs. BS samples was considerable higher, resulting in substantial higher earth pressure at rest. An upper and lower bound presence for preconsolidation stresses is evident, most notably in the strictly loading curves (Figure 3(a)), as earth pressure changed at two stress levels corresponding to the upper and lower bounds of the preconsolidation stress levels. The normally consolidated earth pressure at rest in LH and BS samples was detected based on test 1 and test 2, respectively (Figure 4).

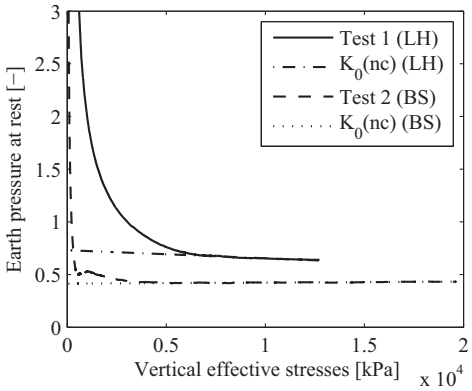

Figure 4: Determination of normally consolidated earth pressure at rest.

$K_0(nc)$decreased slightly as stressed increases above the preconsolidation stresses for both samples; $K_0(nc)$ was given the value OCR=1. The normally consolidated earth pressure at rest for both samples is listed in Table 2, as well as the resulting friction angle based on Jaky (1944) (Eq. 3). Thøgersen (2001) reported the friction angle for a similar Danish Eocene clay was in the 14 º – 19 º range, therefore the back calculated friction angles for LH samples were slightly too high. However, the friction angles for BS samples were unrealistically high, indicating the relation was of little to no use on Søvind Marl, suggesting that the relationship derived by Jaky (1944) cannot be used on Søvind Marl. Results determined $K_0(nc)$was higher in LH compared to BS sample, consistent with Eq. 2, which predicts increased higher plasticity results in higher $K_0(nc)$ values. Table 2 shows that Eq. 2 cannot be applied to estimate normally consolidated earth pressure at rest for most extreme plastic clays. When the plasticity in Table 1 was used in the calculation, Eq. 2 generated a more reliable estimate of the normally consolidated earth pressure at rest for the less plastic BS.

$K_0(oc)$ for all reloading branches of tests 3 to 6 in relationship to the vertical effective stresses is provided in Figure 5.

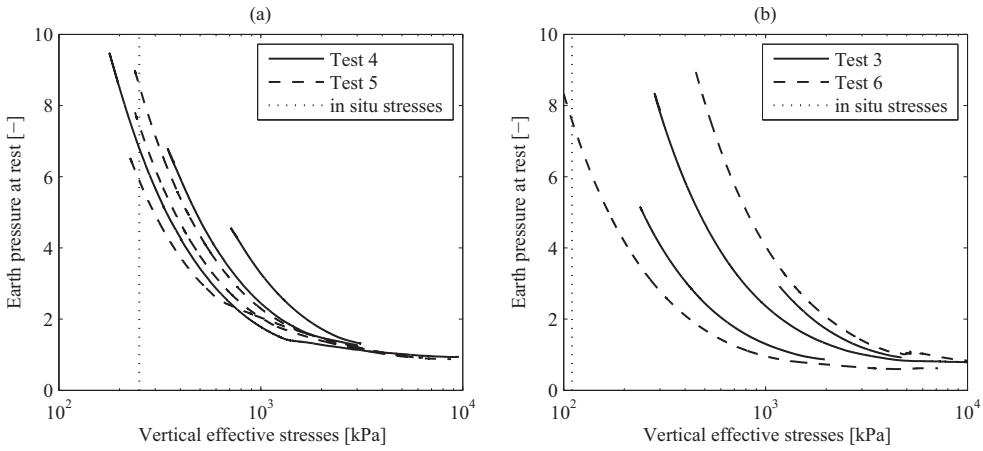

Figure 5: Earth pressure at rest in relation to the vertical stresses. (a) LH samples and (b) BS samples.

The tests yielded very high K_0 values for high overconsolidation ratios. All reloading K_0 curves expressed similar behavior within the sample types (LH or BS). However, a large spread was detected for the BS samples reloading curves.

Figure 6 shows normally consolidated earth pressure at rest based on reloading tests 4 and 5, and 3 and 6 to evaluate the effect of the reloading process on $K_{0(nc)}$.

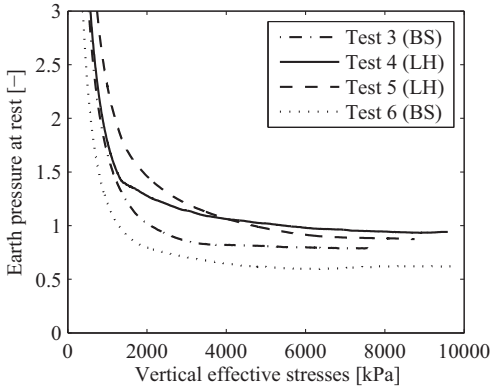

Figure 6: Determination of normally consolidated earth pressure at rest based on reloading tests.

The normally consolidated earth pressure at rest seems to be affected by the reloading process, as these values were much higher than the strictly loading parameters. Consequently, the friction angle calculated using Eq. 3 were also affected, however, it became much too low for LH samples, and was within a more realistic range for the BS samples. Overall, Eq. 3 did not provide reliable friction angle estimate for the normally consolidated earth pressure at. These tests indicated that $K_{0(nc)}$ could not be estimated using the Jaky (1944) relationship (Eq. 3) for these highly plastic clays. Additional tests are necessary to determine is an association exists between friction angle and K_0 for these highly plastic clays with a relatively low expected friction angle.

Table 2: $K_{0(nc)}$ with the connected friction angle.

	K_0(nc) [-]	φ (eq. 3) [º]	K_0 (eq. 2) [-]
Test 1 (LH)	0.68	18.7	1.26
Test 2 (BS)	0.42	35.5	0.62
Test 3 (BS)	0.81	11.0	0.62
Test 4 (LH)	0.96	2.3	1.30
Test 5 (LH)	0.89	6.3	0.84
Test 6 (BS)	0.62	22.3	0.62

6 RELATION WITH OCR

A relation between OCR and $K_{0(oc)}$ was assessed using Eq. 4. The upper bound of the preconsolidation stresses listed in Table 1 was used in the OCR determination. Fits were made by determining $K_{0(nc)}$ and optimizing α. Figure 7 shows the best fit of the measured data to Eq. 4 using $K_{0(oc)}$ for tests 1 and 2 listed in Table 2 and the mean α from each test , the α range from both sample types is listed in Table 3. The ranges observed were high compared to values initial suggested by Meyerhof (1976) and Lancellotta (1993);

however α values in BS samples were consistent with those reported by Lefebvre et al. (1991) and Hamouche et al. (1995).

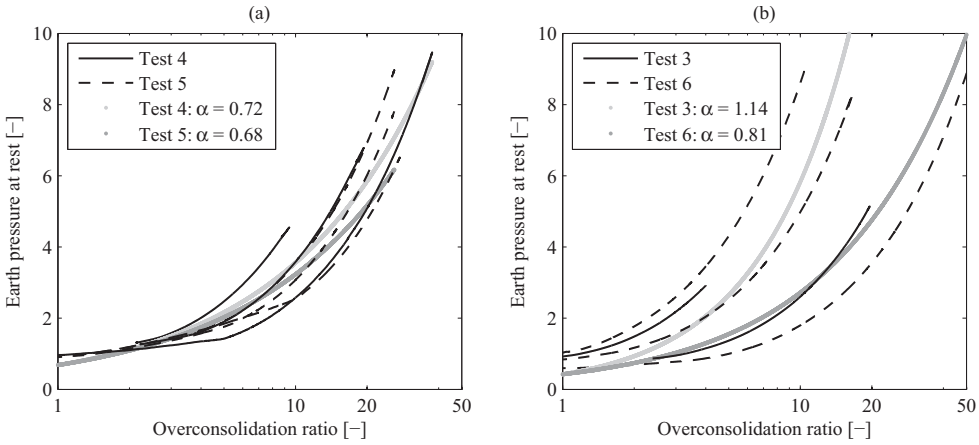

Figure 7: Best fit $K_0(nc)OCR^{\alpha}$ to measured K_0 curves. (a) LH samples and (b) BS samples.

The fit resulted in lower estimated K_0 values for low and high OCRs and a generally poor fit to the measured K_0. LH samples yielded similar α results, as expected due to the similarity in reloading branches. However, a notable variability was observed in BS samples due to the substantial differences in the measured K_0. In Figure 8 $K_0(nc)$ found using the reloading branches (tests 4 and 5 and tests 3 and 6) was used to best fit the measured data using the mean α', the α' ranges are listed in Table 3.

Table 3: Various α using OCR.

	α	α' *
	[-]	[-]
Test 3 (BS)	0.80 – 1.55	0.47 – 0.91
Test 4 (LH)	0.63 – 0.81	0.46 – 0.58
Test 5 (LH)	0.62 – 0.73	0.49 – 0.61
Test 6 (BS)	0.81	0.72 – 1.13

* α' is found from $K_0(nc)_{reload}$

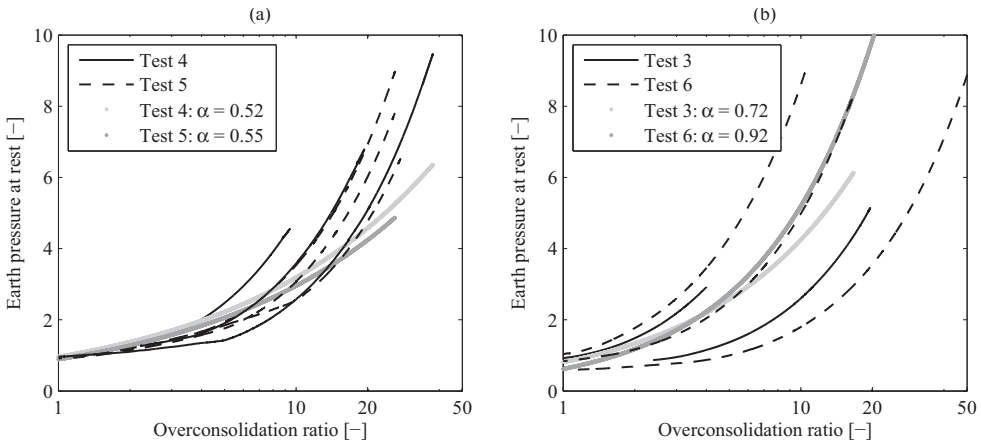

Figure 8: Best $K_0(nc)_{reload}OCR^{\alpha}$ fit to measured K_0 curves. (a) LH samples and (b) BS samples.

By using $K_0(nc)_{reload}$, the curve fit improveed for small *OCR* values. However, it weakened for higher *OCR* values, in particular for LH and BS test 3 samples, where a severe underestimate of K_0 resulted. Test 6 fit was very good considering the wide spread of the measured K_0 curves.

Eq. 5 stipulates that $\alpha=\sin(\varphi)$, however using α from Table 3 back calculated much too high friction angles with an absolute minimum of 38 º. The friction angles were therefore impossible to use in estimations of any kind regarding K_0.

6.1 Relation with OCR_{lab}

The fit of K_0 to OCR using Eq. 4 generally yielded poor results, i.e., it did not follow the measured K_0 curvature. Figure 4 shows the clay recalled the stresses where it becomes normally consolidated. The poor K_0 to OCR fit suggested the "short term" memory was not maintained due to swelling after excavation; the clay did not recall the stresses of unloading conditions, consistent with Krogsbøl et al. (2012). As the sample was subsequently reloaded during testing, the clay responded as if the previous maximum test stresses were the preconsolidation stresses. OCR was then redefined as dependent on the previous maximum stresses in the test, σ'_{unload}, as shown in Eq. 7, incongruent with normal preconsolidation stresses (Krogsbøl et al. 2012):

$$OCR_{lab} = \frac{\sigma'_{unload}}{\sigma'_{v}} \tag{7}$$

Figure 9 shows the relation to OCR_{lab}, using $K_{0(nc)}$ determined using loading tests. Table 4 provides the α range using these assumptions. α values for the reloading branches from the lower bound of the preconsolidation stresses for tests 5 and 6 yielded negative values and were not included in Table 4. The negative α' was obtained as the earth pressure at rest for OCR_{lab} =1 was much too high compared to $K_{0(nc}$, indicating the relation yielded very poor fit for reloading branches with small reloading stresses. This results suggested the fissure influence on K_0 was substantial, and confirms the lower bound of the preconsolidation stresses was not the result of soil preconsolidation.

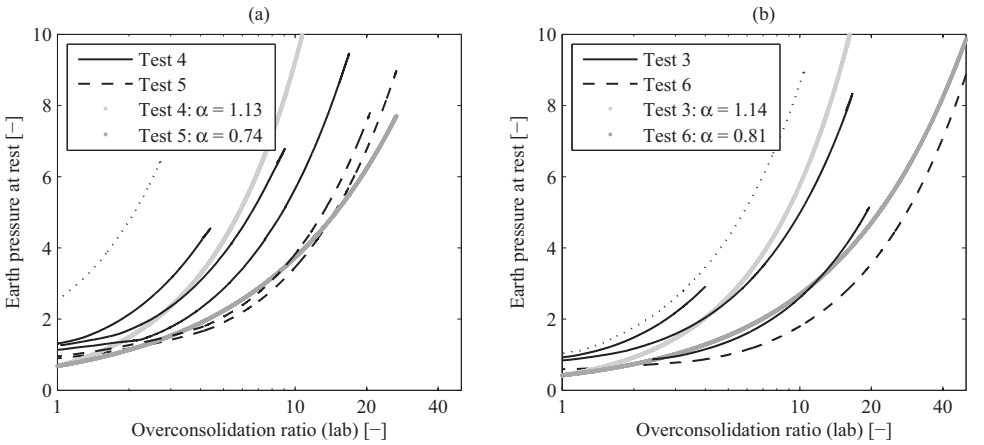

Figure 9: Best $K_0(nc)$ $OCR_{lab}^{\alpha'}$ fit to measured K_0 curves, ··· indicate excluded reloading branches. (a) LH samples and (b) BS samples.

However, the general relation fit improved, as increased variation in α for individual samples was detected. Figure 10 shows the fit using $K_0(nc)$ for each reloading step and OCR_{lab}. The general fit deteriorates, as the fitted curve flattens using $K_0(nc)$ from individual tests.

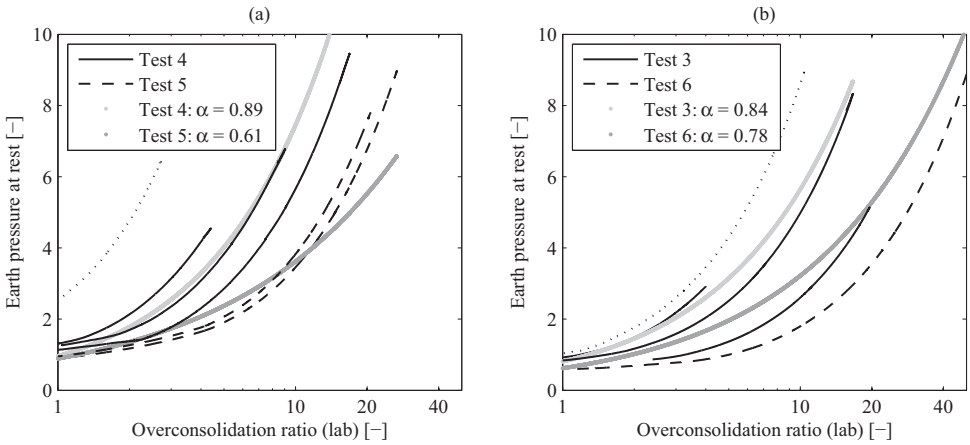

Figure 10: Best $K_0(nc)_{reload}\ OCR_{lab}^{\alpha'}$ fit to measured K_0 curves, ··· indicate excluded reloading branches. (a) LH samples and (b) BS samples.

Table 4: Various α using OCR_{lab}.

	α	α' *
	[-]	[-]
Test 3 (BS)	0.80 – 1.55	0.78 – 0.91
Test 4 (LH)	0.90 – 1.41	0.71 – 1.10
Test 5 (LH)	0.73 – 0.75	0.60 – 0.62
Test 6 (BS)	0.81	0.78

* α' is found from $K_0(nc)_{reload}$

6.2 Mean fit

K_0-curve fit for each sample type was fairly similar. When all tests within each sample type were combined, a very good fit was is obtained using the mean α and $K_0(nc)$ from the loading tests (Figure 11).

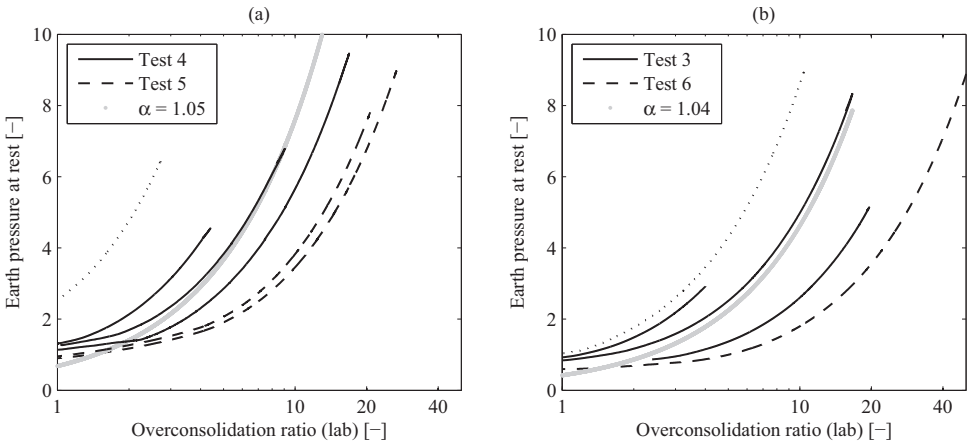

Figure 11: Best K_0(nc) OCR_{reload}^{α} fit to all measured K_0 curves, ··· indicate excluded reloading branches. (a) L H **samples and (b) BS samples.**

K_0 is slightly underestimated when OCR_{reload} =1. It is noteworthy that α was identical for the two sample types. This indicated α was not influenced by clay properties, as these varied substantially for Søvind Marl. The best fit was found applying Eq. 4 with $K_0(nc)$ from the loading tests (tests 1 and 2). Therefore, the reloading process did not notably affect the relation. However, unloading during excavation affected the relation test results, and the unloading stresses should be used to determine test OCRs. The relation fit was acceptable for all reloading branches under reloading stresses above the lower bound of the preconsolidation stresses; therefore the relation is likely valid for all Søvind Marl samples independent of the upper bound of the preconsolidation stresses. K_0 estimates for in situ cases should be made based on the upper bound of the preconsolidation stresses as "short term" memory loss due to excavation did not occur. α was congruent with results reported by Lefebvre et al (1991) and Hamouche et al (1995) for sensitive clays, consistent with Søvind Marl. K_0 Søvind Marl estimates are consequently best expressed as follows:

$$K_0(oc) = K_0(nc)_{measured} \times OCR^{1.05} \quad (8)$$

The Jaky (1944) relationship to $K_0(nc)$ was not valid on highly plastic clays, including Søvind Marl, measured $K_0(nc)$ was used in the relation, which resulted in the best relation for LH and BS, Eq. 9 and 10, respectively:

$$K_0(oc) = 0.68 \times OCR^{1.04} \quad (9)$$

$$K_0(oc) = 0.42 \times OCR^{1.05} \quad (10)$$

7 CONCLUSION

Earth pressure at rest was measured on the highly plastic and overconsolidated Danish Eocene clay Søvind Marl. Six continuous loading oedometer tests with a constant strain rate were conducted using the Aalborg University continuous loading oedometer apparatus. The apparatus distinguishes itself by applying pressurized test water to better saturate and drain the sample during testing. The horizontal pressure is measured by three pressure gauges inserted in the stiff oedometer ring. The CLO provides reliable and continuous description of the horizontal stresses which subsequently provided the earth pressure at rest.

Søvind Marl is highly overconsolidated, but with the appearance of a lower and upper bound of the preconsolidation stresses due to the clays fissured structure, and approximate values of 700 kPa and 6,800 kPa, respectively. This results in high in situ OCRs based on the upper boundary. Tests were made on Søvind Marl samples from two different regions of the formation; LH from the older and BS from the younger regions. The only considerable difference between the two was plasticity; LH samples showed plasticity index up to 200%, whereas BS samples exhibited a 40% index.

The measured earth pressure at rest exhibited high values (<10), and between 6 - 8 in the in situ stress range, caused by high horizontal stresses. The normally consolidated earth pressure at rest was approximately 0.66 for LH samples and 0.42 for BS samples from strictly loading tests. Unloading and reloading affected $K_0(nc)$, as values increased from approximately 0.89 to 0.96 and 0.62 to 0.81 for LH and BS samples, respectively.

$K_0(nc)$ can typically be determined using friction angle by the relationship established by Jaky (1944). However, neither of the measured $K_0(nc)$s could be calculated using Jaky (1944) based on friction angle, as the expected friction angle was much lower than the friction angle required to obtain the measured $K_0(nc)$. Consequently, Jaky (1944) was of very limited to no use on highly plastic clays.

Results showed the measured K_0 was related to Meyerhof's (1976) correlation between K_0 and the overconsolidation ratio. The correlation did not yield a good fit when $K_0(nc)$ obtained from either loading or reloading tests was used in relationship to OCR. The samples were affected by unloading which occurred during excavation; and while the preconsolidation stresses were remembered, the "short-term" memory was affected. Consequently, the stresses from which the clay had been unloaded from were not remembered. Therefore, OCR_{lab} was introduced, which integrated the relationship between the maximum stresses previous executed in the test and the current vertical stresses (Eq. 7). Results showed a good fit between Meyerhof (1976) and the measured data when the loading $K_0(nc)$ was compared to OCR_{lab}, under the conditions the previous maximum stresses were above the lower bound of the preconsolidation stresses, and hence not influenced by the clay fissures. K_0 should therefore be estimated based on the upper bound of the preconsolidation stresses. α was determined at 1.04 and 1.05 for LH and BS samples, respectively. Lefebvre et al (1991) and Hamouche et al (1995) reported comparable α values for sensitive clays, such as Søvind Marl.

REFERENCES

Abdelhamid, M.S. and Krizek, R.J. (1976). At rest lateral earth pressures of a consolidating clay. ASCE Journal of Geotechnical Engineering Division. **102**(7). Pp. 721-738

Andrawes, K.Z. and El-Sohby, M.A. (1973). Factors Affecting Coefficient of Earth Pressure K_0. Journal of the Soil Mechanics and Foundation Division ASCE. **99**(7). Pp. 527-539

Armour Jr., D.W. and Drnevich, V.P. (1986) Improved techniques for the constant-rate-of-strain consolidation test. Consolidation of soils: testing and evaluation, ASTM SPT 892.

ASTM (2012). Standard Test Method for One-dimensional Consolidation Properties of Saturated Cohesive Soils Using Controlled-Strain Loading. ASTM Standard: D4186-06. ASTM

Brooker, E.W. and Ireland, H.O. (1965). Earth pressure at rest related to stress history. Canadian Geotechnical Journal. **2**(1). Pp. 1-15

Davison, L.R. (1989). Continuous loading consolidation tests on soil. PhD thesis (CNAA). Bristol Polytechnic

Dobak, P. (2003). Loading velocity in consolidation analysis. Geological Quarterly, **47**(1). Pp. 13-20

Donath, A. (1891). Untersuchungen über den Erddruk auf Stützwände (in German). Zeitschrift für Bauwesen, **41**. Pp. 491-518

Ducasse. P., Mieussens, C., Moreau, M. and Soyez, B. (1986). Oedometric testing in Laboratories de Ponts et Chaussees, France. ASTM STP 982. Consolidation of Soils: Testing and Evaluation. Pp. 282-298

Gasparre, A. and Coop, M.R. (2008). Quantification of the effects of structure on the compression of a stiff clay. Canadian Geotechnical Journal, **45**: 1324–1334

Gorman, C.T., Hopkins, T.C., Deen, R.C. and Drnevich, V.P. (1977). Constant-rate-of-strain and controlled-gradient testing. Geotechnical Testing Journal. **1**. Pp. 3-15

Grønbech, G.L., Nielsen, B.N., Ibsen, Lars B. and Stockmarr, P. (2015a). Geotechnical properties of Søvind Marl - a plastic Eocene clay. Canadian Geotechnical Journal. **52**

Grønbech, G.L., Ibsen, Lars B. and Nielsen, B.N. (2015b). Preconsolidation of Søvind Marl – a highly fissured Eocene Clay. Accepted with revision in Geotechnical Testing Journal.

Hamilton, J.J. and Crawford, C.B. (1959). Improved determination of preconsolidation pressure of sensitive clay. ASTM STP 254. American Society for Testing and Materials. Pp. 254-271

Hamouche, K., Leroueil, S., Roy, M. and Lutenegger, A.J. (1995). In situ evaluation of K_0 in eastern Canada clays. Canadian Geotechnical Journal, **32**(4). Pp. 677-688

Jaky, J. (1944). The Coefficient of Earth Pressure at Rest. Journal for Society of Hungarian Architects and Engineers, October, pp. 355-358.

Janbu, N. Tokheim, O. and Senneset, K. (1981). Consolidation tests with continuous loading. Proceeding of: X International Conference on Soil Mechanics and Foundation Engineering, Stockholm, Sweden. **1**. Pp. 645-654

Krogsbøl, A., Hededal, O. and Foged, N.. 2012. Deformation properties of highly plastic fissured Palaeogene clay – Lack of stress memory?. In proceedings of NGM 2012, Nordisk Geoteknikermøde Vol. 1/2. 9th-12th of May 2012. Copenhagen, Denmark. 133-140

Ladd, R.S. (1965). Use of electrical pressure transducers to measure soil pressure. Massachusetts Institute of Technology Research Report R65-48. No. 180

Lancellotta, R., 1993. Geotecnica. Zanichelli, II ed., Bologna.

Larsson, L. and Sällfors, G. (1986). Automatic continuous consolidation testing in Sweden. ASTM STP 982. Consolidation of Soils: Testing and Evaluation. Pp. 299-328

Lefebvre, G., Bozozuk, M., Philibert, A.. and Hornych, P. (1991). Evaluating K_0 in Champlain clays with hydraulic fracture tests. Canadian Geotechnical Journal, **28**(3), Pp. 365-377

Lefebvre, G. and Philibert, A. (1979). Measurement of lateral pressures in the one-dimensional consolidation of a structured clay. In proceedings of the 32nd Canadian Geotechnical Conference, Québec, Canada. September. Pp. 2.61-2.75

Lowe, J., Jonas, E. and Obrician, V. (1969). Controlled gradient consolidation test. Journal of Soil Mechanics Division, ASCE, **95**. Pp. 77-97

Massarsch, K.R. (1979). Lateral Earth Pressure in Normally Consolidated Clay. Proceedings of the Seventh European Conference on Soil Mechanics and Foundation Engineering, Brighton, England. Vol 2. Pp. 245-250

Mayne, P.W. and Kulhawy, F.H. (1982). K_0-OCR relationship in soil. Journal of the Geotechnical Enigeering Devision, ASCE. **108**. No. GT6. Pp. 851-872

Mesri, G. and Hayat, T.M. (1993). The coefficient of earth pressure at rest. Canadian Geotechnical Journal. **30**. Pp. 647-666

Meyerhof, G.G. (1976). Bearing capacity and settlement of pile foundations. 11th Terzaghi Lecture. J. Geotech. Eng. Div. ASCE, **102**, No. GT3, Pp. 197–228.

Rowe, P.W. and Barden, L. (1966). A new consolidation cell. Géotechnique. **16**. Pp. 162-170

Sheahan T.C. and Watters. P.J. (1997), Experimental verification of CRS consolidation theory. Journal of geotechnical and geoenvironmental engineering. **125**(5). Pp. 430-437

Smith, R. and Wahls, H. (1969). Consolidation under constant rate of strain. Journal of the Soil Mechanics and Foundation Division ASCE. **90**. Pp. 519-538

Standard Norge (1993). Geoteknisk prøving Laboratoriemetoder Bestemmesle av endimensjonale konsolidaeringegenskaper ved ødometerprøving Metode med kontinuerlig belastning NS 8018 (in Norwegian). Standard Norge. **1**

Thøgersen, L. (2001). Continuous Loading Oedometer Tests with measurement of Horizontal Pressure carried out on the Tertiary Little Belt Clay. AAU Geotechnical Engineering Papers. Laboratory Testing paper. Aalborg University, Denmark

Wissa, A.E.Z., Christian, J.T., Davis, E.H. and Heiberg, S. (1971). Consolidation testing at constant rate of strain. Journal of Soil Mechanics Foundation Division ASCE. **97**(10). Pp. 1393-1413

APPENDIX F
Boring logs

This appendix contains the boring logs from the test sites. LH samples used in oedometer tests originate from boring L*H11 and the triaxial test samples comes from boring L*H9 and L*H11. All BS samples originate in the near proximity of boring B304. Please note that all boring logs are in Danish.

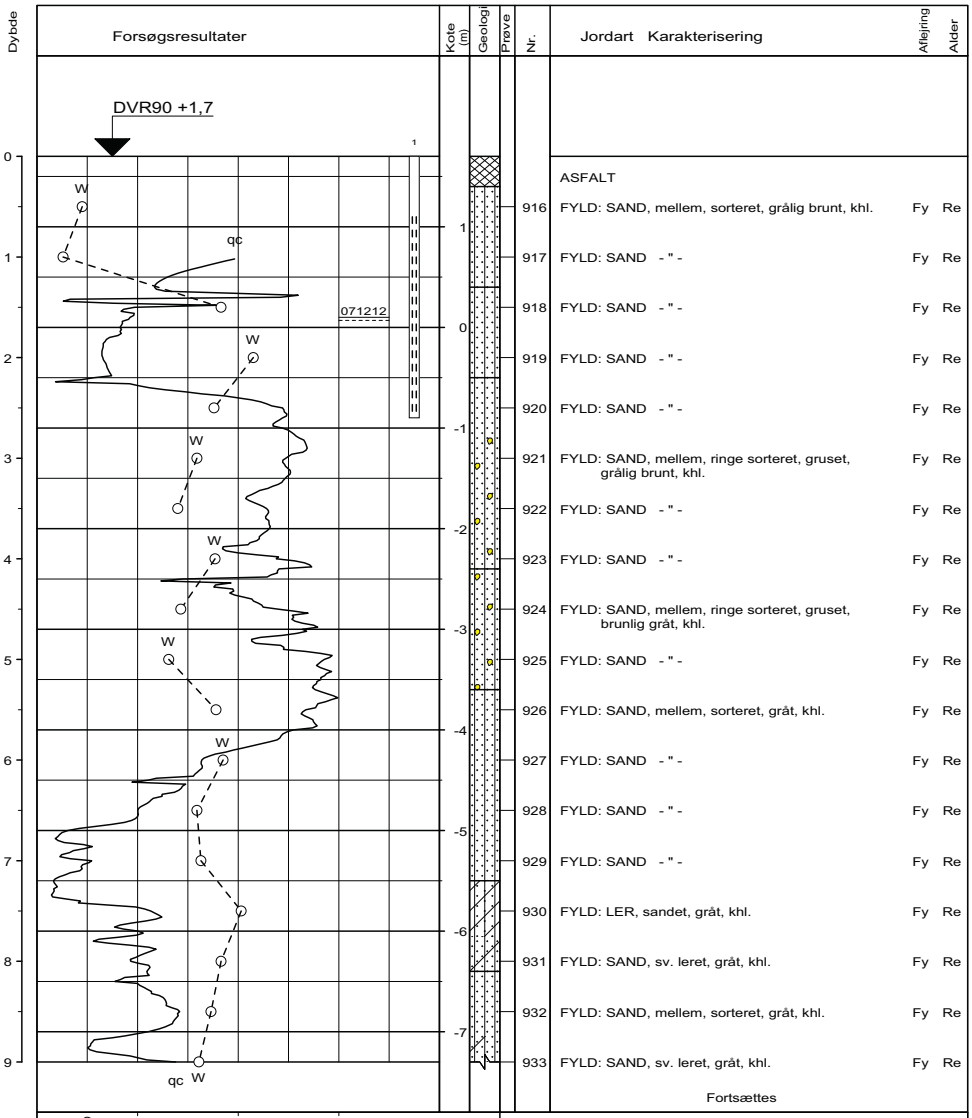

Boremetode : Tørboring med foring

X : 218995 (m) Y : 192907 (m) Plan :

Sag : 25.0705.61 Århus, Light*House

Geolog : JBM Boret af : LER/JQB Dato : 20071204 DGU-nr.: Boring : L*H9

Udarb. af : HLa Kontrol : Godkendt : Dato : Bilag : 3 S. 1 / 6

Grontmij | Carl Bro
Tlf. 98 79 98 00, Fax 98 79 98 01
Sofiendalsvej 94, 9200 Aalborg SV

Boreprofil

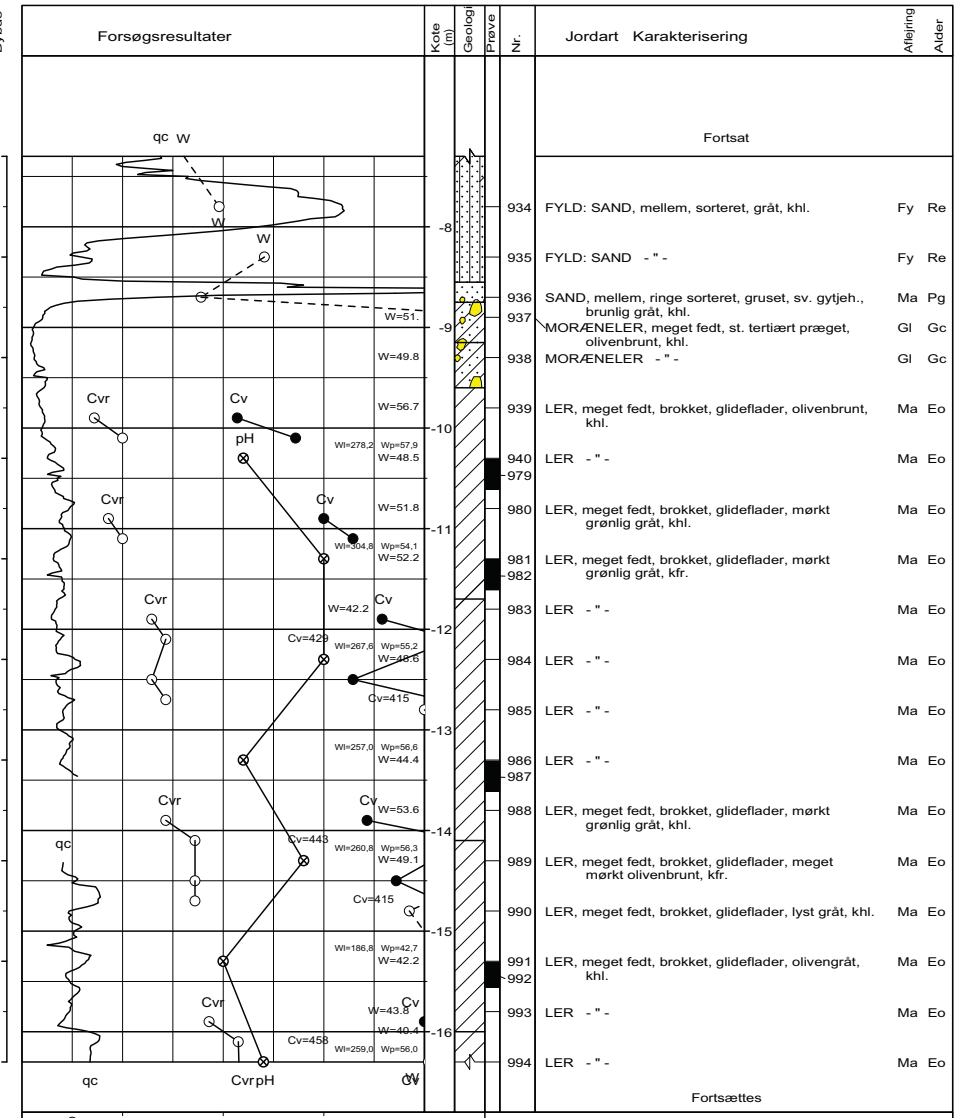

BRregister - PSTGDK 2.0 - 08/07/2008 14:00:39

Sag : 25.0705.61 Århus, Light*House

Geolog : JBM Boret af : LER/JQB Dato : 20071204 DGU-nr.: Boring : L*H9

Udarb. af : HLa Kontrol : Godkendt : Dato : Bilag : 3 S. 2 / 6

Grontmij | Carl Bro
Tlf. 98 79 98 00, Fax 98 79 98 01
Sofiendalsvej 94, 9200 Aalborg SV

Boreprofil

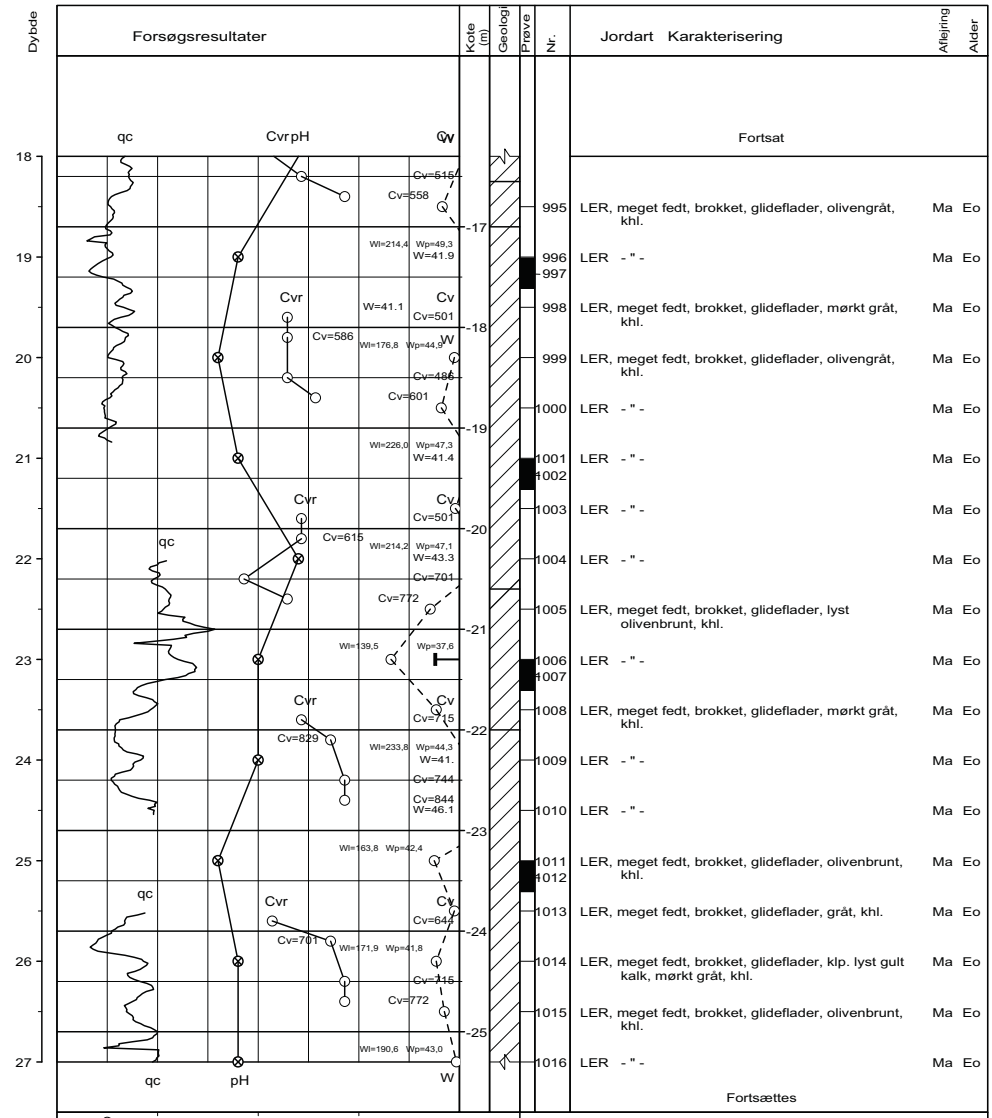

Boremetode : Tørboring med foring

X : 218995 (m) Y : 192907 (m) Plan :

Sag : 25.0705.61 Århus, Light*House

Geolog : JBM Boret af : LER/JQB Dato : 20071204 DGU-nr.: Boring : L*H9

Udarb. af : HLa Kontrol : Godkendt : Dato : Bilag : 3 S. 3 / 6

Grontmij | Carl Bro

Tlf. 98 79 98 00, Fax 98 79 98 01
Sofiendalsvej 94, 9200 Aalborg SV

Boreprofil

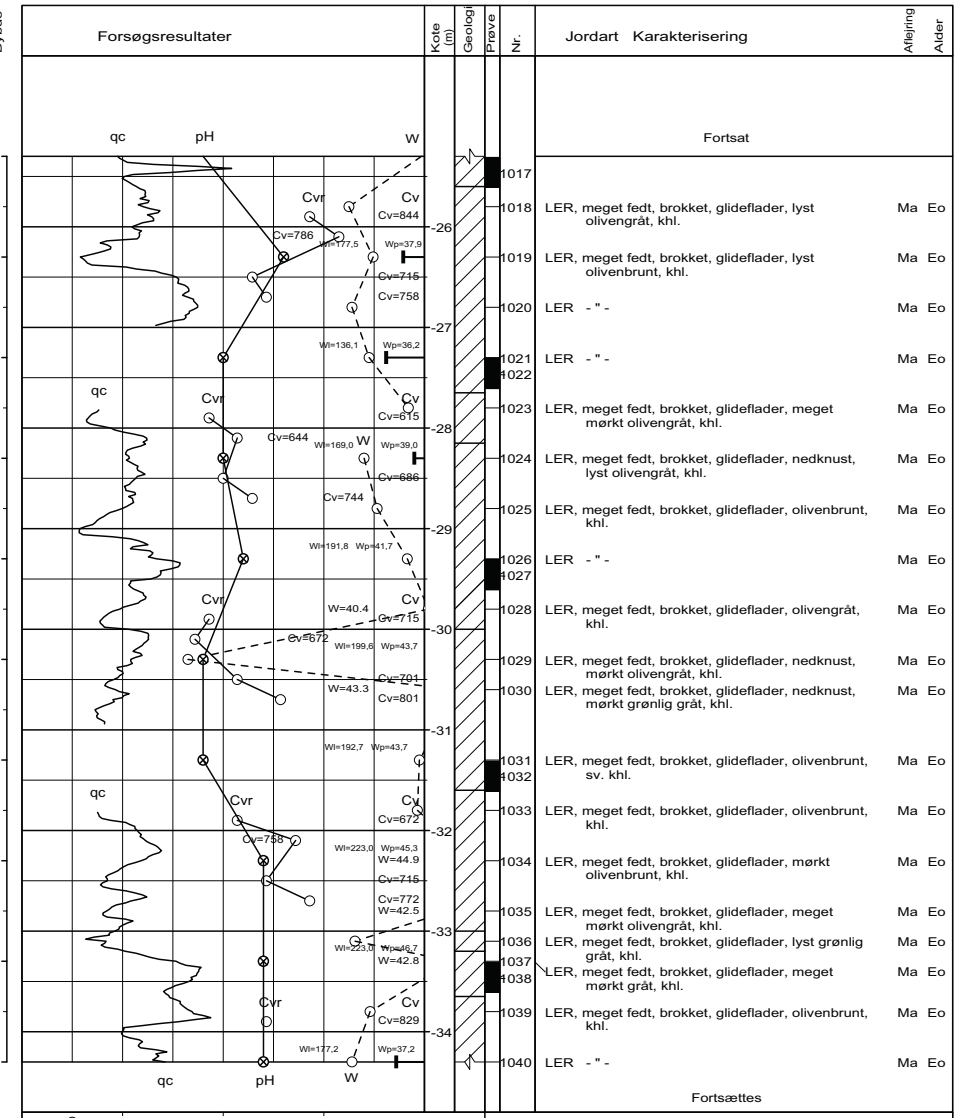

Sag : 25.0705.61 Århus, Light*House

Geolog : JBM Boret af : LER/JQB Dato : 20071204 DGU-nr.: Boring : L*H9

Udarb. af : HLa Kontrol : Godkendt : Dato : Bilag : 3 S. 4 / 6

Grontmij | Carl Bro
Tlf. 98 79 98 00, Fax 98 79 98 01
Sofiendalsvej 94, 9200 Aalborg SV

Boreprofil

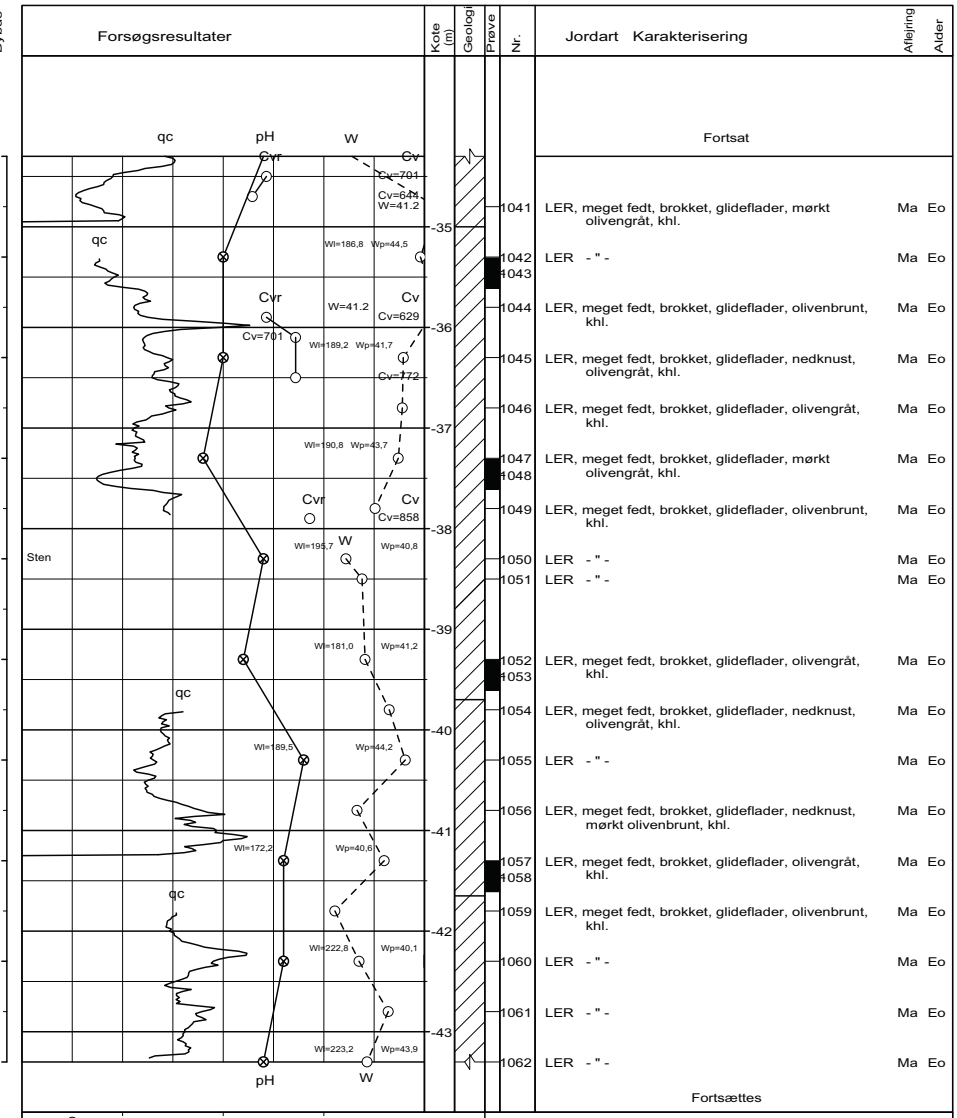

Boremetode : Tørboring med foring

X : 218995 (m) Y : 192907 (m) Plan :

Sag : 25.0705.61 Århus, Light*House

Geolog : JBM Boret af : LER/JQB Dato : 20071204 DGU-nr.: Boring : L*H9

Udarb. af : HLa Kontrol : Godkendt : Dato : Bilag : 3 S. 5 / 6

Grontmij | Carl Bro
Tlf. 98 79 98 00, Fax 98 79 98 01
Sofiendalsvej 94, 9200 Aalborg SV

Boreprofil

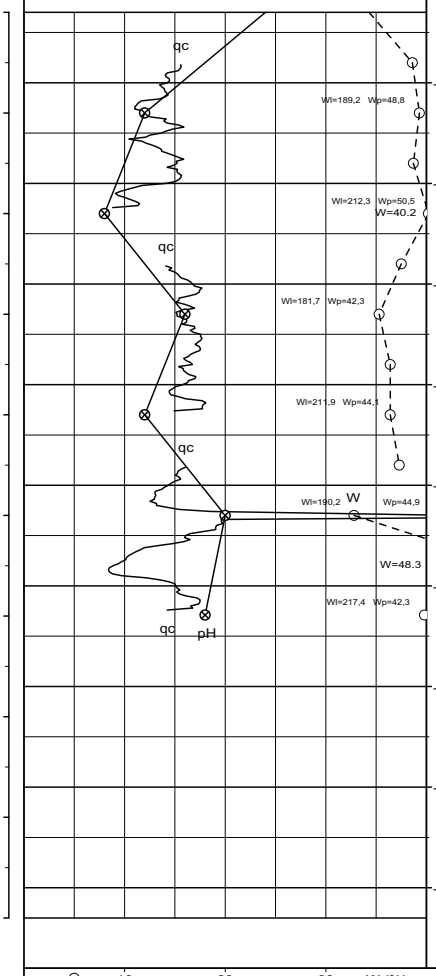

Kote (m)	Geologi	Prøve	Nr.	Jordart Karakterisering	Aflejring	Alder
				Fortsat		
			1063			
			1064	LER, meget fedt, brokket, glideflader, nedknust, olivengrået, khl.	Ma	Eo
			1065	LER, meget fedt, brokket, glideflader, nedknust, meget mørkt grået, khl.	Ma	Eo
			1066	LER, meget fedt, brokket, glideflader, nedknust, mørkt grået, khl.	Ma	Eo
			1067 1068	LER, meget fedt, brokket, glideflader, meget mørkt grået, khl.	Ma	Eo
			1069	LER, meget fedt, brokket, glideflader, nedknust, olivengrået, khl.	Ma	Eo
			1070	LER - " -	Ma	Eo
			1071	LER, meget fedt, brokket, glideflader, olivengrået, khl.	Ma	Eo
			1072 1073	LER - " -	Ma	Eo
			1074	LER, meget fedt, brokket, glideflader, nedknust, olivengrået, khl.	Ma	Eo
			1075	LER, meget fedt, brokket, glideflader, klp. lyst gult kalk, olivengrået, khl.	Ma	Eo
			1076	LER, meget fedt, brokket, glideflader, nedknust, olivengrået, khl.	Ma	Eo
			1077	LER - " -	Ma	Eo

○	10	20 30	W (%)
●○	100	200 300	Cv,Cvr (kN/m²)
		10	qc (MN/m²)
⊗		9	pH

Boremetode : Tørboring med foring

X : 218995 (m) Y : 192907 (m) Plan :

Sag : 25.0705.61 Århus, Light*House

Geolog : JBM Boret af : LER/JQB Dato : 20071204 DGU-nr.: Boring : L*H9

Udarb. af : HLa Kontrol : Godkendt : Dato : Bilag : 3 S. 6 / 6

Grontmij | Carl Bro
Tlf. 98 79 98 00, Fax 98 79 98 01
Sofiendalsvej 94, 9200 Aalborg SV

Boreprofil

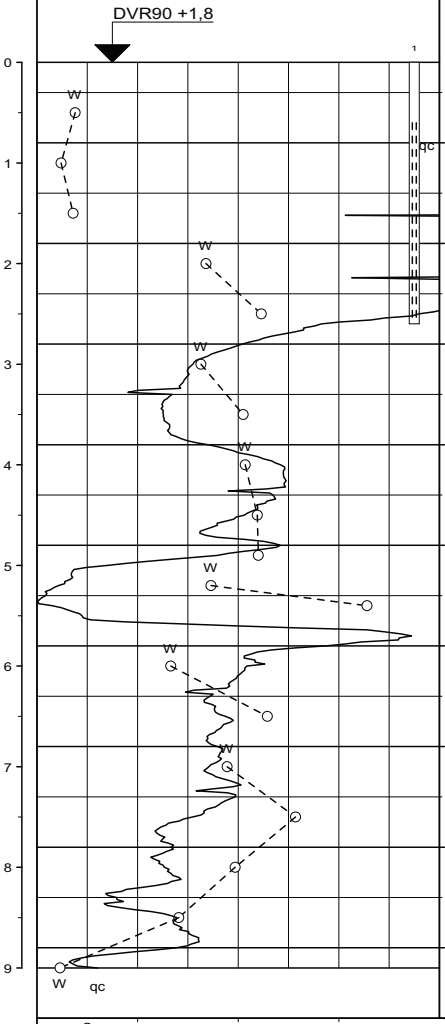

Dybde	Kote (m)	Nr.	Jordart Karakterisering	Aflejring	Alder
		A	ASFALT		
	1	747	FYLD: SAND, mellem, ringe sorteret, gruset, mørkt gulbrunt, khl.	Fy	Re
1		748	FYLD: SAND, mellem, sorteret, grålig brunt, khl.	Fy	Re
		749	FYLD: SAND, mellem, sorteret, træstk., grålig brunt, khl.	Fy	Re
2	0	750	FYLD: SAND, mellem, sorteret, grålig brunt, khl.	Fy	Re
		751	FYLD: SAND, mellem, sorteret, mørkt brunlig gråt, khl.	Fy	Re
3	-1	752	FYLD: SAND - " -	Fy	Re
		753	FYLD: SAND - " -	Fy	Re
4	-2	754	FYLD: SAND - " -	Fy	Re
		755	FYLD: SAND, mellem, sorteret, organiskh., mørkt gråt, khl.	Fy	Re
5	-3	756	FYLD: SAND, mellem, ringe sorteret, gruset, gråt, khl.	Fy	Re
		757	FYLD: SAND, groft, ringe sorteret, gruset, gråt, khl.	Fy	Re
		758	FYLD: SAND, fint, ringe sorteret, siltet, sv. organiskh., gråt, khl.	Fy	Re
6	-4	759	FYLD: SAND, fint sorteret, gråt, khl.	Fy	Re
		760	FYLD: SAND, mellem, sorteret, gråt, khl.	Fy	Re
7	-5	761	FYLD: SAND - " -	Fy	Re
		762	FYLD: SAND - " -	Fy	Re
8	-6	763	FYLD: SAND, mellem, ringe sorteret, gruset, gråt, khl.	Fy	Re
		764	FYLD: SAND - " -	Fy	Re
9	-7	765	FYLD: SAND, mellem, ringe sorteret, gråt, khl.	Fy	Re

Fortsættes

○	10	20	30 W (%)
●○	100	200	300 Cv,Cvr (kN/m²)
		10	qc (MN/m²)
⊗		9	pH

Boremetode : Tørboring med foring

X : 218921 (m) Y : 192840 (m) Plan :

Sag : 25.0705.61 Århus, Light*House

Geolog : JBM Boret af : LER/JQB Dato : 20071015 DGU-nr.: Boring : L*H11

Udarb. af : HLa Kontrol : Godkendt : Dato : Bilag : 5 S. 1 / 8

Grontmij | Carl Bro
Tlf. 98 79 98 00, Fax 98 79 98 01
Sofiendalsvej 94, 9200 Aalborg SV

Boreprofil

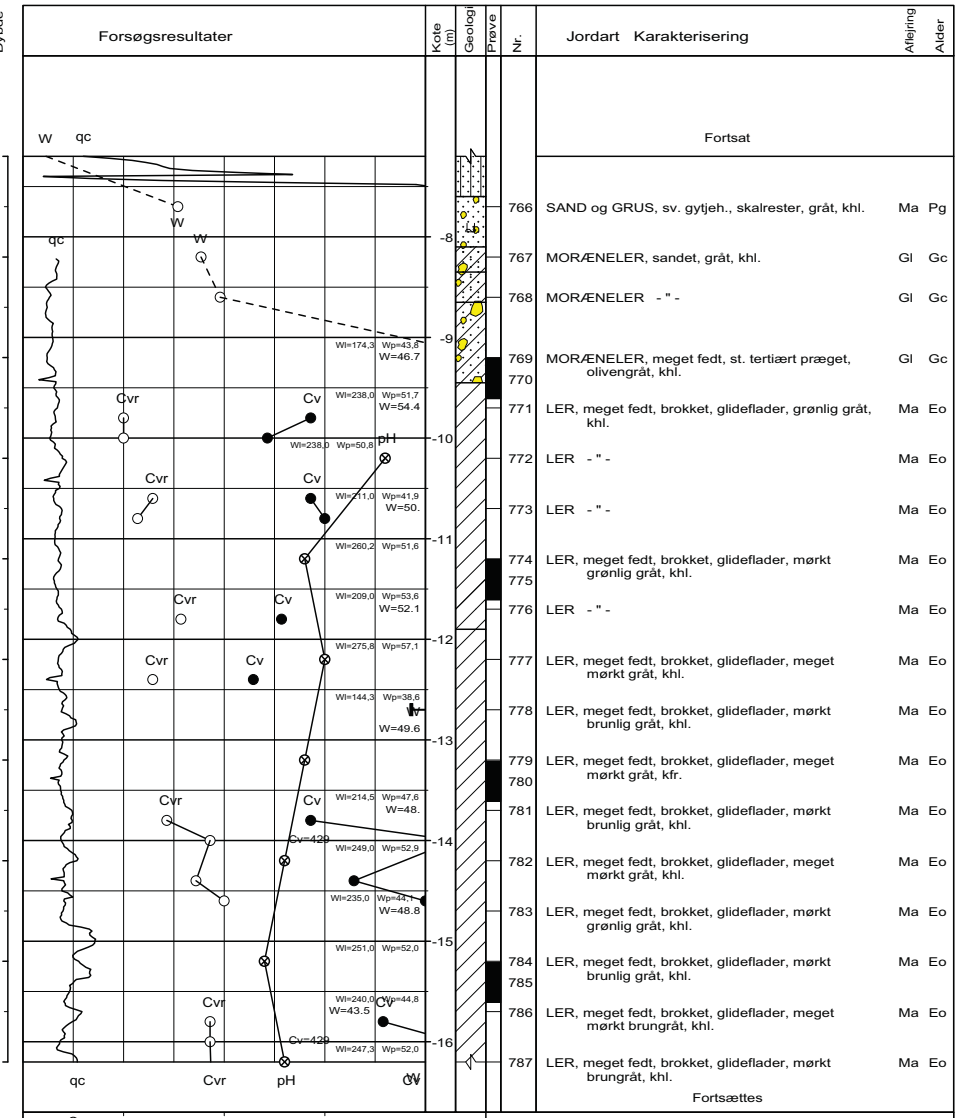

Boremetode : Tørboring med foring

X : 218921 (m) Y : 192840 (m) Plan :

Sag : 25.0705.61 Århus, Light*House

Geolog : JBM Boret af : LER/JQB Dato : 20071015 DGU-nr.: Boring : L*H11

Udarb. af : HLa Kontrol : Godkendt : Dato : Bilag : 5 S. 2 / 8

Grontmij | Carl Bro
Tlf. 98 79 98 00, Fax 98 79 98 01
Sofiendalsvej 94, 9200 Aalborg SV

Boreprofil

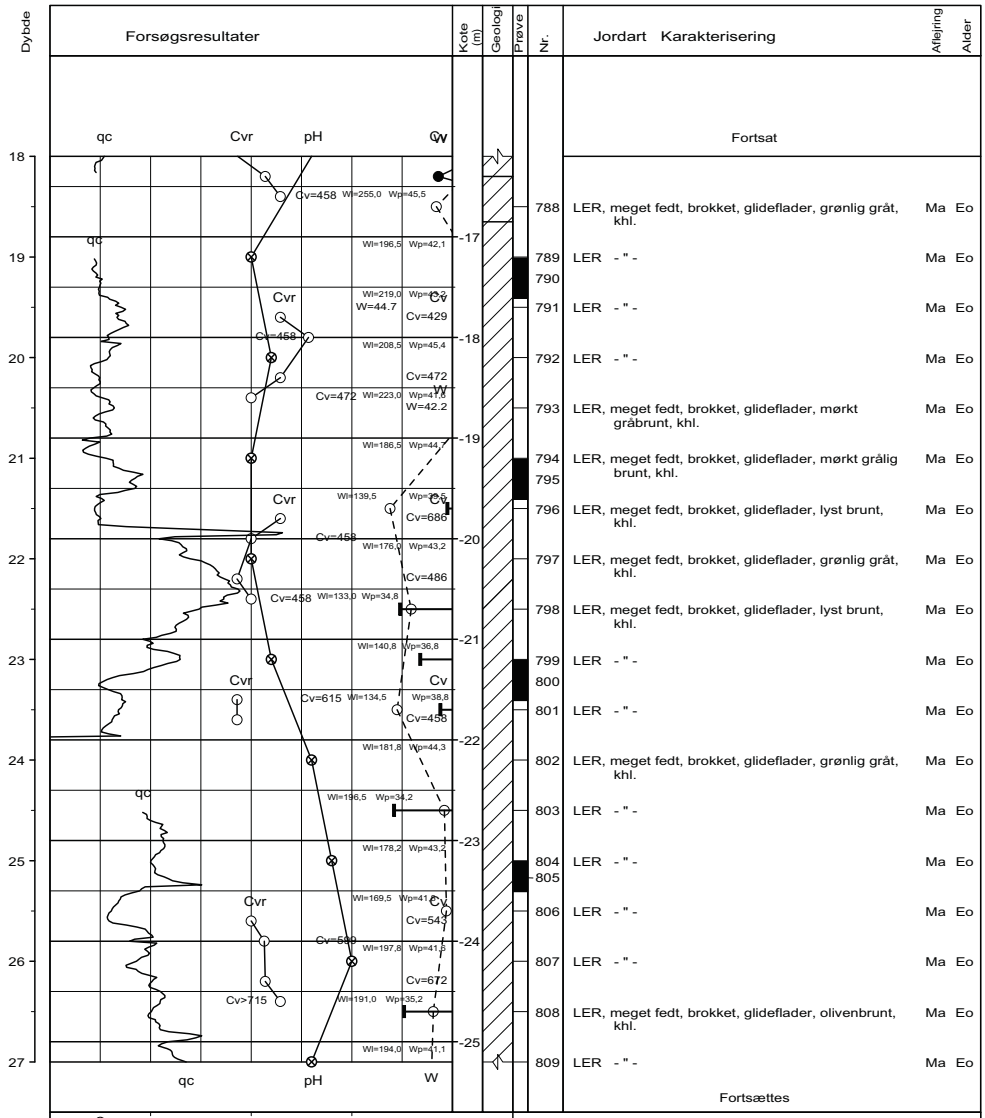

Sag : 25.0705.61 Århus, Light*House

Geolog : JBM Boret af : LER/JQB Dato : 20071015 DGU-nr.: Boring : L*H11

Udarb. af : HLa Kontrol : Godkendt : Dato : Bilag : 5 S. 3 / 8

Grontmij | Carl Bro
Tlf. 98 79 98 00, Fax 98 79 98 01
Sofiendalsvej 94, 9200 Aalborg SV

Boreprofil

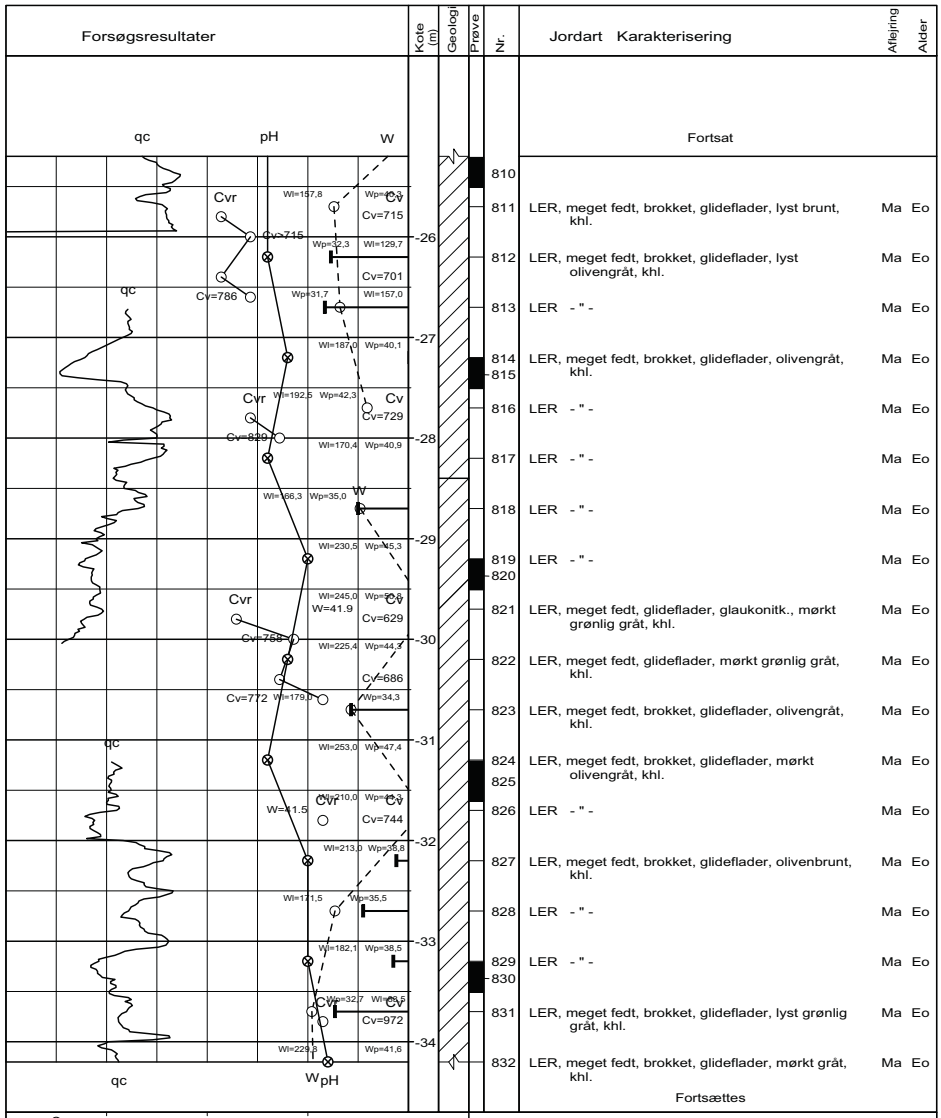

Boremetode : Tørboring med foring

X : 218921 (m) Y : 192840 (m) Plan :

Sag : 25.0705.61 Århus, Light*House

Geolog : JBM Boret af : LER/JQB Dato : 20071015 DGU-nr.: Boring : L*H11

Udarb. af : HLa Kontrol : Godkendt : Dato : Bilag : 5 S. 4 / 8

Grontmij | Carl Bro
Tlf. 98 79 98 00, Fax 98 79 98 01
Sofiendalsvej 94, 9200 Aalborg SV

Boreprofil

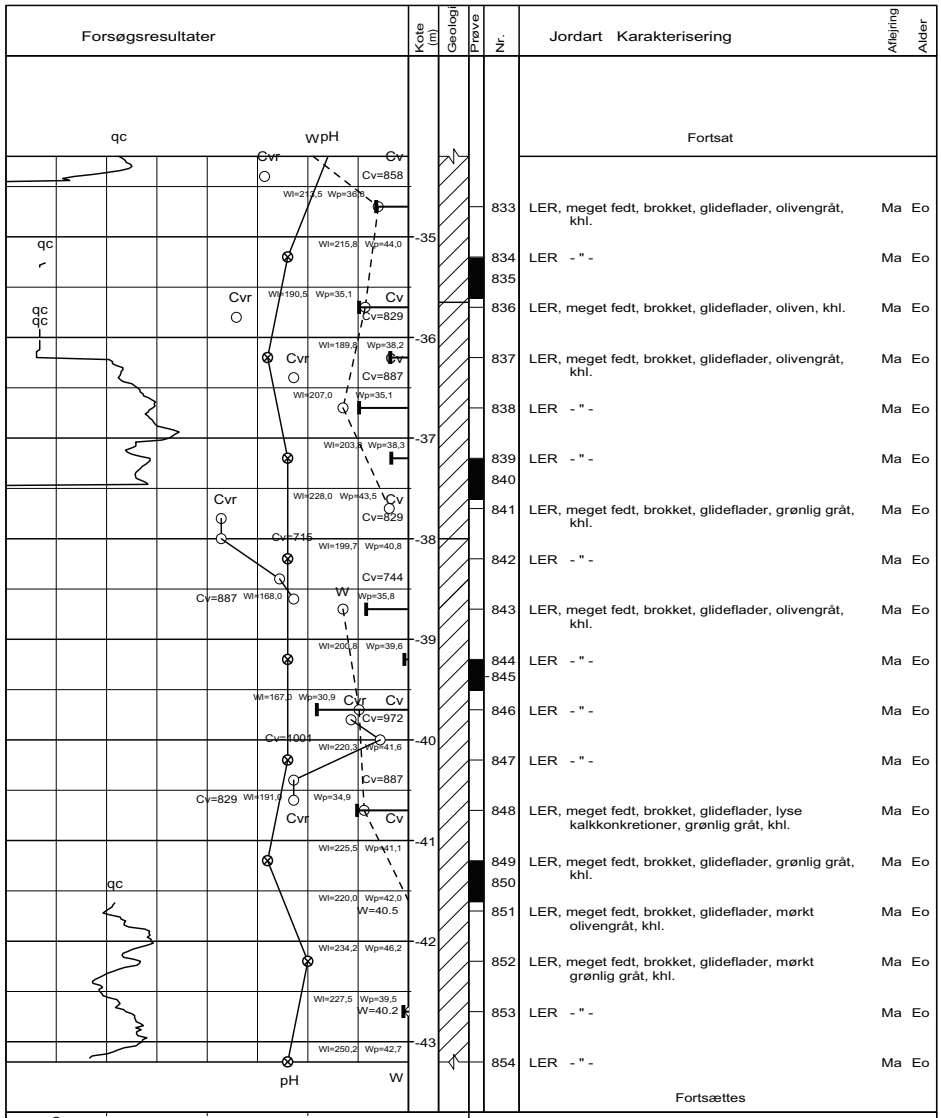

Boremetode : Tørboring med foring

X : 218921 (m) Y : 192840 (m) Plan :

Sag : 25.0705.61 Århus, Light*House

Geolog : JBM Boret af : LER/JQB Dato : 20071015 DGU-nr.: Boring : L*H11

Udarb. af : HLa Kontrol : Godkendt : Dato : Bilag : 5 S. 5 / 8

Grontmij | Carl Bro
Tlf. 98 79 98 00, Fax 98 79 98 01
Sofiendalsvej 94, 9200 Aalborg SV

Boreprofil

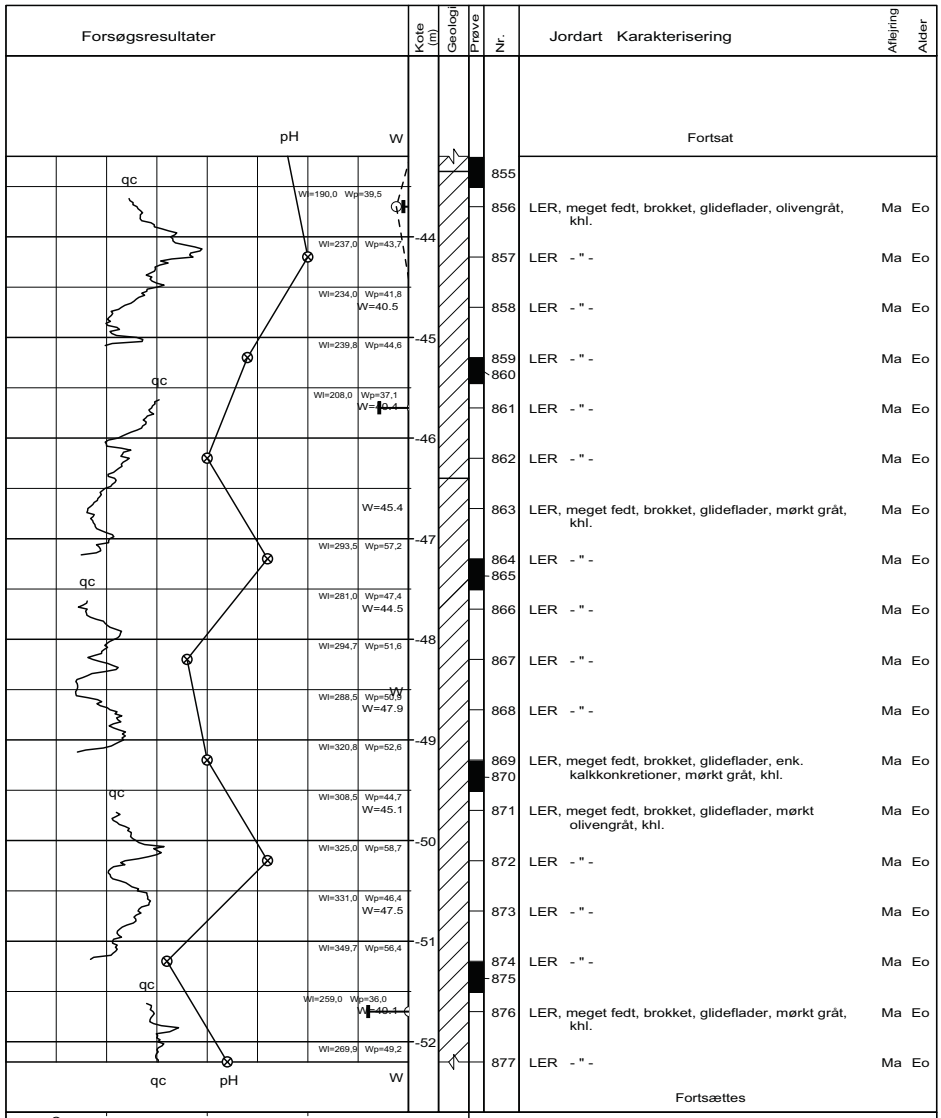

Boremetode : Tørboring med foring

X : 218921 (m) Y : 192840 (m) Plan :

Sag : 25.0705.61 Århus, Light*House

Geolog : JBM Boret af : LER/JQB Dato : 20071015 DGU-nr.: Boring : L*H11

Udarb. af : HLa Kontrol : Godkendt : Dato : Bilag : 5 S. 6 / 8

Grontmij | Carl Bro
Tlf. 98 79 98 00, Fax 98 79 98 01
Sofiendalsvej 94, 9200 Aalborg SV

Boreprofil

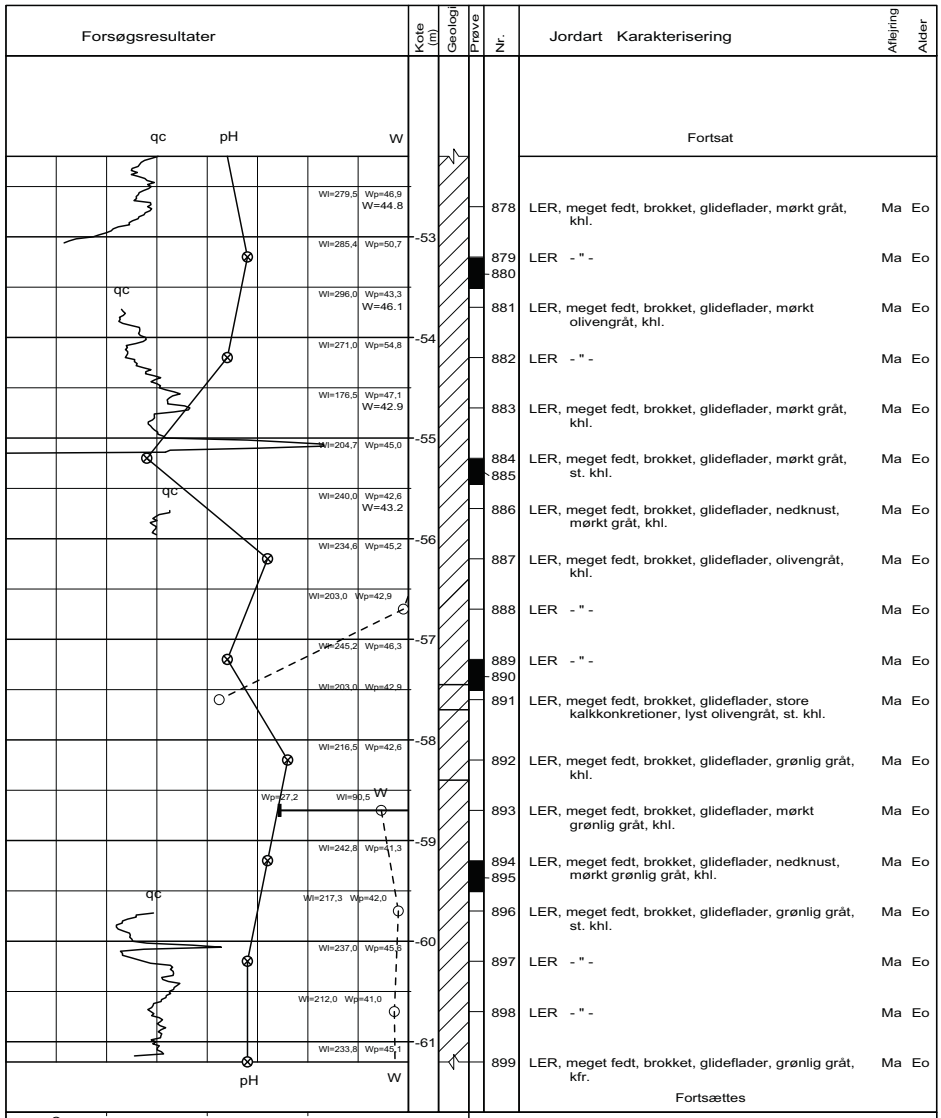

Boremetode : Tørboring med foring

X : 218921 (m) Y : 192840 (m) Plan :

Sag : 25.0705.61 Århus, Light*House

Geolog : JBM Boret af : LER/JQB Dato : 20071015 DGU-nr.: Boring : L*H11

Udarb. af : HLa Kontrol : Godkendt : Dato : Bilag : 5 S. 7 / 8

Grontmij | Carl Bro
Tlf. 98 79 98 00, Fax 98 79 98 01
Sofiendalsvej 94, 9200 Aalborg SV

Boreprofil

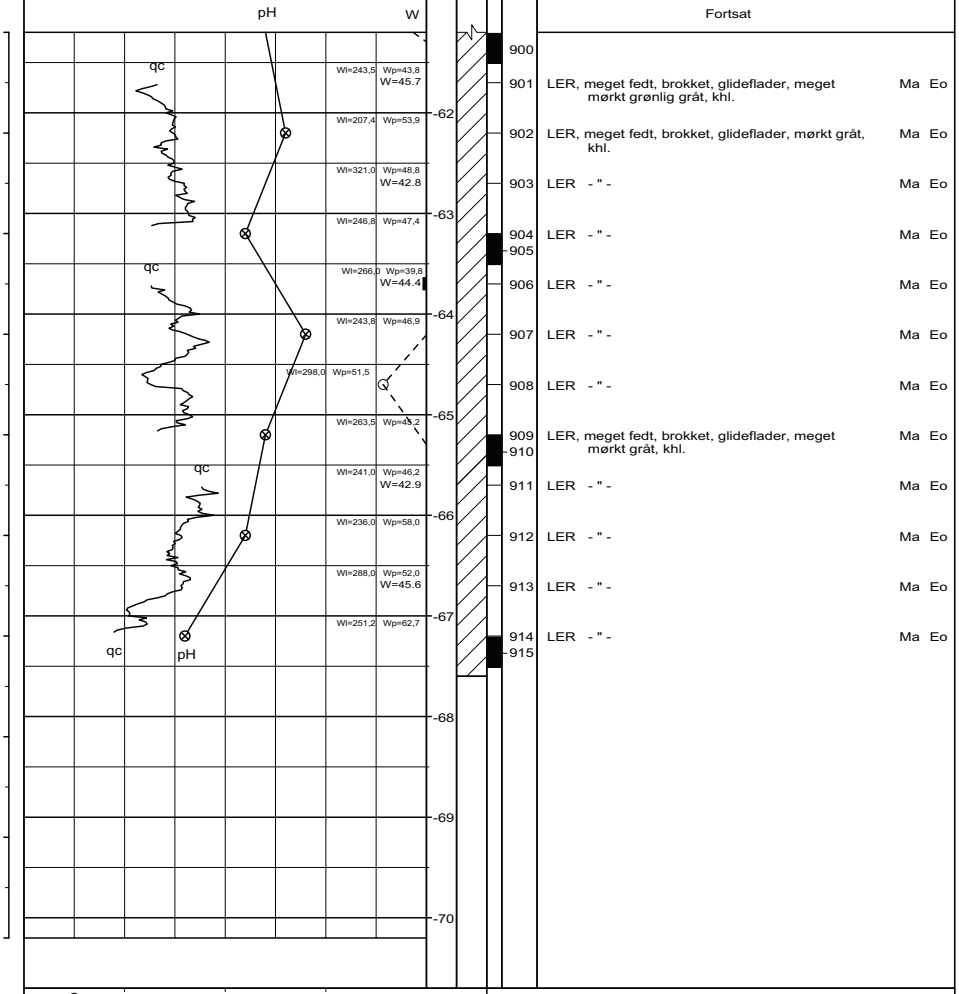

Boremetode : Tørboring med foring

X : 218921 (m) Y : 192840 (m) Plan :

Sag : 25.0705.61 Århus, Light*House

Geolog : JBM Boret af : LER/JQB Dato : 20071015 DGU-nr.: Boring : L*H11

Udarb. af : HLa Kontrol : Godkendt : Dato : Bilag : 5 S. 8 / 8

Grontmij | Carl Bro
Tlf. 98 79 98 00, Fax 98 79 98 01
Sofiendalsvej 94, 9200 Aalborg SV

Boreprofil

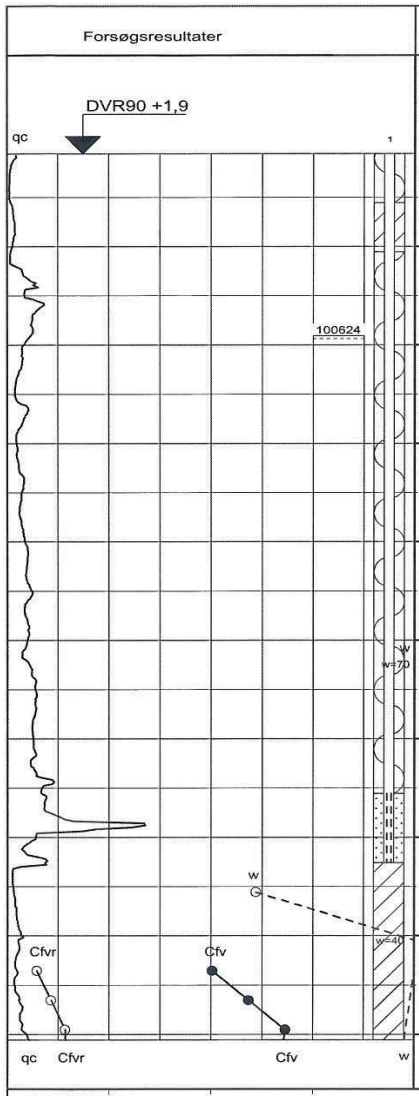

Dybde	Kote (m)	Nr.	Jordart Karakterisering	Aflejring	Alder	Frost	Kalk
			ASFALT, iflg. boreleder				
			STABILT GRUS, brun, iflg. boreleder				
0		1	FYLD: SAND, fin, m. enk. skalfragmenter, brungråt	Fy	Re		-
1	1	2	FYLD: SAND, fin - mellem, sv. gruset, brungråt	Fy	Re		-
		3	FYLD: SAND, fin, slaggebl. m. enk. mørtel og teglstykker, gråsort	Fy	Re		-
2	0	4	FYLD: SAND, fin, m. enk. små skalfragmenter og teglstykker, mørkegråt	Fy	Re		-
		5	FYLD: SAND, fin, m. enk. små skalfragmenter, mørkegråt	Fy	Re		-
3	-1	6	FYLD: SAND - " -	Fy	Re		-
		7	FYLD: SAND, fin, m. enk. grusk. og små skalfragmenter, mørkegråt	Fy	Re		-
4	-2	8	FYLD: SAND - " -	Fy	Re		-
		9	FYLD: SAND, m. enk. små skalfragmenter, gråt	Fy	Re		-
5	-3	10	FYLD: SAND - " -	Fy	Re		-
		11	GYTJE, stedvis sandet, m. enk. grusk., planterester og skalfragmenter, mørkt grønliggråt	Ma	Pg		(+)
		12	SAND, fin - mellem, m. enk. små skalfragmenter, mørkegråt	Ma	Pg		-
6	-4	13	SAND - " -	Ma	Pg		-
		14	SAND, fin - mellem, m. enk. små gytjepletter og skalfragmenter, mørkegråt	Ma	Pg		-
7	-5	15	SAND, fin, siltet, m. gytjelag og enk. små skalfragmenter, mørkegråt	Ma	Pg		-
		16	LER, sandet, siltet, sv. gruset, m. enk. små skalfragmenter, gråt	Ma	Pg		-
8	-6	17	LER, meget fed, m. enk. sandslirer og grusk., gråligt olivenfarvet	Gl	Gc		(+)
		18	LER, meget fed, m. enk. sandslirer, sv. glimmerh., lyst olivengråt	Gl	Gc		(+)
9	-7						

Fortsættes

○	10	20	30	w (%)
△	14	18	22	γ (kN/m³)
●	100	200	300	Cfv,Cfvr (kN/m²)
	10	20	30	qc (MN/m²)

Pr. 4 - 10: Indpumpet postglacialt marint sand. Pr. 15: Lagdelt.
Pr. 16: Tertiært præget. Pr. 17 og 18: Tertiært præget.
Pr. 17 - 23: Viborg ler. N. Oligocæn. Pr. 24 - 55: Søvind mergel. Ø. Eocæn
Boremetode : Tørboring med 6" snegl
Koordinat system : U32EUREF89
X : 575537 (m) Y : 6224513 (m) Plan :

Sag : 72993-G-1 Bestseller. Nyt kontordomicil, Pier 2 Århus Havn

Geolog : LCX Boret af : SNC Dato : 20100407 DGU-nr.: Boring : B/CPT304

Udarb. af : AMU/AWW Kontrol : ELPS Godkendt : ANRS Dato : 25/7-10 Bilag : 1.4 S. 1 / 3

COWI Boreprofil

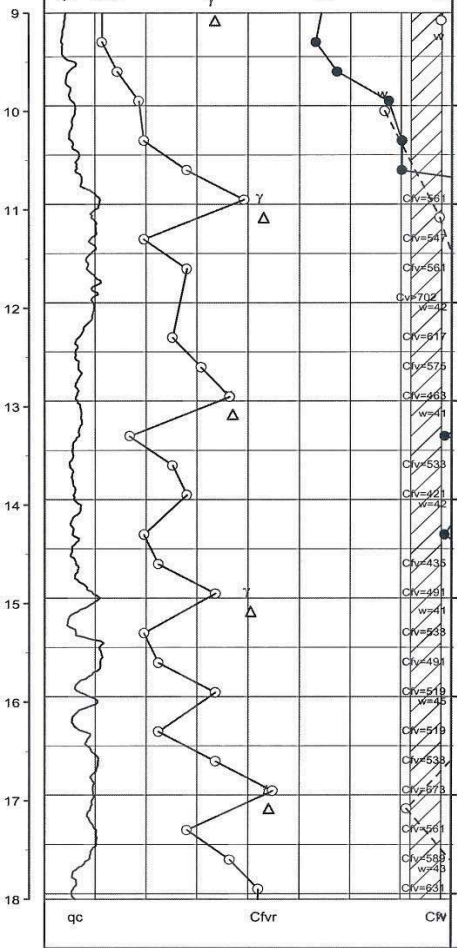

Dybde	Kote (m)	Geo-logi	Prøve	Nr.	Jordart Karakterisering	Aflejring	Alder	Frost	Kalk
					Fortsat				
9				19	LER, meget fed, sv. glimmerh., gråligt olivenfarvet	Ma	Te		(+)
				20	LER -"-	Ma	Te		+
10	-8			21	LER, meget fed, stedvis, glaukonith., sv, glimmerh., gråligt olivenfarvet	Ma	Te		+
				22	LER, meget fed, m. glaukonitpartier, sv. glimmerh., gråligt olivenfarvet	Ma	Te		+
11	-9			23	LER, meget fed, st. glaukonith., sv. glimmerh., lyst olivengråt	Ma	Te		+
				24	LER, meget fed, m. enk. glaukonitk., lyst olivengråt	Ma	Te		+
12	-10			25	LER -"-	Ma	Te		+
				26	LER -"-	Ma	Te		+
13	-11			27	LER -"-	Ma	Te		+
				28	LER, meget fed, lyst olivengråt	Ma	Te		+
14	-12			29	LER -"-	Ma	Te		+
				30	LER -"-	Ma	Te		+
15	-13			31	LER -"-	Ma	Te		+
				32	LER -"-	Ma	Te		+
16	-14			33	LER -"-	Ma	Te		+
				34	LER, meget fed, gråligt olivenfarvet	Ma	Te		(+)
17	-15			35	LER, meget fed, lyst olivengråt	Ma	Te		+
				36	LER -"-	Ma	Te		+
18	-16			37	LER -"-	Ma	Te		+
					Fortsættes				

○	10	20	30	w (%)
△	14	18	22	γ (kN/m³)
●	100	200	300	Cfv,Cfvr (kN/m²)
	10	20	30	qc (MN/m²)

Pr. 4 - 10: Indpumpet postglacialt marint sand. Pr. 15: Lagdelt.
Pr. 16: Tertiært præget. Pr. 17 og 18: Tertiært præget.
Pr. 17 - 23: Viborg ler. N. Oligocæn. Pr. 24 - 55: Søvind mergel. Ø. Eocæn
Boremetode : Tørboring med 6" snegl
Koordinat system : U32EUREF89
X : 575537 (m) Y : 6224513 (m) Plan :

Sag : 72993-G-1 Bestseller. Nyt kontordomicil, Pier 2 Århus Havn

Geolog : LCX Boret af : SNC Dato : 20100407 DGU-nr.: Boring : B/CPT304

Udarb. af : AMU/ÅMN Kontrol : ELPE Godkendt : ANRS Dato : 25/7-10 Bilag : 1.4 S. 2 / 3

COWI

Boreprofil

BRegistar - PSTGFDK 2.0 - 13/07/2010 10:41:45

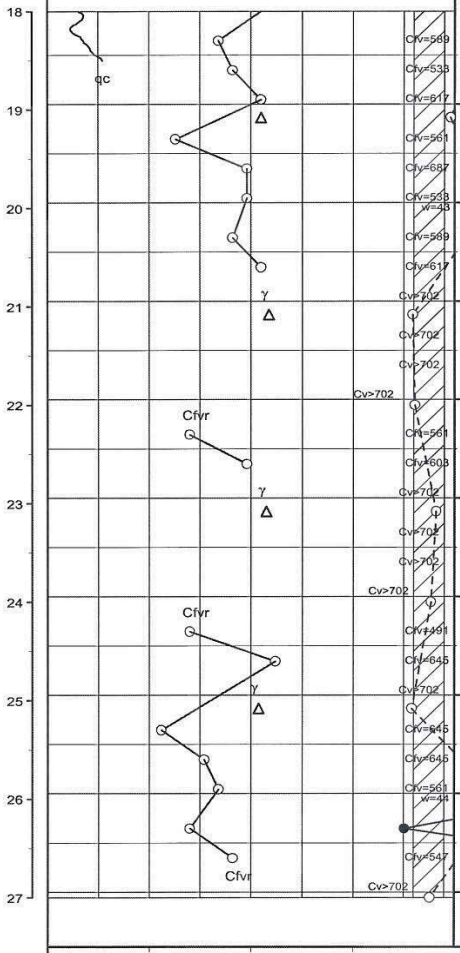

Kote (m)	Geo-logi	Prøve	Nr.	Jordart Karakterisering	Aflejring	Alder	Frost	Kalk
				Fortsat				
-17			38	LER, meget fed, lyst olivengrået	Ma	Te		+
		■	39	LER - " -	Ma	Te		+
			40	LER - " -	Ma	Te		+
-18			41	LER, meget fed, grønlig gråt	Ma	Te		+
			42	LER - " -	Ma	Te		+
-19		■	43	LER, meget fed, lyst olivengrået	Ma	Te		+
			44	LER, meget fed, stedvis m. hærdnede mergelpartier, lyst olivengrået	Ma	Te		+
-20			45	LER, meget fed, stedvis m. enk. hærdnede mergelpartier, lyst olivengrået	Ma	Te		+
			46	LER, meget fed, olivengrået	Ma	Te		-
-21		■	47	LER, meget fed, lyst olivengrået	Ma	Te		+
			48	LER - " -	Ma	Te		+
-22			49	LER, meget fed, m. enk. glaukonitslirer, lyst olivengrået	Ma	Te		+
			50	LER, meget fed, m. enk. glaukonitslirer, olivengrået	Ma	Te		(+)
-23		■	51	LER, meget fed, m. enk. glaukonitslirer, lyst olivengrået	Ma	Te		+
			52	LER, meget fed, lyst olivengrået	Ma	Te		(+)
-24			53	LER, meget fed, m. enk. glaukonitslirer, lyst olivengrået	Ma	Te		(+)
			54	LER - " -	Ma	Te		(+)
-25			55	LER, meget fed, lyst olivengrået	Ma	Te		+

○	10	20	30	w (%)
△	14	18	22	γ (kN/m³)
●	100	200	300	Cfv,Cfvr (kN/m²)
	10	20	30	qc (MN/m²)

Pr. 4 - 10: Indpumpet postglacialt marint sand. Pr. 15: Lagdelt.
Pr. 16: Tertiært præget. Pr. 17 og 18: Tertiært præget.
Pr. 17 - 23: Viborg ler. N. Oligocæn. Pr. 24 - 55: Søvind mergel. Ø. Eocæn
Boremetode : Tørboring med 6" snegl
Koordinat system : U32EUREF89
X : 575537 (m) Y : 6224513 (m) Plan :

Sag : 72993-G-1 Bestseller. Nyt kontordomicil, Pier 2 Århus Havn

Geolog : LCX Boret af : SNC Dato : 20100407 DGU-nr.: Boring : B/CPT304

Udarb. af : AMU/AHM Kontrol : ELPE Godkendt : ANRS Dato : 25/7-10 Bilag : 1.4 S. 3 / 3

COWI Boreprofil

BRegister - FSTGFDK 2.0 - 13/07/2010 10:41:45

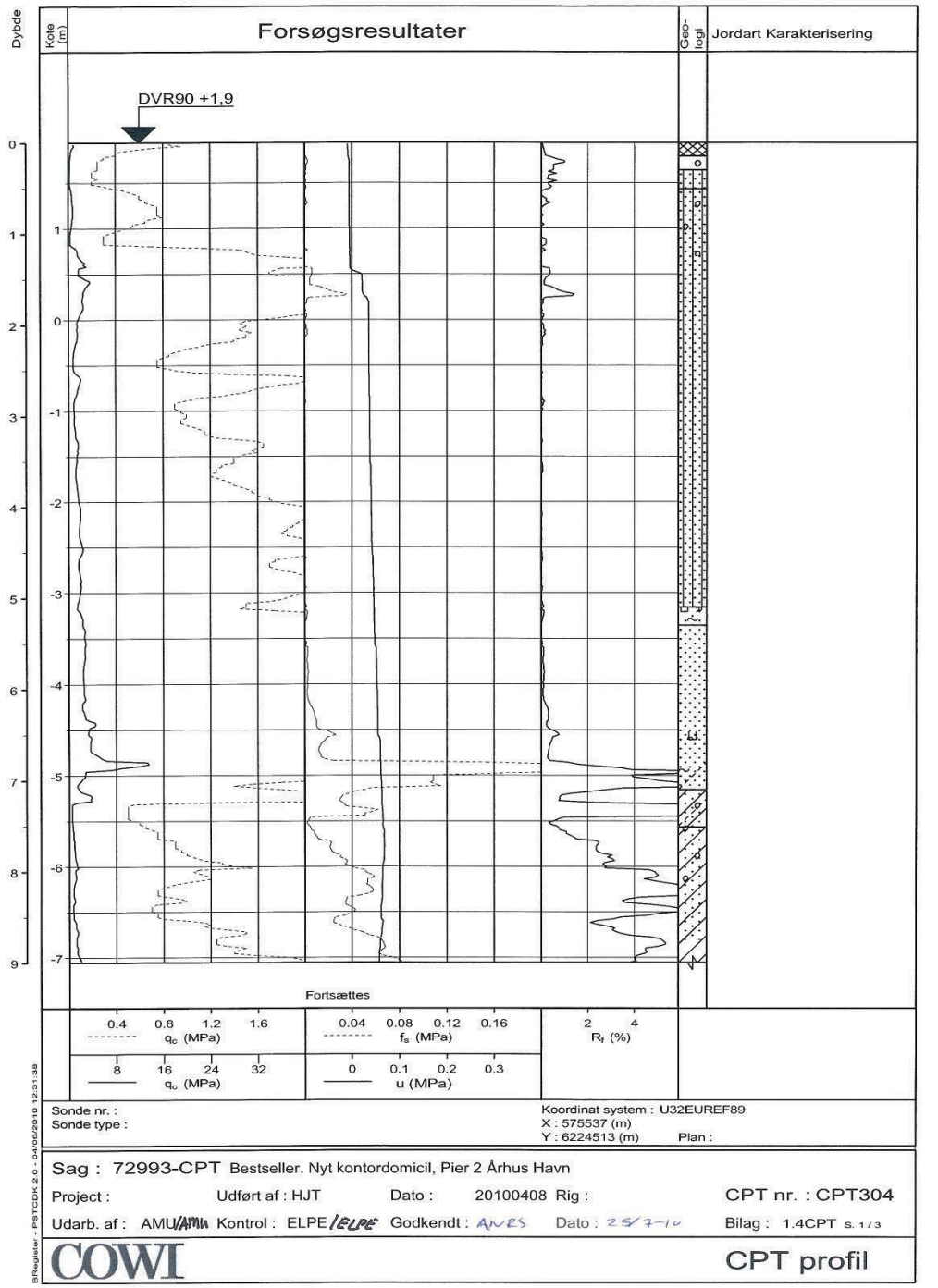
Dybde
Kote (m)
Forsøgsresultater
Geo-logi
Jordart Karakterisering
DVR90 +1,9
0
1
2
3
4
5
6
7
8
9
1
0
-1
-2
-3
-4
-5
-6
-7
Fortsættes
0.4 0.8 1.2 1.6
q_c (MPa)
8 16 24 32
q_c (MPa)
0.04 0.08 0.12 0.16
f_s (MPa)
0 0.1 0.2 0.3
u (MPa)
2 4
R_f (%)
Sonde nr. :
Sonde type :
Koordinat system : U32EUREF89
X : 575537 (m)
Y : 6224513 (m)
Plan :
Sag : 72993-CPT Bestseller. Nyt kontordomicil, Pier 2 Århus Havn
Project :
Udført af : HJT
Dato : 20100408 Rig :
CPT nr. : CPT304
Udarb. af : AMU/AMU Kontrol : ELPE/ELPE Godkendt : ANRS Dato : 25/7-10
Bilag : 1.4CPT s. 1/3
COWI
CPT profil
BTregister - PBTCDK 2.0 - 04/08/2010 12:31:39

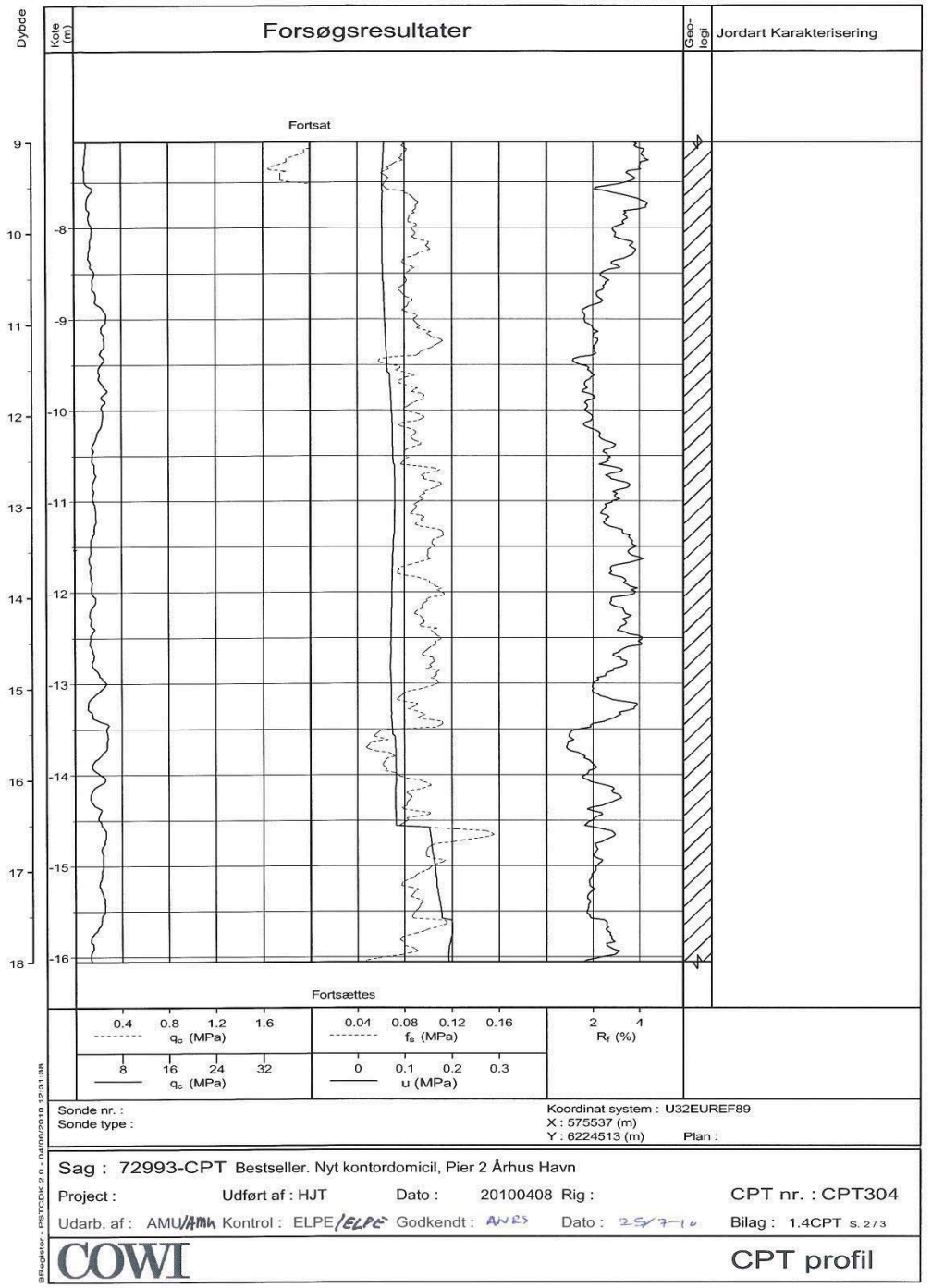

Sonde nr. :
Sonde type :

Koordinat system : U32EUREF89
X : 575537 (m)
Y : 6224513 (m) Plan :

Sag : 72993-CPT Bestseller. Nyt kontordomicil, Pier 2 Århus Havn

Project : Udført af : HJT Dato : 20100408 Rig : CPT nr. : CPT304

Udarb. af : AMU/AMH Kontrol : ELPE/ELPE Godkendt : ANES Dato : 25/7-10 Bilag : 1.4CPT s. 2/3

COWI

CPT profil

BIRegister - PSTCDK 2.0 - 04/06/2010 12:31:38

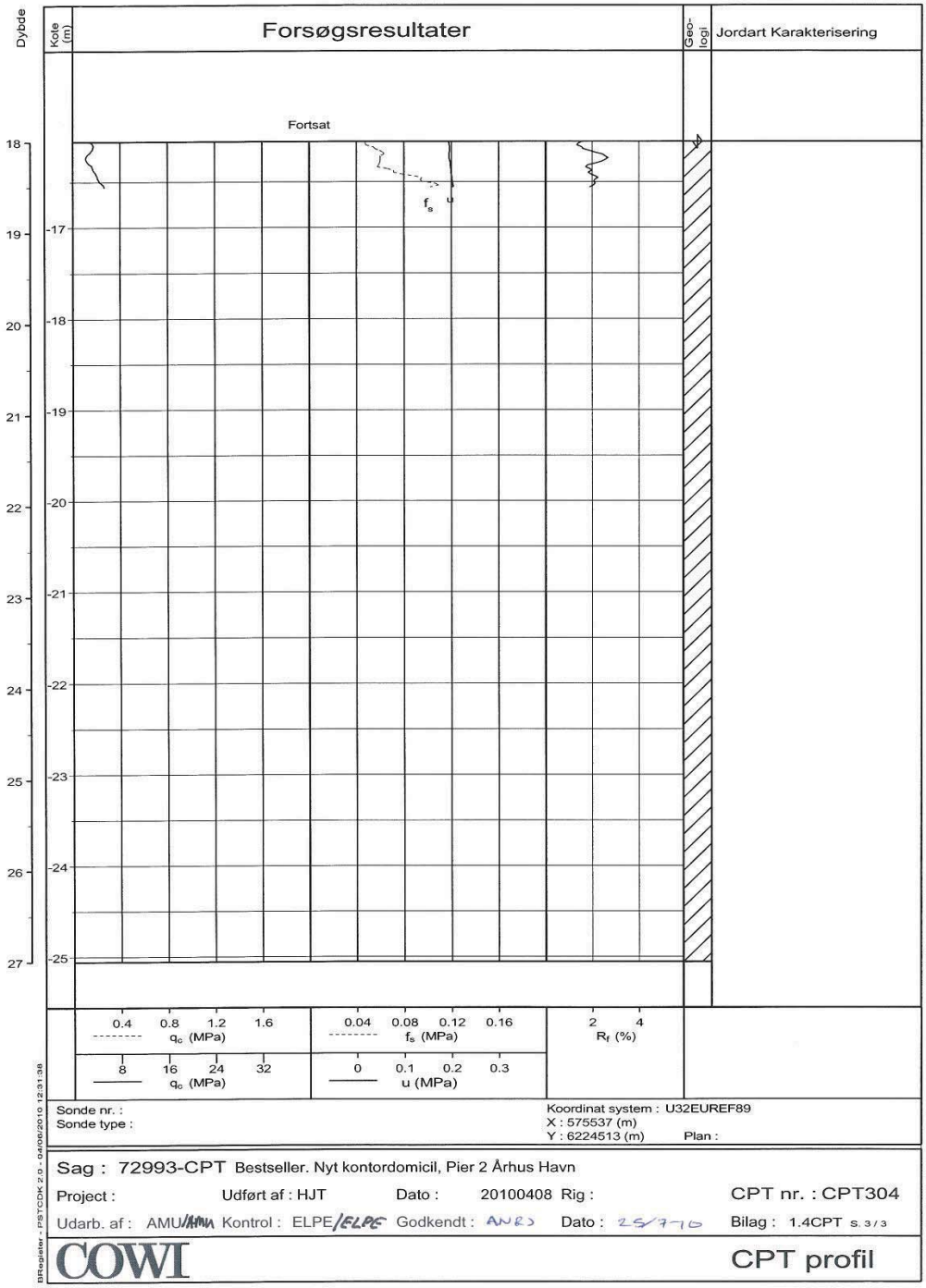

Sonde nr. :
Sonde type :

Koordinat system : U32EUREF89
X : 575537 (m)
Y : 6224513 (m)
Plan :

Sag : 72993-CPT Bestseller. Nyt kontordomicil, Pier 2 Århus Havn

Project : Udført af : HJT Dato : 20100408 Rig : CPT nr. : CPT304

Udarb. af : AMU/AMU Kontrol : ELPE/ELPE Godkendt : ANRJ Dato : 25/7-10 Bilag : 1.4CPT s. 3 / 3

COWI

CPT profil

BRegister - PSTCDK 2.0 - 04/08/2010 12:31:38

APPENDIX G
Additional classification

This appendix contains data and results from classification tests that are not directly presented in an paper. The tests listed below and the results are listed in Table G.1:

- Natural water content, w
- Grain size distribution
- Liquid limit, w_L
- Plastic limit, w_P
- Relative density, G_s
- Chloride (cl^-) content of pore water
- pH of pore water

Table G.1 Classification of BS samples as well as two LH samples.*: G_s found on sample part smaller than 0.063 mm, **: Smaller than 0.063/0.02 mm and ***: test performed twice.

Sample	w_{nat}	Grain size**	w_L	w_P	G_s	cl^-	pH
BS1	39.3	90.7/57.5	90.0	32.3	2.72	1.68	8.28
BS2	39.3	91.1/52.9	80.5	30.0	2.77/2.71*	1.51	8.63
BS3	39.9	91.1/52.6	78.8	31.6	2.72	1.72	8.3
BS4	40.0	92.0/51.3	75.6	31.9	2.72	1.71	8.43
BS5	40.1	90.4/50.8	76.1	32.2	2.72	1.61	8.43
LH815	3.0	91.8/79.7 [94.4/68.4]***	174.3	36.2	2.79	1.0	9.36
LH855	38.2	95.8/81.6	195.3	33.0	2.77	0.8	9.24

APPENDIX H
Incremental Loading Oedometer Tests

This appendix contains data and results from Incremental Loading Oedometer (ILO) tests that are not directly presented in a paper.

Re-loading load programme

Table H.1 Load programme for the re-loading ILO tests.

Step	Re-load (test 1) Load [kg]	σ'_V [kPa]	Re-load (test 2/3) Load [kg]	σ'_V [kPa]	Re-load (test 4) Load [kg]	σ'_V [kPa]
1	0.5	16.2	1	26.9	0.5	14.1
2	1	26.9	2	52.4	1	26.9
3	2	52.4	4	103.5	2	52.4
4	4	103.4	9	231.0	4	103.5
5	8	205.5	19	486.2	8	205.5
6	15.5	396.9	29	741.4	15.5	396.9
7	10.5	269.3	13.5	345.9	8	205.5
8	15.5	396.9	19	486.2	15.5	396.9
9	31	792.4	39	996.5	31	792.4
10	62	1583.4	59	1506.9	62	1583.4
11	125	3191.0	79	2017.2	125	3191.0
12	62	1583.4	99	2527.5	62	1583.4
13	31	792.4	119	3037.9	31	792.4
14	62	1583.4	99	2527.5	62	1583.4
15	125	3191.0	79	2017.2	125	3191.0
16	62	1583.4	59	1506.9	62	1583.4
17	15.5	396.9	39	996.5	15.5	396.9
18	31	792.4	59	1506.9	31	792.4
19	62	1583.4	79	2017.2	62	1583.4
20	125	3191.0	99	2527.5	125	3191.0
21	31	792.4	119	3037.9	31	792.4
22	8	205.5	99	2527.5	8	205.5
23	15.5	396.9	79	2017.2	15.5	396.9
24	31	792.4	99	2527.5	31	792.4
25	62	1583.4	119	3037.9	62	1583.4
26	125	3191.0	139	3548.2	125	3191.0
27	250	6380.6	159	4058.6	250	6380.6
28	-	-	179	4568.9	-	-
29	-	-	199	5079.2	-	-
30	-	-	219	5589.6	-	-

Tolkning af konsolideringsforsøg - Test 1

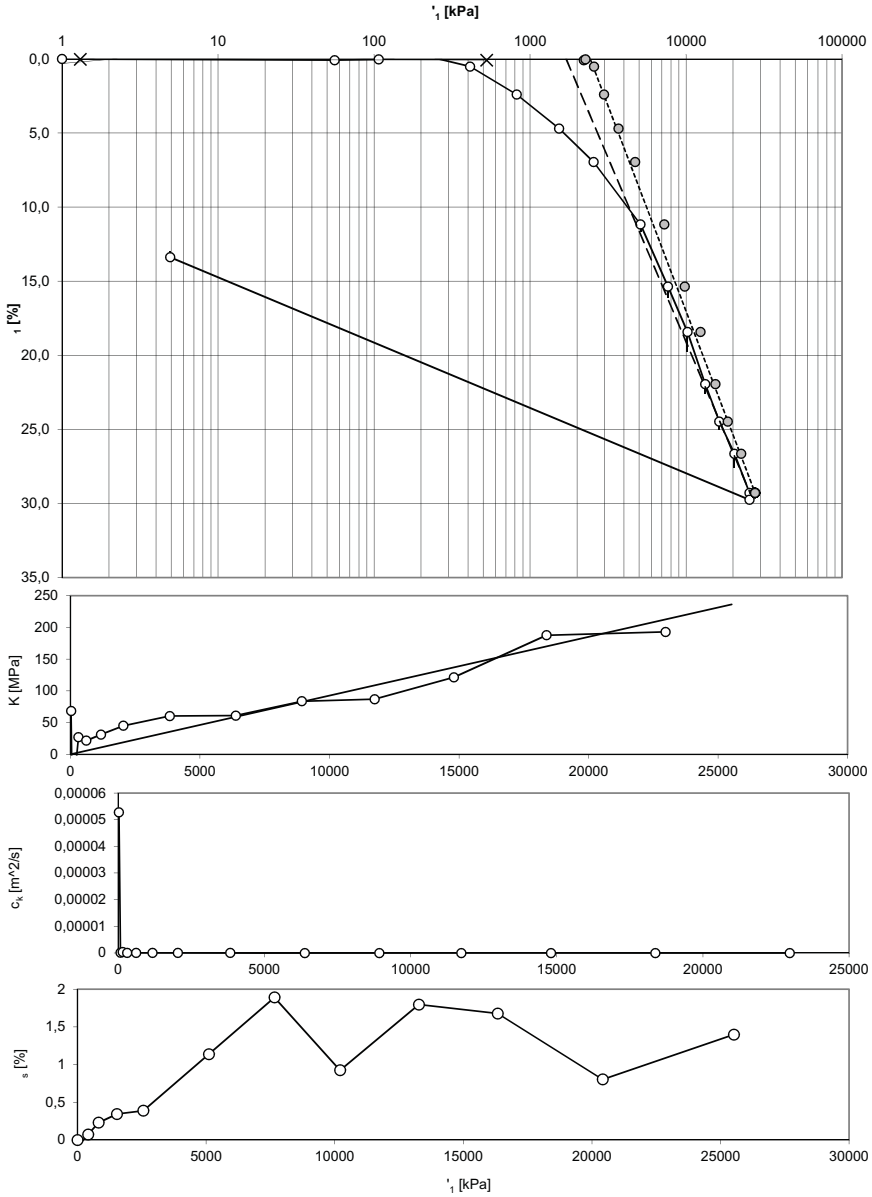

Sag:	Søvind Marl	*Side*	1
Undersøgt d.	April 2012	*Boring nr.*	LH815
Lab. nr.	Test 1		*Samlet belastningsforløb (AC.)*

Forsøgsresultater

		Værdi		Bemærkninger
Tøjningsindeks	Q =	24,88	%	
Krybningstøjningsindeks	Q_s =	1,89	%	
Forbelastningsspænding	$'_{pc}$ =		kPa	
Svelletryk	$'_{sw}$ =		kPa	

Trin	' [kPa]	$_{100}$ [%]	$_{cr}$ [%]	$_{s}$ [%]	K [MPa]	k [m/s]	c_k [m^2/s]
1	56	0,082	-0,259	-0,970	68,25	7,7E-09	5,28E-05
2	107	0,037	-0,442	-1,318	-112,62	-1,2E-11	1,31E-07
3	209	-0,236	-0,001	-0,001	-37,48	-1,1E-10	3,95E-07
4	413	0,515	0,114	0,074	27,20	2,2E-11	5,99E-08
5	821	2,404	0,082	0,230	21,61	1,5E-11	3,15E-08
6	1536	4,694	0,151	0,344	31,20	7,8E-12	2,44E-08
7	2557	6,961	0,197	0,388	45,01	4,4E-12	1,98E-08
8	5108	11,191	0,533	1,138	60,33	2,2E-12	1,32E-08
9	7660	15,376	0,721	1,890	60,97	1,0E-12	6,15E-09
10	10212	18,424	1,337	0,924	83,71	5,8E-13	4,87E-09
11	13274	21,954	0,624	1,796	86,75	4,0E-13	3,49E-09
12	16336	24,475	0,538	1,678	121,43	2,3E-13	2,79E-09
13	20418	26,651	0,952	0,803	187,61	1,7E-13	3,16E-09
14	25522	29,298	0,460	1,397	192,86	1,2E-13	2,41E-09
15	5	13,337	-0,404	-0,875	159,88	1,3E-13	2,12E-09

Tolkning af konsolideringsforsøg - Test 2

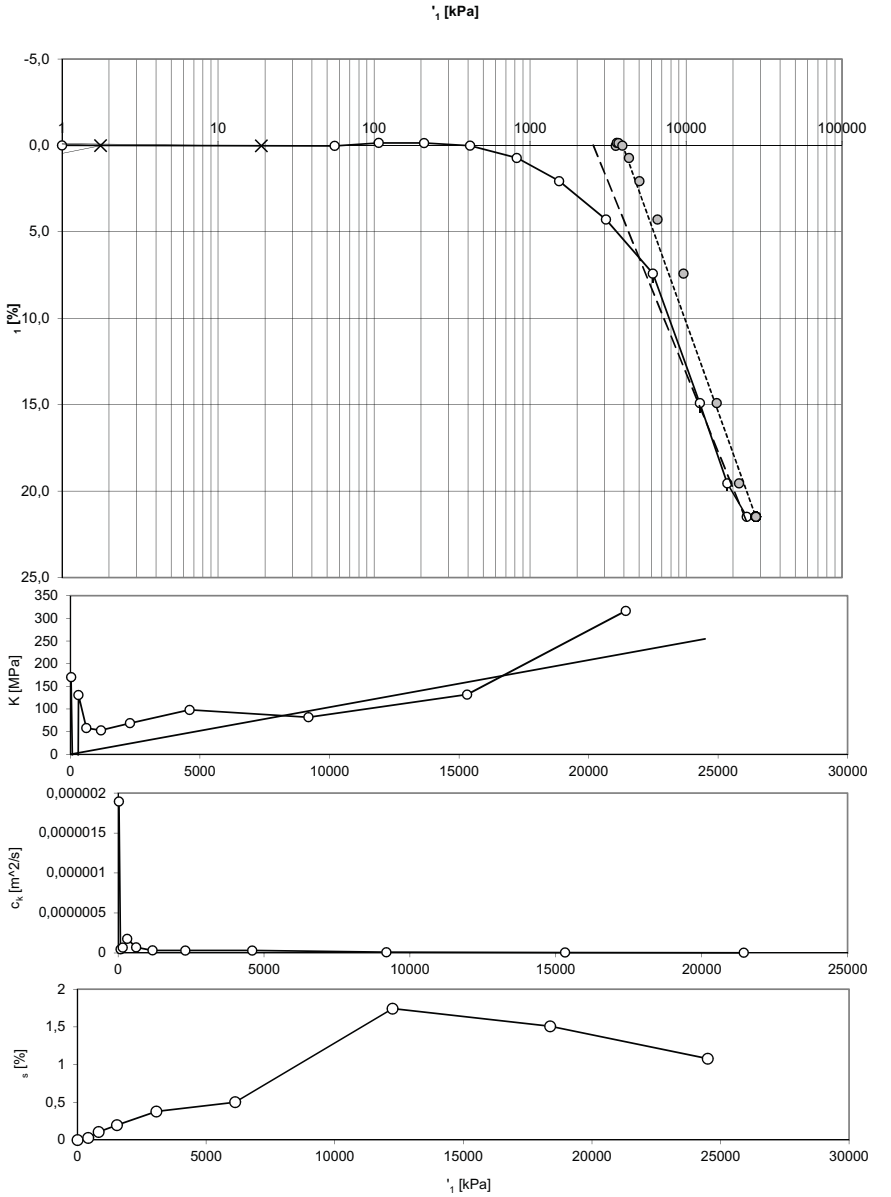

Sag:	Søvind Marl	*Side*	1
Undersøgt d.	8.April 2010	*Boring nr.*	LH840a
Lab. nr.	Test 2		*Samlet belastningsforløb (AC.)*

Forsøgsresultater

		Værdi		Bemærkninger
Tøjningsindeks	Q =	22,15	%	
Krybningstøjningsindeks	Q_s =	1,74	%	
Forbelastningsspænding	$'_{pc}$ =	6973	kPa	
Svelletryk	$'_{sw}$ =		kPa	

Trin	' [kPa]	$_{100}$ [%]	$_{cr}$ [%]	$_{s}$ [%]	K [MPa]	k [m/s]	c_k [m^2/s]
1	56	0,033	-0,205	-0,536	170,14	1,1E-10	1,89E-06
2	107	-0,132	-0,071	-0,150	-30,94	-1,6E-11	4,82E-08
3	209	-0,138	-0,046	-0,122	-1662,92	-4,0E-13	6,72E-08
4	413	0,018	0,010	0,029	130,72	1,4E-11	1,77E-07
5	821	0,724	0,041	0,106	57,86	1,2E-11	7,19E-08
6	1536	2,071	0,077	0,198	53,03	6,1E-12	3,26E-08
7	3067	4,295	0,146	0,378	68,83	4,6E-12	3,18E-08
8	6129	7,415	0,552	0,501	98,16	3,2E-12	3,14E-08
9	12253	14,901	0,532	1,742	81,80	1,2E-12	9,64E-09
10	18377	19,546	0,444	1,508	131,85	4,7E-13	6,14E-09
11	24501	21,481	0,297	1,079	316,37	1,2E-13	3,94E-09

Tolkning af konsolideringsforsøg - Test 3

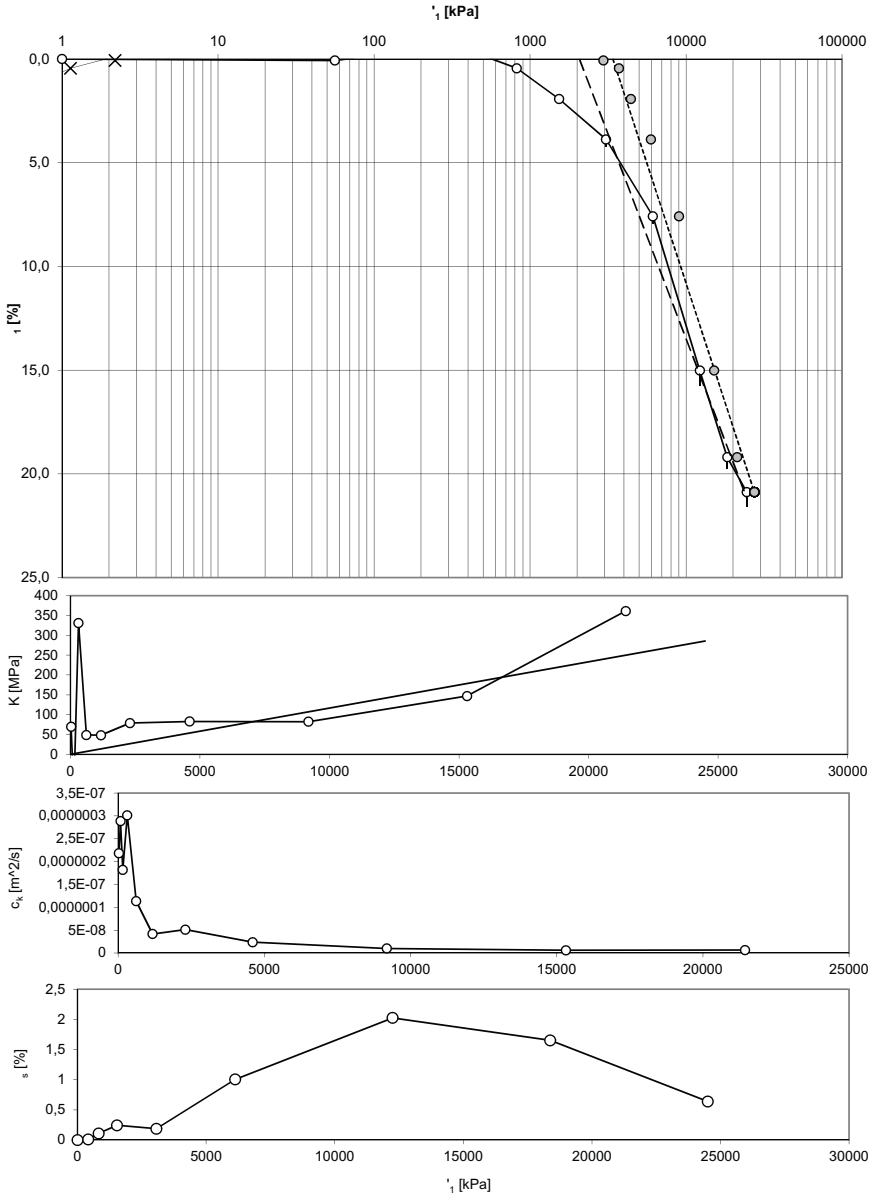

Sag:	Søvind Marl	*Side*	1
Undersøgt d.	19. november 2009	*Boring nr.*	LH840b
Lab. nr.	Test 3		*Samlet belastningsforløb (AC.)*

Forsøgsresultater

		Værdi		Bemærkninger
Tøjningsindeks	Q =	19,74	%	
Krybningstøjningsindeks	Q_s =	2,02	%	
Forbelastningsspænding	$'_{pc}$ =	5785	kPa	
Svelletryk	$'_{sw}$ =		kPa	

Trin	' [kPa]	$_{100}$ [%]	$_{cr}$ [%]	$_{s}$ [%]	K [MPa]	k [m/s]	c_k [m^2/s]
1	56	0,080	-0,340	-0,848	69,69	3,1E-11	2,19E-07
2	107	-0,195	-0,316	-0,903	-18,53	-1,6E-10	2,89E-07
3	209	-0,449	-0,128	-0,259	-40,17	-4,5E-11	1,82E-07
4	413	-0,387	0,038	0,008	330,95	9,1E-12	3,01E-07
5	822	0,451	0,042	0,109	48,70	2,3E-11	1,13E-07
6	1536	1,936	0,095	0,244	48,12	8,7E-12	4,17E-08
7	3067	3,879	0,340	0,188	78,77	6,5E-12	5,11E-08
8	6129	7,581	0,350	1,004	82,71	2,9E-12	2,37E-08
9	12253	15,018	0,723	2,023	82,35	1,2E-12	9,87E-09
10	18377	19,186	0,573	1,652	146,92	4,1E-13	6,07E-09
11	24501	20,882	0,695	0,638	361,01	1,8E-13	6,56E-09

Tolkning af konsolideringsforsøg - Test 4

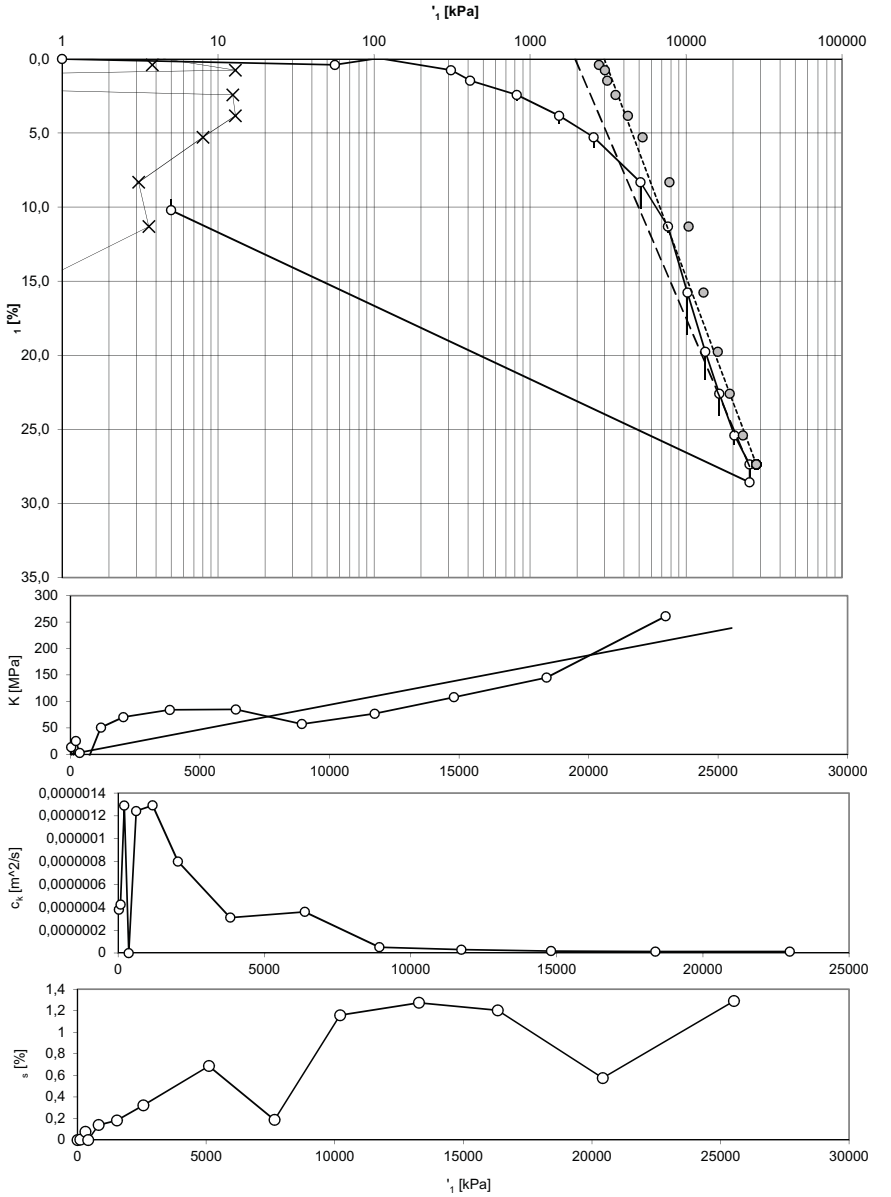

Sag:	Søvind Marl	*Side*	1
Undersøgt d.	April 2012	*Boring nr.*	BS3
Lab. nr.	Test 4		*Samlet belastningsforløb (AC.)*

Forsøgsresultater

		Værdi		Bemærkninger
Tøjningsindeks	Q =	24,63	%	
Krybningstøjningsindeks	Q_s =	1,29	%	
Forbelastningsspænding	$'_{pc}$ =		kPa	
Svelletryk	$'_{sw}$ =		kPa	

Trin	' [kPa]	$_{100}$ [%]	$_{cr}$ [%]	$_{s}$ [%]	K [MPa]	k [m/s]	c_k [m^2/s]
1	56	0,414	-0,547	-1,389	13,55	2,8E-10	3,80E-07
2	107	-0,056	0,004	0,004	-10,87	-3,9E-10	4,24E-07
3	311	0,755	0,237	0,078	25,18	5,1E-10	1,29E-06
4	413	4,719	0,000	0,000	2,57	5,4E-13	1,40E-10
5	822	2,419	0,403	0,140	-17,75	-7,0E-10	1,24E-06
6	1536	3,829	0,508	0,182	50,68	2,5E-10	1,29E-06
7	2557	5,277	0,718	0,321	70,48	1,1E-10	8,01E-07
8	5108	8,310	1,773	0,687	84,14	3,7E-11	3,10E-07
9	7660	11,314	0,438	0,187	84,94	4,2E-11	3,60E-07
10	10212	15,768	2,839	1,158	57,28	9,0E-12	5,13E-08
11	13274	19,759	1,888	1,274	76,73	3,8E-12	2,93E-08
12	16336	22,592	1,518	1,203	108,08	1,6E-12	1,74E-08
13	20418	25,409	0,661	0,576	144,96	8,7E-13	1,26E-08
14	25522	27,365	1,210	1,290	260,89	4,7E-13	1,23E-08
15	5	10,221	-0,779	-2,067	148,84	1,7E-13	2,46E-09

Sag:	Søvind Marl	*Side*	2
Undersøgt d.	April 2012	*Boring nr.*	BS3
Lab. nr.	Test 4		*Samlet belastningsforløb (AC.)*

Tolkning af konsolideringsforsøg - Re-load (test 1)

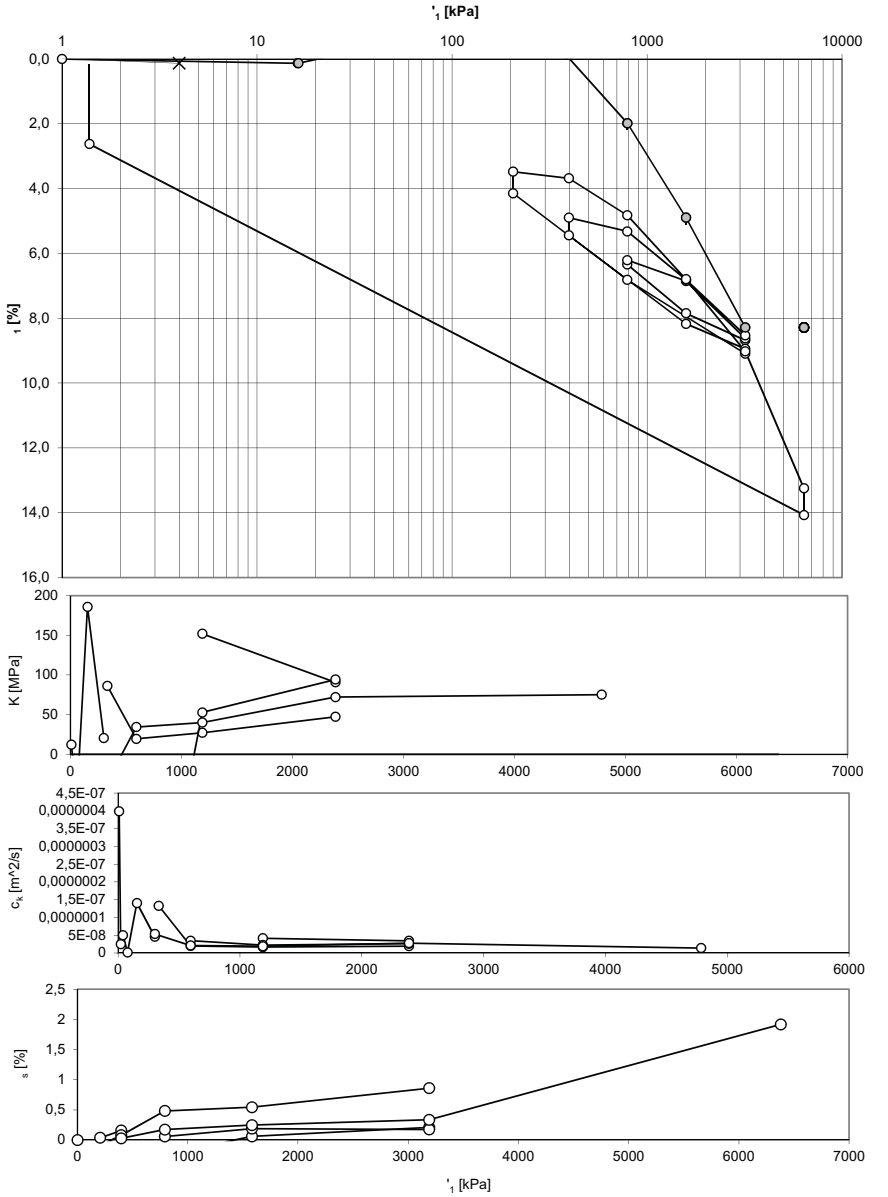

Sag:	Søvind Marl	*Side*	1
Undersøgt d.	April 2012	*Boring nr.*	LH815
Lab. nr.	Re-load (test 1)		*Samlet belastningsforløb (AC.)*

Forsøgsresultater

		Værdi		Bemærkninger
Tøjningsindeks	Q =	#VÆRDI!	%	
Krybningstøjningsindeks	Q_s =	1,92	%	
Forbelastningsspænding	$'_{pc}$ =	0	kPa	
Svelletryk	$'_{sw}$ =		kPa	

Trin	' [kPa]	$_{100}$ [%]	$_{cr}$ [%]	$_{s}$ [%]	K [MPa]	k [m/s]	c_k [m^2/s]
1	16	0,133	-0,279	-3,850	12,15	3,3E-10	3,99E-07
2	27	-0,146	-0,361	-1,051	-3,84	-6,5E-11	2,49E-08
3	52	-0,443	-0,363	-0,770	-8,58	-5,9E-11	5,02E-08
4	103	-1,049	-0,199	-0,566	-8,43	-2,0E-12	1,67E-09
5	206	-0,994	0,018	0,037	185,73	7,6E-12	1,41E-07
6	397	-0,068	0,056	0,157	20,68	2,2E-11	4,56E-08
7	269	-0,178	-0,018	-0,035	116,49	5,3E-12	6,18E-08
8	397	-0,030	0,047	0,080	86,25	1,5E-11	1,33E-07
9	792	1,987	0,193	0,482	19,61	1,0E-11	2,00E-08
10	1583	4,899	0,242	0,543	27,16	6,2E-12	1,68E-08
11	3191	8,297	0,399	0,859	47,31	4,1E-12	1,94E-08
12	1583	7,843	-0,035	-0,077	353,63	1,2E-12	4,22E-08
13	792	6,330	-0,134	-0,237	52,30	3,1E-12	1,64E-08
14	1583	6,850	0,074	0,060	152,03	2,7E-12	4,16E-08
15	3191	8,622	0,321	0,210	90,76	3,8E-12	3,44E-08
16	1583	8,169	-0,019	-0,037	355,15	1,2E-12	4,15E-08
17	397	5,426	-0,544	-1,428	43,26	2,9E-12	1,24E-08
18	792	5,320	0,022	0,058	-374,90	-9,2E-13	3,46E-08
19	1583	6,819	0,106	0,189	52,78	4,2E-12	2,23E-08
20	3191	8,524	0,569	0,176	94,29	2,8E-12	2,62E-08
21	792	6,805	-0,119	-0,227	139,52	1,4E-12	1,97E-08
22	205,517	4,131971792	-0,66421	-1,863114	21,95733	1,65E-12	3,62E-09
23	396,893	3,680805337	0,051832	0,0281614	-42,41798	-1,261E-11	5,35E-08
24	792,402	4,827299499	0,082401	0,1737806	34,49732	6,152E-12	2,12E-08
25	1583,42	6,80091382	0,127546	0,2480988	40,07974	4,742E-12	1,9E-08
26	3190,98	9,0291904	0,171881	0,3349456	72,14346	3,831E-12	2,76E-08
28	1,38275	2,607988856	-2,44973	-7,46015	59,8325	1,008E-12	6,03E-09

Sag:	Søvind Marl	*Side*	2
Undersøgt d.	April 2012	*Boring nr.*	LH815
Lab. nr.	Re-load (test 1)		*Samlet belastningsforløb (AC.)*

Tolkning af konsolideringsforsøg - Re-load (test 2/3)

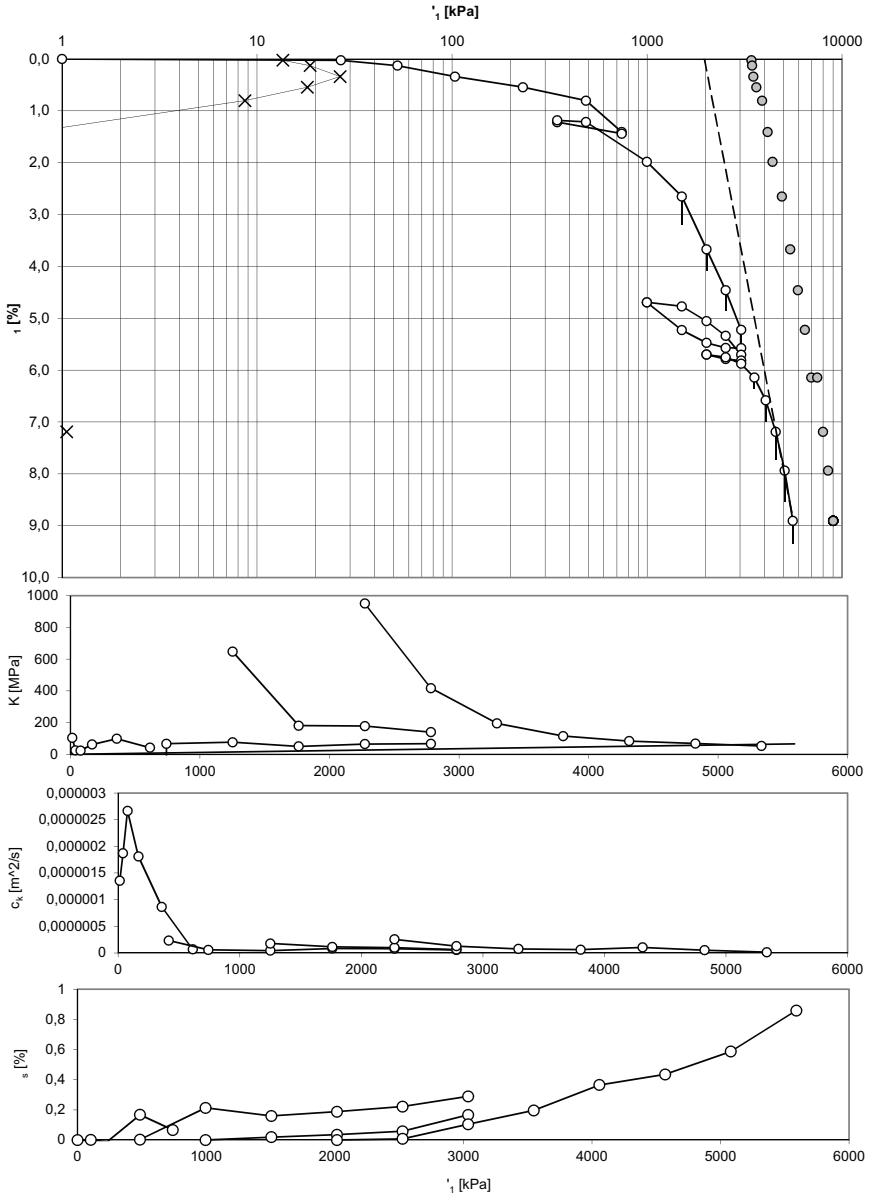

Sag:	Søvind Marl	*Side*	1
Undersøgt d.	19. november 2009	*Boring nr.*	LH840
Lab. nr.	Re-load (test 2/3)		*Samlet belastningsforløb (AC.)*

Forsøgsresultater

		Værdi		Bemærkninger
Tøjningsindeks	Q =	19,53	%	
Krybningstøjningsindeks	Q_s =	0,86	%	
Forbelastningsspænding	$'_{pc}$ =	6812	kPa	
Svelletryk	$'_{sw}$ =		kPa	

Trin	' [kPa]	$_{100}$ [%]	$_{cr}$ [%]	$_{s}$ [%]	K [MPa]	k [m/s]	c_k [m^2/s]
1	27	0,026	-0,002	-0,003	104,47	1,3E-10	1,36E-06
2	52	0,130	-0,001	-0,002	24,54	7,6E-10	1,87E-06
3	103	0,340	0,001	0,001	24,22	1,1E-09	2,67E-06
4	231	0,546	-0,007	-0,011	62,14	2,9E-10	1,81E-06
5	486	0,805	0,084	0,167	98,38	8,8E-11	8,67E-07
6	741	1,413	0,032	0,067	41,97	1,6E-11	6,92E-08
7	346	1,220	-0,035	-0,076	204,42	1,3E-12	2,56E-08
8	486	1,219	0,002	0,003	-94383,84	-2,5E-14	2,35E-07
9	997	1,985	0,103	0,213	66,71	9,0E-12	6,01E-08
10	1507	2,651	0,553	0,160	76,55	6,0E-12	4,62E-08
11	2017	3,673	0,407	0,188	49,93	1,7E-11	8,47E-08
12	2528	4,463	0,384	0,222	64,66	1,3E-11	8,22E-08
13	3038	5,228	0,351	0,289	66,69	8,5E-12	5,66E-08
14	2528	5,571	0,000	0,000	-148,73	-1,3E-11	1,92E-07
15	2017	5,478	-0,003	-0,011	547,33	2,4E-12	1,30E-07
16	1507	5,224	-0,003	-0,014	201,16	3,0E-12	6,10E-08
17	997	4,693	0,000	0,000	96,10	5,1E-12	4,94E-08
18	1507	4,772	0,032	0,019	647,64	2,8E-12	1,78E-07
19	2017	5,054	0,051	0,035	180,98	6,3E-12	1,15E-07
20	2528	5,340	0,098	0,058	178,04	5,7E-12	1,01E-07
21	3038	5,705	0,109	0,166	139,94	4,7E-12	6,62E-08
22	2527,55	5,785926285	0,00502	0,0202522	-631,3152	-4,465E-12	2,82E-07
23	2017,21	5,70255739	0,000248	0,000433	612,141	1,716E-12	1,05E-07
24	2527,55	5,756257902	0,011978	0,0080727	950,3358	2,7E-12	2,57E-07
25	3037,88	5,878528171	0,043078	0,1044079	417,3829	3,089E-12	1,29E-07
26	3548,22	6,140268385	0,209266	0,1963904	194,9778	3,946E-12	7,69E-08
28	4568,89	7,190750849	0,529429	0,4347791	83,88082	1,259E-11	1,06E-07
29	5079,22	7,938779876	0,601555	0,5868878	68,22398	7,767E-12	5,3E-08
30	5589,56	8,907265061	0,448814	0,8579452	52,69417	2,766E-12	1,46E-08

Tolkning af konsolideringsforsøg - Re-load (test 4)

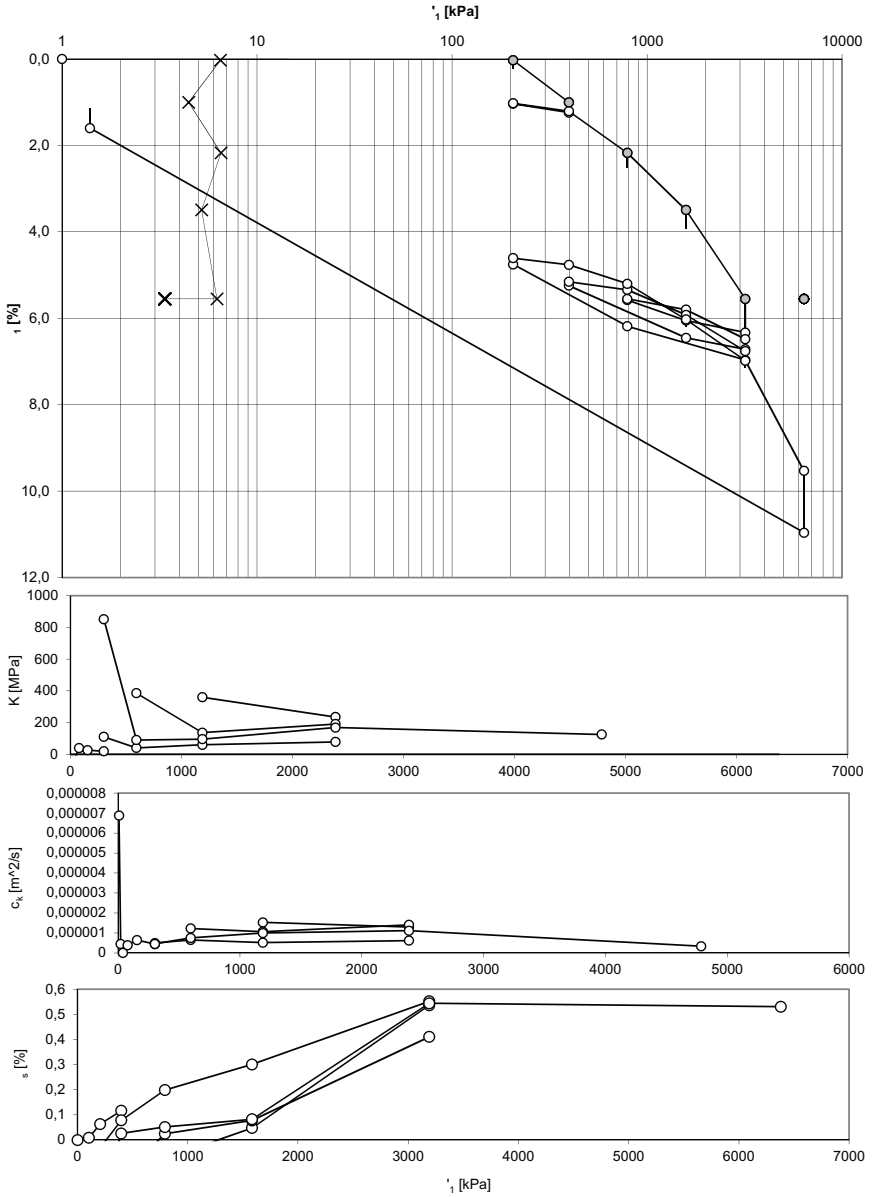

Sag:	Søvind Marl	*Side*	1
Undersøgt d.	April 2012	*Boring nr.*	BS3
Lab. nr.	Re-load (Test 4)		*Samlet belastningsforløb (AC.)*

Forsøgsresultater

		Værdi		Bemærkninger
Tøjningsindeks	Q =	#VÆRDI!	%	
Krybningstøjningsindeks	Q_s =	0,55	%	
Forbelastningsspænding	$'_{pc}$ =	0	kPa	
Svelletryk	$'_{sw}$ =		kPa	

Trin	' [kPa]	$_{100}$ [%]	$_{cr}$ [%]	$_{s}$ [%]	K [MPa]	k [m/s]	c_k [m^2/s]
1	14	-0,009	-0,382	-7,608	-150,94	-4,6E-10	6,88E-06
2	27	-0,390	-0,173	-0,283	-3,35	-1,4E-09	4,57E-07
3	52	-0,492	-0,013	-0,039	-24,91	-7,5E-13	1,87E-09
4	103	-0,363	0,015	0,009	39,59	9,9E-11	3,94E-07
5	206	0,023	0,206	0,064	26,45	2,5E-10	6,50E-07
6	397	1,005	0,236	0,116	19,49	2,3E-10	4,46E-07
7	206	1,035	-0,011	-0,030	-633,00	-3,0E-12	1,92E-07
8	397	1,208	0,055	0,078	110,61	4,5E-11	5,01E-07
9	792	2,172	0,329	0,199	41,05	1,6E-10	6,54E-07
10	1583	3,492	0,438	0,301	59,89	8,7E-11	5,20E-07
11	3191	5,547	0,779	0,552	78,25	8,0E-11	6,23E-07
12	1583	6,052	-0,002	-0,002	-317,97	-5,0E-11	1,59E-06
13	792	5,581	-0,027	-0,074	167,87	2,5E-11	4,17E-07
14	1583	5,801	0,051	0,048	360,30	4,2E-11	1,53E-06
15	3191	6,484	0,234	0,536	235,11	5,6E-11	1,31E-06
16	1583	6,451	-0,005	-0,009	4771,78	3,9E-12	1,86E-06
17	397	5,238	-0,090	-0,151	97,89	3,0E-11	2,90E-07
18	792	5,341	0,062	0,025	385,32	3,2E-11	1,23E-06
19	1583	5,921	0,115	0,078	136,48	7,8E-11	1,07E-06
20	3191	6,763	0,203	0,410	190,80	7,4E-11	1,41E-06
21	792	6,180	-0,020	-0,041	411,39	2,4E-11	1,01E-06
22	205,523	4,740912731	-0,14545	-0,246616	40,77577	3,878E-11	1,58E-07
23	396,898	4,763377184	0,018201	0,0263731	851,9045	5,342E-12	4,55E-07
24	792,408	5,200666391	0,172931	0,0519158	90,44581	8,344E-11	7,55E-07
25	1583,43	6,028074003	0,169547	0,0824925	95,60216	1,046E-10	1E-06
26	3190,98	6,980204877	0,174948	0,5438988	168,8377	6,618E-11	1,12E-06
28	1,38862	1,581846098	-0,45709	-1,01258	80,30682	3,009E-12	2,42E-08

Sag:	Søvind Marl	*Side*	2
Undersøgt d.	April 2012	*Boring nr.*	BS3
Lab. nr.	Re-load (Test 4)		*Samlet belastningsforløb (AC.)*

APPENDIX I
Continuous Loading Oedometer Tests

This appendix contains raw data from Continuous Loading Oedometer (CLO)tests. First the swell pressure,σ'_{sw}, was measured (first picture in each test), then the tests were loaded to in situ stresses, σ'_{V0}, and back to swell pressure (these steps are not included in these graphs). The data is only adjusted in regards to zero point measurements. If one measurement was believed to be unreliable (because of faulty transducer), this measurement was ignored in the analysis of the test. An example of this is displacement transducer 2 in test 5 (laboratory number 130603). Select analysed data from each test is presented after the raw data; horizontal lines separate each step.

Laboratory number 130601 - Test 6

Zero point measurements

Table I.1 Zero point measurements for test 6.

Transducer	Zero measurement
Cell pressure	111 kPa
Load cell	57.6 + 20 kg
Pore pressure	0 kPa
Displacement 1	2.333 mm
Displacement 2	2.481 mm
Horizontal pressure 1	515.7 kPa
Horizontal pressure 2	-348.4 kPa
Horizontal pressure 3	152.3 kPa

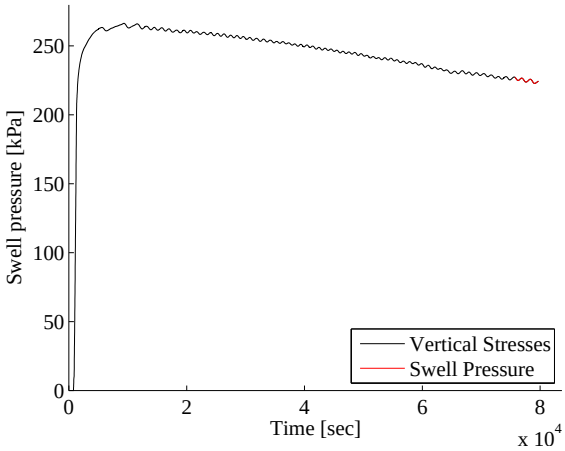

Figure I.1 130601 - Swell pressure.

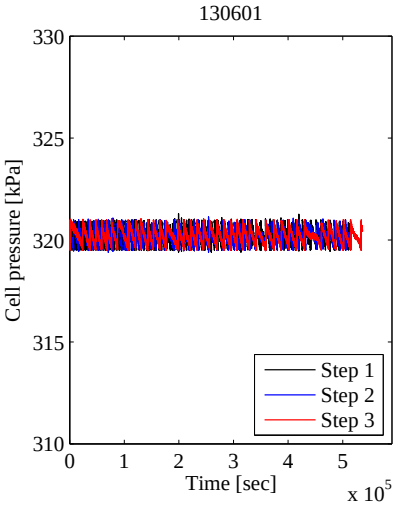

Figure I.2 130601 - Cell pressure.

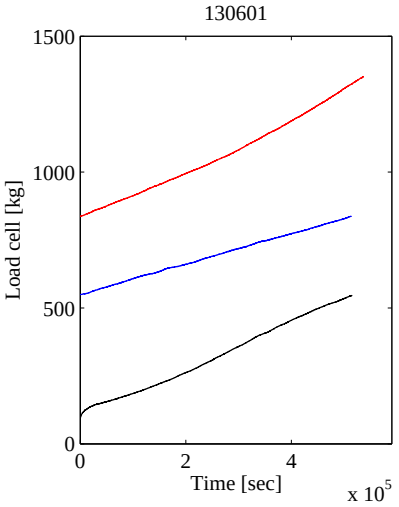

Figure I.3 130601 - Load cell.

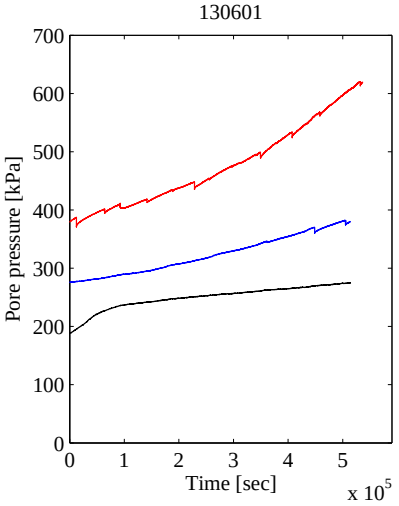

Figure I.4 130601 - Pore pressure.

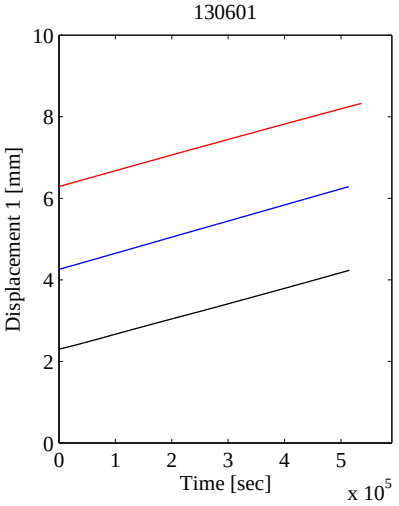

Figure I.5 130601 - Displacement 1.

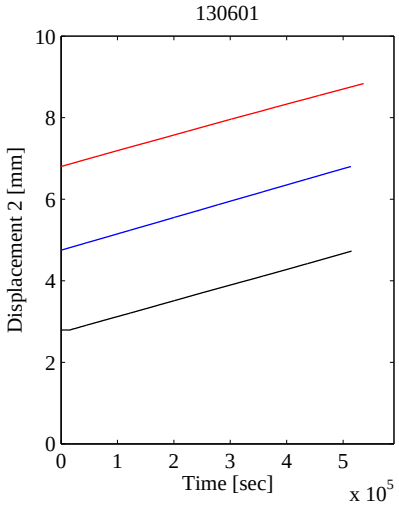

Figure I.6 130601 - Displacement 2.

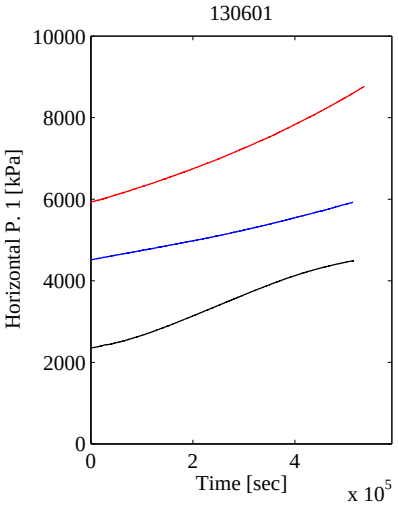

Figure I.7 130601 - Horizontal pressure 1.

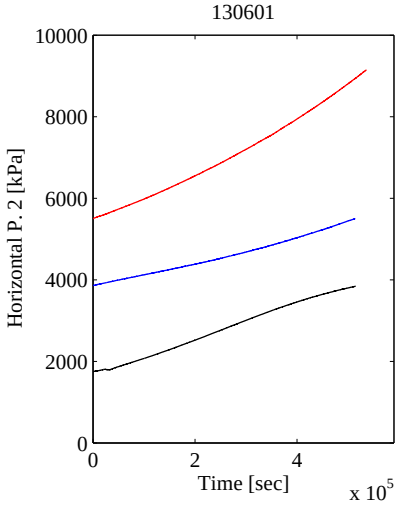

Figure I.8 130601 - Horizontal pressure 2.

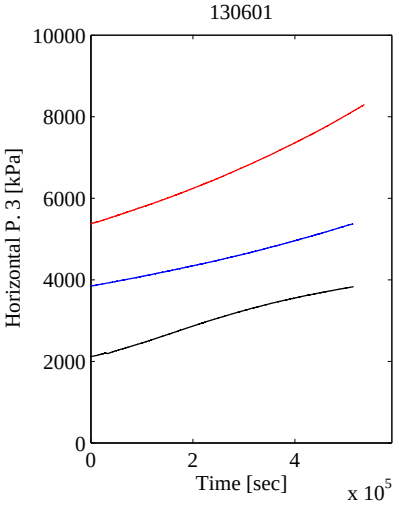

Figure I.9 130601 - Horizontal pressure 3.

Table I.2 Select data from 130601.

σ'_V	σ'_H	ε_V
241.6	1782.3	0.50
501.2	1789.6	0.52
787.8	1880.6	0.99
1084.2	2059.1	1.62
1862.6	2498.2	2.89
3815.2	3358.2	5.42
5052.1	3831.6	7.65
5887.1	4189.0	9.64
7554.7	5119.5	13.61
7711.5	5210.6	13.92
9212.1	6044.0	16.37
12296.4	7871.6	20,14

Laboratory number 130602 - Test 7

Zero point measurements

Table I.3 Zero point measurements for test 7.

Transducer	Zero measurement
Cell pressure	110 kPa
Load cell	57.9 + 20 kg
Pore pressure	-12.5 kPa
Displacement 1	3.488 mm
Displacement 2	3.736 mm
Horizontal pressure 1	485.6 kPa
Horizontal pressure 2	0 kPa
Horizontal pressure 3	362.5 kPa

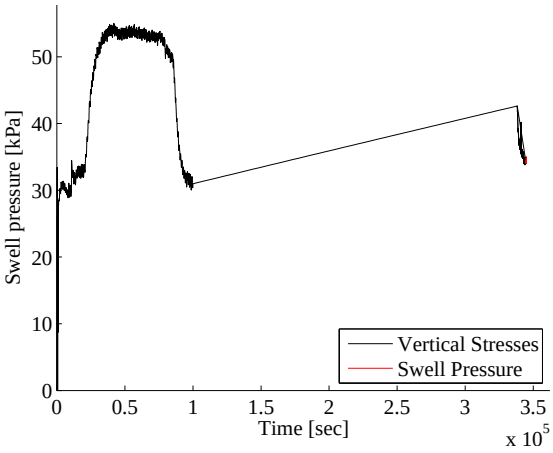

Figure I.10 130602 - Swell pressure.

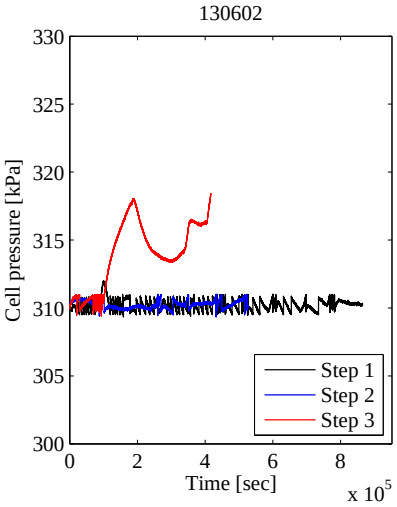

Figure I.11 130602 - Cell pressure.

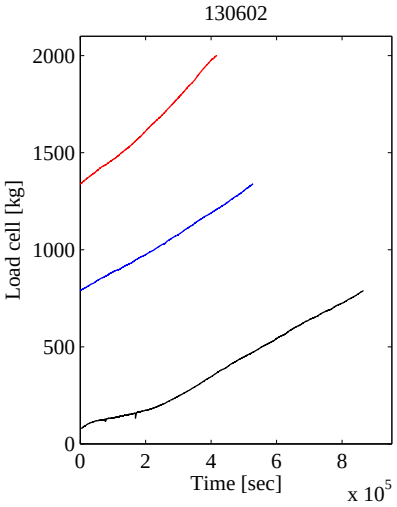

Figure I.12 130602 - Load cell.

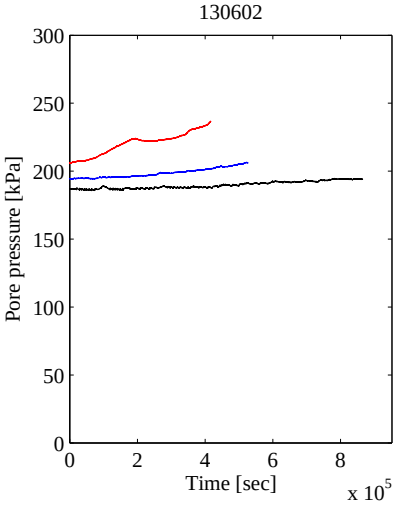

Figure I.13 130602 - Pore pressure.

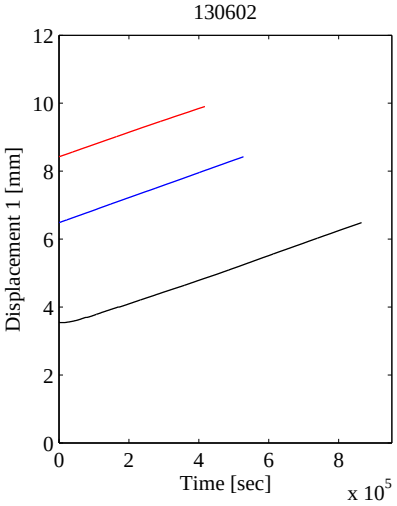

Figure I.14 130602 - Displacement 1.

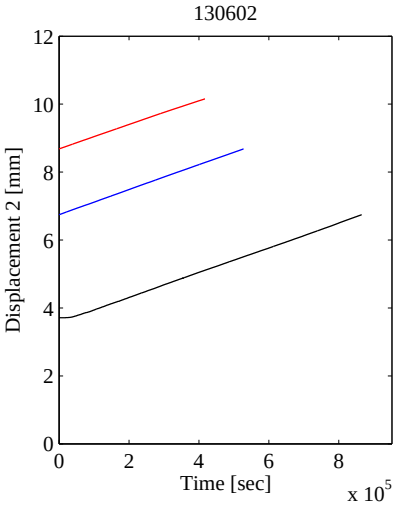

Figure I.15 130602 - Displacement 2.

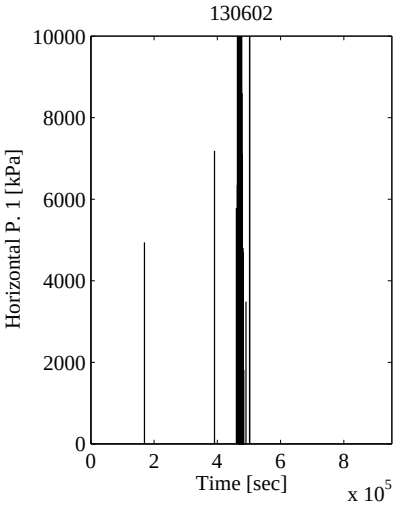

Figure I.16 130602 - Horizontal pressure 1.

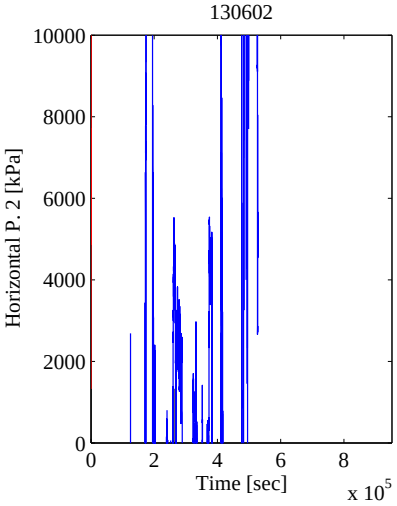

Figure I.17 130602 - Horizontal pressure 2.

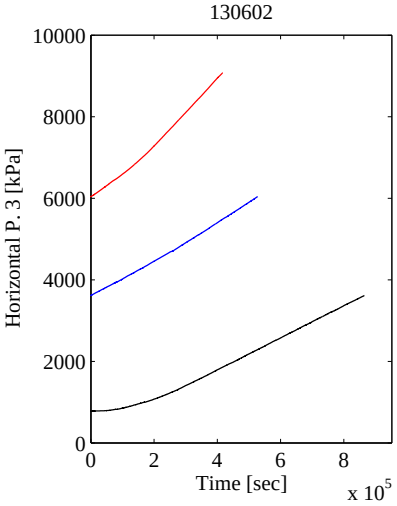

Figure I.18 130602 - Horizontal pressure 3.

Table I.4 Select data from 130602.

σ'_V	σ'_H	ε_V
57.1	220.3	0.05
185.0	221.5	0.06
448.1	236.9	0.33
614.5	311.7	0.94
803.5	422.1	1.54
1052.0	558.6	2.17
1881.8	905.5	3.36
3119.7	1362.4	4.75
5868.5	2476.1	8.19
7259.3	3048.0	10.00
8242.6	3451.2	11.23
9681.9	4111.1	13.08
12763.7	5427.5	16.37
14142.4	6012.2	17.67
16835.5	7268.8	19.70
19592.4	8480.7	21.38

Laboratory number 130603 - Test 5

Zero point measurements

Table I.5 Zero point measurements for test 5.

Transducer	Zero measurement
Cell pressure	108 kPa
Load cell	58.2 + 20 kg
Pore pressure	-18.4 kPa
Displacement 1	2.498 mm
Displacement 2	2.566 mm
Horizontal pressure 1	0 kPa
Horizontal pressure 2	0 kPa
Horizontal pressure 3	0 kPa

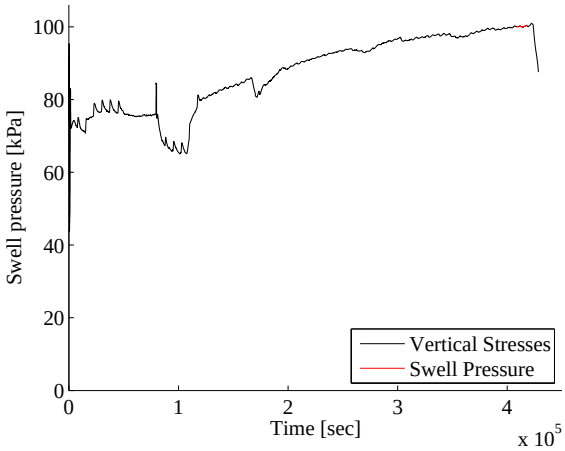

Figure I.19 130603 - Swell pressure.

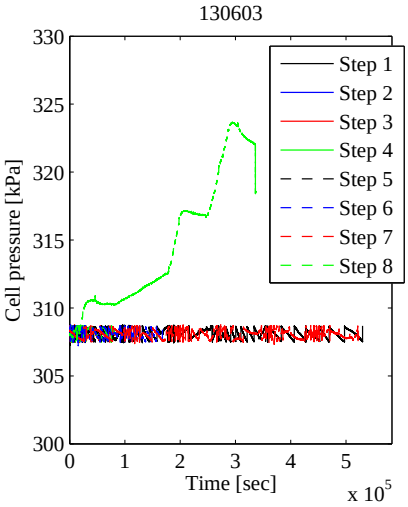

Figure I.20 130603 - Cell pressure.

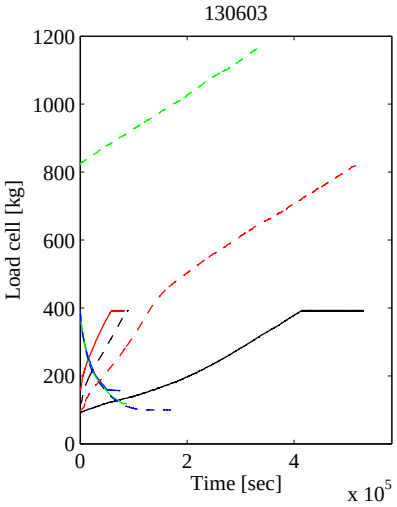

Figure I.21 130603 - Load cell.

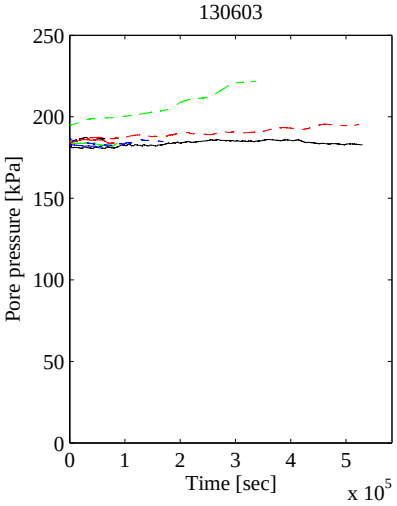

Figure I.22 130603 - Pore pressure.

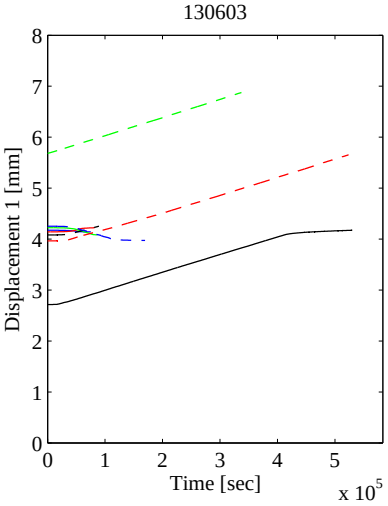

Figure I.23 130603 - Displacement 1.

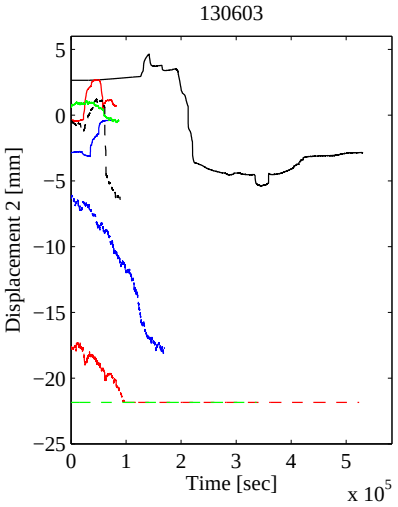

Figure I.24 130603 - Displacement 2.

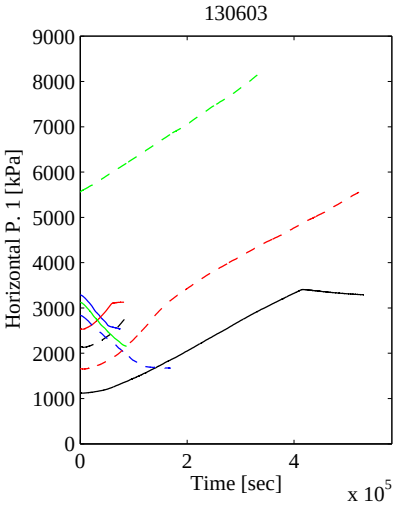

Figure I.25 130603 - Horizontal pressure 1.

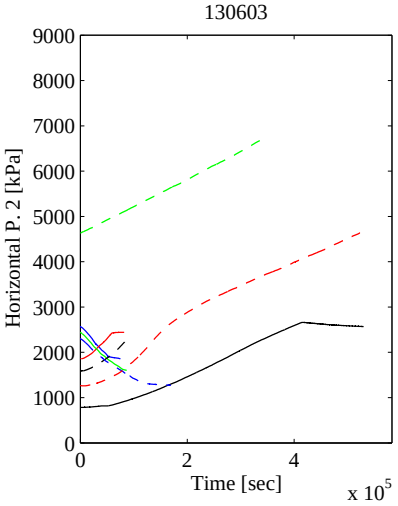

Figure I.26 130603 - Horizontal pressure 2.

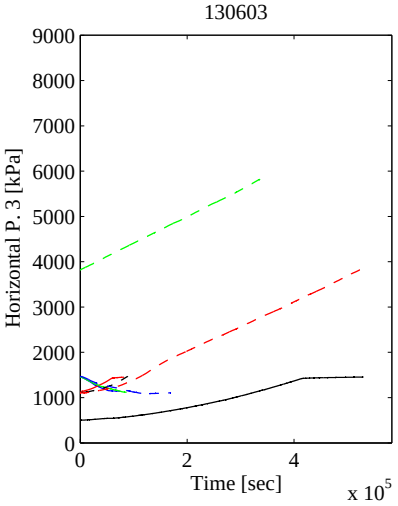

Figure I.27 130603 - Horizontal pressure 3.

Table I.6 Select data from 130603. step 1-4.

σ'_V	σ'_H	ε_V
96.7	898.2	0.73
189.6	905.7	0.73
406.3	973.2	1.07
612.1	1189.3	1.66
1195.2	1774.1	2.84
836.2	3003.3	4.92
3189.5	3153.7	5.54
2091.7	3035.9	5.59
1565.0	2882.1	5.58
1004.6	2561.1	5.56
791.7	2327.8	5.48
1233.8	2327.2	5.48
1495.4	2354.0	5.48
2631.0	2671.4	5.52
3190.2	2994.1	5.75
2036.5	2892.5	5.75
1173.8	2590.8	5.74
762.1	2335.9	5.64
548.3	2174.6	5.47
398.0	2007.2	5.29

Table I.7 Select data from 130603. step 5-8.

σ'_V	σ'_H	ε_V
666.8	1989.5	5.28
1571.4	2103.0	5.3
2218.7	2298.5	5.49
2844.6	2572.5	5.7
3188.2	2780.7	5.84
2447.2	2751.1	5.85
2037.9	2697.5	5.84
1151.0	2437.3	5.83
733.9	2229.3	5.72
459.9	2048.4	5.49
296.6	1858.4	5.27
206.2	1606.7	4.92
254.8	1588.5	4.89
745.7	1619.6	4.9
1340.4	1774.6	5.12
1964.2	2033.0	5.43
2418.3	2262.0	5.63
3642.8	2994.5	6.16
4895.4	3970.2	7.29
7397.4	5833.7	10.24
8141.5	6421.0	11.19
9644.5	7682.2	12.94
11093.8	8933.0	14.59

Laboratory number 130604 - Test 8

Zero point measurements

Table I.8 Zero point measurements for test 8.

Transducer	Zero measurement
Cell pressure	108 kPa
Load cell	58.2 + 20 kg
Pore pressure	-20 kPa
Displacement 1	1.622 mm
Displacement 2	1.155 mm
Horizontal pressure 1	0 kPa
Horizontal pressure 2	-101 kPa
Horizontal pressure 3	-8 kPa

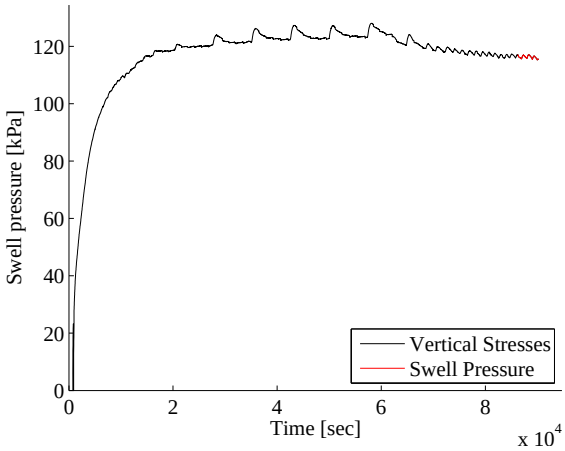

Figure I.28 130604 - Swell pressure.

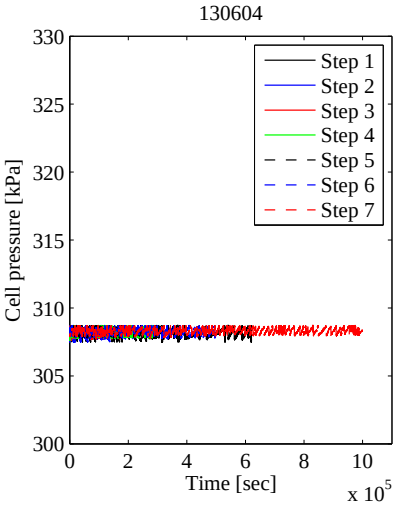

Figure I.29 130604 - Cell pressure.

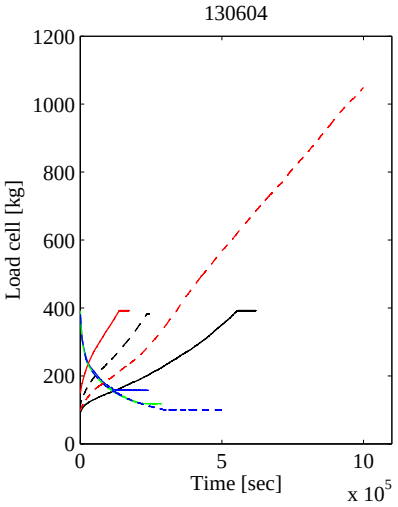

Figure I.30 130604 - Load cell.

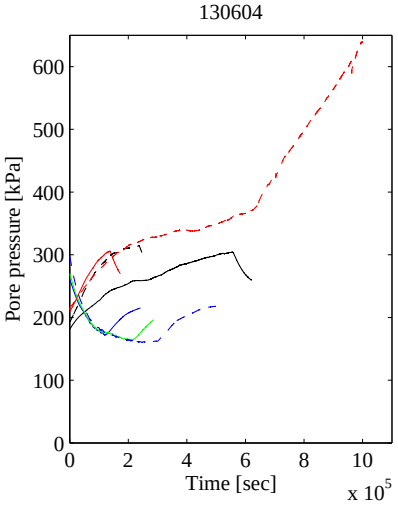

Figure I.31 130604 - Pore pressure.

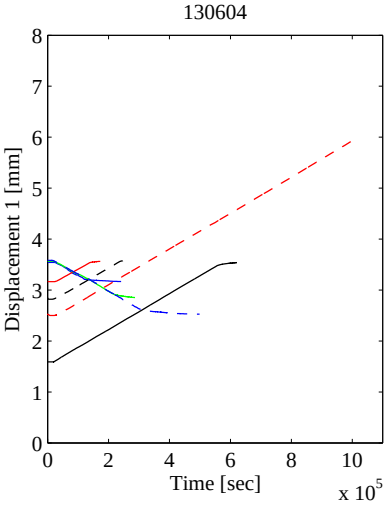

Figure I.32 130604 - Displacement 1.

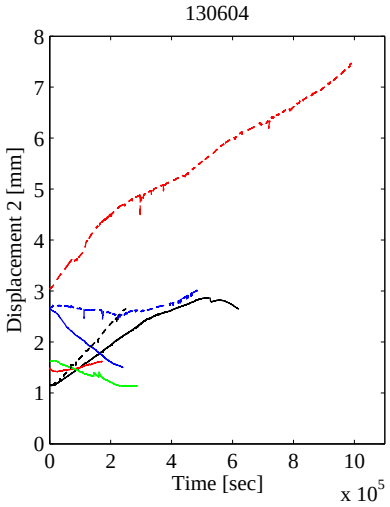

Figure I.33 130604 - Displacement 2.

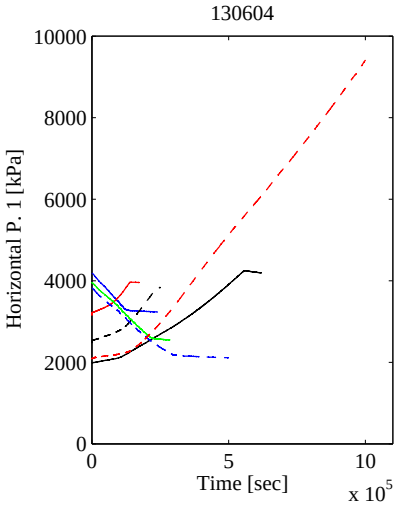

Figure I.34 130604 - Horizontal pressure 1.

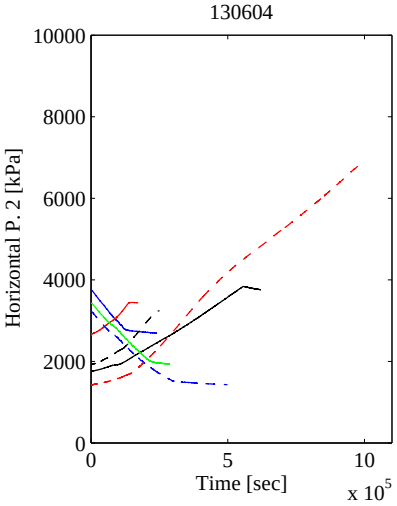

Figure I.35 130604 - Horizontal pressure 2.

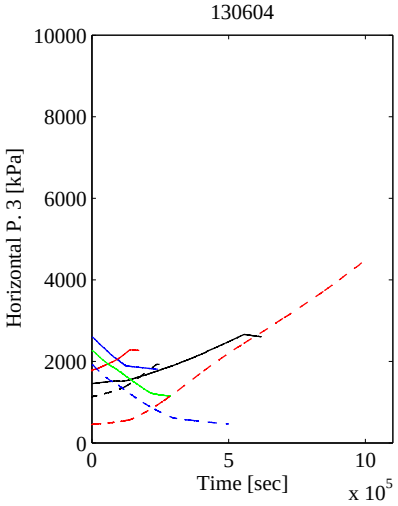

Figure I.36 130604 - Horizontal pressure 3.

Table I.9 Select data from 130604. step 1-4.

σ'_V	σ'_H	ε_V
112.0	2128.4	-0.11
273.4	2137.7	-0.11
504.7	2191.7	0.25
680.1	2258.4	0.85
1033.8	2653.1	2.00
2011.1	3606.9	4.35
3136.7	4489.4	6.39
3111.9	4486.3	7.17
2479.0	4461.8	7.18
1773.7	4320.7	7.17
1334.8	4064.6	6.94
921.9	3629.4	6.33
770.8	3291.3	5.93
762.0	3264.9	5.15
910.9	3280.1	5.14
1365.7	3316.4	5.14
1933.4	3431.3	5.40
2601.3	3719.2	5.95
3130.3	4110.4	6.47
3127.3	4109.7	7.25
1704.1	3962.6	7.25
1370.1	3807.1	7.08
853.1	3370.9	6.40
515.8	2755.8	5.53
402.9	2463.6	5.03
385.0	2395.9	4.88

Table I.10 Select data from 130604. step 5-7.

σ'_V	σ'_H	ε_V
373.1	2381.4	4.11
595.6	2393.2	3.99
1159.7	2488.4	4.31
1322.6	2543.7	4.52
1559.3	2651.9	4.87
2337.1	3255.5	5.80
3008.7	3825.6	6.52
3005.3	3824.8	7.31
2087.3	3758.4	7.31
1592.3	3631.8	7.23
1254.6	3441.4	6.97
875.4	3129.1	6.43
448.9	2379.6	5.30
202.3	1802.1	3.96
181.7	1704.9	3.79
196.9	1694.3	3.02
261.9	1701.8	2.96
589.3	1719.0	2.97
768.1	1737.9	3.18
1013.7	1789.7	3.63
1364.7	1933.3	4.34
1671.6	2256.2	4.94
2629.6	3107.8	6.11
4862.8	4979.0	8.44
7253.0	6908.5	11.38
9587.7	9029.8	14.37

Laboratory number 130605 - Test 9

Zero point measurements

Table I.11 Zero point measurements for test 9.

Transducer	Zero measurement
Cell pressure	111 kPa
Load cell	55.8 + 20 kg
Pore pressure	-20 kPa
Displacement 1	3.921 mm
Displacement 2	3.669 mm
Horizontal pressure 1	0 kPa
Horizontal pressure 2	0 kPa
Horizontal pressure 3	0 kPa

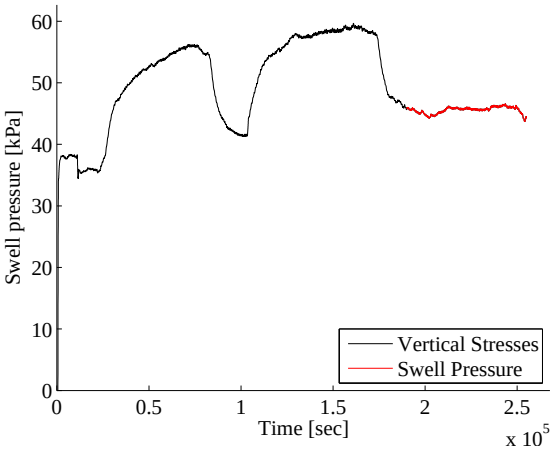

Figure I.37 130605 - Swell pressure.

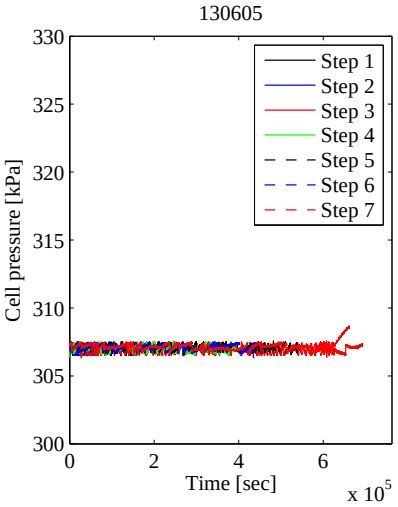

Figure I.38 130605 - Cell pressure.

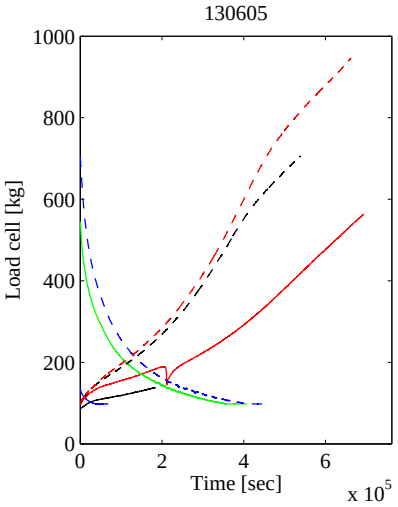

Figure I.39 130605 - Load cell.

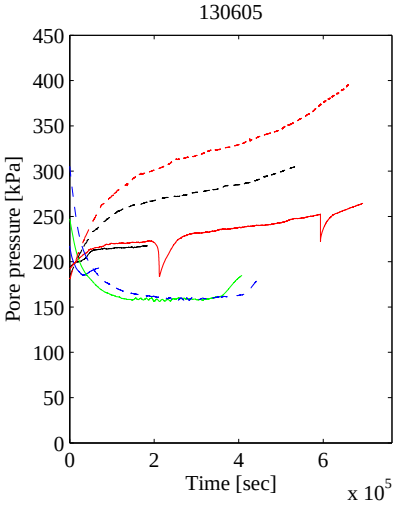

Figure I.40 130605 - Pore pressure.

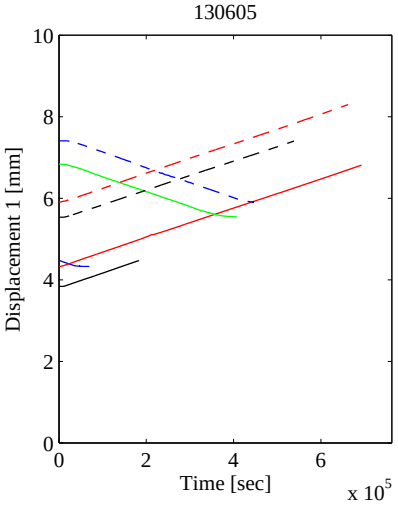

Figure I.41 130605 - Displacement 1.

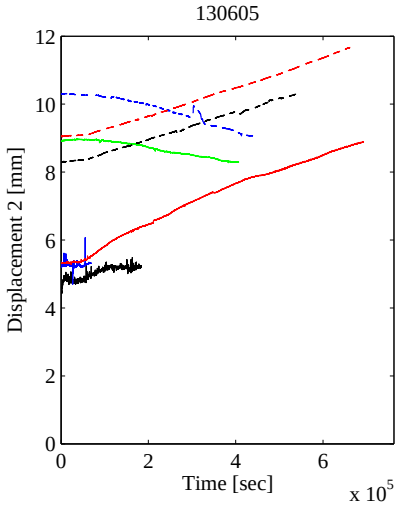

Figure I.42 130605 - Displacement 2.

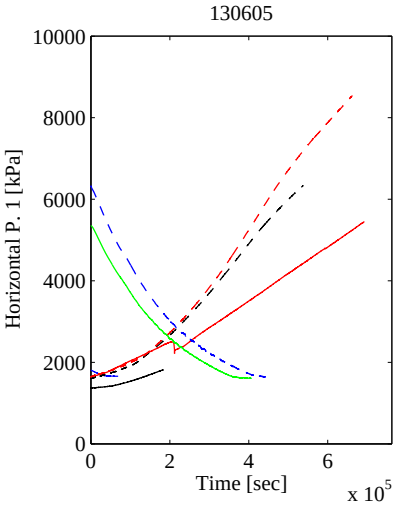

Figure I.43 130605 - Horizontal pressure 1.

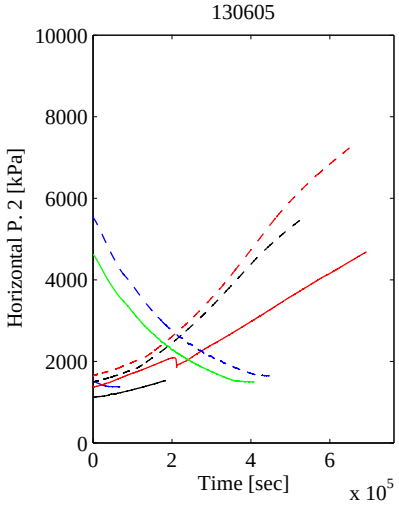

Figure I.44 130605 - Horizontal pressure 2.

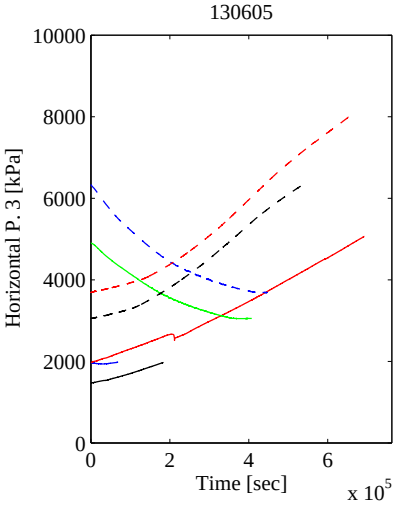

Figure I.45 130605 - Horizontal pressure 3.

Table I.12 Select data from 130605. step 1-4.

σ'_V	σ'_H	ε_V
78.4	1120.0	-0.27
178.1	1130.9	-0.27
290.0	1154.9	-0.04
373.8	1224.9	0.44
427.5	1301.8	0.81
516.3	1421.7	1.31
621.3	1558.8	1.83
461.0	1543.0	1.80
394.6	1530.7	1.73
280.4	1493.1	1.54
231.0	1473.4	1.35
295.5	1477.8	1.37
360.9	1487.2	1.42
534.2	1541.0	1.66
795.5	1801.0	2.53
1536.6	2568.2	5.05
2879.1	3564.4	7.06
4927.6	4824.4	9.64
3643.4	4631.5	9.71
2230.6	4072.2	9.34
1415.5	3516.3	8.69
72.7	2633.2	7.47
238.6	1864.5	5.43

Table I.13 Select data from 130605. step 5-7.

σ'_V	σ'_H	ε_V
410.8	1878.3	5.39
786.2	1954.0	5.82
1101.6	2094.5	6.39
1924.7	2728.2	7.59
3964.8	4099.8	9.38
5669.7	5274.7	10.79
6349.0	5802.4	11.60
4932.8	5662.9	11.63
2932.4	4980.2	11.34
1855.4	4313.7	10.73
906.9	3240.5	9.43
428.7	2509.3	7.97
239.9	2136.9	6.62
404.6	2158.4	6.68
805.3	2234.1	7.13
1179.4	2381.9	7.74
2063.2	2967.7	8.98
5250.0	5026.5	11.38
6973.9	6200.3	12.58
8751.1	7649.8	14.59

Laboratory number 130606 - Test 10

Zero point measurements

Table I.14 Zero point measurements for test 10.

Transducer	Zero measurement
Cell pressure	107 kPa
Load cell	54.1 + 20 kg
Pore pressure	-15 kPa
Displacement 1	2.873 mm
Displacement 2	1.709 mm
Horizontal pressure 1	0 kPa
Horizontal pressure 2	0 kPa
Horizontal pressure 3	0 kPa

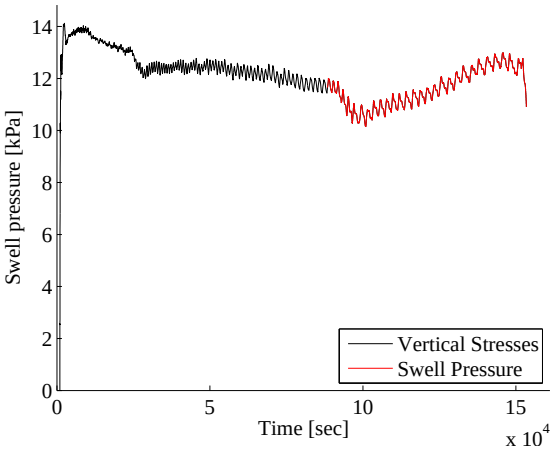

Figure I.46 130606 - Swell pressure.

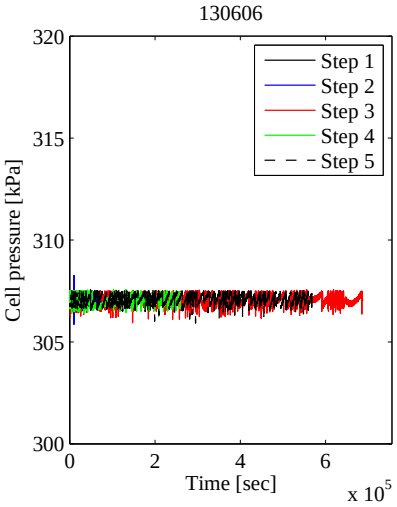

Figure I.47 130606 - Cell pressure.

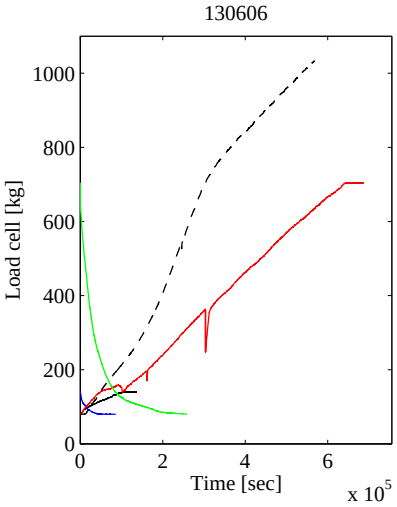

Figure I.48 130606 - Load cell.

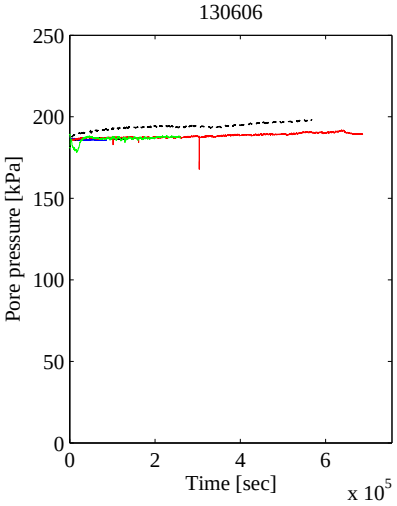

Figure I.49 130606 - Pore pressure.

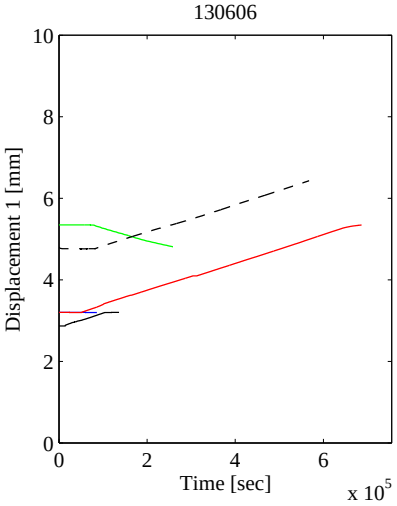

Figure I.50 130606 - Displacement 1.

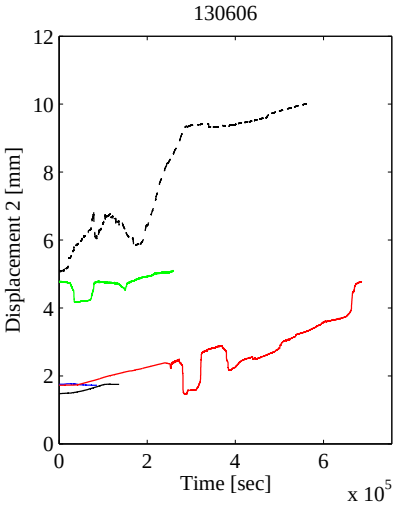

Figure I.51 130606 - Displacement 2.

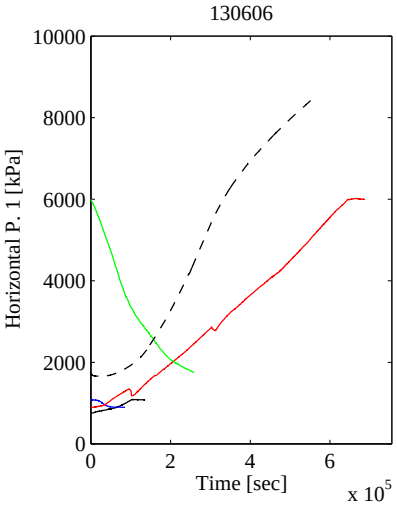

Figure I.52 130606 - Horizontal pressure 1.

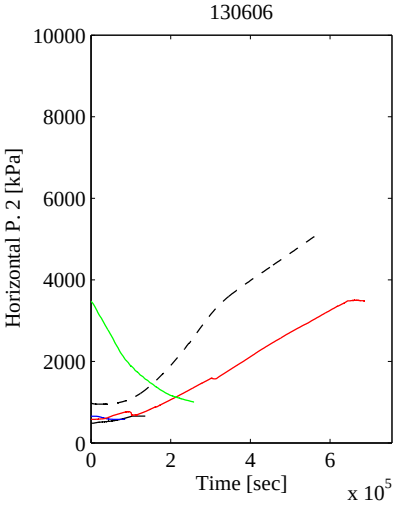

Figure I.53 130606 - Horizontal pressure 2.

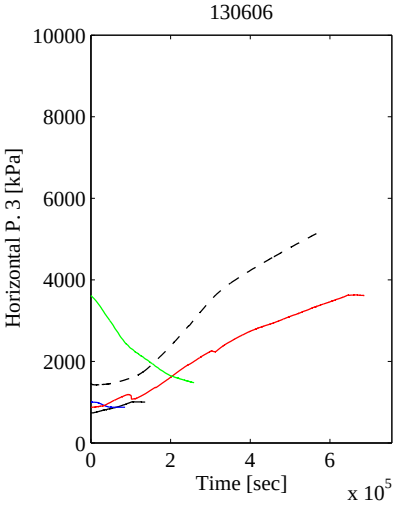

Figure I.54 130606 - Horizontal pressure 3.

Table I.15 Select data from 130606. step 1-3.

σ'_V	σ'_H	ε_V
65.3	458.9	-0.02
195.0	470.6	-0.02
327.1	511.0	0.26
470.9	564.4	0.55
676.2	711.5	1.09
417.6	709.0	1.10
190.1	691.9	1.10
83.2	608.5	1.10
65.5	582.5	1.09
208.9	586.4	1.09
467.2	612.2	1.09
688.8	702.4	1.09
807.2	843.8	1.45
1967.6	1492.3	3.16
3873.8	2575.7	5.00
5449.4	3495.5	6.75
6440.4	4164.0	8.24

Table I.16 Select data from 130606. step 4-5.

σ'_V	σ'_H	ε_V
5060.2	4096.5	8.25
3345.6	3832.5	8.25
1538.2	3247.7	8.25
761.5	2634.7	8.23
530.9	2323.3	7.97
289.9	1828.0	7.45
115.0	1425.2	6.93
65.8	1207.0	6.46
66.6	1145.1	6.30
219.2	1143.7	6.30
685.5	1164.2	6.30
1413.9	1328.6	6.53
2221.9	1714.8	7.11
3395.7	2306.3	7.67
4875.6	3006.6	8.19
6362.3	3799.0	8.72
7830.3	4844.6	9.89
8779.9	5450.9	10.82
9794.0	6061.5	11.86

APPENDIX J
Undrained triaxial tests

This appendix contains data from the undrained triaxial tests. Each test was first saturated by applying a back pressure of 200 kPa. After saturation, all samples were re-consolidated to the lower bound of the preconsolidation stresses (as physical limitations of the triaxial apparatus hindered reaching the upper bound of the preconsolidation stresses). Hereafter, the stresses in the sample were taken to the stress level from where the shearing step was planned to start (listed in Table J.1). Samples were an-iostropic consolidated whenever the apparatus would allow it. Finally, the samples were taken to failure by undrained compression. For each consolidation step, the axial and volumetric strains, pore pressure, horizontal and vertical stresses are graphically presented. For each shearing step, the cell pressure, pistol force, pore pressure and axial deformation are graphically presented, and the total deviatoric and mean stresses along with excess pore pressure and axial strain are listed in the following table.

Table J.1 Load programme for undrained shear triaxial test.

Laboratory number	Test number	σ'_{shear}	shear state
130607	1	300	in situ
130608	2	210	in situ
130609	3	370	in situ
130610	4	525	in situ
130611	5	375	OCR=2
130612	6	750	OCR=1
130613	7	1125	$1.5\times\sigma'_{pc}$

Laboratory number 130607 - Test 1

Re-consolidation step

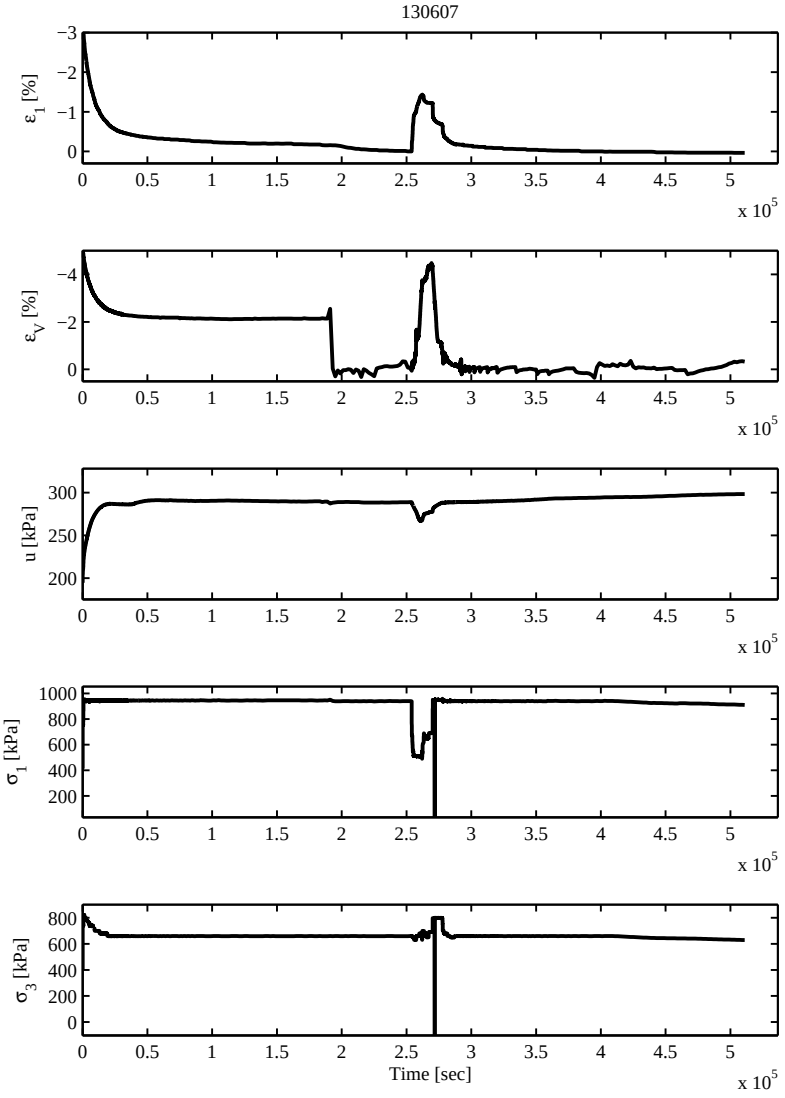

Figure J.1 Re-consolidation test 1.

Step to shearing stresses

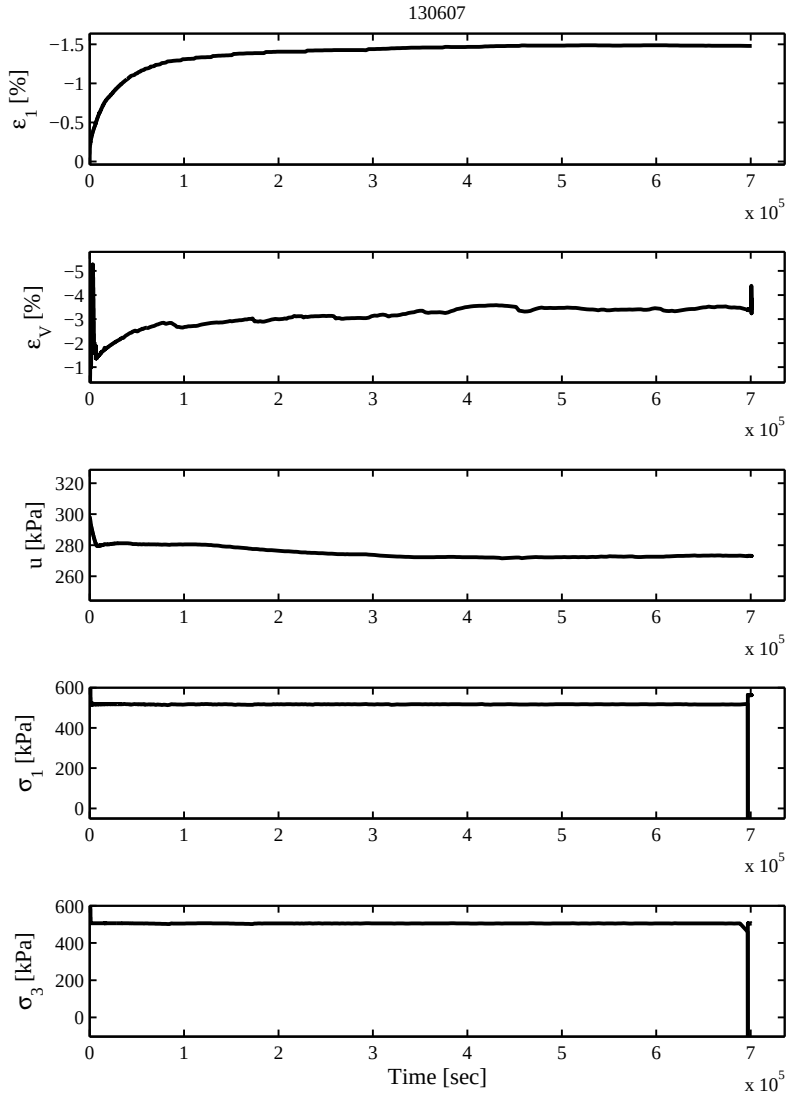

Figure J.2 To shearing stresses test 1.

Shearing step

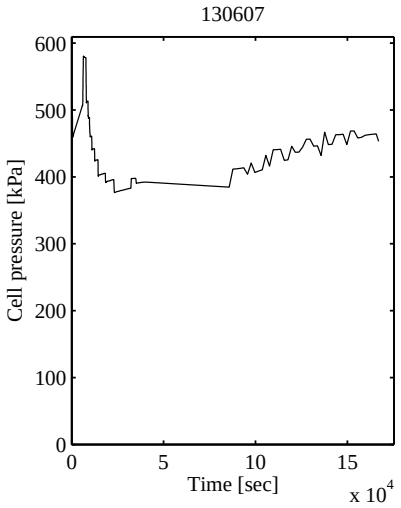

Figure J.3 130607 - Cell pressure.

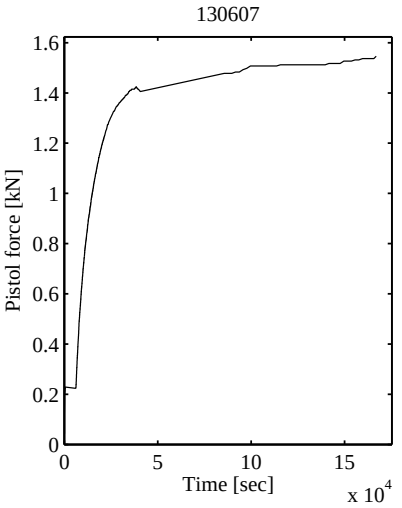

Figure J.4 130607 - Pistol force.

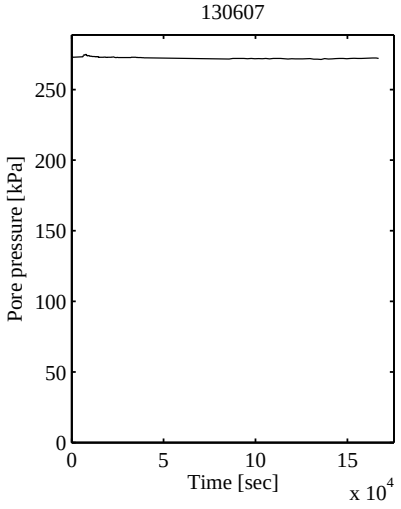

Figure J.5 130607 - Pore pressure.

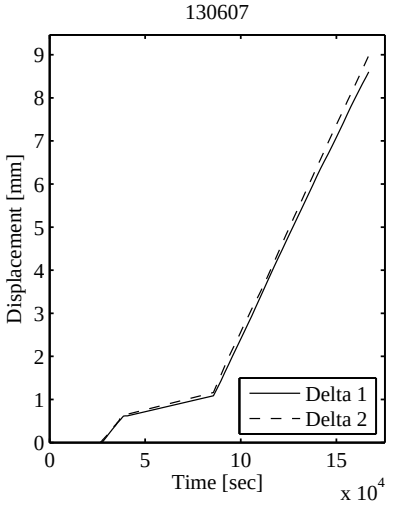

Figure J.6 130607 - Displacements.

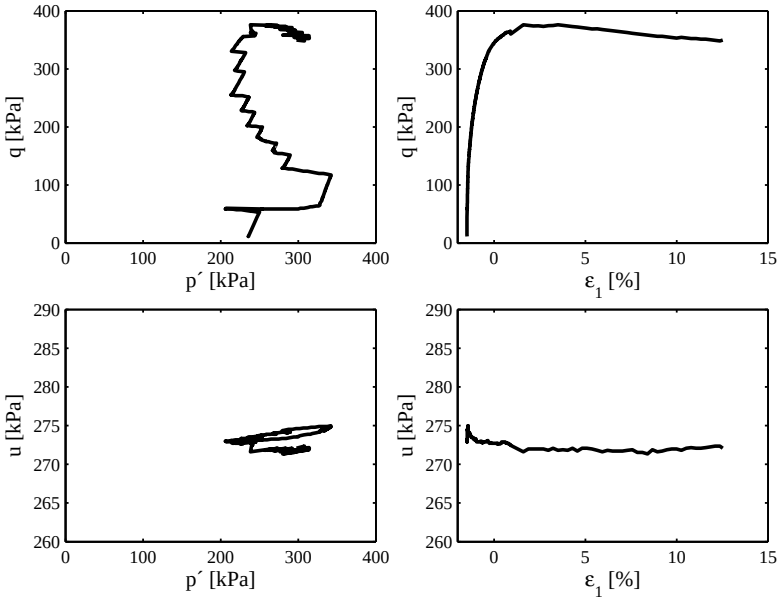

Figure J.7 Shearing step test 1.

Table J.2 Data triaxial test 1.

q [kPa]	p [kPa]	u [kPa]	ε_1 [%]	q [kPa]	p [kPa]	u [kPa]	ε_1 [%]
11.5	509.0	273.2	-1.48	260.3	489.3	272.9	-0.95
58.8	526.5	273.2	-1.47	270.3	493.4	272.9	-0.88
77.9	605.7	274.5	-1.46	293.8	503.2	273.0	-0.70
109.8	614.9	274.7	-1.44	313.5	498.5	272.9	-0.51
137.8	558.4	274.1	-1.41	349.2	497.1	272.7	0.14
159.4	540.9	274.0	-1.35	365.2	513.7	272.5	0.89
179.7	525.9	273.7	-1.30	376.2	510.0	271.6	1.60
196.1	526.2	273.6	-1.24	372.1	540.1	271.7	4.55
212.5	512.4	273.4	-1.18	361.5	577.0	271.9	7.57
225.1	517.1	273.4	-1.13	353.3	586.4	272.1	10.53
237.7	504.2	273.2	-1.07	349.8	569.8	272.1	12.53
249.0	508.7	273.2	-1.01				

Laboratory number 130608 - Test 2

Re-consolidation step

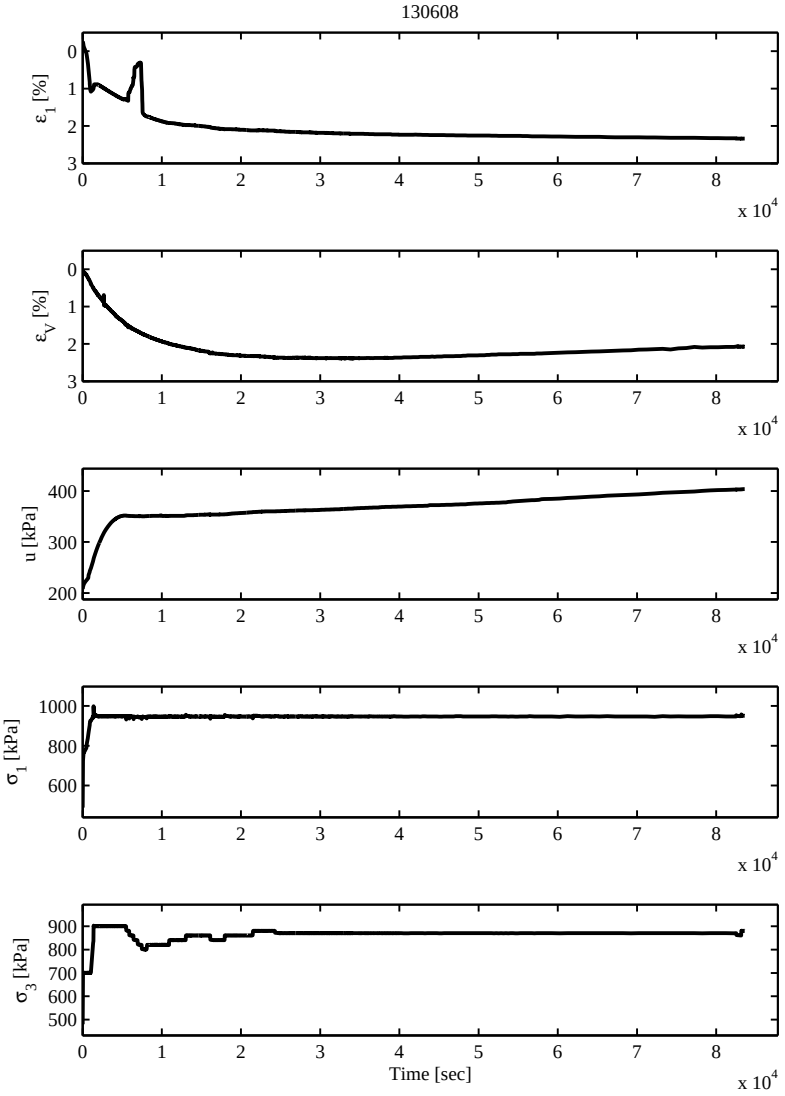

Figure J.8 Re-consolidation test 2.

Step to shearing stresses

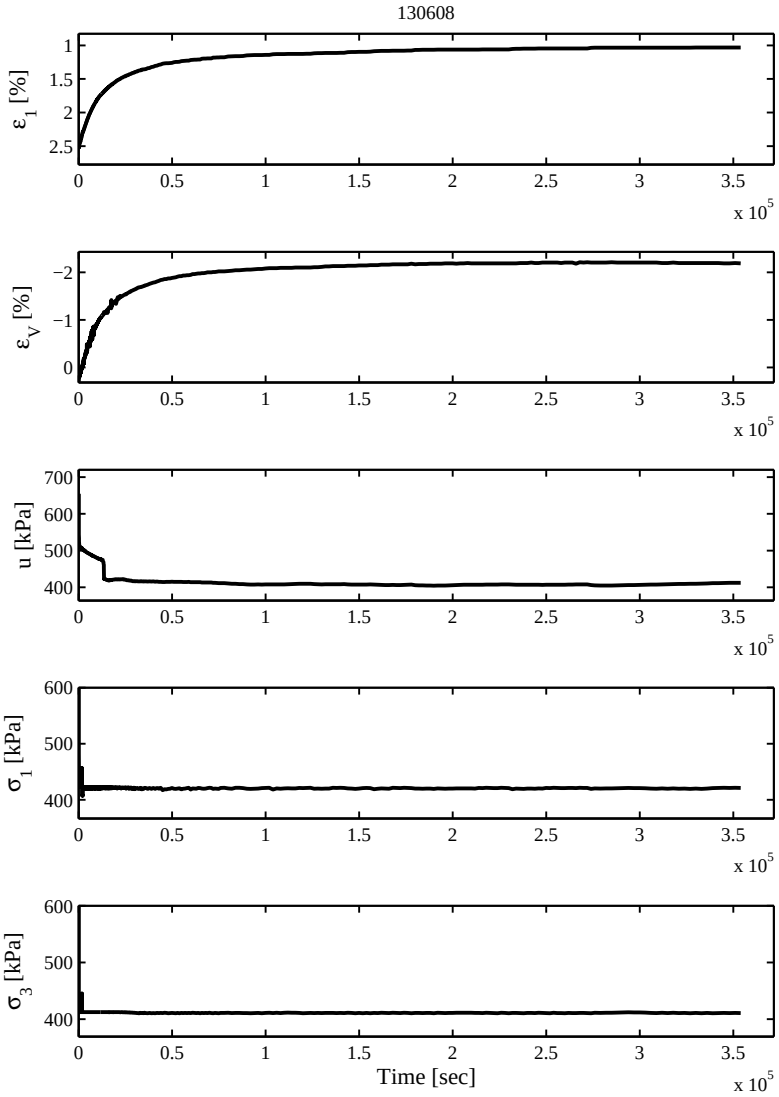

Figure J.9 To shearing stresses test 2.

Shearing step

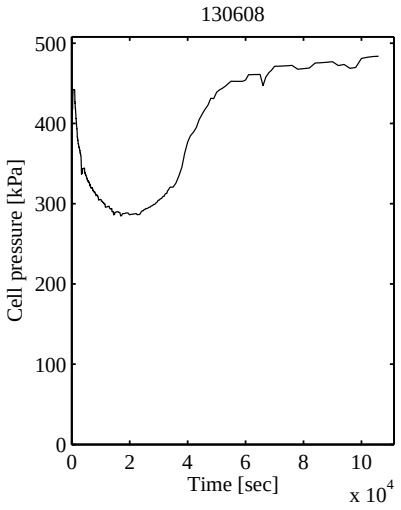

Figure J.10 130608 - Cell pressure.

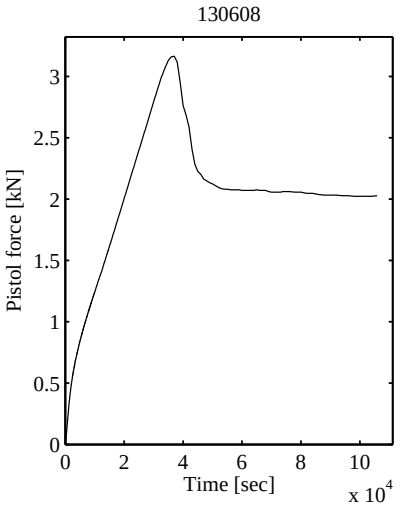

Figure J.11 130608 - Pistol force.

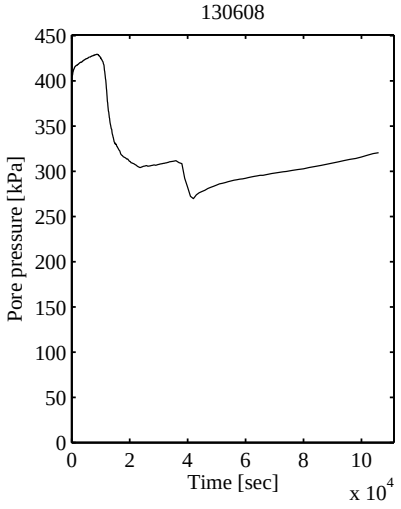

Figure J.12 130608 - Pore pressure.

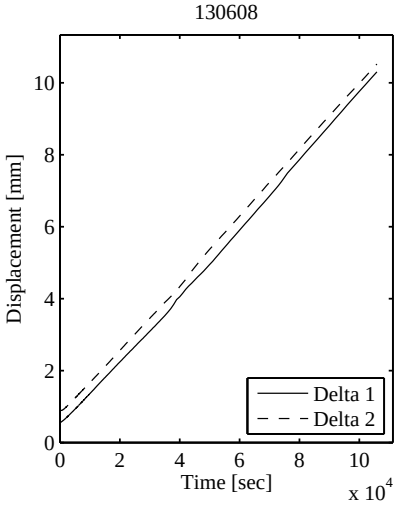

Figure J.13 130608 - Displacements.

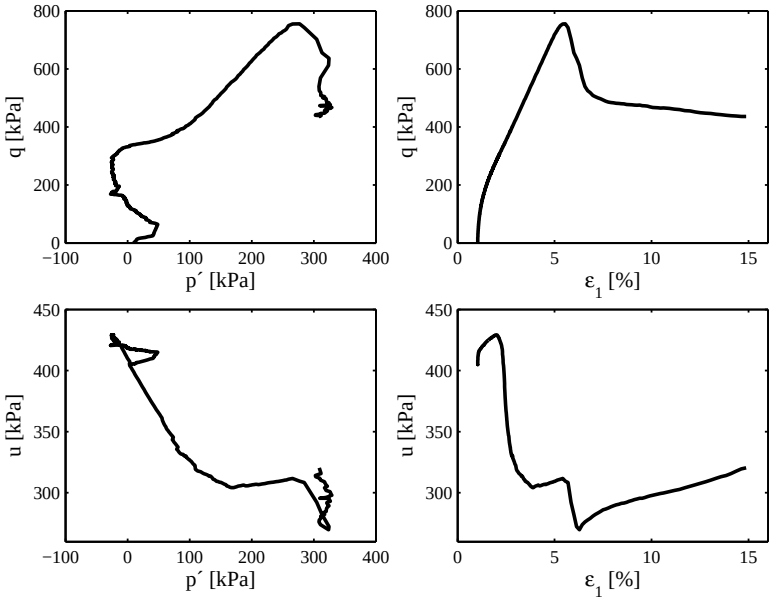

Figure J.14 Shearing step test 2.

Table J.3 Data triaxial test 2.

q [kPa]	p [kPa]	u [kPa]	ε_1 [%]	q [kPa]	p [kPa]	u [kPa]	ε_1 [%]
-3.6	409.3	405.1	1.04	695.4	540.0	308.5	4.83
52.3	459.6	413.5	1.07	701.0	543.0	308.7	4.87
103.2	433.0	416.9	1.15	720.9	553.3	309.4	5.02
187.7	406.7	422.6	1.43	755.1	586.6	309.5	5.55
208.0	405.1	424.3	1.53	742.4	593.1	308.4	5.70
227.2	402.9	425.5	1.63	612.4	593.4	269.7	6.28
274.6	403.4	428.8	1.94	486.0	608.5	287.6	7.77
304.1	406.7	426.2	2.14	469.1	623.0	297.4	9.92
388.3	415.7	334.9	2.73	449.1	626.0	307.8	12.52
503.6	454.8	309.2	3.53	436.0	629.2	320.5	14.87
603.6	495.6	305.7	4.20				

Laboratory number 130609 - Test 3

Re-consolidation step

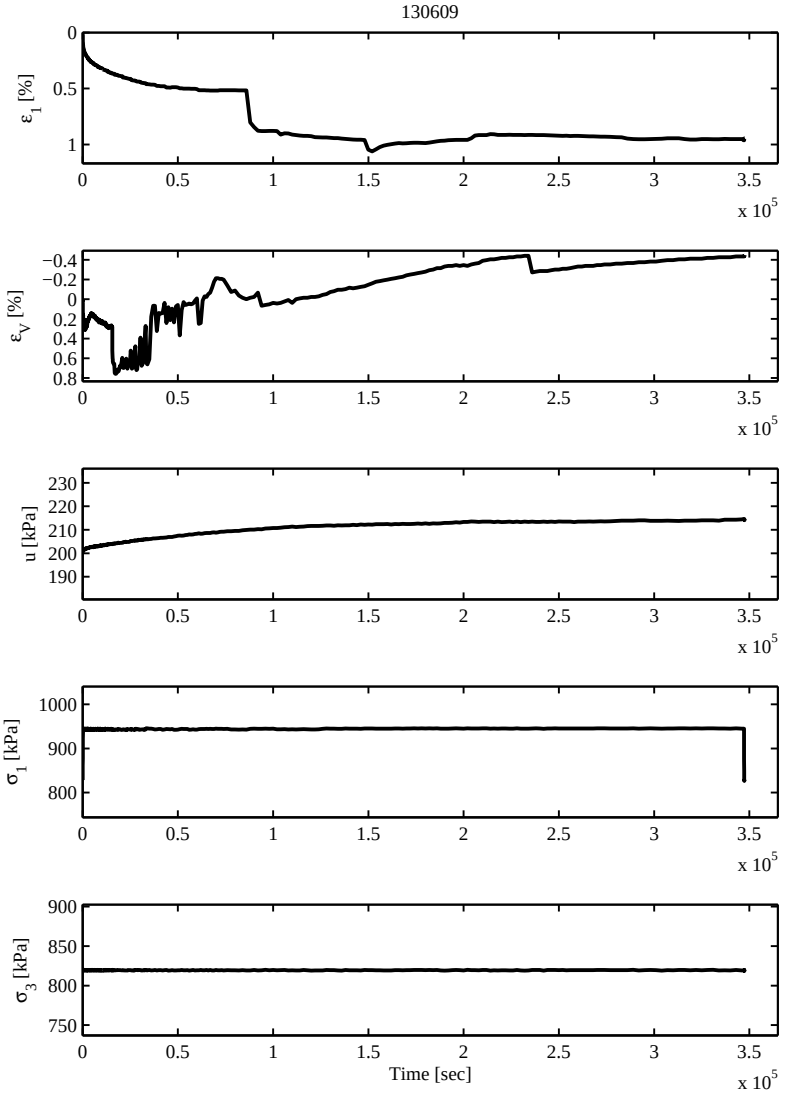

Figure J.15 Re-consolidation test 3.

Step to shearing stresses

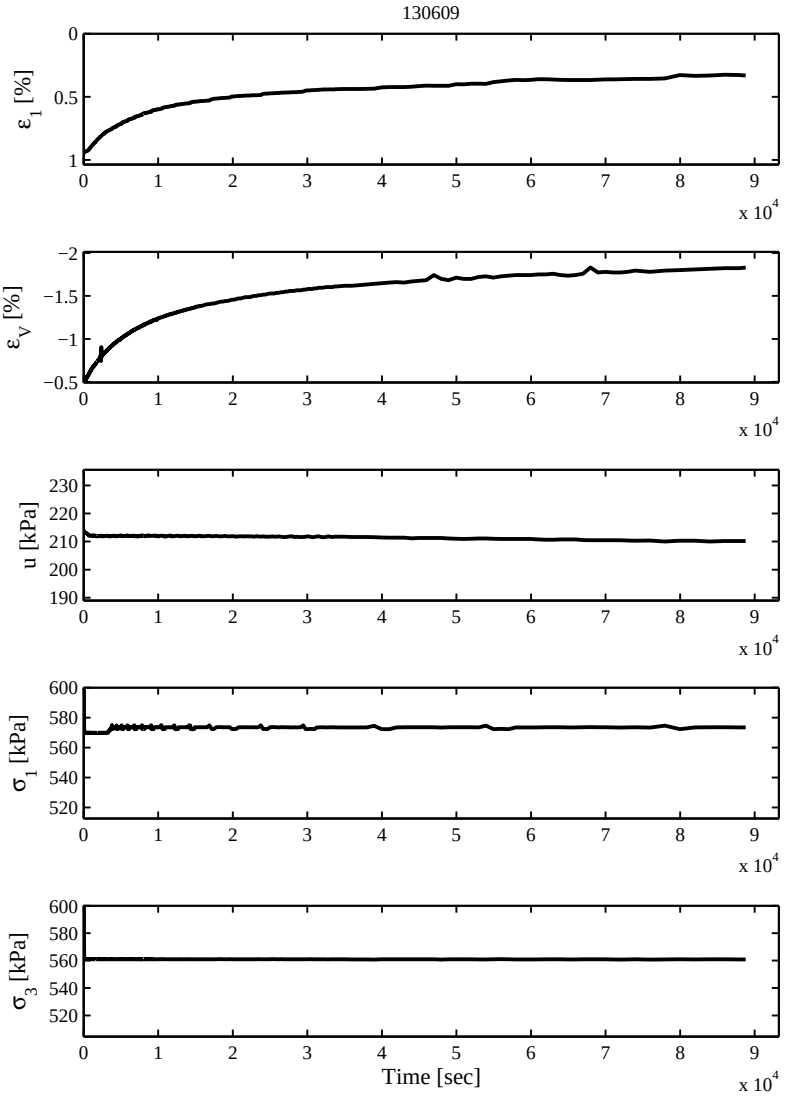

Figure J.16 To shearing stresses test 3.

Shearing step

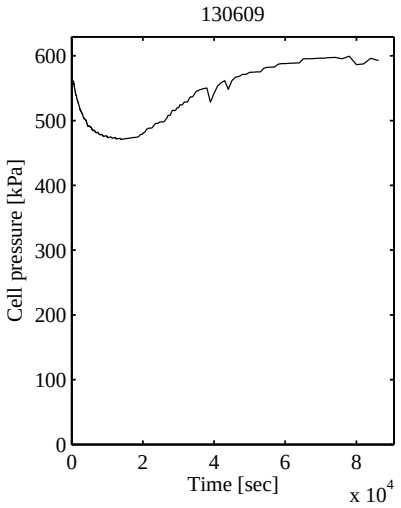

Figure J.17 130609 - Cell pressure.

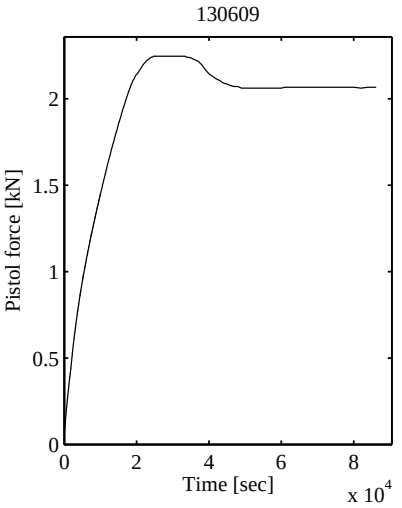

Figure J.18 130609 - Pistol force.

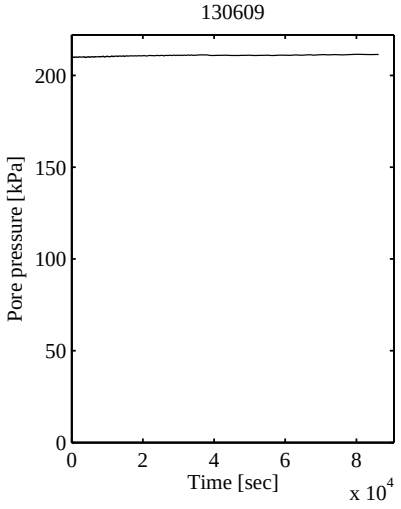

Figure J.19 130609 - Pore pressure.

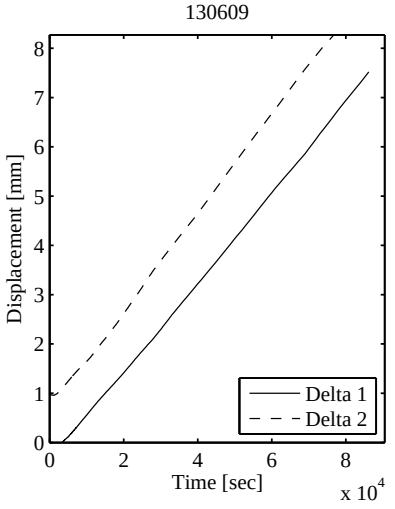

Figure J.20 130609 - Displacements.

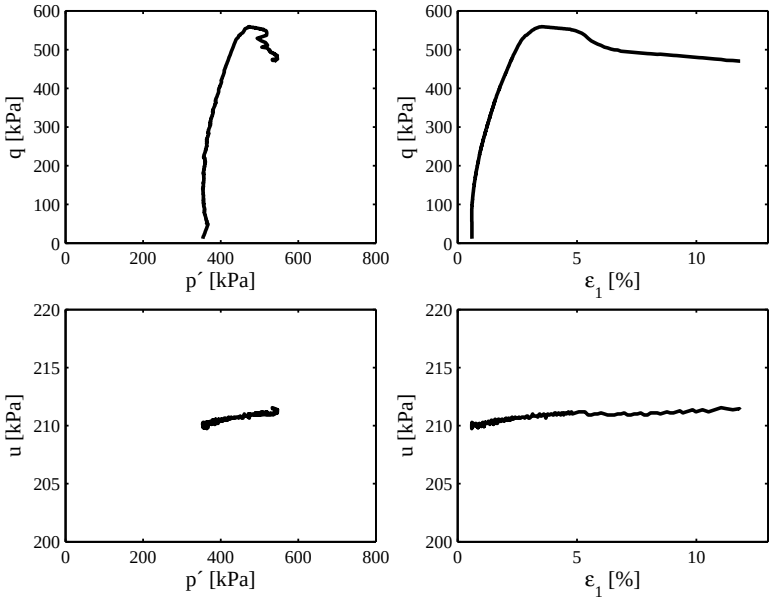

Figure J.21 Shearing step test 3.

Table J.4 Data triaxial test 3.

q [kPa]	p [kPa]	u [kPa]	ε_1 [%]	q [kPa]	p [kPa]	u [kPa]	ε_1 [%]
11.3	563.8	210.1	0.61	458.2	624.0	210.6	2.15
64.9	571.9	210.0	0.60	513.7	645.2	210.7	2.57
104.9	565.5	210.0	0.62	539.8	661.5	210.8	2.93
145.9	565.6	210.0	0.68	553.9	673.4	210.8	3.23
181.9	566.4	210.2	0.77	559.5	684.3	210.8	3.52
211.6	568.8	209.8	0.87	559.3	684.3	210.9	3.57
238.8	570.7	210.0	0.96	559.0	684.1	211.0	3.61
263.4	574.9	210.3	1.06	557.1	693.8	211.0	3.94
285.4	577.7	210.3	1.16	554.5	709.0	211.1	4.40
307.4	583.5	210.3	1.26	522.6	715.8	210.9	5.60
326.9	587.2	210.2	1.36	490.7	746.1	210.9	7.81
346.4	591.2	210.2	1.45	480.3	757.1	211.2	9.98
364.6	598.0	210.5	1.55	470.4	749.9	211.4	11.83
411.6	610.9	210.4	1.83				

Laboratory number 130610 - Test 4

Re-consolidation step

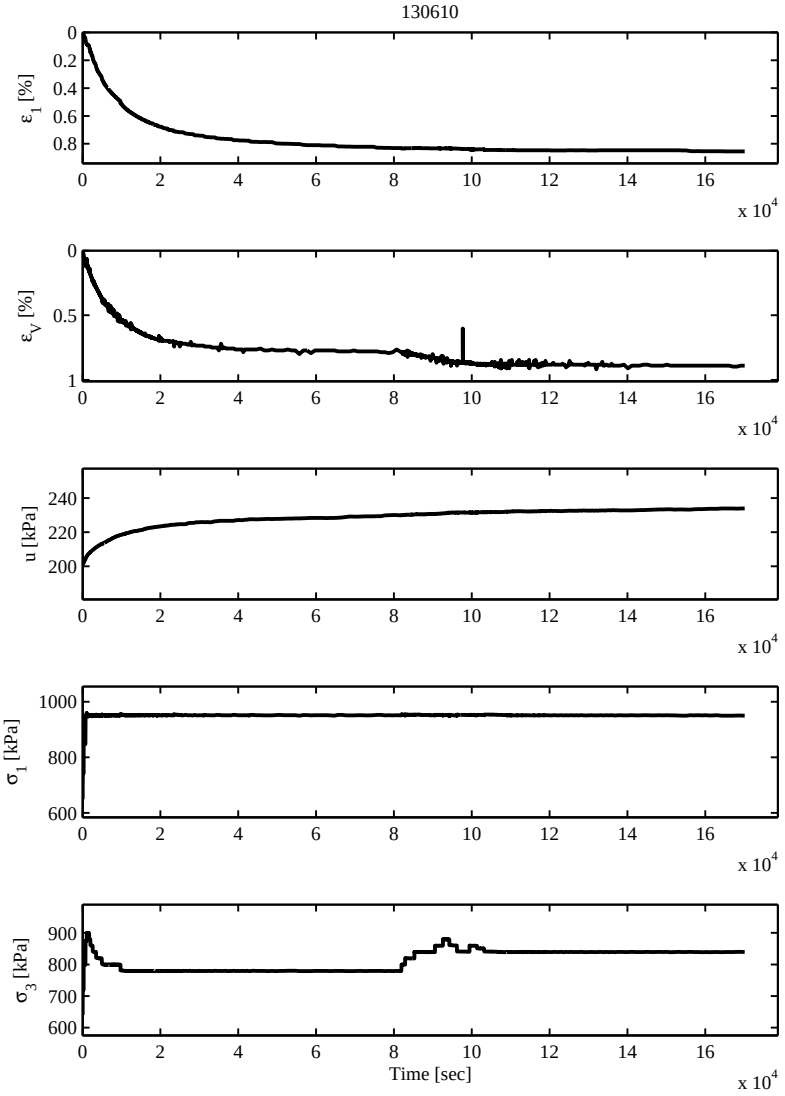

Figure J.22 Re-consolidation test 4.

Step to shearing stresses

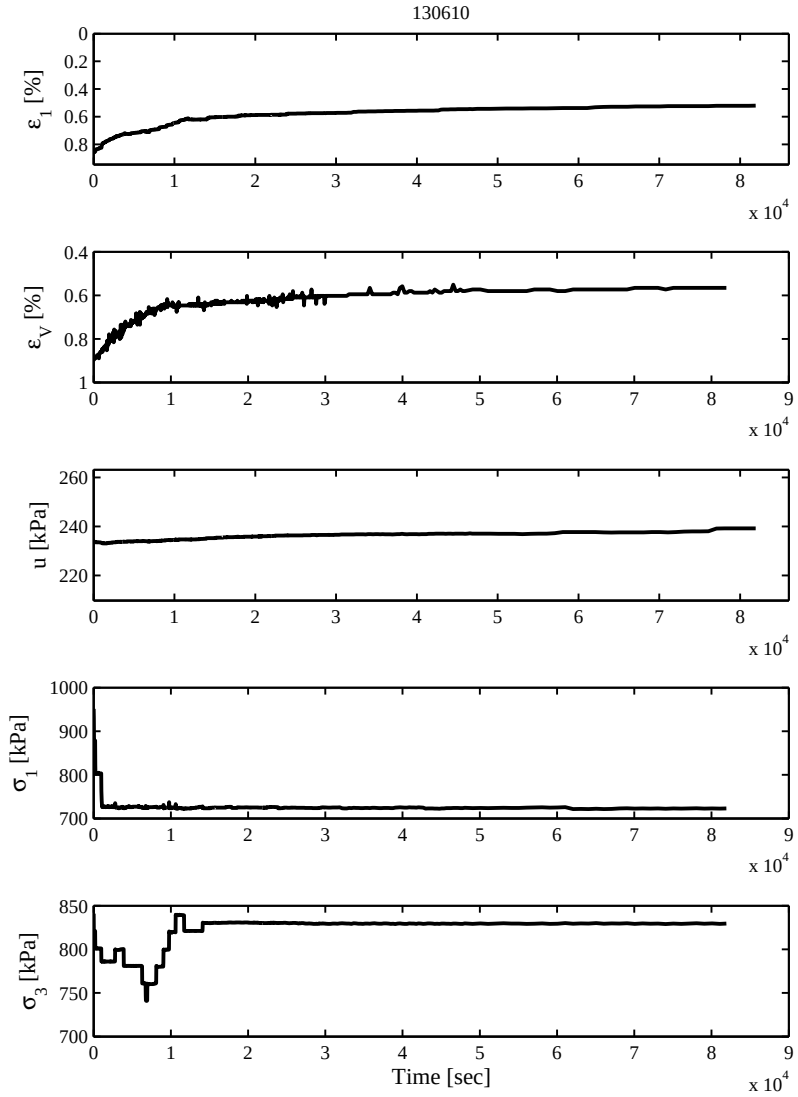

Figure J.23 To shearing stresses test 4.

Shearing step

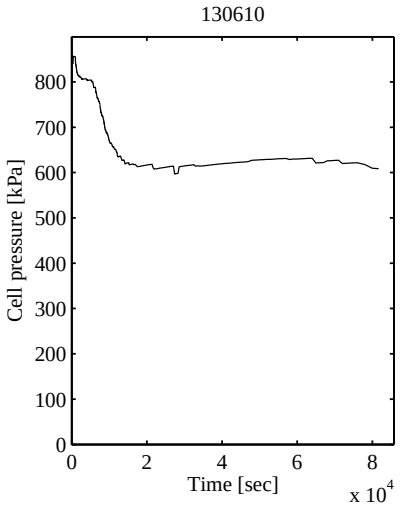

Figure J.24 130610 - Cell pressure.

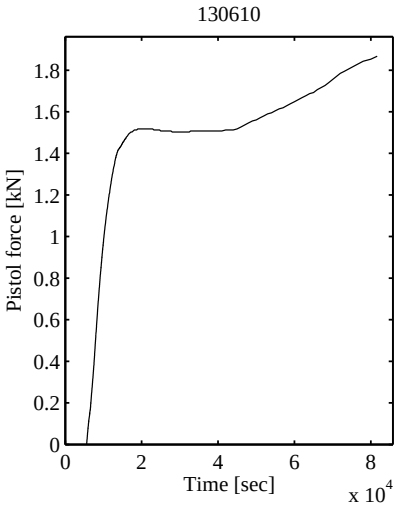

Figure J.25 130610 - Pistol force.

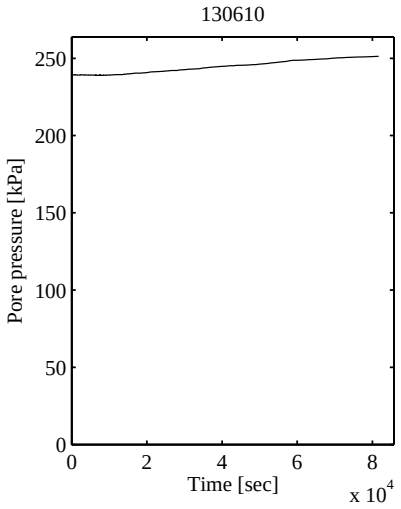

Figure J.26 130610 - Pore pressure.

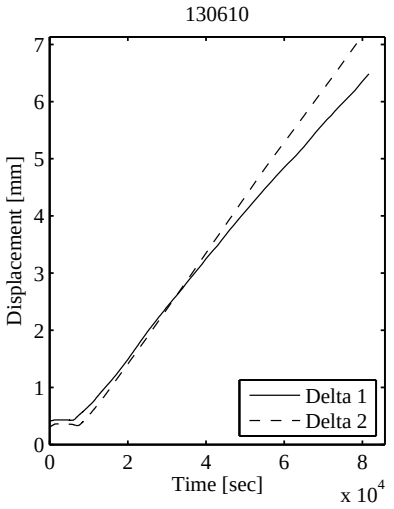

Figure J.27 130610 - Displacements.

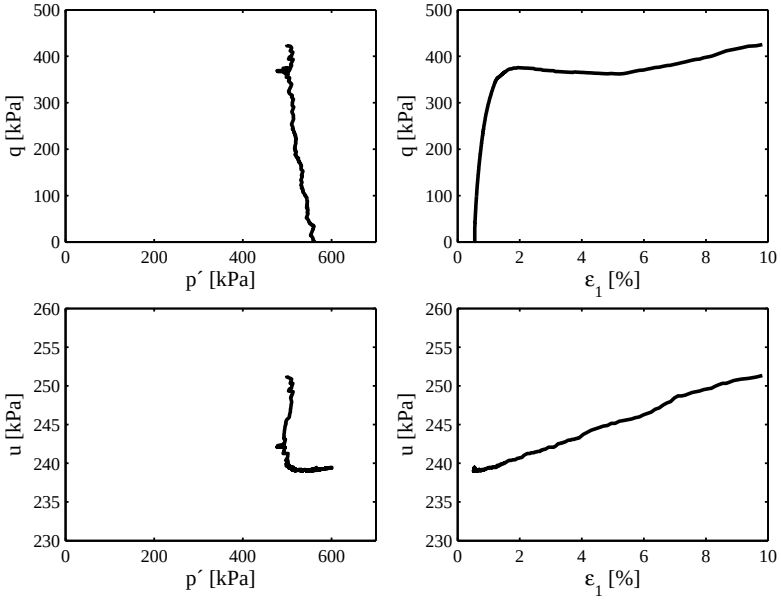

Figure J.28 Shearing step test 4.

Table J.5 Data triaxial test 4.

q [kPa]	p [kPa]	u [kPa]	ε_1 [%]	q [kPa]	p [kPa]	u [kPa]	ε_1 [%]
-106.2	795.4	239.1	0.52	346.8	742.5	239.5	1.22
-57.3	836.6	239.5	0.54	366.4	740.1	240.1	1.52
-17.0	810.0	239.2	0.56	375.7	740.2	240.6	1.93
-13.4	795.4	239.2	0.56	372.1	733.7	241.4	2.54
29.4	797.9	239.1	0.55	365.7	737.9	243.0	3.60
68.4	785.9	239.0	0.58	364.2	738.0	244.3	4.30
119.6	772.3	239.1	0.63	368.0	749.9	245.9	5.73
173.2	765.4	239.1	0.70	384.4	757.7	248.7	7.10
219.3	759.0	239.2	0.78	405.9	762.1	250.1	8.42
279.8	749.8	239.3	0.93	425.1	750.1	251.3	9.82

Laboratory number 130611 - Test 5

Re-consolidation step

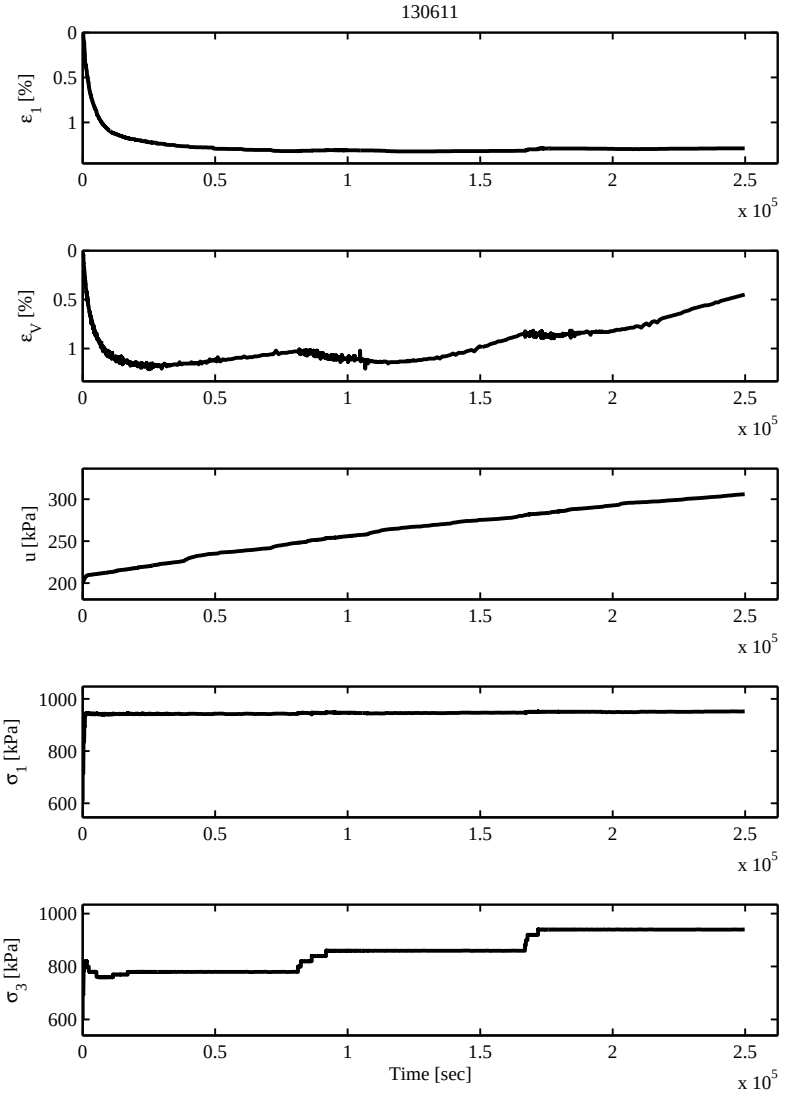

Figure J.29 Re-consolidation test 5.

Step to shearing stresses

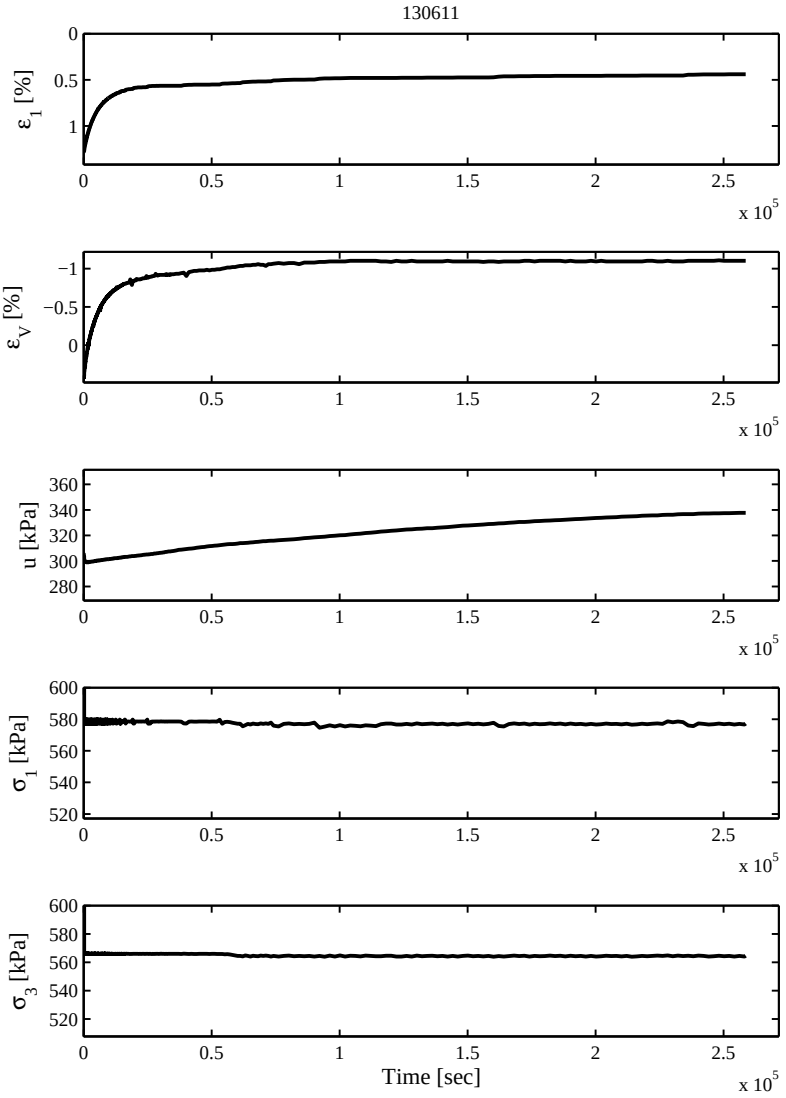

Figure J.30 To shearing stresses test 5.

Shearing step

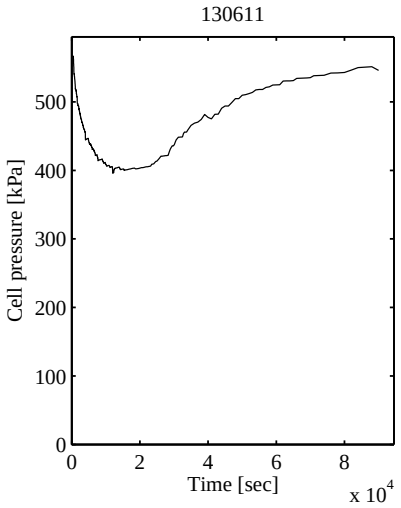

Figure J.31 130611 - Cell pressure.

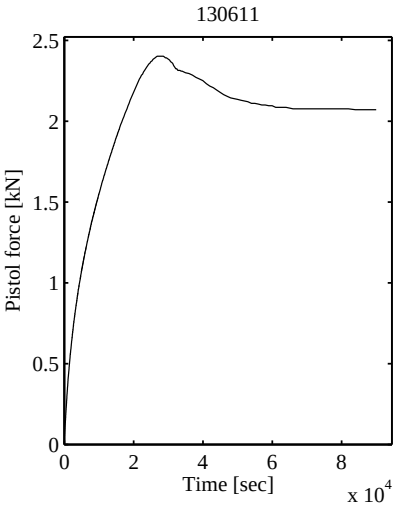

Figure J.32 130611 - Pistol force.

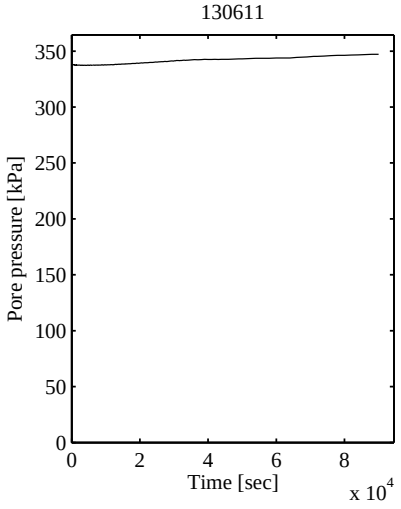

Figure J.33 130611 - Pore pressure.

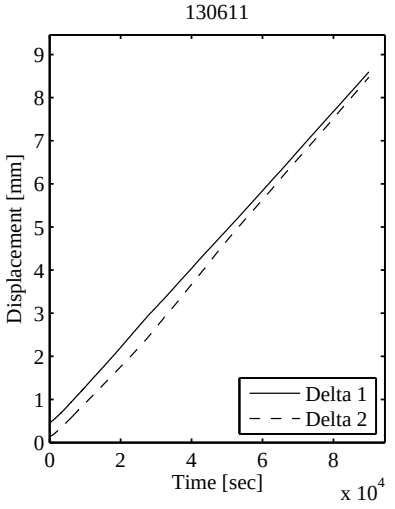

Figure J.34 130611 - Displacements.

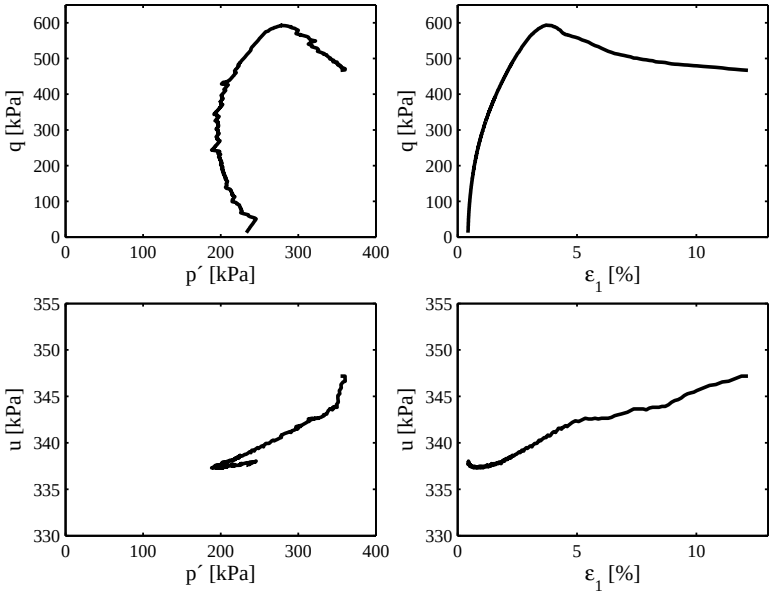

Figure J.35 Shearing step test 5.

Table J.6 Data triaxial test 5.

q [kPa]	p [kPa]	u [kPa]	ε_1 [%]	q [kPa]	p [kPa]	u [kPa]	ε_1 [%]
12.5	570.8	337.6	0.44	390.5	539.5	337.8	1.56
80.7	563.7	337.7	0.48	433.4	541.3	337.9	1.85
136.5	544.9	337.5	0.56	473.6	559.7	338.4	2.16
178.5	540.6	337.4	0.65	535.1	581.0	339.2	2.73
214.2	537.0	337.4	0.74	589.6	613.6	340.4	3.55
245.0	526.6	337.3	0.84	593.4	618.8	340.6	3.71
270.7	534.4	337.4	0.93	585.9	632.9	341.3	4.15
297.5	533.4	337.4	1.05	556.6	655.9	342.3	5.07
318.2	533.6	337.4	1.15	504.5	682.1	343.5	7.25
338.8	534.1	337.5	1.25	486.8	693.3	344.1	8.83
356.9	534.5	337.6	1.35	479.3	698.7	345.6	10.03
373.7	537.9	337.7	1.46	466.8	701.6	347.2	12.16

Laboratory number 130612 - Test 6

Re-consolidation step to shearing stresses

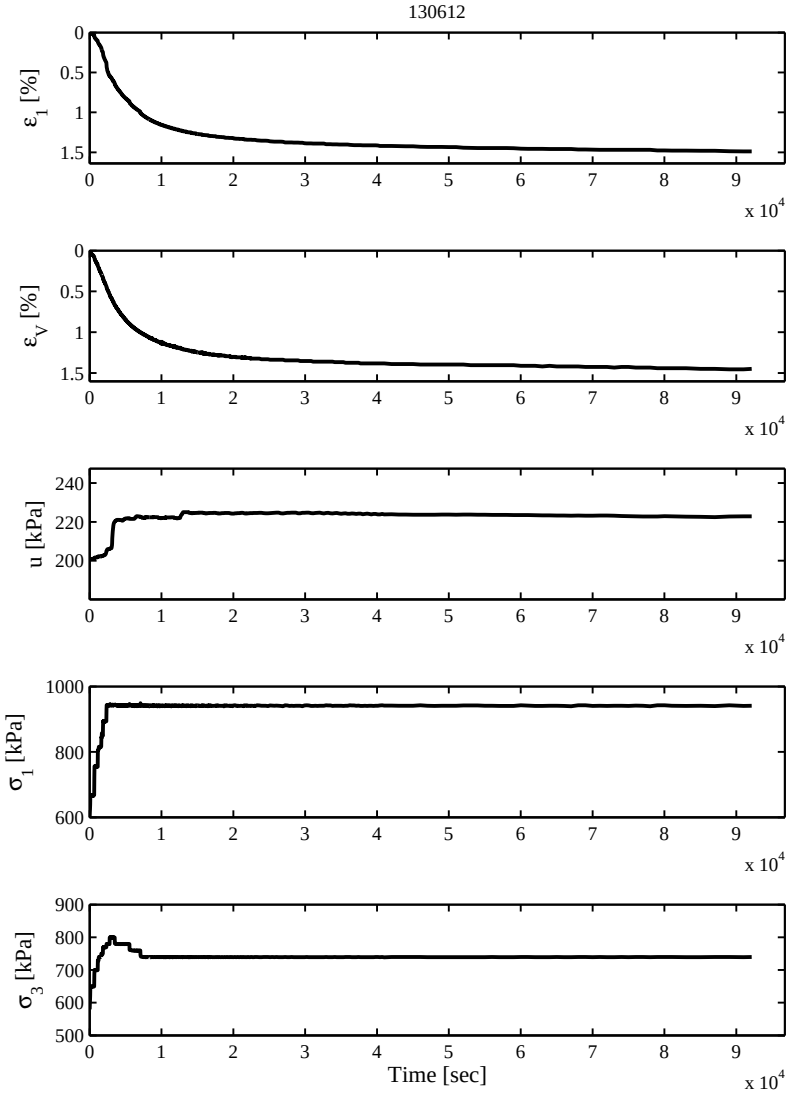

Figure J.36 Re-consolidation to shearing stresses test 6.

Shearing step

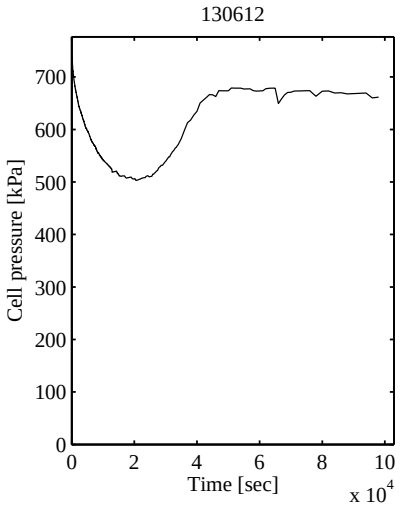

Figure J.37 130612 - Cell pressure.

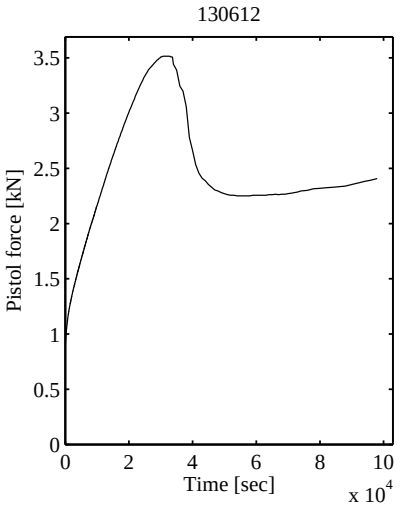

Figure J.38 130612 - Pistol force.

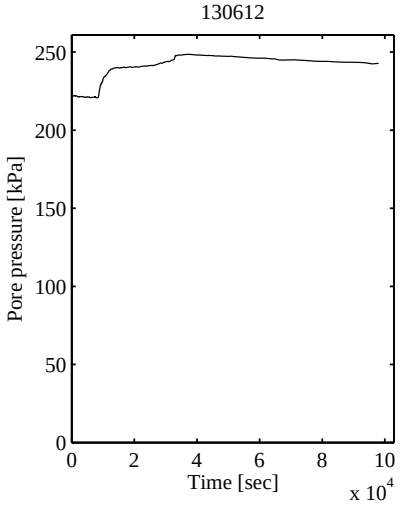

Figure J.39 130612 - Pore pressure.

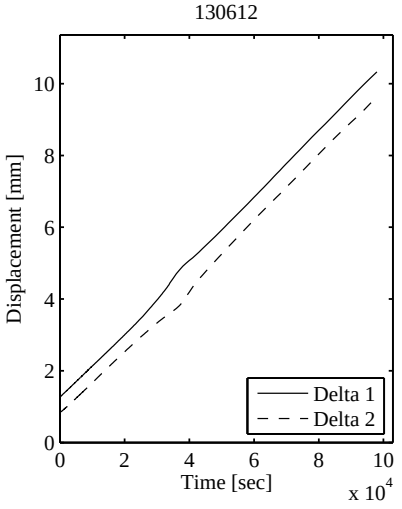

Figure J.40 130612 - Displacements.

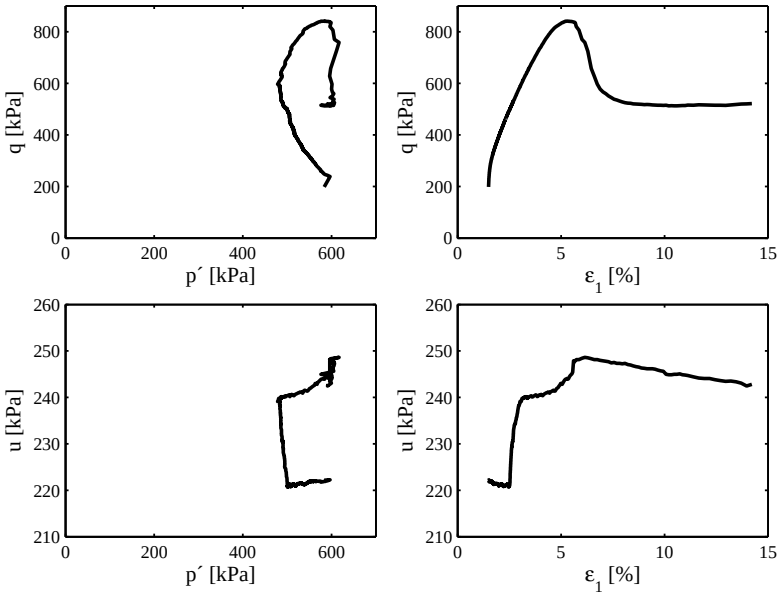

Figure J.41 Shearing step test 6.

Table J.7 Data triaxial test 6.

q [kPa]	p [kPa]	u [kPa]	ε_1 [%]	q [kPa]	p [kPa]	u [kPa]	ε_1 [%]
198.5	805.7	222.2	1.50	742.8	751.0	240.6	4.04
286.6	785.5	221.9	1.59	801.2	776.8	241.3	4.52
320.1	770.6	221.8	1.68	827.2	801.3	242.4	4.90
346.4	756.4	221.4	1.78	841.3	825.8	244.1	5.29
370.1	749.8	221.5	1.88	820.0	844.6	248.2	5.73
391.4	741.3	221.1	1.98	724.2	859.3	248.5	6.30
412.7	736.2	221.2	2.08	577.7	848.1	248.0	6.89
453.9	726.8	221.0	2.28	531.1	850.7	247.3	7.83
473.8	725.8	221.2	2.38	519.1	850.2	246.5	8.76
509.9	720.6	227.0	2.58	514.5	850.3	245.6	9.94
529.7	719.9	231.3	2.68	514.9	845.6	244.4	11.39
575.9	721.8	238.2	2.96	521.7	835.4	242.8	14.22
628.8	727.6	240.1	3.26				

Laboratory number 130613 - Test 7

Re-consolidation step

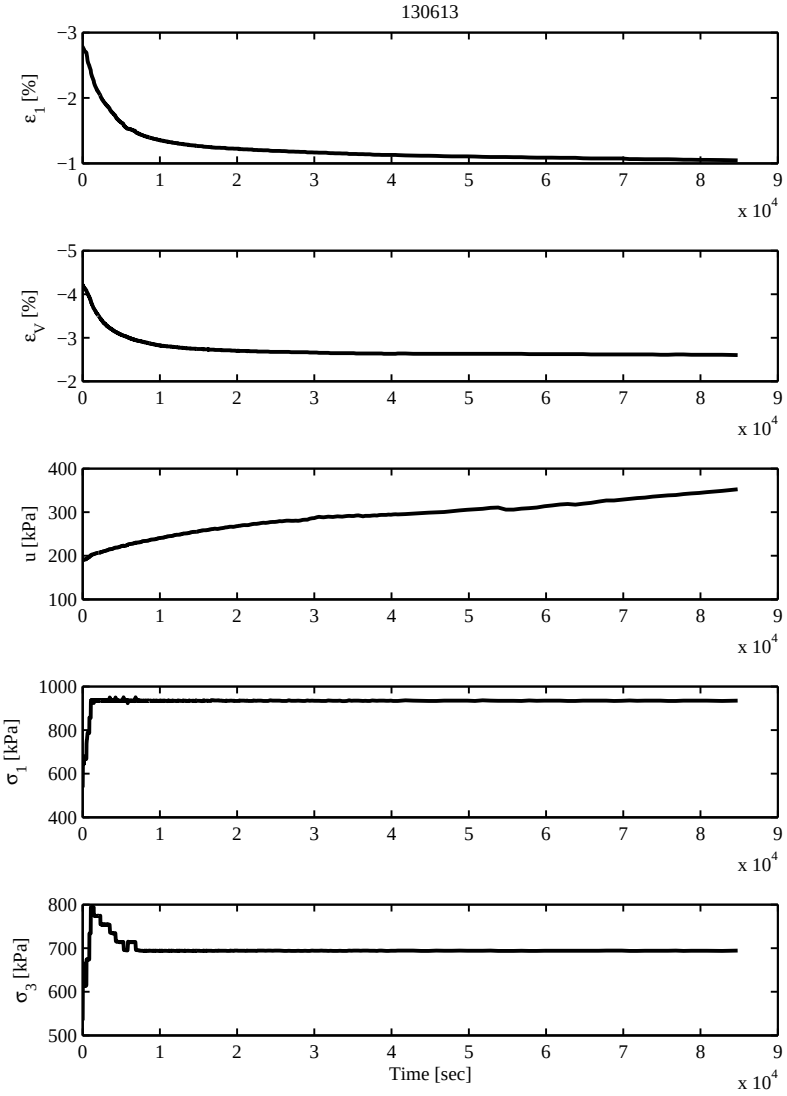

Figure J.42 Re-consolidation test 7.

Step to shearing stresses

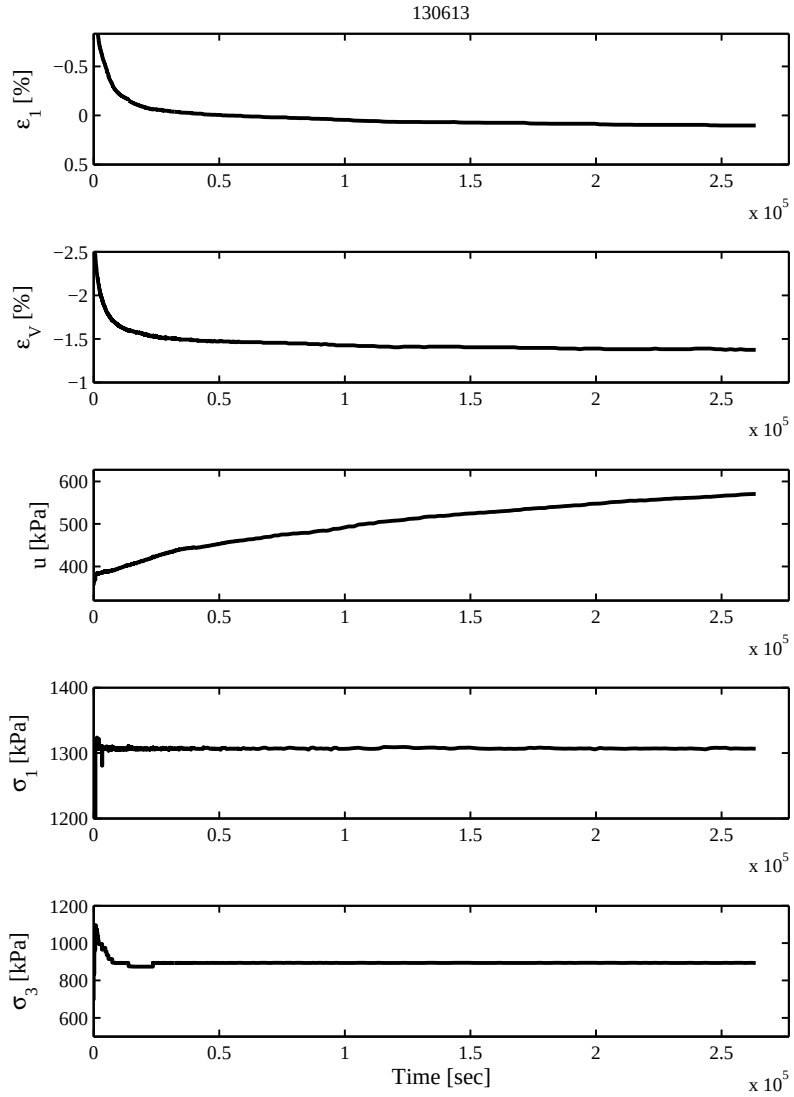

Figure J.43 To shearing stresses test 7.

Shearing step

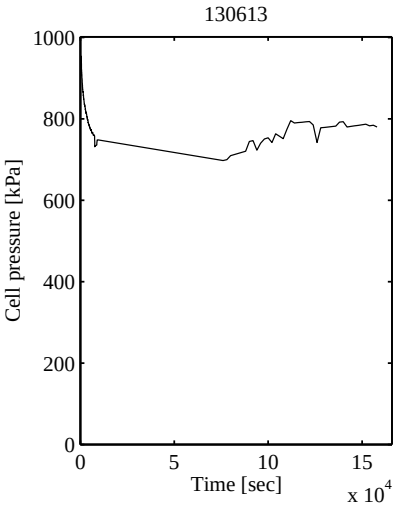

Figure J.44 130613 - Cell pressure.

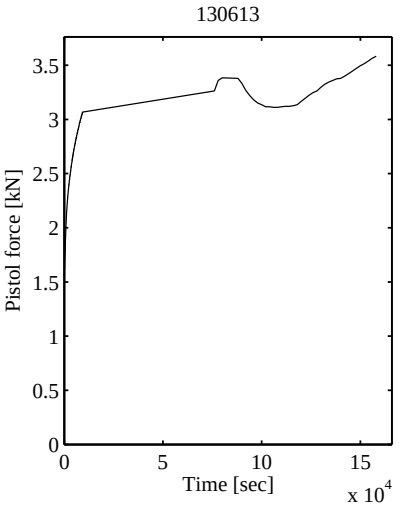

Figure J.45 130613 - Pistol force.

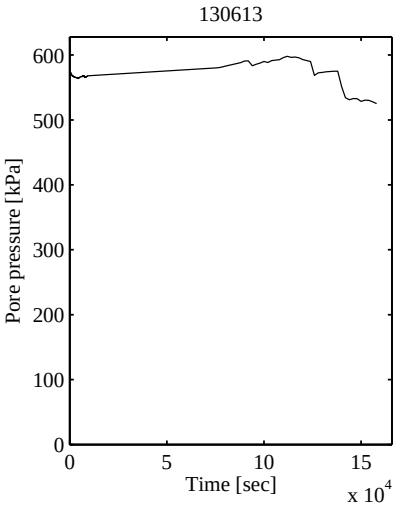

Figure J.46 130613 - Pore pressure.

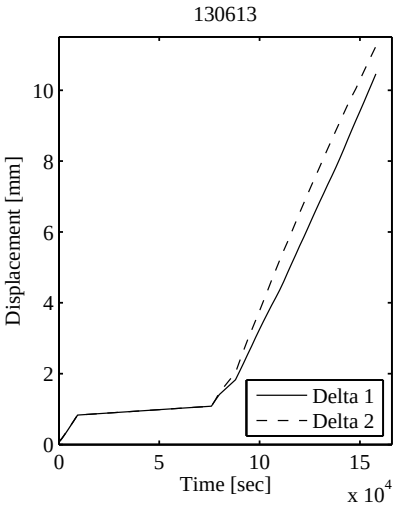

Figure J.47 130613 - Displacements.

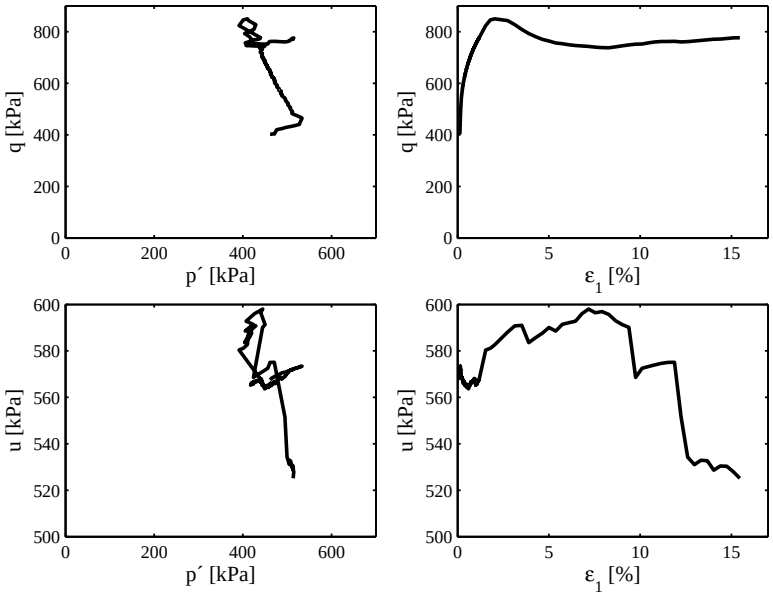

Figure J.48 Shearing step test 7.

Table J.8 Data triaxial test 7.

q [kPa]	p [kPa]	u [kPa]	ε_1 [%]	q [kPa]	p [kPa]	u [kPa]	ε_1 [%]
402.2	1029.0	567.5	0.13	823.6	971.9	580.4	1.54
512.7	1074.7	571.1	0.18	845.9	981.9	581.1	1.79
578.1	1050.2	568.2	0.26	849.8	993.0	582.7	2.05
618.6	1036.8	566.6	0.36	827.1	1020.2	590.8	3.13
647.7	1027.1	565.5	0.46	808.2	1016.0	591.0	3.52
673.1	1017.5	564.6	0.55	753.2	1014.4	591.4	5.73
694.7	1011.4	565.4	0.66	741.3	1039.7	593.0	8.65
709.1	1009.4	566.7	0.73	762.3	1046.0	575.1	11.88
726.9	1008.7	567.2	0.83	768.3	1040.1	532.7	13.68
756.3	985.9	566.0	1.03	776.7	1038.7	525.1	15.46
773.8	1005.9	567.2	1.16				

SUMMARY

The thesis regards the characterisation and determination of properties of Søvind Marl, a Danish highly fissured and plastic clay. Highly fissured, plastic clays are present at great depths several places in Denmark, where extensive development activity is currently ongoing. Nonetheless, the knowledge of these highly clays is very limited. The thesis consists of three parts based on five scientific papers and a monograph covering a range of different geotechnical tests and properties.

The first part describes the geotechnical description and properties of Søvind Marl in order to get a general knowledge of the material and an idea of potential challenges. The second part deals with the preconsolidation and stiffness of Søvind Marl. This study herein evaluates the preconsolidation stresses and clarifies and discusses potential difficulties. During continuous loading oedometer tests, the earth pressure at rest is measured at various stress levels and assessed to known correlations. The third part concerns the strength parameters of Søvind Marl. The study consists of conducting undrained triaxial tests normalised using SHANSEP to determine the undrained shear strength, and the study will determine the correlation factors from field tests to undrained shear strength. Finally, the thesis is concluded with recommendations for further work within the field of plastic clays.

ISSN: 2246-1248
ISBN: 978-87-7112-227-5

AALBORG UNIVERSITY PRESS